The ecology, sonic environment, and acoustic occurrence of subarctic baleen whales in the Bering Strait over a decade of change

Erica Danielle Escajeda

A dissertation

submitted in partial fulfillment of the

requirements for the degree of

Doctor of Philosophy

University of Washington

2023

Reading Committee:

Kristin L. Laidre, Chair

Kathleen M. Stafford

Trevor A. Branch

Program Authorized to Offer Degree:

School of Aquatic and Fishery Sciences

Authors: Erica Escajeda, Kathleen M. Stafford, Rebecca A. Woodgate, Kristin L. Laidre
Title: Variability in fin whale (*Balaenoptera physalus*) occurrence in the Bering Strait and southern Chukchi Sea in relation to environmental factors
Journal: Deep Sea Research Part II
Publisher: Elsevier Ltd.

Authors: Erica D. Escajeda, Kathleen M. Stafford, Rebecca A. Woodgate, Kristin L. Laidre
Title: Quantifying the effect of ship noise on the acoustic environment of the Bering Strait
Journal: Marine Pollution Bulletin
Publisher: Elsevier Ltd.

University of Washington

ABSTRACT

The ecology, sonic environment, and acoustic occurrence of subarctic baleen whales in the Bering Strait over a decade of change

Erica Danielle Escajeda

Chair of the Supervisory Committee:

Kristin L. Laidre

School of Aquatic and Fishery Sciences and Applied Physics Laboratory

The southern Chukchi Sea is a productive, shallow continental shelf ecosystem that is undergoing rapid change due to climate warming. Annual sea ice cover has declined significantly, potentially allowing for more temperate species to move further north into the Arctic and stay for longer periods. Monitoring the presence and occupation patterns of top predators, such as baleen whales, is important for detecting shifts in species assemblages and distributions in response to climate change. This dissertation examines the acoustic occurrence of three subarctic baleen whales in the Chukchi Sea—fin whales (*Balaenoptera physalus*), humpback whales (*Megaptera novaeangliae*), and gray whales (*Eschrichtius robustus*)—and seeks to uncover patterns in their presence, the environmental drivers that draw them into the Arctic, and how ships affect the acoustic habitat of the region during the open-water season.

In Chapter 2, I use acoustic recordings from three moored hydrophones in the Bering Strait region from 2009–2015 to identify fin whale calls during the open-water season (July–

November) and investigate the potential influence of local environmental conditions on fin whale presence. The results show significant interannual variability in the acoustic presence of fin whales with the greatest detections of calls in years with contrasting environmental conditions (2012 and 2015). Colder temperatures, lower salinities, slower water velocities, and weak southward winds prevailed in 2012 while warmer temperatures, higher salinities, faster water velocities, and moderate southward winds prevailed in 2015. Most detections (96%) were recorded at the mooring site, Site A3, nearest the confluence of the nutrient-rich Anadyr and Bering Shelf water masses, ~ 35 km north of Bering Strait, indicating that productive water masses may influence the occurrence of fin whales.

In Chapter 3, I expanded my efforts to include humpback and gray whales and added two years of acoustic and environment data, 2017 and 2018, to the dataset from Chapter 2. Using recordings and *in situ* environmental data from Site A3 collected from 2009 to 2018, I identified fin, humpback, and gray whale calls during the open-water season (May–December), and examined the timing of migration as well as investigated potential environmental drivers of whale presence. The acoustic presence of humpback and fin whales varied across the years with the highest occurrence of humpback calls in 2009, 2017, and 2018 and the highest occurrence of fin whale calls in 2015, 2017, and 2018. The years 2013 and 2015 had the highest proportion of recordings with gray whale calls. Fin whales had significantly later departure dates during the study period (~ 3 days yr^{-1}, $p = 0.02$), likely on account of warmer temperatures in the Chukchi Sea in the later years of the study (2017 and 2018). Individual models for the three species identified day of the year, sea-surface temperatures, near-bottom temperatures, and the presence of a thermal front the previous month as drivers of fin, humpback, and gray whale presence.

In Chapter 4, I characterized ship activity in the Bering Strait during the open-water season (July–November) for 2013–2015 and quantified the impact of ship noise on third-octave frequency bands used by baleen whales (25–1000 Hz). Peak ship activity occurred in July–September with the greatest overlap in ship noise and whale vocalizations observed in October. Ships elevated sound levels by ~ 4 dB on average for all third-octave frequency bands combined, and sound levels exceeding 100 dB re 1 µPa for the 250-Hz third-octave frequency band were recorded from two large vessels over 11 km away from the hydrophones. The results show that ship noise has the potential to impact baleen whales in the Bering Strait and serve as a baseline for measuring future impacts of ship activity in the region.

Overall, the results presented within this dissertation provide a snapshot of the presence of subarctic baleen whales in the Bering Strait during a time of change in the Pacific Arctic. It is clear from this work that fin whales, humpback whales, and gray whales are important components of the summertime marine ecosystem of the Chukchi Sea. Continued study of their presence in the region will be important for tracking further changes in the region. Additionally, the results presented here serve as a baseline for measuring future changes to the marine soundscape as shipping and other anthropogenic activities continue to increase in the Pacific Arctic.

TABLE OF CONTENTS

LIST OF TABLES

dates indicate when the hydrophone started and stopped recording, however we only analyzed recordings for the open-water season (May through freeze-up in November/December of each year).

Table 3.2. Melt-out (sea-ice concentration < 80%) and freeze-up (sea-ice conc. ≥ 80%) initiation dates along with the start/end dates and length of the open-water period for the Chukchi Sea (boundaries in Fig. 3.1).

Table 3.3. List of variables included in the best model for each species (model with lowest AICc score). A check mark (✓) indicates that the variable was included in the model. Smoothers are: cs = cubic spline, pb = penalized b-spline smoothers. Variables in **bold** text were included in all three species' models.

Table 3.4. Results of the incremental R^2 test on the final models for each species. The R^2 value listed for each predictor variable is the R^2 for the full model with that variable removed. The ΔR^2 indicates the change in R^2 from that of the full model, and the percent (%) change indicates how much the full-model R^2 changed with that variable removed. The R^2 values were calculated using the Cox-Snell equation (Cox and Snell 1989).

Table S3.1. Results of the Pearson correlation tests between seasonal means for near-bottom temperature and salinities ('SBE Temp' and 'SBE Salt'), sea-surface temperatures (SST), water speeds, and wind speeds. Pink shading denotes correlations with an absolute value > 0.7.

Table S3.2. Summary of sampling dates and units for the prey datasets: National Oceanic and Atmospheric Administration (NOAA) Bering Arctic Subarctic Integrated Survey (BASIS); NOAA Ecosystems and Fisheries Oceanography Coordinated Investigations joint research program (EcoFOCI); and benthic zooplankton density collected during Distributed Biological Observatory surveys (DBO; https://www.pmel.noaa.gov/dbo/; Grebmeier and Cooper 2019a, 2019b). See Figs. 2 and 3 for sampling locations. *The National Oceanic and Atmospheric Administration (NOAA) EcoFOCI dataset was compiled by Dr. David Kimmel (NOAA – National Marine Fisheries Service).

Table S3.3. Results of the linear regression for the departure dates (y) for each species vs. seasonal means of environmental variables (x). Only the variables with a significant, linear relationship to the departure dates ($p < 0.05$) are listed below, including seasonal means for sea-surface temperatures (SST, °C), near bottom temperatures (measured with SBE-16 instrument, °C), and water speeds (measured by ADCP instrument, cm s^{-1}). Seasons were defined as follows: winter = 21 Dec–20 Mar, spring = 21 Mar–20 Jun, summer = 21 Jun–20 Sep, and fall = 21 Sep–20 Dec. Winter here indicates the previous winter to the arrival of the whales to the Bering Strait.

Table S3.4. Best models for each species according to Akaike information criterion with a correction for small sample sizes (AICc) along with their R^2 values (Cox-Snell). Other models that had ΔAICc < 10 are also listed. Note that the two models for gray whale had the same AICc

score and R^2 value, thus we chose the model with fewer variables. The smoothing terms are specified next to the variable names: cs = cubic spline, pb = penalized b-spline smoothers. DOY = day of the year; SBE Temp = daily mean near-bottom temperatures; SBE Salt = daily mean near-bottom salinities; Water Speed = daily mean water speeds; Wind Speed = daily mean wind speeds; SST Grad = SST gradient (represents presence of a thermal front); SST Grad Lagged = SST Gradient lagged by one month.

Table 4.1. Hydrophone deployment data, including latitude and longitude (in decimal degrees) and recording settings. Dates are in the format 'yyyy-mm-dd.' Mooring names are from the Bering Strait mooring program (Woodgate et al., 2015). See Fig. 4.1 for the mooring locations.

Table 4.2. Correlation coefficients and *p*-values from Pearson correlation tests between daily median third-octave sound levels measured for the 63-Hz, 125-Hz, and 250-Hz bands. The correlation coefficients were used in the autoregressive correlation factors for the generalized least squares regression models (See Section 4.3.2).

Table 4.3. Total numbers of recordings with ship noise, baleen whale vocalizations, or a combination of both for each mooring. Note that there were ship recordings with other marine mammal species present, we focus on whales only here.

Table 4.4. Coefficients ("Coef.") and *p*-values from the generalized least squares (GLS) regression models examining the relationship between daily mean wind (m/s) and water speeds (cm/s), and daily median sound levels recorded for the 63-Hz, 125-Hz, and 250-Hz third-octave bands at Sites A2 and A4 (2013–2015 combined). All *p*-values were significant (significance threshold = 0.05).

Table 4.5. Total counts of vessels by type observed in the Bering Strait region (i.e., within 100-km of Sites A2 and A3) during May–November for the years 2013–2015 according to the U.S. Coast Guard's Nationwide Automatic Identification System (NAIS) data. The vessel types were defined by the NAIS dataset and are based on the U.S. Coast Guard's Authoritative Vessel Identification Service (AVIS) database. Note that only large vessels (> 300 gross tonnage), passenger vessels (≥ 100 gross tons and carrying a minimum of 12 passengers), and large fishing vessels are required to carry AIS transponders by the International Maritime Organization (IMO). Sailing and smaller vessels are not required to carry AIS transponders, and consequently, their numbers may be underrepresented in the totals presented here.

Table 4.6. Number of unique vessels by type (total n = 378) along with the average speed over ground (SOG, knots) and the standard deviation in parentheses calculated using all unique vessels combined for each vessel type. Note that there were 34 ships with unknown vessel type that were not included in the table below.

LIST OF FIGURES

both the near-surface (triangles) and the near-bottom sensor (circles). The icons are then shaded to convey the presence (black) or absence (white) of fin whale calls for that day.

Fig. S2.14. Water mass composition at the A2 mooring site. The bounds for each water mass were calculated using daily mean temperatures and salinities from both the near-surface (triangles) and the near-bottom sensor. The icons are then shaded to convey the presence (black) or absence (white) of fin whale calls for that day. Note that years 2009–2011 were omitted since the hydrophone did not record data that year.

Fig. 3.1. Map of study area and the Bering Strait region. The white circle around A3 indicates the extent of the 30-km buffer which we used to calculate the sea-surface temperature gradient for indicating the presence of a thermal front near A3. The four wind data points from NOAA's National Center for Atmospheric Prediction (NCEP) North American Regional Reanalysis (NARR) dataset are included (stars). The inset map shows the study area (orange box) along with the boundaries for the Chukchi Sea as defined by the International Hydrographic Organization (IHO, http://www.marineregions.org/gazetteer.php?p=details&id=4257).

Fig. 3.2. Sampling stations for (A) the Bering Arctic Subarctic Integrated Survey (BASIS), and (B) the benthic invertebrate dataset (Grebmeier and Cooper 2019a, 2019b).

Fig. 3.3. (A) Sampling stations for the NOAA EcoFOCI zooplankton dataset. (B) Annual mean density (number per m^3) of *Calanus* spp. copepods in the four sampling zones.

Fig. 3.4. Proportion of hourly recordings with whale calls by month during the open-water season for humpback whales, fin whales, and gray whales at the A3 mooring site. Vertical lines separate each year while the gray shaded areas indicate periods with no recordings.

Fig. 3.5. Proportion of October–November recordings with whale calls by year for each species.

Fig. 3.6. Graphical representation of Chukchi Sea ice melt-out (< 80% concentration) in the spring, and freeze-up (≥ 80% concentration) in the fall for the study period (2009–2018) (light blue). The dark blue area represents the open-water period (sea-ice concentration ≤ 15%).

Fig. 3.7. Plots of (A) seasonal mean near-bottom ('SBE Temp') and sea-surface (SST) temperatures, and (B) near-bottom salinities ('SBE Salt').

Fig. 3.8. (A) Arrival and (B) departure days of the year for fin whales (FW; circles), humpback whales (HB; squares), and gray whales (GW; triangles). Arrival dates shown for the years that had recordings available in spring (2014–2016, 2018). Linear regressions are shown as dotted. The days of the year when sea ice concentrations reached < 80% in the Chukchi Sea ('CS Ice Melt') and ≥ 80% concentration ('CS Ice Freeze') are included with the arrival and departure dates for illustrative purposes (dashes).

Fig. 3.9. Results from the Pearson correlation tests (*r*) and linear regression between departure days for fin whales (top) and humpback whales (bottom) and seasonal mean sea-surface temperatures (SST; from the NOAA Optimum Interpolation Sea Surface Temperature [OISST] dataset; °C), and near-bottom temperatures (from SBE-16 instrument; °C). Seasons were defined as follows: winter = 21 Dec–20 Mar, spring = 21 Mar–20 Jun, summer = 21 Jun–20 Sep, and fall = 21 Sep–20 Dec. See Table S3.3 for the linear equations.

Fig. 3.10. Results from the Pearson correlation test (*r*) and linear regression between fin whale departure days and winter mean water speeds (ADCP data; cm s^{-1}). Winter was defined by the period 21 December–20 March.

Fig. 3.11. Plots of the additive smoothing fits for the best fin whale model with the smoothed functions for the daily probability of a calling fin whale being present in relation to temporal (day of the year, DOY), and environmental conditions. Daily means were used for the environmental covariates, including near-bottom temperature, sea surface temperatures (SST), and water speed. The 'SST Gradient' represents the maximum difference in daily mean SSTs between grid cells within a 30-km buffer around site A3, which was then lagged by one month ('Lagged SST Gradient'). The lines indicate the effect of the covariate on the probability and the gray areas represent the standard errors for the effect of the smoothed term.

Fig. 3.12. Plots of the additive smoothing fits for the best humpback whale model with the smoothed functions for the daily probability of a calling humpback whale being present in relation to temporal (day of the year, DOY), and environmental conditions. Daily means were used for the environmental covariates, including near-bottom temperature and salinity, sea-surface temperatures (SST), water speed, and wind speed. The 'SST Gradient' represents the maximum difference in daily mean SSTs between grid cells within a 30-km buffer around site A3, which was then lagged by one month ('Lagged SST Gradient'). The lines indicate the effect of the covariate on the probability and the gray areas represent the standard errors for the effect of the smoothed term.

Fig. 3.13. Plots of the additive smoothing fits for the best gray whale model with the smoothed functions for the daily probability of a calling gray whale being present in relation to temporal (day of the year, DOY), and environmental conditions. Daily means were used for the environmental covariates including near-bottom temperature and salinity, sea-surface temperatures (SST), water speed, and wind speed. The 'Lagged SST Gradient' represents the maximum difference in daily mean SSTs between grid cells within a 30-km buffer around site A3 lagged by one month. The lines indicate the effect of the covariate on the probability and the gray areas represent the standard errors for the effect of the smoothed term.

Fig. S3.1. Map of the Distributed Biological Observatory (DBO) sampling regions (figure from Grebmeier et al. 2019).

Fig. S3.2. Chart of the sampling periods for all three prey datasets: BASIS forage fish dataset (top, green squares), EcoFOCI *Calanus* spp. dataset (middle, blue squares), and the benthic amphipod dataset (bottom, yellow squares). The start dates of the hydrophone recordings are represented by the bold squares and the gray shading represents the recording periods.

Fig. S3.3. Vector plots of daily mean water speed (cm s^{-1}) at the A3 mooring site.

Fig. S3.4. Seasonal means for water speed (cm s^{-1}) measured at the A3 mooring site. Note that 2016 was omitted since we do not have acoustic data for that year. The seasons were defined as follows: Winter ('W') = 21 Dec–20 Mar; Spring = 21 Mar–20 Jun; Summer ('Su') = 21 Jun–20 Sep; Fall = 21 Sep–20 Dec. Water speeds throughout the seasons were highly variable with standard deviations ranging from 13 cm s^{-1} to 27 cm s^{-1}. A linear regression of the seasonal means with year shows a significant increasing trend over the study period ($p = 0.02$).

Fig. S3.5. Vector plots of daily mean wind speed (cm s^{-1}) at the A3 mooring site. The gray dashed line at 10 m s^{-1} indicates strong wind speeds.

Fig. S3.6. Plot of the daily maximum sea-surface temperature (SST) gradient (°C) within a 30-km radius of the A3 mooring site for the open-water season (1 May through freeze-up; see Table 3.2). The SST gradient is a proxy for the presence of a thermal front—the higher the gradient, the stronger the front. The plot is overlaid with a bar plot of the hours per day with fin whale calls with bold lines indicating the start and end of the recording period.

Fig. S3.7. Plot of the daily maximum sea-surface temperature (SST) gradient (°C) within a 30-km radius of the A3 mooring site for the open-water season (1 May through freeze-up; see Table 3.2). The SST gradient is a proxy for the presence of a thermal front—the higher the gradient, the stronger the front. The plot is overlaid with a bar plot of the hours per day with humpback whale calls with bold lines indicating the start and end of the recording period.

Fig. S3.8. Plot of the daily maximum sea-surface temperature (SST) gradient (°C) within a 30-km radius of the A3 mooring site for the open-water season (1 May through freeze-up; see Table 3.2). The SST gradient is a proxy for the presence of a thermal front—the higher the gradient, the stronger the front. The plot is overlaid with a bar plot of the hours per day with gray whale calls with bold lines indicating the start and end of the recording period.

Fig. S3.9. Proportion of recordings with gray whale calls by month. Only the years with both spring and fall recordings are shown. In some years, particularly 2013 and 2014, a peak in gray whale calls is evident in the spring and fall, possibly reflecting the spring and fall migration of gray whales into and from the study region.

Fig. 4.1. Map of the study area with the three mooring locations—Sites A2 and A4 in the eastern channel of the strait, and Site A3 north of the strait. The nearest NCEP-NARR wind data point is located southwest of the strait (65°N, 170°W; Mesinger et al., 2006). The two white circles

represent 100-km buffers around Sites A2 and A3, respectively, and were used for identifying ships within the Bering Strait region. Depth data were taken from the International Bathymetric Chart of the Arctic Ocean version 3.0 (500-m resolution; Jakobsson et al., 2012). The top left inset shows the tracklines for all vessels that transited the Bering Strait between June–November 2013.

Fig. 4.2. Summary of our approach for selecting the ship transmissions from the AIS data for characterizing ship activity in the Bering Strait and for the received level (RL) vs. range to receiver analysis. SOG = speed over ground in knots; MMSI = Maritime Mobile Service Identity number.

Fig. 4.3. Summary of our approach to dividing the ambient and ship acoustic files into wind and water speed categories for the ship vs. ambient sound level analysis.

Fig. 4.4. Total counts of unique vessels that transited within 100 km of the Bering Strait region (n = 412 vessels), defined as merged 100-km buffers around Sites A2 and A3 (see Fig. 4.1). Note that the totals are likely underestimates since not all vessels are required to carry AIS transponders

Fig. 4.5. Median sound pressure levels (SPL) measured across third-octave frequency bands (Hz) for recordings with ship noise (circles) plotted against ambient SPLs (triangles) for (A) days with low water speeds (≤40 cm/s), and (B) days with high water speeds (>40 cm/s) visualized by whether the recording occurred on a day with high wind speeds (>10 knots; solid lines and points), or low wind speeds (≤10 knots; dotted lines and hollow points). Total sample sizes for the ship recordings are as follows: low water/high wind = 34 recordings; low water/low wind = 26 recordings; high water/high wind = 55 recordings; and high water/low wind = 40 recordings. Ambient sample sizes are as follows: low water/high wind = 4,377 recordings; low water/low wind = 1,189 recordings; high water/high wind = 4,788 recordings; and high water/low wind = 1,706 recordings. Note that the x-axis is log-scaled.

Fig. 4.6. Received levels (RL) for the 250-Hz third-octave frequency band (TOL) vs. slant range to the recorder (km) for the loudest vessels from the select dataset of unique ship events (n = 8; color points) plotted against the RLs for all select ship events (total n = 73; gray points). A ‘ship event’ is a ship recording matched with the AIS tracks of a single vessel that was traveling at speeds > 5 knots and passed within 10 km of the mooring (see Section 4.3.5). Vessel type is listed for each of the loudest vessels along with its length and mean speed over ground (SOG) in knots (kts). Each point represents the RL measured over each minute of the ship event recording and corresponds to an AIS transmission.

ACKNOWLEDGEMENTS

It is difficult to imagine that I will be able to capture the deep gratitude I feel for those who have helped me complete my PhD in these short pages, but I will give it my best. First and foremost, I am very grateful for my advisor, Kristin Laidre, and my co-advisor, Kate Stafford, who took me on as a student. Their expert guidance trained me to be a more effective scientist, and I am very thankful for their patience as I chased intellectual rabbit holes during my doctorate research. Joining Kristin's lab as a master's student was a dream come true, and I am very grateful for the opportunity afforded me by the National Science Foundation's Graduate Research Fellowship Program (NSF GRFP) to continue as a PhD student. Thank you, Kristin, for all the meetings to keep me on track, for the many hours you spent reading manuscript drafts, and for always being responsive to emails, even when you were half a world away! Thank you, Kate, for patiently teaching me how to use passive acoustics and program hydrophones, for always reminding me to think about the biology, ecology, and behavior of my study species first. I am forever grateful for the fieldwork opportunities you provided me in the Arctic. Spending four days stuck in the sea ice on an icebreaker is a memory that I will cherish forever.

I was incredibly lucky to be trained by not only two world-class women scientists, but also a third. I had the pleasure of collaborating with Rebecca Woodgate as a coauthor on all three of my dissertation chapters. Thank you, Rebecca, for always being warm and kind, for generously giving your time to provide insightful and detailed feedback, and for challenging me to have a deeper understanding of the statistics I used for my analyses. I am a better scientific writer because of you.

Behind every successful graduate student is a hard-working committee who sat through multiple progress presentations, read early drafts, and provided guidance every step of the way. I

had the best team: Trevor Branch, Lisa Eisner, and Joseph Sisneros. Thank you, Trevor, for our many conversations where we pondered what drives whales to behave the way they do, for reminding me to keep the history of whaling in mind and consider the toll it continues to enact on whales today, and for guiding me on how to approach quantitative analyses. Thank you, Lisa, for always being kind and encouraging. I am very grateful for your valuable insights into the prey and biological oceanography of the Bering-Chukchi Sea system. Thank you, Joe, for your enthusiasm and insights on animal communication.

Looking back on my doctorate journey, some of the most fulfilling experiences I had were teaching undergraduate students. I am forever grateful that I had the example of José Guzman to follow for how to be an empathetic teacher and mentor. You gave me the freedom to experiment with different pedagogical approaches while providing support and guidance when I needed it. I will miss the chaos that is teaching introductory Marine Biology every fall. I also wish to thank my other supervisors that have been instrumental in my training as an instructor: Camrin Braun, Miles Logsdon, Amy Kennedy, Amy Van Cise, and Glenn VanBlaricom. Thank you, Glenn, for mentoring me in the early stages of my graduate career. I will forever have your voice in my head when beginning the writing process. Rest in peace.

Not to sound cheesy, but it is true when they say it takes a village—I am so grateful for the wonderful community of colleagues and friends I have met during my time at the University of Washington. First and foremost, I am so grateful to have been part of the Laidre Lab: Jessie Hale, Jenny Stern, Marie Zahn, Sarah Teman, and Ben Cohen—thank you for cheering me on and supporting me every step of the way. Thank you, Divya Panicker and Irina Trukhanova, for your friendship and encouragement. Thank you to all the students and colleagues I met through the Northwest Student Chapter of the Society for Marine Mammalogy (NWSSMM). I will miss

our annual meetings which always felt like a family reunion. To my UW Society for the Advancement of Chicanos/Hispanics and Native Americans in Science (SACNAS) Chapter family—Anthony Salazar, Ari Gomez, Jeffrey Buenaflor, Macarena Aloi, Audrey Ragsac, Jessica Soto, and Joe Camacho—thank you for providing me an outlet to give back to the community while providing me with an invaluable support network and friend group outside of my department. My sincere thanks to all the students, professors, and staff who made the School of Aquatic and Fishery Sciences (SAFS) such a welcoming and nurturing environment for conducting my graduate work. I cannot imagine a better place to have received my scientific training. Special thanks to Samantha Scherer and Amy Fox for patiently answering my many questions and helping me navigate the bureaucracy of graduate school. Thank you to the UW Polar Science Center community for the hallway hellos, the coffee hour conversations, and for making me feel welcome.

This work would not have been possible without the support and technical expertise of Jim Johnson and the crew of the *Norseman II* who helped deploy and service the moorings. My dissertation work was supported by an NSF GRFP fellowship as well as a SAFS fellowship. I am also grateful for the UW College of the Environment for providing funding to attend meetings and conferences during my graduate career.

I would not be here if not for the support of my wonderful family. Thank you to my parents who nurtured a love for wild places in me from an early age and who encouraged me to follow my dreams. I am very grateful for my in-laws, Jerry and Karen, for their love and support. Finally, I cannot begin to express my gratitude for my partner in life, Alex – thank you for being my sounding board, my cheerleader, my comfort, and my inspiration. I would not have been able to complete this journey without you.

DEDICATION

To Alex

To my parents who have always believed in me

To the people and animals of the Arctic whose home is quickly changing

CHAPTER 1. Introduction

1.1 A Time of Change

Climate change is rapidly transforming Earth's ecosystems, especially marine systems where the rate of change is outpacing that of terrestrial systems (Poloczanska et al. 2013). Prominent among the biological responses to climate change are shifts in distribution and phenology—the timing of important life history events (Parmesan 2006). For baleen whales, whose ranges and distributions are often closely related to water temperature (MacLeod 2009), warmer temperatures associated with climate change could lead to range expansions and contractions, as well as shifts in the timing of their migrations (Ramp et al. 2015; Szesciorka et al. 2020; Ingman et al. 2021; Citta et al. 2023). Tracking changes in the distributions of baleen whales is complicated by the fact that many populations are still recovering from intensive whaling that took place in the early to late 20th century (Zerbini et al. 2016). The movement of a species into a region where they were not recently observed could be a reaction to better conditions brought on by climate change, or the species reclaiming portions of their historical range, or both. Identifying environmental conditions that are favorable for whales and how these conditions are changing is an important step in understanding how baleen whales may respond to climate change.

Despite decades of research, fundamental questions regarding whale behavior and ecology remain: why do whales migrate (Horton et al. 2022), how do they navigate (Bingman and Cheng 2005), and how do they find their patchily-distributed prey (Torres 2017)? While researchers are working to uncover the biology and ecology of baleen whales, climate change is quickly reshaping the oceans, obscuring the line between novel and basal patterns. Nowhere else is this transformation more evident than in the Arctic where temperatures are warming twice as

fast as the rest of the planet (Druckenmiller et al. 2022). Warmer temperatures are causing ice to retreat earlier in the spring and form later in the fall (Markus et al. 2009; Frey et al. 2015), leading to longer ice-free periods during the summer (Comiso et al. 2008; Cavalieri and Parkinson 2012; Vaughan et al. 2013). The steady decline of sea ice has cascading impacts on the Arctic marine food web, especially in shallow continental seas such as the Bering and Chukchi seas (Fig. 1.1) where primary production is tightly coupled to sea ice (Hunt et al. 2002; Arrigo et al. 2014; Kikuchi et al. 2020; Stabeno et al. 2020). While the impacts of sea-ice decline on Arctic marine cetaceans such as bowhead whales (*Balaena mysticetus*) are well documented in the Pacific Arctic (Laidre et al. 2015), how declining ice and associated environmental factors affect subarctic whales that summer in the region is unclear.

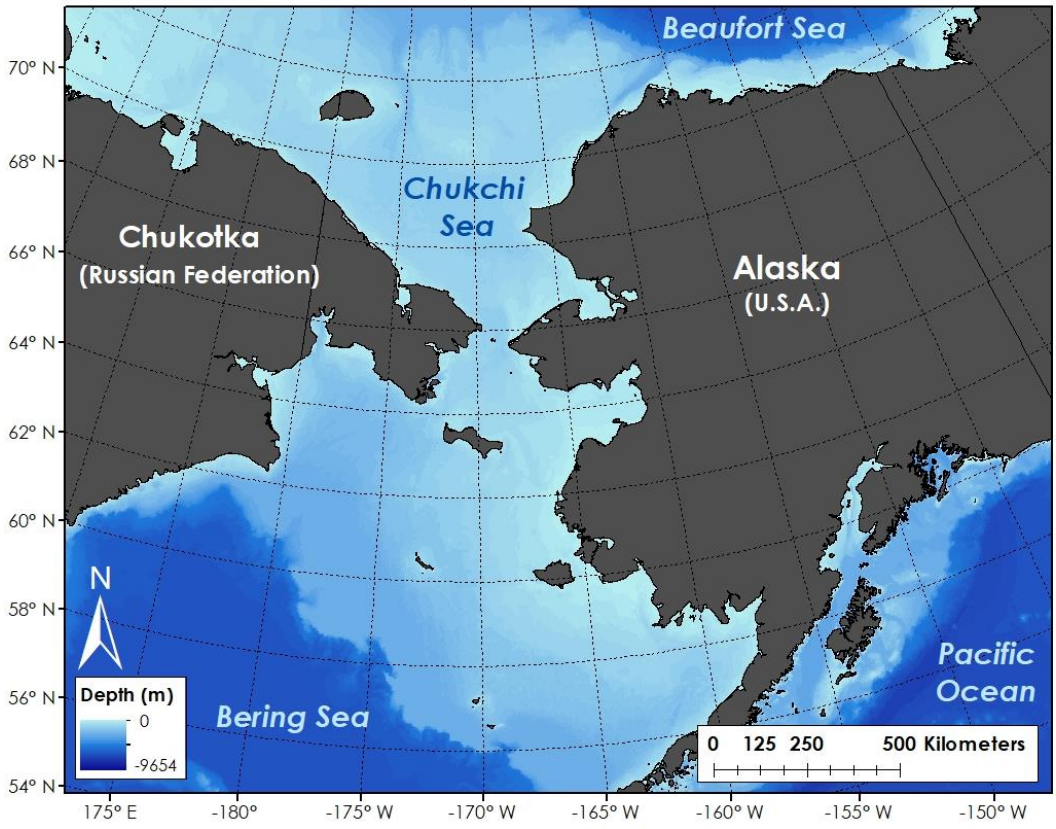

Fig. 1.1. Map of the Pacific Arctic. Bathymetry data were taken from the Alaska Region Digital Elevation Model *v.* 2 (ARDEM; http://research.cfos.uaf.edu/bathy/).

Climate change may benefit subarctic baleen whales, at least in the short term, by permitting expansion into new habitats (Kovacs et al. 2011; Moore, 2016), increasing primary production (Arrigo and van Dijken 2015), and allowing whales to stay longer in feeding areas (Perryman et al. 2002). However, declining sea ice is also opening the Arctic to increased ship activity (Eguíluz et al. 2016), which may impact the acoustic habitat for these species. There has been increased interest in recent years in studying the ambient soundscape of the Arctic with the aim of documenting baseline sound levels and measuring the contribution of anthropogenic noise to the soundscape (Merchant et al. 2014; Ahonen et al. 2017; Halliday et al. 2017; Insley et al. 2017). The Bering Strait presents an ideal location to study the effect of ship noise on ambient sound levels given that the region is a natural bottleneck for ships transiting into the Arctic from the Bering Sea.

This dissertation examines the acoustic occurrence of three subarctic baleen whales in the Chukchi Sea—fin whales (*Balaenoptera physalus*), humpback whales (*Megaptera novaeangliae*), and gray whales (*Eschrichtius robustus*)—and seeks to uncover patterns in their presence in the region, the environmental drivers that draw them into the Pacific Arctic, and how ships affect their acoustic habitat during the open-water season. Putting these research questions in context requires an exploration into the factors that shape whale behavior and habitat selection, including how whales find their food, what conditions are favorable for baleen whales, how the region is changing in the Anthropocene, and what methods are most effective for studying whales in this region.

1.2 How do whales find their food?

Determining what attracts subarctic whales to the Pacific Arctic first requires an understanding of how whales find their prey. Baleen whales migrate between lower latitude breeding areas and

higher latitude feeding areas each year, taking advantage of the seasonal bounty of prey initiated by spring phytoplankton blooms (Rice and Wolman 1971; Mizroch et al. 2009; Calambokidis et al. 2001). As they travel along their migration routes, baleen whales employ a series of sensory modalities at various scales for tracking down their patchily-distributed prey (Kenney et al. 2001; Torres 2017).

Their memory of previously successful feeding grounds likely determines a whale's first-order decisions on where to migrate (Kenney et al. 2001). The first foraging ground a whale visits is with its mother; consequently, maternally-directed fidelity to feeding grounds is commonly found in some whale populations (Baker et al. 1990; Clapham and Seipt 1991; Barendse et al. 2013). How the whales navigate to those familiar feeding grounds, though, is unclear. At large scales (> 100 km), it is thought that baleen whales employ magnetoreception (detection of the Earth's magnetic fields; Kirschvink et al. 1986), gravitaxis (sensing the Earth's gravity field; Horton et al. 2017), and/or perception of temperature and salinity gradients found in currents and fronts to orient themselves in the direction of favorable feeding areas (Torres 2017). Once the whales draw closer, at scales of 10–100 km, individuals may then cue into acoustic signals from conspecifics to zero-in on areas where other whales are feeding (Torres 2017). Warming sea temperatures, declining sea ice, and fluctuating salinity along with increased anthropogenic noise may interfere with the detection of vital cues that whales use to navigate and find their prey. Identifying those cues is critical to understanding the resiliency of whales to climate change.

Given their large size and energy requirements, whales must find dense, reliable patches of food (Piatt and Methven 1992; Goldbogen et al. 2011). The location and size of whales' feeding ranges are therefore linked to the distribution and predictability of their prey (Stevick et

al. 2006; Filatova et al. 2022). Gray whales are benthic foragers, specializing in tube-dwelling infaunal amphipods such as *Ampelisca macrocephala* (Lilljeborg 1852; Highsmith and Coyle 1991). Benthic invertebrate communities change on longer timescales than pelagic prey (Grebmeier 2012) and have a more predictable distribution, which results in high fidelity of gray whales to their feeding grounds (Heide-Jørgensen et al. 2012; Filatova et al. 2022). Eastern North Pacific gray whales undertake one of the longest known migrations of any mammal (Mate et al. 2015), swimming thousands of miles from the warm calving lagoons of Baja California, Mexico, to the cold feeding grounds of the Bering and Chukchi seas (Fig. 1.2; Rice and Wolman 1971). The fact that gray whales migrate great distances to reach the Pacific Arctic is a testament to the quality and density of prey found in the Bering and Chukchi seas—two of the most productive marine ecosystems in the world (Grebmeier et al. 2006; Zerbini et al. 2016).

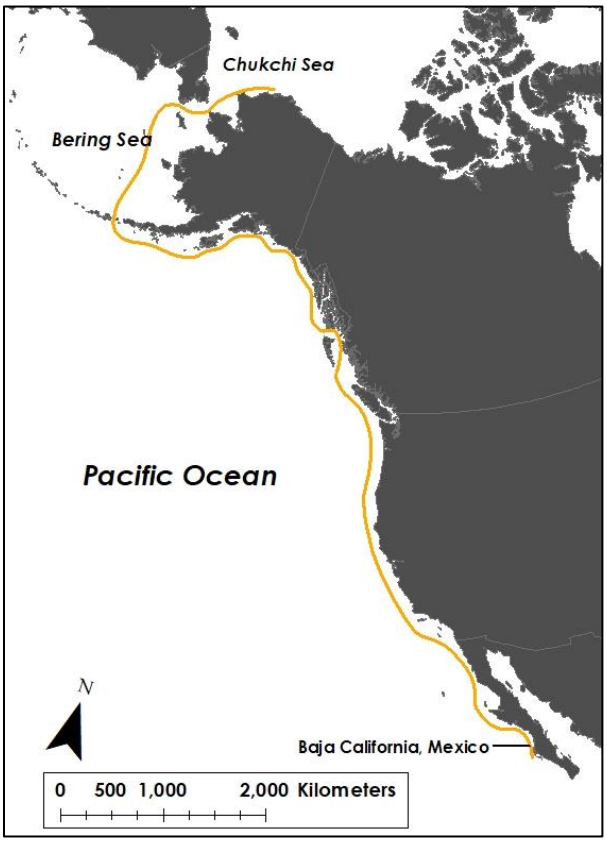

Fig. 1.2. Approximate migration route of eastern North Pacific gray whales (orange line).

What draws fin and humpback whales in the Pacific Arctic, however, is less clear. Both fin and humpback whales are generalist pelagic predators, feeding primarily on krill and forage fish species (Nemoto 1959). Nemoto (1959) analyzed the stomach contents of fin whales caught in the northern Bering Sea (north of 58 °N) in the 1950s and found that the main prey species were capelin (*Mallotus villosus*), juvenile Alaska pollock (*Gadus chalcogrammus*), and Pacific herring (*Clupea pallasii*), while saffron cod (*Eleginus gracilis*) and Arctic krill (*Thysanoessa raschii*) were also common. The stomachs of humpback whales harvested in the North Pacific had very similar contents as fin whales, including krill (*Euphausia pacifica*, *T. inermis*, *T. longipes*, *T. spinifera*), and forage fish species such as capelin, juvenile Alaska pollock, sand lance (*Ammodytes* spp.), and Atka mackerel (*Pleurogrammus monopterygius*) (Nemoto 1959). Since fin and humpback whales pursue pelagic prey, it is likely that both species cue into the presence of currents, temperature gradients, and other oceanographic features that determine the distribution and presence of their prey. What features, then, make for good feeding opportunities for these whales in the Chukchi Sea?

1.3 What conditions are favorable for subarctic baleen whales in the Pacific Arctic?

The northern Bering and Chukchi seas are productive, shallow continental shelf seas (Grebmeier et al. 2006) that are influenced by seasonal ice cover (Stabeno et al. 2012; Hermann et al. 2016) and the inflow of Pacific water which enters through the narrow Bering Strait (Fig. 1.3; Woodgate et al. 2005). The southern Chukchi Sea is an advective system whose productivity is shaped by the seasonal presence of distinct water masses, or currents. These water masses deliver nutrients, phytoplankton, and zooplankton to the Chukchi Sea and are defined by their temperature and salinity properties (Coachman et al. 1975). The water masses also have varying levels of nutrients, which determine the community composition of the phytoplankton and

zooplankton found within them (Hopcroft et al. 2010; Eisner et al. 2013; Pisareva et al. 2015; Danielson et al. 2017; Pinchuk and Eisner, 2017; Sigler et al. 2017). Three water masses dominate in the north Bering Sea and southern Chukchi Sea: the Anadyr Water which is cold, saline, and nutrient-rich, and flows on the western side of the region; the Alaskan Coastal Water which is warm, fresh, and nutrient-poor, and flows on the eastern side of the region; and the Bering Shelf Water which is cold and less salty than the Anadyr Water, and flows through the central north Bering Sea (Fig. 1.3; Coachman et al. 1975). Spatial and temporal variability in the distribution of zooplankton is determined by the distribution of the various water masses (Danielson et al. 2017) as well as rates of transport through the Bering Strait (Spear et al. 2019), which in turn, affects the distribution of forage fishes (Eisner et al. 2013; De Robertis et al. 2017; Sigler et al. 2017).

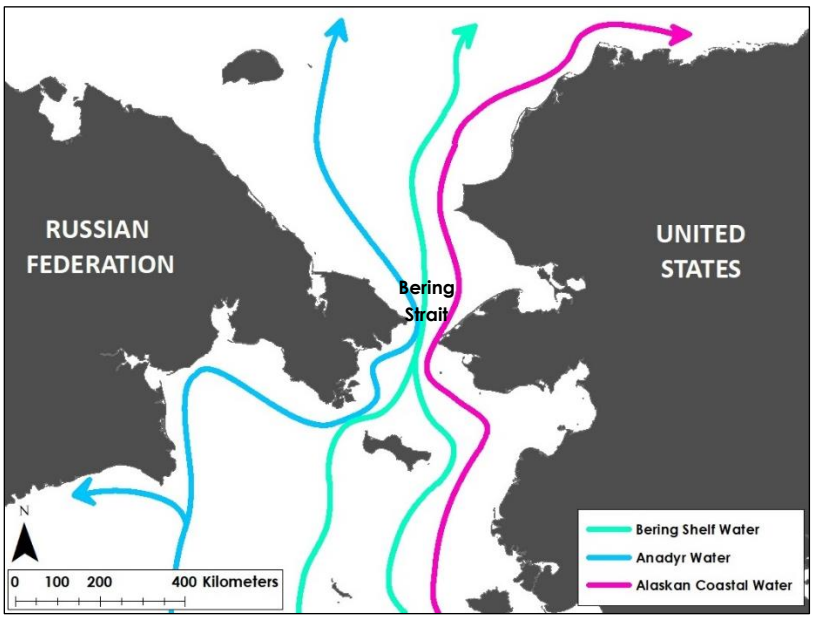

Fig. 1.3. Map of the typical annual mean flow patterns of the three dominant water masses in the Bering Strait region.

Pelagic fish species such as Arctic cod (*Boreogadus saida*), Pacific herring, capelin, and sand lance feed on pelagic zooplankton such as *Calanus* spp. copepods and euphausiids, linking

their distributions to that of their zooplankton prey. Additionally, many of these species are sensitive to specific ranges of water temperatures (Andrews et al. 2016; De Robertis et al. 2017). Arctic cod and capelin are typically found in colder temperatures, while herring are found in warmer waters (Andrews et al. 2016; De Robertis et al. 2017). Both the population dynamics and dispersal of pelagic fish are coupled to variation in environmental conditions (De Robertis et al. 2017). Fin and humpback whales likely maximize feeding success by targeting areas that are important to their prey, such as spawning locations, and/or oceanographic features that accrue prey.

An important mesoscale oceanographic feature that aggregates prey are fronts (Scales et al. 2014). Fronts in the Bering Sea form important feeding habitats for seabirds and marine mammals alike (Schneider et al. 1987; Springer et al. 1996), however less research has been conducted on the importance of fronts as feeding habitat in the north Bering (Russel et al. 1993) and Chukchi seas (Moore et al. 1995; Highsmith et al. 2006; Bluhm et al. 2007). Average flow in the southeast Bering Sea is northward, creating a network of fronts that stretches from the Bering Sea, through the Anadyr Strait west of St. Lawrence Island, continuing through the Bering Strait and into the Chukchi Sea (Fig. 1.4; Belkin and Cornillon 2003). A front created by the confluence of warm and cold-water masses regularly forms north of the Bering Strait in summer, attracting feeding fin, humpback, and gray whales (Bluhm et al. 2007; Clarke et al. 2013; Clarke et al. 2016; Brower et al. 2018; Moore et al. 2022). The location and intensity of fronts created by the water masses of the Chukchi Sea are likely important factors that drive patterns in subarctic baleen whale occurrence.

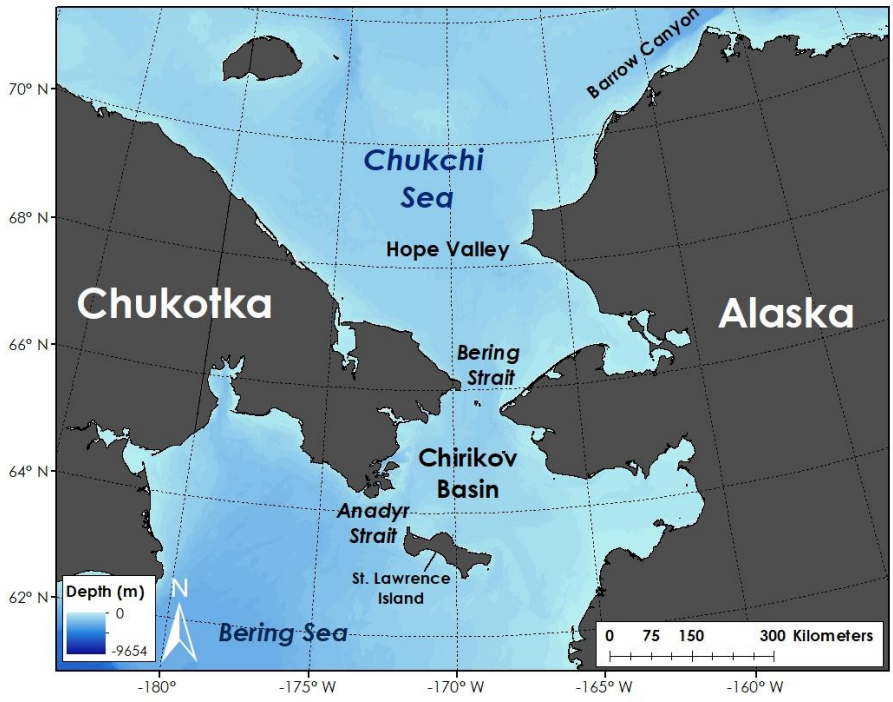

Fig. 1.4. Map of the Pacific Arctic with key locations labeled. Bathymetry data were taken from the Alaska Region Digital Elevation Model *v.* 2 (ARDEM; http://research.cfos.uaf.edu/bathy/).

The spatial distribution of benthic communities is similarly shaped by the presence of water masses as well as sediment properties (Grebmeier et al. 1989; Feder et al. 2005, 2007; Denishenko et al. 2015). Nutrient deposition is controlled by currents, which in turn are affected by bathymetry (Pisareva et al. 2015) and the position of the ice edge (Denishenko 2002). Water speed also affects sediment grain size; areas with fast water speeds have coarser, more gravel-like sediments, while areas with slower water speeds have softer, more muddy sediments. Sediment grain size impacts biodiversity in benthic communities and determines species dominance (Grebmeier et al. 2006). Infaunal amphipods, such as *Ampelisca macrocephala*, require soft sediments (Highsmith et al. 2006), therefore areas with slower water speeds and softer sediments are likely important feeding areas for gray whales in the Chukchi Sea.

Gray whales are known to feed on a wide variety of benthic invertebrates (reviewed in Nerini 1984) in addition to ampeliscid amphipods. Although their primary form of feeding is

through suction of benthic sediments, gray whales have also been observed skim-feeding at the surface for pelagic zooplankton (Moore et al. 2022). Gray whales likely rely on fronts to aggregate such pelagic prey (Bluhm et al. 2007). Once they discover a good prey patch, gray whales exhibit high fidelity to a region, traveling less than a kilometer in a day (Heide-Jørgensen et al. 2012). Foraging hotspots for gray whales in the Pacific Arctic (Fig. 1.4) include the northeastern Chukchi Sea (Clarke et al. 1989; Brower et al. 2017), the northern coast of Chukotka (Berzin 1984; Heide-Jørgensen et al. 2012), the mouth of Barrow Canyon (Kuletz et al. 2015), the Chirikov Basin north of St. Lawrence Island (Moore et al. 2003), and the Hope Valley in the central and southern Chukchi Sea (Berzin 1984; Moore et al. 2000; Clarke and Moore 2002; Moore et al. 2003; Bluhm et al. 2007). These hotspots have remained relatively consistent over the past decades, except for the Chirikov Basin.

In the 1980s and early 1990s, gray whales were commonly observed feeding in the Chirikov Basin (Moore et al. 2003). By the late 1990s, however, the Chirikov Basin could no longer support the entire gray whale population, resulting in an unusual mortality event (UME) in 1999–2000 (Moore et al. 2003). Possible causes for the collapse include diminished amphipod abundance due to overgrazing gray whales (Highsmith and Coyle 1991, 1994), changes in nutrient deposition (Coyle et al. 2007), and the prevalence of coarser sediment in the basin due to faster current speeds, leading to a reduction in the abundance of tube-building ampeliscid amphipods (Moore et al. 2003). The gray whale UME of 1999–2000 alerted researchers to the presence of changing conditions in the Pacific Arctic as well as the sensitivity of gray whales to changes in their benthic prey, making gray whales an important sentinel species (Moore 2008).

1.4 How is the Pacific Arctic changing?

Increased sightings of fin and humpback whales in the Chukchi Sea in recent years (Brower et al. 2018) suggest that these two species are reclaiming portions of their previous range as their populations recover to pre-whaling levels (Zerbini et al. 2006; Clarke et al. 2013). Alternatively, and perhaps concurrently, recent environmental shifts could have led to more favorable conditions in the Chukchi Sea for the two species (Clarke et al. 2013). If the latter is true, it is important to understand the nature of these environmental shifts and how they could in turn impact Arctic marine mammals. More subarctic cetaceans in the area along with longer ice-free seasons could lead to temporal and spatial range overlap with Arctic marine mammals, potentially resulting in increased competition for resources (Laidre and Heide-Jørgensen 2012; Clarke et al. 2013). Additionally, when considering direct anthropogenic impacts on marine mammals in the Alaskan Arctic such as shipping, subarctic cetaceans as a group are often overlooked.

Environmental changes such as increased water speeds through the Strait (Woodgate et al. 2012), warmer annual temperatures (Danielson et al. 2020), increased primary production (Arrigo and van Dijken 2015), and declines in sea ice cover during the spring and fall (Serreze et al. 2016) are transforming the Pacific Arctic. Coincident with these environmental shifts is a dramatic increase in the number of ships passing through the Bering Strait (Huntington et al. 2015). Increased global shipping has contributed to a ~ 10 dB increase in sound levels in lower frequency bands used by fin whales (< 80 Hz; Andrew et al. 2002; McDonald et al. 2006). In addition, ship noise masks important biological signals (Clark et al. 2009; Pine et al. 2018), increases stress hormone levels (Rolland et al. 2012), provokes avoidance behavior (Nowacek et al. 2007; Southall et al. 2007), and promotes vocal behavior changes in baleen whales (Parks et al. 2011; Dunlop et al. 2014). Consequently, understanding how elevated ship noise affects the

available acoustic habitat for marine mammals is a research priority (Richardson et al. 1995; Nowacek et al. 2007; Moore et al. 2012; McKenna et al. 2017).

1.5 How do we study whales in the Bering Strait?

Though visual surveys have been conducted in the Chukchi Sea for decades (Clarke et al. 2019), our understanding of the occurrence of fin and humpback whales in the region is still rather limited. Visual surveys are constrained by weather, availability of observation platforms (ships or planes), observer availability, and visibility, among other factors. Additionally, whales only surface for short periods of time, making observing and identifying whales challenging. Passive acoustic monitoring (PAM), on the other hand, has finer scale temporal resolution (minutes to hours), can be deployed and left undisturbed for long stretches of time, and is able to capture the presence of species during inclement weather, when the seas are ice-covered, and during the night (Mellinger et al. 2007).

Light quickly attenuates in water whereas sound can travel over great distances. Therefore, marine mammals rely primarily on hearing to navigate their world. Baleen whales use sound to orient themselves in their habitat (George et al. 1989), find mates (Darling and Bérubé 2001; Croll et al. 2002), avoid predators (Cummings and Thompson 1971), and keep in contact with each other (Payne and Webb 1971). Each species produces unique vocalizations, allowing researchers to identify species using differences in frequency, duration, and amplitude patterning in the vocalizations. The ability to identify baleen whales using their calls and songs enables researchers to study behavior, occurrence over time, and abundance (Mellinger et al. 2007). The main limitation to PAM, however, is that an individual must be calling to be detected. Also, in some species, such as fin and humpback whales, only males produce songs in addition to other vocalizations (Payne and McVay 197; Darling and Bérubé 2001; Croll et al. 2002).

Consequently, passive acoustic studies are often biased towards the detection of only a portion of the population, and we cannot assume absence of a species based on acoustic data alone.

The use of passive acoustic surveys in the Bering and Chukchi seas has greatly improved our knowledge of the occurrence of visually cryptic and rare species such as North Pacific right whales (*Eubalaena japonica*; Wright et al. 2019), as well as more common but dispersed species, such as fin and humpback whales. Recent passive acoustic surveys in the Pacific Arctic reveal an interannual pattern in the presence of both fin and humpback whales. Delarue et al. (2013) noted low fin whale detections in the northeast Chukchi Sea in 2009 and 2010, while more fin whales were heard in 2007. Woodgate et al. (2015) observed fin whale calls in the southern Chukchi Sea throughout 2009 with a peak in detections in 2012. Woodgate et al. (2015) also recorded more humpback whale calls in 2009 and 2012 than in 2010 and 2011. Environmental variability likely explains the observed patterns of interannual variability of the two species (Delarue et al. 2013), however the connection between the presence of these species and environmental conditions has yet to be explored. Investigating possible explanations for previously observed interannual variability in the presence of fin and humpback whales, as well as identifying any similar patterns for gray whales, formed the main motivation for this dissertation.

1.6 Dissertation Overview

The primary goal of this dissertation is to document and investigate patterns in the acoustic presence of subarctic baleen whales in the Bering Strait, including identifying migration timing and environmental factors that influence their presence in the region. This work began with the mystery of why calling fin whales are abundant in some years and not in others during the open-water season in the Chukchi Sea. Chapter 2 seeks to uncover the answer to this mystery, comparing environmental conditions in years with high abundance of calling whales to those of

years with low abundance. Chapter 3 expands on this effort to include humpback and gray whales in addition to examining the migration timing of all three species in relation to environmental conditions, and exploring potential drivers of whale presence. Finally, Chapter 4 examines the impact of ship noise on ambient sound levels for the open-water season with a focus on the Bering Strait region.

In Chapter 2, published in *Deep Sea Research Part II* (Escajeda et al. 2020), my coauthors and I use acoustic recordings from three moored hydrophones in the Bering Strait region from 2009–2015 to identify fin whale calls during the open-water season (July–November) and investigate the potential influence of local environmental conditions on the interannual variability in fin whale presence. We examined near-surface and near-bottom temperatures (T) and salinities (S), wind and water velocities through the strait, water mass presence as estimated using published T/S boundaries, and satellite-derived sea surface temperatures and sea-ice concentrations. Our results show significant interannual variability in the acoustic presence of fin whales with the greatest detections of calls in years with contrasting environmental conditions (2012 and 2015). Colder temperatures, lower salinities, slower water velocities, and weak southward winds prevailed in 2012 while warmer temperatures, higher salinities, faster water velocities, and moderate southward winds prevailed in 2015. Most detections (96%) were recorded at the mooring site nearest the confluence of the nutrient-rich Anadyr and Bering Shelf water masses, Site A3, indicating that productive water masses may influence the occurrence of fin whales. The disparity in environmental conditions between 2012 and 2015 suggests there may be multiple environmental factors or other unexamined variables working in combination that draw fin whales into the Pacific Arctic. The lack of a distinct connection between fin whales and environmental conditions motivated me to examine other

factors beyond the Bering Strait region that could impact fin whale presence. Exploring the connection between subarctic whale presence and environmental conditions in the Pacific Arctic and beyond formed the foundation of Chapter 3.

In Chapter 3 (*manuscript in preparation*), I added two years of acoustic and environment data (2017 and 2018) to the acoustic dataset from Chapter 2, expanding the study period to 2009–2018. Focusing on data from Site A3, I identified fin, humpback, and gray whale calls during the open-water season (May–December), examined migration timing, and tested for potential environmental drivers of whale presence. The acoustic presence of fin and humpback whales varied across the years, with most recordings with calls observed in the late fall months (October through November). We observed the highest proportion of recordings with humpback whale calls for the peak months of October–November in 2009, 2017, and 2012 (66–80% of recordings had humpback whale calls), and the highest proportion of recordings with fin whale calls for October–November in 2015, 2017, and 2018 (75–79% of recordings). We observed the highest proportion of recordings with gray whale calls for October–November in 2013 and 2015 (46 and 51% of recordings, respectively). Fin whales departed the Bering Strait ~ 3 days later per year over the duration of the study ($p = 0.02$). Significant positive correlations between fall water temperatures (all Pearson $r \geq 0.71$, $p < 0.03$) and departure dates for fin and humpback whales suggest that warmer water temperatures may allow both species to delay their southward migrations. Individual models for each species identified day of the year, water temperatures, and the presence of a thermal front in the previous month as factors that influence the acoustic presence of all three species during the open-water season.

In Chapter 4, published in *Marine Pollution Bulletin* (Escajeda et al. 2023), my coauthors and I characterized ship activity in the Bering Strait during the open-water season (July–

November) for 2013–2015 and quantified the impact of ship noise on third-octave sound levels (TOLs) for frequency bands used by baleen whales (25–1000 Hz). Peak ship activity occurred in July–September with the greatest overlap in ship noise and whale vocalizations observed in October. Ships elevated sound levels by ~ 4 dB on average for all TOL bands combined, and 250-Hz TOLs exceeding 100 dB re 1 µPa were recorded from two large vessels over 11 km away from the hydrophones. Our results show that ship noise has the potential to impact baleen whales in the Bering Strait and serve as a baseline for measuring future changes in ship activity in the region.

Overall, the results presented within this dissertation provide a snapshot of the presence of subarctic baleen whales in the Bering Strait during a time of change in the Pacific Arctic. It is clear from this work that fin, humpback, and gray whales are important components of the summer marine ecosystem of the Chukchi Sea. Continued study of their presence in the region will be important for tracking changes in the Chukchi Sea. Additionally, the results presented in this dissertation serve as a baseline for measuring future changes to the marine soundscape of the Bering Strait as shipping and other anthropogenic activities continue to transform the Arctic.

1.7 References

Ahonen H, Stafford KM, de Steur L, et al (2017) The underwater soundscape in western Fram Strait: Breeding ground of Spitsbergen's endangered bowhead whales. Marine Pollution Bulletin 123:97–112. https://doi.org/10.1016/j.marpolbul.2017.09.019

Andrew RK, Howe BM, Mercer JA, Dzieciuch MA (2002) Ocean ambient sound: Comparing the 1960s with the 1990s for a receiver off the California coast. Acoustics Research Letters Online 3:65–70. https://doi.org/10.1121/1.1461915

Andrews AG, Strasburger WW, Farley EV, et al (2016) Effects of warm and cold climate conditions on capelin (*Mallotus villosus*) and Pacific herring (*Clupea pallasii*) in the eastern Bering Sea. Deep Sea Research Part II: Topical Studies in Oceanography 134:235–246. https://doi.org/10.1016/j.dsr2.2015.10.008

Arrigo KR, Perovich DK, Pickart RS, et al (2014) Phytoplankton blooms beneath the sea ice in the Chukchi Sea. Deep Sea Research Part II: Topical Studies in Oceanography 105:1–16. https://doi.org/10.1016/j.dsr2.2014.03.018

Arrigo KR, van Dijken GL (2015) Continued increases in Arctic Ocean primary production. Progress in Oceanography 136:60–70. https://doi.org/10.1016/j.pocean.2015.05.002

Baker CS, Palumbi SR, Lambertsen RH, et al (1990) Influence of seasonal migration on geographic distribution of mitochondrial DNA haplotypes in humpback whales. Nature 344:238–240. https://doi.org/10.1038/344238a0

Barendse J, Best PB, Carvalho I, Pomilla C (2013) Mother knows best: Occurrence and associations of resighted humpback whales suggest maternally derived fidelity to a southern hemisphere coastal feeding ground. PLoS ONE 8:e81238. https://doi.org/10.1371/journal.pone.0081238

Belkin I, Cornillon P (2003) SST fronts of the Pacific coastal and marginal seas. Pacific Oceanography 1:90–113

Berzin AA (1984) Soviet studies on the distribution and numbers of the gray whale in the Bering and Chukchi seas from 1968 to 1982. In: Jones ML, Swartz SL, Leatherwood S (eds) The Gray Whale: *Eschrichtius robustus*. Academic Press, Massachusetts, pp 409–419

Bingman VP, Cheng K (2005) Mechanisms of animal global navigation: comparative perspectives and enduring challenges. Ethology Ecology & Evolution 17:295–318. https://doi.org/10.1080/08927014.2005.9522584

Bluhm BA, Coyle KO, Konar B, Highsmith R (2007) High gray whale relative abundances associated with an oceanographic front in the south-central Chukchi Sea. Deep Sea Research Part II: Topical Studies in Oceanography 54:2919–2933. https://doi.org/10.1016/j.dsr2.2007.08.015

Brower AA, Ferguson MC, Schonberg SV, et al (2017) Gray whale distribution relative to benthic invertebrate biomass and abundance: Northeastern Chukchi Sea 2009–2012. Deep Sea Research Part II: Topical Studies in Oceanography 144:156–174. https://doi.org/10.1016/j.dsr2.2016.12.007

Brower AA, Clarke JT, Ferguson MC (2018) Increased sightings of subArctic cetaceans in the eastern Chukchi Sea, 2008–2016: population recovery, response to climate change, or increased survey effort? Polar Biology 41:1033–1039. https://doi.org/10.1007/s00300-018-2257-x

Calambokidis J, Steiger GH, Straley JM, et al (2001) Movements and population structure of humpback whales in the North Pacific. Marine Mammal Science 17:769–794. https://doi.org/10.1111/j.1748-7692.2001.tb01298.x

Cavalieri DJ, Parkinson CL (2012) Arctic sea ice variability and trends, 1979-2010. The Cryosphere 6:881–889. https://doi.org/10.5194/tc-6-881-2012

Citta JJ, Breed GA, Okkonen SR, et al (2023) Shifts in bowhead whale distribution, behavior, and condition following rapid sea ice change in the Bering Sea. Continental Shelf Research 256:104959. https://doi.org/10.1016/j.csr.2023.104959

Clapham PJ, Seipt IE (1991)f Resightings of independent fin whales, *Balaenoptera physalus*, on maternal summer ranges. Journal of Mammalogy 72(4):788–790. https://doi.org/10.2307/1381844.

Clark C, Ellison W, Southall B, et al (2009) Acoustic masking in marine ecosystems: intuitions, analysis, and implication. Marine Ecology Progress Series 395:201–222. https://doi.org/10.3354/meps08402

Clarke JT, Moore SE, Ljungblad DK (1989) Observations on gray whale (*Eschrichtius robustus*) utilization patterns in the northeastern Chukchi Sea, July-October 1982-1987. Canadian Journal of Zoology 67:2646–2654

Clarke J, Moore S (2002) A note on observations of gray whales in the southern Chukchi and northern Bering Seas, August-November, 1980-89. Journal of Cetacean Research and Management 4:283–288

Clarke J, Stafford K, Moore S, et al (2013) Subarctic cetaceans in the southern Chukchi Sea: Evidence of recovery or response to a changing ecosystem. Oceanography 26:136–149. https://doi.org/10.5670/oceanog.2013.81

Clarke JT, Kennedy AS, Ferguson MC (2016) Bowhead and gray whale distributions, sighting rates, and habitat associations in the Eastern Chukchi Sea, summer and fall 2009–15, with a retrospective comparison to 1982–91. Arctic 69:359. https://doi.org/10.14430/arctic4597

Clarke JT, Brower AA, Ferguson MC, et al (2019) Distribution and relative abundance of marine mammals in the Eastern Chukchi Sea, Eastern and Western Beaufort Sea, and Amundsen Gulf, 2019. Marine Mammal Laboratory, Alaska Fisheries Science Center, NMFS, NOAA, Seattle, WA

Coachman LK, Aagaard K, Tripp RB (1975) Bering Strait: The regional physical oceanography. University of Washington Press, Seattle, WA

Comiso JC, Parkinson CL, Gersten R, Stock L (2008) Accelerated decline in the Arctic sea ice cover. Geophysical Research Letters 35:L01703. https://doi.org/10.1029/2007GL031972

Coyle KO, Highsmith RC (1994) Benthic amphipod community in the northern Bering Sea: Analysis of potential structuring mechanisms. Marine Ecology Progress Series 107:233–244

Coyle KO, Bluhm B, Konar B, et al (2007) Amphipod prey of gray whales in the northern Bering Sea: Comparison of biomass and distribution between the 1980s and 2002–2003. Deep Sea Research Part II: Topical Studies in Oceanography 54:2906–2918. https://doi.org/10.1016/j.dsr2.2007.08.026

Croll DA, Clark CW, Acevedo A, et al (2002) Only male fin whales sing loud songs. Nature 417:809

Cummings W, Thompson P (1971) Gray whales, *Eschrichtius robustus*, avoid the underwater sounds of killer whales, *Orcinus orca*. Fishery Bulletin 69:525–530

Danielson SL, Eisner L, Ladd C, et al (2017) A comparison between late summer 2012 and 2013 water masses, macronutrients, and phytoplankton standing crops in the northern Bering and Chukchi Seas. Deep Sea Research Part II: Topical Studies in Oceanography 135:7–26. https://doi.org/10.1016/j.dsr2.2016.05.024

Danielson SL, Ahkinga O, Ashjian C, et al (2020) Manifestation and consequences of warming and altered heat fluxes over the Bering and Chukchi Sea continental shelves. Deep Sea Research Part II: Topical Studies in Oceanography 177:104781. https://doi.org/10.1016/j.dsr2.2020.104781

Darling JD, Bérubé M (2001) Interactions of singing humpback whales with other males. Marine Mammal Science 17:570–584. https://doi.org/10.1111/j.1748-7692.2001.tb01005.x

De Robertis A, Taylor K, Wilson CD, Farley EV (2017) Abundance and distribution of Arctic cod (*Boreogadus saida*) and other pelagic fishes over the U.S. Continental Shelf of the Northern Bering and Chukchi Seas. Deep Sea Research Part II: Topical Studies in Oceanography 135:51–65. https://doi.org/10.1016/j.dsr2.2016.03.002

Delarue J, Martin B, Hannay D, Berchok CL (2013) Acoustic occurrence and affiliation of fin whales detected in the northeastern Chukchi Sea, July to October 2007–10. Arctic 66:159–172

Denisenko SG (2002) Zoobenthos and ice distribution in the Arctic seas. Proceedings of the Zoological Institute 296:39–46

Denisenko S, Grebmeier J, Cooper L (2015) Assessing bioresources and standing stock of zoobenthos (key species, high taxa, trophic groups) in the Chukchi Sea. Oceanography 28:146–157. https://doi.org/10.5670/oceanog.2015.63

Druckenmiller ML, Thoman RL, Moon TA (2022) NOAA Arctic Report Card 2022: Executive Summary. https://doi.org/10.25923/YJX6-R184

Dunlop RA, Cato DH, Noad MJ (2014) Evidence of a Lombard response in migrating humpback whales (*Megaptera novaeangliae*). The Journal of the Acoustical Society of America 136:430–437. https://doi.org/10.1121/1.4883598

Eguíluz VM, Fernández-Gracia J, Irigoien X, Duarte CM (2016) A quantitative assessment of Arctic shipping in 2010–2014. Sci Rep 6:30682. https://doi.org/10.1038/srep30682

Eisner L, Hillgruber N, Martinson E, Maselko J (2013) Pelagic fish and zooplankton species assemblages in relation to water mass characteristics in the northern Bering and southeast Chukchi seas. Polar Biology 36:87–113. https://doi.org/10.1007/s00300-012-1241-0

Escajeda E, Stafford KM, Woodgate RA, Laidre KL (2020) Variability in fin whale (*Balaenoptera physalus*) occurrence in the Bering Strait and southern Chukchi Sea in relation to environmental factors. Deep Sea Research Part II: Topical Studies in Oceanography 177:104782. https://doi.org/10.1016/j.dsr2.2020.104782

Escajeda ED, Stafford KM, Woodgate RA, Laidre KL (2023) Quantifying the effect of ship noise on the acoustic environment of the Bering Strait. Marine Pollution Bulletin 187:114557. https://doi.org/10.1016/j.marpolbul.2022.114557

Feder HM, Jewett SC, Blanchard A (2005) Southeastern Chukchi Sea (Alaska) epibenthos. Polar Biology 28:402–421. https://doi.org/10.1007/s00300-004-0683-4

Feder HM, Jewett SC, Blanchard AL (2007) Southeastern Chukchi Sea (Alaska) macrobenthos. Polar Biology 30:261–275. https://doi.org/10.1007/s00300-006-0180-z

Filatova OA, Fedutin ID, Pridorozhnaya TP, Hoyt E (2022) Bottom-feeding gray whales *Eschrichtius robustus* demonstrate a finer scale of site fidelity than pelagic-feeding humpback whales *Megaptera novaeangliae* on an Arctic feeding ground. Polar Biology 45:1013–1021. https://doi.org/10.1007/s00300-022-03048-x

George JC, Clark C, Carroll GM, Ellison WT (1989) Observations on the ice-breaking and ice navigation behavior of migrating bowhead whales (*Balaena mysticetus*) near Point Barrow, Alaska, spring 1985. Arctic 42:24–30. https://doi.org/10.14430/arctic1636

Goldbogen JA, Calambokidis J, Oleson E, et al (2011) Mechanics, hydrodynamics and energetics of blue whale lunge feeding: efficiency dependence on krill density. Journal of Experimental Biology 214:131–146. https://doi.org/10.1242/jeb.048157

Grebmeier JM, Feder HM, McRoy CP (1989) Pelagic-benthic coupling on the shelf of the northern Bering and Chukchi Seas. III. Benthic food supply and carbon cycling. Marine Ecology Progress Series 51:253–268

Grebmeier JM, Cooper LW, Feder HM, Sirenko BI (2006) Ecosystem dynamics of the Pacific-influenced Northern Bering and Chukchi Seas in the Amerasian Arctic. Progress in Oceanography 71:331–361. https://doi.org/10.1016/j.pocean.2006.10.001

Grebmeier JM (2012) Shifting patterns of life in the Pacific Arctic and Sub-Arctic seas. Annual Review of Marine Science 4:63–78. https://doi.org/10.1146/annurev-marine-120710-100926

Grebmeier JM, Bluhm BA, Cooper LW, et al (2015) Time-series benthic community composition and biomass and associated environmental characteristics in the Chukchi Sea during the RUSALCA 2004–2012 program. Oceanography 28:116–133

Halliday WD, Insley SJ, Hilliard RC, et al (2017) Potential impacts of shipping noise on marine mammals in the western Canadian Arctic. Marine Pollution Bulletin 123:73–82. https://doi.org/10.1016/j.marpolbul.2017.09.027

Heide-Jørgensen MP, Laidre KL, Litovka D, et al (2012) Identifying gray whale (*Eschrichtius robustus*) foraging grounds along the Chukotka Peninsula, Russia, using satellite telemetry. Polar Biology 35:1035–1045. https://doi.org/10.1007/s00300-011-1151-6

Hermann AJ, Gibson GA, Bond NA, et al (2016) Projected future biophysical states of the Bering Sea. Deep Sea Research Part II: Topical Studies in Oceanography 134:30–47. https://doi.org/10.1016/j.dsr2.2015.11.001

Highsmith RC, Coyle KO (1991) Amphipod life histories: community structure, impact of temperature on decoupled growth and maturation rates, productivity, and P:B ratios. American Zoologist 31:861–873

Highsmith RC, Coyle KO, Bluhm BA, Konar B (2006) Gray whales in the Bering and Chukchi seas. In: Estes JA, DeMaster DP, Doak DF, et al. (eds) Whales, whaling, and ocean ecosystems. University of California Press, Berkeley, pp 303–313

Hopcroft RR, Kosobokova KN, Pinchuk AI (2010) Zooplankton community patterns in the Chukchi Sea during summer 2004. Deep Sea Research Part II: Topical Studies in Oceanography 57:27–39. https://doi.org/10.1016/j.dsr2.2009.08.003

Horton TW, Hauser N, Zerbini AN, et al (2017) Route fidelity during marine megafauna migration. Frontiers in Marine Science 4:422. https://doi.org/10.3389/fmars.2017.00422

Horton TW, Palacios DM, Stafford KM, Zerbini AN (2022) Baleen whale migration. In: Clark CW, Garland EC (eds) Ethology and Behavioral Ecology of Mysticetes. Springer International Publishing, Cham, pp 71–104

Hunt GL, Stabeno P, Walters G, et al (2002) Climate change and control of the southeastern Bering Sea pelagic ecosystem. Deep Sea Research Part II: Topical Studies in Oceanography 49:5821–5853. https://doi.org/10.1016/S0967-0645(02)00321-1

Huntington HP, Daniel R, Hartsig A, et al (2015) Vessels, risks, and rules: Planning for safe shipping in Bering Strait. Marine Policy 51:119–127. https://doi.org/10.1016/j.marpol.2014.07.027

Ingman K, Hines E, Mazzini PLF, et al (2021) Modeling changes in baleen whale seasonal abundance, timing of migration, and environmental variables to explain the sudden rise in entanglements in California. PLoS ONE 16:e0248557. https://doi.org/10.1371/journal.pone.0248557

Insley SJ, Halliday WD, De Jong T (2017) Seasonal patterns in ocean ambient noise near Sachs Harbour, Northwest Territories. Arctic 70:239. https://doi.org/10.14430/arctic4662

Kenney R, Mayo C, Winn H (2001) Migration and foraging strategies at varying spatial scales in western North Atlantic right whales: A review of hypotheses. Journal of Cetacean Research and Management 2:251–260

Kikuchi G, Abe H, Hirawake T, Sampei M (2020) Distinctive spring phytoplankton bloom in the Bering Strait in 2018: A year of historically minimum sea ice extent. Deep Sea Research Part II: Topical Studies in Oceanography 181–182:104905. https://doi.org/10.1016/j.dsr2.2020.104905

Kirschvink JL, Dizon AE, Westphal JA (1986) Evidence from strandings for geomagnetic sensitivity in cetaceans. Journal of Experimental Biology 120:1–24. https://doi.org/10.1242/jeb.120.1.1

Kovacs KM, Lydersen C, Overland JE, Moore SE (2011) Impacts of changing sea-ice conditions on Arctic marine mammals. Marine Biodiversity 41:181–194. https://doi.org/10.1007/s12526-010-0061-0

Kuletz KJ, Ferguson MC, Hurley B, et al (2015) Seasonal spatial patterns in seabird and marine mammal distribution in the eastern Chukchi and western Beaufort seas: Identifying biologically important pelagic areas. Progress in Oceanography 136:175–200. https://doi.org/10.1016/j.pocean.2015.05.012

Laidre KL, Heide-Jørgensen MP (2012) Spring partitioning of Disko Bay, West Greenland, by Arctic and Subarctic baleen whales. ICES Journal of Marine Science 69:1226–1233. https://doi.org/10.1093/icesjms/fss095

Laidre KL, Stern H, Kovacs KM, et al (2015) Arctic marine mammal population status, sea ice habitat loss, and conservation recommendations for the 21st century. Conservation Biology 29:724–737. https://doi.org/10.1111/cobi.12474

MacLeod C (2009) Global climate change, range changes and potential implications for the conservation of marine cetaceans: a review and synthesis. Endangered Species Research 7:125–136. https://doi.org/10.3354/esr00197

Markus T, Stroeve JC, Miller J (2009) Recent changes in Arctic sea ice melt onset, freezeup, and melt season length. Journal of Geophysical Research 114:C12024. https://doi.org/10.1029/2009JC005436

Mate BR, Ilyashenko VY, Bradford AL, et al (2015) Critically endangered western gray whales migrate to the eastern North Pacific. Biology Letters 11:20150071. https://doi.org/10.1098/rsbl.2015.0071

McDonald MA, Hildebrand JA, Wiggins SM (2006) Increases in deep ocean ambient noise in the Northeast Pacific west of San Nicolas Island, California. The Journal of the Acoustical Society of America 120:711–718. https://doi.org/10.1121/1.2216565

McKenna MF, Gabriele C, Kipple B (2017) Effects of marine vessel management on the underwater acoustic environment of Glacier Bay National Park, AK. Ocean & Coastal Management 139:102–112. https://doi.org/10.1016/j.ocecoaman.2017.01.015

Mellinger D, Stafford K, Moore S, et al (2007) An overview of fixed passive acoustic observation methods for cetaceans. Oceanography 20:36–45. https://doi.org/10.5670/oceanog.2007.03

Merchant ND, Pirotta E, Barton TR, Thompson PM (2014) Monitoring ship noise to assess the impact of coastal developments on marine mammals. Marine Pollution Bulletin 78:85–95. https://doi.org/10.1016/j.marpolbul.2013.10.058

Mizroch SA, Rice DW, Zwiefelhofer D, et al (2009) Distribution and movements of fin whales in the North Pacific Ocean. Mammal Review 39:193–227. https://doi.org/10.1111/j.1365-2907.2009.00147.x

Moore SE, George JC, Coyle KO, Weingartner TJ (1995) Bowhead whales along the Chukotka Coast in autumn. Arctic 48:155–160

Moore SE (2000) Variability of cetacean distribution and habitat selection in the Alaskan Arctic, Autumn 1982–91. Arctic 53:448–460

Moore SE, deMaster DP, Dayton PK (2000) Cetacean habitat selection in the Alaskan Arctic during summer and autumn. Arctic 53:432–447

Moore SE, Grebmeier JM, Davies JR (2003) Gray whale distribution relative to forage habitat in the northern Bering Sea: Current conditions and retrospective summary. Canadian Journal of Zoology 81:734–742. https://doi.org/10.1139/z03-043

Moore SE (2008) Marine mammals as ecosystem sentinels. Journal of Mammalogy 89:534–540

Moore SE, Reeves RR, Southall BL, et al (2012) A new framework for assessing the effects of anthropogenic sound on marine mammals in a rapidly changing Arctic. BioScience 62:289–295. https://doi.org/10.1525/bio.2012.62.3.10

Moore SE (2016) Is it 'boom times' for baleen whales in the Pacific Arctic region? Biology Letters 12:20160251. https://doi.org/10.1098/rsbl.2016.0251

Moore SE, Clarke JT, Okkonen SR, et al (2022) Changes in gray whale phenology and distribution related to prey variability and ocean biophysics in the northern Bering and eastern Chukchi seas. PLoS ONE 17:e0265934. https://doi.org/10.1371/journal.pone.0265934

Nemoto T (1959) Food of baleen whales with reference to whale movements. Scientific Report of the Whales Research Institute 14:149–290

Nerini M (1984) A review of gray whale feeding ecology. In: Jones ML, Swartz SL, Leatherwood S (eds) The Gray Whale *Eschrichtius Robustus*. Academic Press, Florida, pp 423–450

Nowacek DP, Thorne LH, Johnston DW, Tyack PL (2007) Responses of cetaceans to anthropogenic noise. Mammal Review 37:81–115. https://doi.org/10.1111/j.1365-2907.2007.00104.x

Parks SE, Johnson M, Nowacek D, Tyack PL (2011) Individual right whales call louder in increased environmental noise. Biology Letters 7:33–35. https://doi.org/10.1098/rsbl.2010.0451

Parmesan C (2006) Ecological and evolutionary responses to recent climate change. Annual Review of Ecology, Evolution, and Systematics 37:637–669. https://doi.org/10.1146/annurev.ecolsys.37.091305.110100

Payne RS, McVay S (1971) Songs of humpback whales. Science 173:585–597. https://doi.org/10.1126/science.173.3997.585

Perryman WL, Donahue MA, Perkins PC, Reilly SB (2002) Gray whale calf production 1994–2000: Are observed fluctuations related to changes in seasonal ice cover? Marine Mammal Science 18:121–144. https://doi.org/10.1111/j.1748-7692.2002.tb01023.x

Piatt JF, Methven DA (1992) Threshold foraging behavior of baleen whales. Marine Ecology Progress Series 84:205–210

Pinchuk AI, Eisner LB (2017) Spatial heterogeneity in zooplankton summer distribution in the eastern Chukchi Sea in 2012–2013 as a result of large-scale interactions of water masses. Deep Sea Research Part II: Topical Studies in Oceanography 135:27–39. https://doi.org/10.1016/j.dsr2.2016.11.003

Pine MK, Hannay DE, Insley SJ, et al (2018) Assessing vessel slowdown for reducing auditory masking for marine mammals and fish of the western Canadian Arctic. Marine Pollution Bulletin 135:290–302. https://doi.org/10.1016/j.marpolbul.2018.07.031

Pisareva M, Pickart R, Iken K, et al (2015) The relationship between patterns of benthic fauna and zooplankton in the Chukchi Sea and physical forcing. Oceanography 28:68–83. https://doi.org/10.5670/oceanog.2015.58

Poloczanska ES, Brown CJ, Sydeman WJ, et al (2013) Global imprint of climate change on marine life. Nature Climate Change 3:919–925. https://doi.org/10.1038/nclimate1958

Ramp C, Delarue J, Palsbøll PJ, et al (2015) Adapting to a warmer ocean—seasonal shift of baleen whale movements over three decades. PLoS ONE 10:e0121374. https://doi.org/10.1371/journal.pone.0121374

Rice DW, Wolman AA (1971) The life history and ecology of the gray whale (*Eschrichtius robustus*). Allen Press, Lawrence, KS

Richardson WJ, Greene, Jr. CR, Malme CI, Thomson DH (1995) Marine mammals and noise. Academic Press, San Diego, California

Rolland RM, Parks SE, Hunt KE, et al (2012) Evidence that ship noise increases stress in right whales. Proceedings of the Royal Society B: Biological Sciences 279:2363–2368. https://doi.org/10.1098/rspb.2011.2429

Russell RW, Harrison NM, Hunt Jr GL (1993) Foraging at a front: Hydrography, zooplankton, and avian planktivory in the northern Bering Sea. Marine Ecology Progress Series 182:77–93

Scales KL, Miller PI, Hawkes LA, et al (2014) On the front line: Frontal zones as priority at-sea conservation areas for mobile marine vertebrates. Journal of Applied Ecology 51:1575–1583. https://doi.org/10.1111/1365-2664.12330

Schneider D, Harrison NM, Hunt GL (1987) Variation in the occurrence of marine birds at fronts in the Bering Sea. Estuarine, Coastal and Shelf Science 25:135–141. https://doi.org/10.1016/0272-7714(87)90031-X

Serreze MC, Crawford AD, Stroeve JC, et al (2016) Variability, trends, and predictability of seasonal sea ice retreat and advance in the Chukchi Sea. Journal of Geophysical Research: Oceans 121:7308–7325. https://doi.org/10.1002/2016JC011977

Sigler MF, Mueter FJ, Bluhm BA, et al (2017) Late summer zoogeography of the northern Bering and Chukchi seas. Deep Sea Research Part II: Topical Studies in Oceanography 135:168–189. https://doi.org/10.1016/j.dsr2.2016.03.005

Southall BL, Bowles AE, Ellison WT, et al (2007) Marine mammal noise exposure criteria: Initial scientific recommendations. Aquatic Mammals 33:411–521. https://doi.org/10.1578/AM.33.4.2007.411

Spear A, Duffy-Anderson J, Kimmel D, et al (2019) Physical and biological drivers of zooplankton communities in the Chukchi Sea. Polar Biology 42:1107–1124. https://doi.org/10.1007/s00300-019-02498-0

Springer AM, McRoy CP, Flint MV (1996) The Bering Sea green belt: Shelf-edge processes and ecosystem production. Fisheries Oceanography 5:205–223. https://doi.org/10.1111/j.1365-2419.1996.tb00118.x

Stabeno PJ, Farley Jr. EV, Kachel NB, et al (2012) A comparison of the physics of the northern and southern shelves of the eastern Bering Sea and some implications for the ecosystem. Deep Sea Research Part II: Topical Studies in Oceanography 65–70:14–30. https://doi.org/10.1016/j.dsr2.2012.02.019

Stabeno PJ, Mordy CW, Sigler MF (2020) Seasonal patterns of near-bottom chlorophyll fluorescence in the eastern Chukchi Sea: 2010–2019. Deep Sea Research Part II: Topical Studies in Oceanography 177:104842. https://doi.org/10.1016/j.dsr2.2020.104842

Stevick PT, Allen J, Clapham PJ, et al (2006) Population spatial structuring on the feeding grounds in North Atlantic humpback whales (*Megaptera novaeangliae*). Journal of Zoology 270:244–255. https://doi.org/10.1111/j.1469-7998.2006.00128.x

Szesciorka AR, Ballance LT, Širović A, et al (2020) Timing is everything: Drivers of interannual variability in blue whale migration. Sci Rep 10:7710. https://doi.org/10.1038/s41598-020-64855-y

Torres LG (2017) A sense of scale: Foraging cetaceans' use of scale-dependent multimodal sensory systems. Marine Mammal Science 33:1170–1193. https://doi.org/10.1111/mms.12426

Vaughan D, Comiso JC, Allison I, et al (2013) Observations: Cryosphere. Climate Change 2013: The Physical Science Basis. Observations: Cryosphere in Climate Change 2013: The Physical Science Basis 317–382

Woodgate RA, Aagaard K, Weingartner TJ (2005) A year in the physical oceanography of the Chukchi Sea: Moored measurements from autumn 1990–1991. Deep Sea Research Part II: Topical Studies in Oceanography 52:3116–3149. https://doi.org/10.1016/j.dsr2.2005.10.016

Woodgate RA, Weingartner TJ, Lindsay R (2012) Observed increases in Bering Strait oceanic fluxes from the Pacific to the Arctic from 2001 to 2011 and their impacts on the Arctic Ocean water column. Geophysical Research Letters 39:2012GL054092. https://doi.org/10.1029/2012GL054092

Woodgate R, Stafford K, Prahl F (2015) A synthesis of year-round interdisciplinary mooring measurements in the Bering Strait (1990–2014) and the RUSALCA years (2004–2011). Oceanography 28:46–67. https://doi.org/10.5670/oceanog.2015.57

Wright DL, Berchok CL, Crance JL, Clapham PJ (2019) Acoustic detection of the critically endangered North Pacific right whale in the northern Bering Sea. Marine Mammal Science 35:311–326. https://doi.org/10.1111/mms.12521

Zerbini AN, Waite JM, Laake JL, Wade PR (2006) Abundance, trends and distribution of baleen whales off Western Alaska and the central Aleutian Islands. Deep Sea Research Part I: Oceanographic Research Papers 53:1772–1790. https://doi.org/10.1016/j.dsr.2006.08.009

Zerbini AN, Friday NA, Palacios DM, et al (2016) Baleen whale abundance and distribution in relation to environmental variables and prey density in the Eastern Bering Sea. Deep Sea Research Part II: Topical Studies in Oceanography 134:312–330. https://doi.org/10.1016/j.dsr2.2015.11.002

CHAPTER 2. Variability in fin whale (*Balaenoptera physalus*) occurrence in the Bering Strait and southern Chukchi Sea in relation to environmental factors

[Escajeda E, Stafford KM, Woodgate RA, Laidre KL (2020) Variability in fin whale (*Balaenoptera physalus*) occurrence in the Bering Strait and southern Chukchi Sea in relation to environmental factors. Deep Sea Research Part II: Topical Studies in Oceanography 177:104782. https://doi.org/10.1016/j.dsr2.2020.104782]

2.1 Abstract

Fin whales (*Balaenoptera physalus*) are common summer visitors to the Pacific Arctic, migrating through the Bering Strait and into the southern Chukchi Sea to feed on seasonally-abundant prey. The abundance and distribution of fin whales in the Chukchi Sea varies from year-to-year, possibly reflecting fluctuating environmental conditions. We hypothesized that fin whale calls were most likely to be detected in years and at sites where productive water masses were present, indicated by low temperatures and high salinities, and where strong northward water and wind velocities, resulting in increased prey advection, were prevalent. Using acoustic recordings from three moored hydrophones in the Bering Strait region from 2009–2015, we identified fin whale calls during the open-water season (July–November) and investigated potential environmental drivers of interannual variability in fin whale presence. We examined near-surface and near-bottom temperatures (T) and salinities (S), wind and water velocities through the strait, water mass presence as estimated using published T/S boundaries, and satellite-derived sea surface temperatures and sea-ice concentrations. Our results show significant interannual variability in the acoustic presence of fin whales with the greatest detections of calls in years with contrasting environmental conditions (2012 and 2015). Colder temperatures, lower salinities, slower water velocities, and weak southward winds prevailed in 2012 while warmer temperatures, higher salinities, faster water velocities, and moderate southward winds prevailed in 2015. Most detections (96%) were recorded at the mooring site

nearest the confluence of the nutrient-rich Anadyr and Bering Shelf water masses, ~35 km north of Bering Strait, indicating that productive water masses may influence the occurrence of fin whales. The disparity in environmental conditions between 2012 and 2015 suggests there may be multiple combinations of environmental factors or other unexamined variables that draw fin whales into the Pacific Arctic.

2.2 Introduction

The Arctic has undergone unprecedented environmental shifts as a result of climate warming (Post et al., 2019). Prominent among these shifts is the loss of sea-ice cover during the summer (Comiso et al., 2008; Cavalieri and Parkinson, 2012; Vaughan et al., 2013; Wood et al., 2015a,b; Walsh et al., 2017) along with earlier melting in the spring and delayed onset of freezing in the fall (Markus et al., 2009; Stroeve et al., 2014; Frey et al., 2015; Stabeno et al., 2019; Baker et al., this issue). Environmental shifts as a result of climate change are especially evident in the Chukchi Sea where annual sea-ice cover has declined by ~13 days each decade from 1979 to 2013 (Laidre et al., 2015), extending the open-water season (Grebmeier et al., 2010; Stroeve et al., 2014; Wood et al., 2015b; Woodgate, 2018). Declining sea ice is expected to result in range expansions of temperate and subarctic species into the Arctic (Root et al., 2003; Wassmann et al., 2011; Laidre and Heide-Jørgensen, 2012; Woodgate et al., 2015). Subarctic cetaceans, such as fin whales (*Balaenoptera physalus*), are thought to be expanding their range and residence time in the Chukchi Sea (Woodgate et al., 2015), which could lead to increased competition with Arctic cetaceans (Clarke et al., 2013).

Fin whales are a cosmopolitan mysticete whose range extends through most of the world's oceans (Mizroch et al., 1984). Though their exact migration patterns are unclear, fin whales are thought to breed in lower latitudes during winter and migrate to high-latitude areas,

such as the Bering and Chukchi seas, in summer to feed on seasonally abundant prey (Mizroch et al., 1984, 2009). Fin whale diets vary seasonally and spatially across the North Pacific, but typically include euphausiids and forage fish species (Pike, 1950; Nemoto, 1959; Nemoto and Kasuya, 1965; Mizroch et al., 1984; Flinn et al., 2002; Witteveen and Wynne, 2016). Fin whales are generally thought to avoid sea ice, though they have been observed swimming along the ice edge in the Arctic (Sleptsov, 1961; Mizroch et al., 1984).

Fin whales produce low frequency signals (< 100 Hz), with high intensities (source levels up to 189 dB re 1 μPa at 1m) and short durations (≤ 1 s; Watkins, 1981; Watkins et al., 1987; Širović et al., 2007). The most commonly documented call is a short (~1 s) down-sweep generally starting around 25 Hz and ending at 15 Hz with peak energy centered near 20 Hz (Watkins, 1981; Watkins et al., 1987). The fin whale "20-Hz pulse" can occur in regular sequences, forming a stereotyped song that lasts from < 1 h to ~33 h (Watkins et al., 1987). Such sequences are believed to be produced by males as a mating display starting in the fall and lasting through spring (Watkins et al., 2000; Croll et al., 2002; Stafford et al., 2007). Fin whales also produce 20-Hz and higher frequency pulses in short, irregular sequences that may serve as contact calls (Watkins, 1981; McDonald et al., 1995; Edds-Walton, 1997), especially during the summer months (Širović et al., 2013).

Historical records dating back to the early 20th century suggest fin whales commonly occurred in the southwest Chukchi Sea during the summer (Mizroch et al., 2009). Soviet and Japanese whaling expeditions in the 1930–1940s captured fin whales as far west as Cape Schmidt (68°55'18.3"N 179°27'42.7"W), and as far north as the central Chukchi Sea (69°04′N, 171°06′W) and Wrangel Island (Tomilin, 1957; Nemoto, 1959; Sleptsov, 1961; Mizroch et al., 2009; Fig. 2.1). Fin whales were observed in the Chukchi Sea as early as June (Nikulin, 1946)

and stayed in the area until October (Nikulin, 1946; Nasu, 1960; Votrogov and Ivashin, 1980). Sleptsov (1961) describes fin whales as 'one of the numerous baleen whales that inhabit the Chukchi Sea' and reported seeing hundreds of fin whales in the span of six days between the Bering Strait and Cape Serdtse-Kamen in September 1939. By the mid-20th century, intense whaling in the North Pacific had taken a toll on fin whale populations and fin whales were rarely seen in the Chukchi Sea. Only a few sightings of fin whales were recorded between 1958 and 1981 (Nasu, 1960; Votrogov and Ivashin, 1980). More recent visual and acoustic observations of fin whales chart their presence in portions of the northeastern Chukchi Sea (Delarue et al., 2013), southcentral Chukchi Sea (Clarke et al., 2015; Brower et al., 2018), and the southern Chukchi Sea north of the Bering Strait (Tsujii et al., 2016).

We hypothesize that observed spatial variability in fin whale presence may be connected to environmental variability in the study region. In addition to the seasonal cycle of sea ice, the Chukchi Sea is characterized by the presence of distinct water masses defined by differences in temperature and salinity which vary from year to year (Coachman et al., 1975). The water masses in the Chukchi Sea have varying levels of nutrients and chlorophyll-*a* (chl-*a*), leading to distinct phytoplankton and zooplankton communities (Hopcroft et al., 2010; Eisner et al., 2013; Pisareva et al., 2015; Danielson et al., 2017; Sigler et al., 2017). Large, chain-forming diatoms are found in areas with high chl-*a* concentrations, such as the productive Anadyr Water (AW) in the western Chukchi Sea, whereas smaller phytoflagellates occur in low-nutrient areas, such as the less productive Alaskan Coastal Water (ACW) in the eastern Chukchi Sea (Springer and McRoy, 1993; Eisner et al., 2013; Danielson et al., 2017). Consequently, large copepods and other zooplankton groups are found in the AW while smaller copepods are ubiquitous in the ACW zooplankton community (Eisner et al., 2013; Sigler et al., 2017). It might be therefore

expected that fin whales would occupy areas where the AW, or similarly productive water masses, dominate.

The Chukchi Sea is a highly advective ecosystem that is heavily influenced by the inflow of Pacific Water which enters through the Bering Strait (Woodgate et al., 2005a; Fig. 2.1). Advection from the northern Bering Sea provides the main source of zooplankton for the Chukchi Sea and is an important factor in determining zooplankton biomass and secondary production (Weingartner, 1997; Kitamura et al., 2017). High northward water velocities through the strait likely translate to increased advection of Pacific-origin prey into the Chukchi Sea. Therefore, we hypothesize that years with high detections of fin whale calls will have high northward (along-channel) water velocities.

The Bering Strait is divided into two channels by the Diomede Islands roughly mid-strait (Fig. 2.1). The western channel of Bering Strait is comparatively cold and salty due to the prevalence of the AW, while the eastern channel tends to be warmer and fresher due to the presence of the ACW (Coachman et al., 1975; Woodgate et al., 2005b, 2015). The cold and salty Bering Shelf Water (BSW) passes through the central strait (Coachman et al., 1975; Woodgate et al., 2005b). Variability in wind strength and direction can influence the position of these water masses and overall transport in the strait. Strong along-channel (northward) winds through Bering Strait may push the less productive surface ACW against the Alaskan coast via Ekman transport, allowing the more productive AW to shift east and replace it in the surface waters (Woodgate, 2018). Similarly, southward winds spread the ACW westwards across the surface of the strait and draw AW to the east at depth (Woodgate et al., 2015). Thus, wind changes could affect feeding opportunities for fin whales at different depths across the strait. Northward winds are linked to northward flow through the strait (Woodgate et al., 2005a), which leads to higher

advection of prey into the Chukchi Sea, in general. Therefore, we hypothesize that fin whale occurrence may be related to northward wind velocity through the strait.

Given that the Bering Strait is the only gateway from the Pacific Ocean into the Chukchi Sea (Fig. 2.1), the region is an ideal study area for recording the occurrence of migrating fin whales. In this paper, we investigate whether fin whales exhibited any interannual variation in their acoustic presence during the open-water season (July−November) from 2009−2015 and explore correlations between the acoustic presence of fin whales and environmental variation in the Bering Strait region. We hypothesize that high levels of fin whale calls occur in the years when and at the mooring sites where the highly productive AW and BSW are prevalent, when/where there are higher northward water velocities (and thus primarily northward winds) through the strait, and in years when sea ice forms later in the fall, allowing fin whales to remain in the Chukchi Sea longer into the season.

2.3 Methods

2.3.1 *Acoustic Data*

Acoustic data were collected from three AURAL-M2 hydrophones (Autonomous Underwater Recorder for Acoustic Listening-Model 2, Multi-Électronique, Inc.; sensitivity of −154 dB re 1 V/µPa and 16-bit resolution) attached to oceanographic moorings positioned within the eastern channel of the Bering Strait (A2 in the center of the eastern channel, and A4 in the Alaskan Coastal Current (ACC) on the east side of the channel), and a central strait location ~35 km north of the strait in the southern Chukchi Sea (A3; Fig. 2.1). Hydrophones were first installed on the moorings in September 2009 and recorded through 2015. Each hydrophone was positioned 4–8 m above the seafloor and sampled at 8192 Hz or 16384 Hz with various hourly duty cycles and recording start dates (Table 2.1). We assume that calls recorded during the hydrophones' duty

cycle are representative of fin whale acoustic activity for the entire hour in which the calls were recorded.

We quantified fin whale calling activity as the number of hours per day with fin whale calls present, hereafter referred to as 'fin whale hours' (FWH). Note that since we were only able to detect calling whales, we could not assume the absence of fin whales during any hour, nor could we estimate the abundance of fin whales using call abundance alone. The term 'recording years' refers to years that each hydrophone actively recorded data. Analysis of the recordings was restricted to the recording start date (typically July) until the end of November, called here as the 'recording period.' Given the shallow depth of the study area, it is likely that all calls from individuals within 10–20 km of the hydrophones were recorded (Woodgate et al., 2015). If we use the conservative call detection range of 10 km, the hydrophones cover a total of 892 km^2, or ~3% of the study area (Fig. 2.1). Hydrophones at A2 and A4 cover ~64% of the eastern channel area (~900 km^2), while the width of the A3 10-km call detection buffer covers ~10% of the across-strait distance at its latitude north of the strait.

We identified hours with fin whale 20-Hz pulses using the spectrogram correlation tool implemented in Ishmael (2014 version; Mellinger and Clark 2000; Mellinger, 2002). Detector parameters included a threshold of 10 to reduce the number of false detections and a smoothing time constant of 0.3 s. Each hour identified by the detector was then manually verified to contain fin whale calls by inspecting the spectrogram in Ishmael (FFT 4096, Hanning window, spectrogram equalization enabled with a time constant of 30 s) and eliminating any false positives from the dataset. The hours before and after a true positive FWH were examined to capture any hours with calls that were not picked up by the detector, adding a total of 269 FWH to our detections (~11% of the total number of FWH for all three sites).

To investigate spatial and temporal patterns in the presence of fin whales, we compared FWH between years and sites using a nonparametric two-sample Wilcoxon rank-sum test under the null hypothesis of equal distributions. Since all hydrophones recorded in October, we restricted our interannual comparisons of FWH within each mooring site and between the three sites to October only to avoid issues with unequal recording period lengths. We also compared the date of departure of calling fin whales from the study region by calculating the 95% quantile of the cumulative distribution of days with fin whale calls starting on 1 October of each year, following the procedure of Hauser et al. (2017). We used a significance threshold of 0.05 for all statistical tests and assumed independence between daily values.

2.3.2 *Environmental Data Collection*

Six environmental variables were recorded *in-situ* by other sensors on the same moorings, including: near-bottom temperature and salinity (40–55 m depth) measured by Sea-Bird (SBE) SBE16 and SBE37 sensors; near-surface temperature and salinity (14–19 m depth) measured by the ISCAT system developed at the University of Washington (e.g. Woodgate et al., 2015), which includes a SBE37 temperature-salinity-pressure sensor in an ice-resistant housing; and water velocity (cm s^{-1}) and direction (°) measured by Teledyne's Workhorse Acoustic Doppler Current Profilers (ADCPs). The ADCPs measured water velocity in 2-m bins from ~15 m to ~45 m depth (see Supplemental Tables S1–S3 for instrument depths). For simplicity, we used only data from the ADCP bin closest to ~30 m depth. Note that henceforth the term 'near-surface' refers to measurements taken by the ISCATs and 'near-bottom' refers to those taken by the SBEs. Some ISCAT recorders were lost/stopped recording before the 30 November cut-off date (see Woodgate et al., 2015 and Supplemental Tables S1–S3 for data gaps along with other mooring sensor information). Note that the ISCAT for A3 stopped recording in August 2014, 45

days after deployment, thus near-surface temperature and salinity data are not available for fall 2014.

In addition to the *in-situ* data, we examined northward wind velocity, and satellite-derived sea surface temperatures (SST) and sea-ice concentrations. Wind velocity data were obtained from the National Center for Environmental Prediction (NCEP) R1 dataset, with a spatial resolution at the Bering Strait of 2.5°. We used the National Oceanic and Atmospheric Administration's (NOAA) Optimum Interpolation satellite sea surface temperature (OISST) gridded product with a 0.25° resolution (https://www.esrl.noaa.gov/psd/; Reynolds et al., 2007). Daily mean SSTs were extracted from the cell containing each mooring's position.

For sea-ice concentrations, we sought datasets with the highest resolution available. We required data from different passive microwave sea-ice satellites to cover the entire duration of the study. For years 2009 and 2010, we used Advanced Microwave Scanning Radiometer – Earth Observing System (AMSR-E) sea-ice concentration data with a resolution of 6.25 km from the Integrated Climate Date Center (ICDC, icdc.cen.uni-hamburg.de; Kaleschke et al., 2001; Spreen et al., 2008). The AMSR-E satellite failed in early October 2011, consequently for 2011 and 2012 we used data from the Special Scanning Microwave/Imager (SSM/I) with a spatial resolution of 25 km (Cavalieri 1996). High resolution Advanced Microwave Scanning Radiometer 2 (AMSR-2) data with a grid resolution of 6.25 km were used for 2013–2015 (Beitsch et al. 2014; Kaleschke and Tian-Kunze, 2016).

We derived daily mean sea-ice concentration for the area of the Chukchi Sea as defined by the International Hydrographic Organization (IHO; http://www.marineregions.org/gazetteer.php?p=details&id=4257), and for a custom study area polygon (Fig. 2.1). The study area polygon was defined by the bounds set by Cape Serdtse-

Kamen, Russian Federation, in the northwest; Nunyamo, Russian Federation, to the southwest; York, Alaska, USA, on the Seward Peninsula to the southeast; and Cape Espenberg, Alaska, USA, to the northwest (Fig. 2.1). We determined the study area polygon by estimating where sea ice, if present, could potentially create a migration barrier for fin whales. All satellite-derived data were visualized in ArcMap (v. 10.1) using the WGS 1984 datum and projected in a custom polar stereographic projection with a central meridian of –171°W.

2.3.3 *Environmental Data Analysis*

To ensure consistency when comparing the environmental data over time, we calculated summary statistics for October data since there were no data gaps in the *in-situ* temperature and salinity data in this month (except for a gap in the near-surface data for 2014 at A3). For the ADCP data, we elected to compare the monthly mean northward water velocities for June to November to capture the summertime peak in transport through the Bering Strait (Woodgate et al., 2005b). We investigated correlations between days with fin whale calls present (i.e., FWH > 0) and select individual environmental variables using non-parametric Kendall's rank correlation tests. The Kendall's rank coefficient, tau (τ), indicates the direction of association ($-1 < \tau < 1$) and the resulting *p*-value indicates presence of a statistically significant correlation under the null hypothesis of non-correlation between the samples.

We tested for interactions between fin whale presence and along-channel (northward) wind patterns within the Bering Strait by comparing the daily mean northward wind velocity on days when the number of FWH reached above a certain threshold (≥1 h, ≥6 h, ≥12 h, and ≥18 h) and days without any FWH. We calculated summary statistics for northward wind velocities in October only, including an overall mean along-channel wind velocity as well as mean wind velocity for days with no FWHs and days with FWHs above a threshold (see categories above).

We then compared the overall October mean along-channel wind velocity to the mean wind velocities for days with and without FWHs using a Wilcoxon rank sum test.

For the sea ice analysis, we calculated the melt-out and freeze-up dates as the day of the year when the sea ice concentration within the study area decreased/increased below/above 80%, respectively, following Markus et al. (2009) and Stroeve et al. (2014). We defined an area as 'ice-free' if the mean sea ice concentration was ≤15%, a threshold commonly used to indicate the presence of sea ice (Serreze et al., 2009, 2016; Stroeve et al., 2012). We calculated the melt period length using the number of days between the initiation of melting (≤80% concentration) and when the study area was ice-free (≤15% concentration). For the freeze-up period length, we calculated the number of days between the first day sea ice concentration reached >15% and the first day the sea ice reached ≥80% concentration in the fall. We compared the calculated fin whale departure date and sea ice freeze-up date for each year using a two-sided Pearson correlation test after testing for normality.

2.3.4 *Water Masses*

Water mass presence for each day was estimated for the near-surface and near-bottom using temperature and salinity (T/S) bounds suggested by Danielson et al. (2017). These authors distinguish five water mass categories: the Alaskan Coastal Water (ACW), Bering Chukchi Summer Water (BCSW), Bering Chukchi Winter Water (BCWW), Melt Water (MW), and water from the Atlantic layer in the Arctic (AtlW). Danielson et al. (2017) combine the Anadyr Water (AW) and the Bering Shelf Water (BSW) into one water mass, the BCSW, since the T/S properties of these two water masses are often indistinguishable from each other. Note that since the T/S bounds of these waters vary interannually (Coachman et al., 1975), there are limitations to the representativeness of the above water mass identifications.

Chi-squared tests of independence were performed for each mooring site using pooled presence/absence of fin whale calls for each day across all recording years along with the daily water mass designations to determine whether there was a significant association between the presence of fin whale calls and water mass. If a chi-squared test was inappropriate (e.g. in the case of small sample sizes), a Fisher's exact test was applied instead. Fisher's exact test evaluates the significance of association, or contingency between two categorical variables, and is insensitive to sample sizes. All analyses were performed using the statistical software R (v. 3.5.3; R Core Team, 2019).

2.4 Results

2.4.1 *Fin Whale Detections*

We processed a total of 52,272 audio files collected from ~July to November 2009−2015 (Table 2.1). Fin whales were detected at all three sites, with the highest frequency and abundance of fin whale hours (FWH) at site A3 by a large margin (Fig. 2.2; Supplemental Figs. S1–S3). About one third (34.4%) of the total recording days at A3 had at least 1 h with fin whale calls, compared to only 4.6% at A2 and 1.5% at A4. Calling fin whales were detected in all recording years at A2 and A3, but were only detected in 2014 and 2015 at A4. October had the highest occurrence of FWH across all sites (68.4%), and given the hydrophones all had data from October, we restricted our statistical tests to this month. Wilcoxon rank-sum tests revealed statistically significant differences in the distribution of FWH in October at the three mooring sites (A2 and A3: W = 5259.5, $p < 0.001$, n = 186 days; A2 and A4: W = 8423, $p = 0.006$, n = 124 days; A3 and A4: W = 1709, $p < 0.001$, n = 124 days). The earliest detection of fin whale calls across all sites and years occurred on 23 July 2013 at A3, and the latest fin whale detection occurred on 20 November 2015 at A3 (Table 2.2). Annual fin whale departure dates using the

95% quantile were only calculated for A3 given the lack of data at A2 and A4 (see Supplemental Fig. S2.4 for the cumulative distribution of days with fin whale calls at A3). Fin whale departure dates at A3 did not show any statistically significant trend ($R^2 = 0.20$, $p = 0.311$; Fig. 2.3).

At A3, fin whale calling activity was highest in 2012 and 2015 (52 and 71 days with at least one FWH, respectively), while calling activity was the lowest in 2010 (22 days) followed by 2011 and 2013 (28 days). The Wilcoxon tests comparing FWH in October between years at A3 show significant differences in the distributions fin whale detections across years, with significant values ($p < 0.01$) between all consecutive years except 2009 and 2010 ($p = 0.736$) and 2010 and 2011 ($p = 0.463$; Table 2.3). Wilcoxon tests comparing FWH in 2012 and 2015 to the other years detected significantly different distributions ($p < 0.01$), except for the test between 2012 and 2014 ($p = 0.614$; Table 2.3).

Fin whale calls were less common at A2, though 2015 had relatively higher call activity with 40 h with fin whale calls compared to 2–10 h in each of the other six years. At A4, fin whale calls were only detected in 2014 (1 h) and 2015 (19 h). Insufficient sample sizes precluded any statistical comparisons of fin whale vocal activity between years for A2 and A4.

2.4.2 *Sea-ice Conditions and Analyses*

Sea-ice conditions within the study area were highly variable from year to year. Melt-out dates ranged from as early as 27 April (2011) to as late as 20 May (2010; Table 2.4). The number of days between the initiation of melting (< 80% concentration) and ice-free conditions in the study area (< 15% concentration) ranged from 21 days (2015) to 41 days (2013; Table 2.4). The study area was typically ice-free starting in late May to early June, with the earliest ice-free date occurring on 24 May 2015 and the latest on 17 June 2010. On average, freeze-up dates (≥ 80% concentration) occurred in early to mid-December, with the earliest freeze-up on 28 November

2009 and the latest on 25 December 2010. The freeze-up periods for each year were typically much shorter than the melt periods, with the number of days between the ice-free date and freeze-up initiation ranging from five days (2014) to 23 days (2010 and 2012; Table 2.4).

Fin whale departure dates for each year at A3 were compared to the sea ice freeze-up date for the study area and the Chukchi Sea, as well as the day of the year when the daily mean near-surface and near-bottom temperatures first reached ≤ 0°C (Fig. 2.4). Two-sided Pearson correlation tests indicated no significant correlation between fin whale departure date and sea ice freeze-up date for the study area (t = –1.046, p = 0.344) or the Chukchi Sea (t = –0.308, p = 0.771). The latest fin whale departure date occurred on 17 November 2011 and 2015 when the mean sea ice concentrations were ~0.8% and 4.9% in the study area, and 21.0% and 18.2% in the Chukchi Sea, respectively (Table 2.4).

2.4.3 *Environmental Conditions at the Moorings*

Environmental data at the three mooring sites exhibited strong interannual and spatial variation. The highest temperatures and lowest salinities on average were seen at A4 (e.g. 2013 October near-surface mean temperature = 3.5 °C, SD = 0.7 °C; near-surface mean salinity = 30.3 psu, SD = 1.3 psu). Conversely, A2 and A3 had lower temperatures and higher salinities than A4 (A2: 2013 October near-surface mean temperature = 3.3 °C, SD = 0.7 °C, near-surface mean salinity = 31.1 psu, SD = 1 psu; A3: 2013 October near-surface mean temperature = 2.9 °C, SD = 0.8 °C, near-surface mean salinity = 31.7 psu, SD = 0.8 psu; Fig. 2.5). This spatial structure, with warm fresh waters near the Alaskan Coast, typically indicates the presence of the Alaskan Coastal Current (see discussion in Woodgate et al., 2015). There were also significant interannual differences across all three sites. The lowest near-surface and near-bottom

temperatures occurred in 2012 while the highest temperatures occurred in 2015 (Fig. 2.5; Woodgate, 2018).

Northward water velocities were on average the highest at sites A2 and A4 during the open-water season (Fig. 2.6), consistent with known seasonality in the flow due to weaker opposing southward winds in summer (Woodgate et al., 2005b). The year 2012 had the weakest northward water velocity throughout the open-water season while 2014 had sustained high northward velocities throughout the season (Fig. 2.6; Woodgate, 2018). Overall, northward water velocities weakened over the period between July and November with the slowest northward water velocities occurring in November, except in 2012 and 2014 when the seasonal minimum velocities were seen in September and October (Fig. 2.6). Direction of flow at all three sites was primarily northward during the open-water season (see Supplemental Figs. S5−S11 for plots of the water and wind velocity vectors along with fin whale acoustic presence at A3 during the open-water season). For a more detailed overview of variation in Bering Strait transport through 2015, see Woodgate (2018).

Due to low fin whale detections at A2 and A4, we focused our wind analysis on site A3 and used wind data from the grid point closest to the mooring (67.5°N, 190°W, ~140 km to the northwest of A3). On average, along-channel winds were mainly southward during the month of October, with the strongest mean winds occurring in 2013 (October $\overline{x}$ = –6.2 m/s, SD = 5.4 m/s) and the weakest mean winds in 2012 (October $\overline{x}$ = –0.4 m/s, SD = 8.1 m/s; Table 2.5). Note that the negative sign indicates a southward direction.

2.4.4 *Environmental Analyses*

We focused our environmental analyses on the A3 mooring site due to the relative lack of fin whale detections at A2 and A4. The Kendall's rank correlation tests between FWH on days with

fin whale calls (i.e., FWH > 0) and the environmental variables produced statistically significant ($p < 0.05$) though small correlations for daily mean water speed, and along-channel wind and water velocities pooled for all seven years (2009–2015; Table 2.6). We ran a second test using October data only and found similar results, as well as the addition of significant correlations between FWH and near-surface temperature and SST at site A3 (Table 2.6).

Days with fin whale calls mostly had southward mean wind velocities while days without calls (i.e., FWH = 0) mostly had northward overall mean winds (Table 2.5; Fig. 2.7). The Wilcoxon test comparing the overall mean along-channel wind velocity for October of each year against the means for days with and without FWHs revealed that days without FWH and days with FWH ≥ 6 and 12 hr had statistically significant differences in along-channel wind velocities in 2011 and 2014 only (Table 2.5). Insufficient data precluded any tests for days with FWH ≥ 18 hrs.

2.4.5 *Water Mass Composition at the Moorings*

Water mass composition at A2 and A3 during the open water season was dominated by the presence of the Bering Chukchi Summer Water (BCSW) at both the near-surface (>70% of days at both sites) and near-bottom levels (>90% of days at both sites) for all recording years (see Supplemental Figs. S12–S14 for plots with the water mass composition at the three sites during the open water season). The water mass composition at A4 was similarly dominated by BCSW at the near-bottom (73% of days in July−November) and to a lesser extent in the near-surface (51% of days in July−November). The cold and salty Bering Chukchi Winter Water (BCWW) appeared in both levels in the water column in November at all three sites, when it is assumed that fin whales are beginning their migration south. A fresher, colder signal, that falls within the Melt Water (MW) category as defined by Danielson et al. (2017), appeared in the near-surface at

all three sites in September and October 2012 and 2013, with the strongest signal in 2012. However, since the sea-ice edge is far away from the mooring sites in September and October, the freshening observed in 2012 and 2013 was likely due to fresh waters from either the Alaskan Coastal Current (ACC) or the Siberian Coastal Current (SCC). The SCC is a cold, fresh current present seasonally in the Chukchi Sea only in some years (Weingartner et al., 1999). Also noteworthy was a warm Alaskan Coastal Water (ACW) signal in the near-surface at A2 in 2013, 2014, and 2015 and at A3 in 2010 and 2015.

We conducted a side-by-side comparison of the daily water mass designations for A2 and A3 and noted the number of days when at least one of the water mass designations at A2 did not match those from A3. Out of 726 days when both moorings were recording and had data for both instruments, 14 days (~2% of total days) had different water mass composition in the near-bottom water and 69 days (~10% of total days) for the near-surface water. In contrast, A2 and A4 had different water mass compositions on 203 days (~39%) for the near-surface and 127 days (24%) for the near-bottom. The comparison between A3 and A4 yielded 311 days (60%) with different water mass composition at the near-surface and 136 days (26%) at the near-bottom. These results indicate that despite close spatial proximity, A2 and A4 had very different water mass composition while A2 and A3 had similar water mass composition.

2.4.6 *Water Mass Analyses*

The chi-squared tests of independence between the pooled FWH and the near-surface/near-bottom water mass designations at site A3 suggest that the occurrence of fin whale calls during the study period was statistically dependent on the occurrence of water masses (both tests using near-surface and near-bottom water mass designations: $p < 0.001$). We repeated the tests of independence for each recording year at A3, using the Fisher's Exact Test to compare the daily

near-surface and near-bottom water mass designations to the total FWH for each day. The results show a significant relationship for 2009, 2011, 2012, and 2015 (all $p < 0.02$), signifying that fin whale presence was statistically dependent on water mass presence for these years. We were unable to execute the Fisher's Exact test for 2013 (near-bottom water mass) and 2014 (both near-surface and near-bottom) due to the fact that only one water mass (BCSW) was present at both levels in the water column, resulting in zeros in both the expected and observed columns of the test's contingency tables.

We were unable to perform a chi-squared test for independence for A2 and A4 due to the presence of small expected values ($E_{i,j} < 5$) in the contingency tables generated by the test. At A4, fin whale calls were only heard on days when the BCSW was present at both levels of the water column. Calling fin whales were only heard at A2 on days when the BCSW was present in the near-bottom waters. We applied a Fisher's Exact Test to the A2 near-surface water mass designations and found that fin whale calls and water mass occurrence in the near-surface waters were statistically independent of each other ($p = 0.48$).

2.5 Discussion

The results of this study show a pattern of interannual and spatial variation in the presence of acoustically-active fin whales in the Bering Strait region. Across all three sites, the year 2015 had the most fin whale detections followed by 2012, though these years had contrasting temperatures and salinities, sea-ice conditions, water velocity and wind patterns. Site A3, where the Anadyr Water (AW) and Bering Shelf Water (BSW) were most prevalent, had the most hours with fin whale calls, supporting our hypothesis that water masses may affect the occurrence of fin whales. We found small but significant correlations between FWH and northward wind and water velocities, near-surface temperatures and SST at site A3. However, our *p*-values for the

correlation tests were potentially too low and likely overestimated the real significance of the tests given that days with fin whale calls were likely not independent of each other. In addition, the statistically significant correlations between FWH and environmental variables were small (< 0.25). Thus, we conclude that it is not possible to prove a strong relationship between individual environmental parameters and FWH with our data. More data and greater spatial coverage are necessary to prove any significant association between days with fin whale calls and environmental factors in the Bering Strait region.

Most fin whale calls were heard in October, potentially due to fact that fin whale 20-Hz pulses serve primarily a reproductive purpose (Watkins et al., 2000; Croll et al., 2002; Stafford et al., 2007) and thus, tend to be heard closer to the winter mating season (Stafford et al., 2007). Consequently, fin whale vocalizations may not be a reliable indication of when fin whales first pass northwards through the Bering Strait. Additionally, the dates of departure from the Bering Strait region presented here only apply to vocal fin whales since we could not detect non-vocal whales, which could have remained in the area beyond these dates. Due to this inherent bias, the departure dates presented in this study only provide an approximation for when fin whales leave the region. The departure dates from the A3 mooring site did not exhibit a significant trend (Fig. 2.3), therefore it is not possible to determine whether fin whales are extending their residence time in the Chukchi Sea from our data. Perhaps this is not surprising given that we only have seven years of data, and interannual variability is substantial. In general, the fin whale departure dates at A3 occurred in early November, ranging from 31 October (2010) to 17 November (2011 and 2015). What signaled the fin whales to leave the Chukchi Sea is not clear. Sea-ice concentrations in the study area around the last detection dates were well below ‘ice-free’ levels (< 15%; Table 2.4), indicating that the Bering Strait was still navigable and free of sea ice. It is

possible, though, that fin whales respond to cooling water temperatures since all departure dates occurred before near-surface and near-bottom water temperatures at A3 reached below 0 °C (Fig. 2.4).

The overwhelming majority of fin whale calls were detected at site A3, where calling fin whales were heard every year. There are multiple possible explanations for the spatial variability observed in fin whale detections. First, site A3 is situated at the confluence of two productive water masses, the AW and BSW, which likely provide better feeding opportunities for fin whales. The dominant water mass detected at A3 was the Bering Chukchi Summer Water (BCSW), which is composed of the AW and BSW, and thus has high nutrient levels and larger zooplankton (Eisner et al., 2013; Ershova et al., 2015; Danielson et al., 2017). Though fin whale calls were also detected on days when other fresher water masses were present at A3, including days in 2015 when Alaskan Coastal Water (ACW) was present in the near-surface (Fig. S2.13). Fin whale calls were also detected on days in September 2012 when a fresh, cold signal appeared in the near-surface waters at A3, possibly indicating the presence of the Siberian Coastal Current (SCC).

The SCC occasionally flows into the Bering Strait during periods with strong or persistent southward winds (Weingartner et al., 1999). Ershova et al. (2015) detected the presence of the SCC in the central Chukchi Sea in September 2012, therefore it is possible that the reach of the SCC extended to the A3 site that month. Fig. S2.8 shows that winds measured in September 2012 were predominantly southward, which has been shown to cause the ACW to deviate away from the Alaskan coast and towards the western Chukchi Sea (Woodgate et al., 2015; Pisareva, 2018; Morris, 2019). Often the presence of the cold and fresh SCC creates a front (Weingartner et al., 1999), which could isolate and cluster prey. In 1992–1993, Moore et al.

(1995) observed bowhead whales (*Balaena mysticetus*) feeding in close association with salinity and thermal fronts along the Chukotka coast. Moreover, *Thysanoessa inermis*, a common fin whale prey (Nemoto 1959; Witteveen and Wynne, 2016), was found to be the dominant zooplankton species collected from a dense prey patch near a front, lending support to the potential importance of the SCC in creating favorable feeding conditions for fin whales at A3.

In addition to its proximity to productive water masses, A3 may be situated close to oceanographic features created by currents, such as island wake eddies, that are known to create favorable foraging opportunities for baleen whales (Johnston et al., 2005a; Chenoweth et al., 2011). Eddies create upwelling zones which promote phytoplankton blooms (Hasegawa et al., 2009) and have been shown to be important feeding habitat for auklets and other planktivores in the Bering and Chukchi seas (Piatt and Springer, 2003). In the Bay of Fundy, Canada, island wake eddy systems were found to be important feeding grounds for fin whales as well as minke whales (*B. acutorostrata*) and harbor porpoises (*Phocoena phocoena*; Johnston et al., 2005a,b). Currents moving past the Diomede Islands generate island wake eddies (Coachman et al., 1975; Woodgate et al., 2015) that are then carried northwards towards A3, according to satellite SST data (Woodgate, pers. comm.). The island wake eddies may create opportune feeding conditions for fin whales at A3.

In contrast, site A2 had fin whale detections in all recording years but in lower abundance, while fin whale calls were largely absent from site A4. Given its position in the less-productive ACC, A4 may present lower quality feeding areas for fin whales than the other two sites. Though A2 had similar water mass composition as A3, water velocities were higher at A2, potentially transporting prey out of the area. Therefore, fin whales may be less inclined to stay in the region around A2 due to fewer feeding opportunities. Also, the position of site A3 north and

towards the middle of the Bering Strait gives it an advantage over A2 in capturing the calls of fin whales migrating through the western strait. While A2 and A4 can only record the calls of fin whales passing through the east channel of the strait, A3 can potentially record calling whales migrating through both channels.

While the spatial variability in fin whale detections may be explained, the exact environmental mechanisms for the observed temporal variability are less clear. Both 2012 and 2015 stand out as years with the highest number of fin whale detections at A3, yet the two years had very different environmental conditions. The year 2012 had the coldest October mean temperatures (near-bottom October mean at A3 = 1.0 °C), late sea ice breakup (16 May), anomalously low flow (Woodgate, 2018), and weak mean northward wind velocities in the fall. On the other hand, 2015 had a very warm annual mean temperature (near-bottom October mean at A3 = 3.6 °C), earlier sea ice breakup (4 May), high flow (Woodgate, 2018), and variable northward wind velocities. Our results suggest that at A3, the occurrence of fin whale calls is more strongly related to southward winds than northward winds, but this relation does not hold for all years (Table 2.5). Thus, we cannot attribute interannual variation in the acoustic presence of fin whales to any one environmental predictor. Instead, we believe that a combination of conditions not only in the Chukchi Sea, but also in the Bering Sea, contributes to the abundance of fin whales in the study area. We hypothesize a series of 'push' and 'pull' factors below that may have influenced the observed interannual variation in the presence of acoustically-active fin whales.

Pull factors imply that conditions in the Chukchi Sea were favorable for zooplankton and other fin whale prey in 2012 and 2015, thus drawing more fin whales into the area to feed. The abundance of hours with fin whale calls at A3 in 2012 may point to the fact that the year was

particularly cold, and thus, productive. Colder temperatures are more favorable for the secondary production of *Calanus* copepods (Kimmel et al., 2018), a prominent constituent of the Chukchi Sea zooplankton. Cold years in the Bering and Chukchi seas have been also found to have higher zooplankton biomass and abundance (Ohashi et al., 2013; Ershova et al., 2015; Pinchuk and Eisner, 2017), and thus stronger recruitment for walleye pollock (*Gadus chalcogrammus*) and Pacific cod (*G. macrocephalus*; Stabeno et al., 2012), which are zooplankton predators like fin whales. Friday et al. (2013) observed twice as many fin whales along the eastern Bering Sea shelf in 2008 and 2010 when temperatures were cold than they did in 2002, a warm year. In their August−September 2012 sampling of the Chukchi Sea, Danielson et al. (2017) observed an abnormally high biomass of large copepods as well as a predominance of the BCSW in the bottom water at multiple sampling stations. During the same sampling period, Pinchuk and Eisner (2017) report a high abundance of *Calanus glacialis* and widespread distribution of Pacific-origin zooplankton in 2012, adding evidence to our hypothesis that 2012 was a favorable year for fin whale prey.

Conversely, 2015 was a warm year with high salinities. High salinities are usually indicative of high AW content and thus are typically associated with high nutrient levels (Danielson et al., 2017). Consequently, 2015 may have had higher zooplankton abundance due to a nutrient-rich environment. Pinchuk and Eisner (2017) found a strong correlation between the biomass of Pacific-origin zooplankton and high salinities associated with the BCSW, which was the dominant water mass at A3 in 2015 (Supplementary Figs. S12–S14). It is also possible that the earlier sea-ice retreat and warmer water temperatures observed in 2015 created better conditions for Pacific-origin copepods and euphausiids. Matsuno et al. (2011) found that Pacific copepod species (e.g. *Eucalanus bungii*) expanded into the Chukchi Sea in 2007, a year with

relatively early sea-ice retreat and abnormally high sea surface temperatures, similar to 2015. A notable pull factor for 2015 could also have been the strong water velocities measured in the Bering Strait. Strong velocities likely led to higher transport of both nutrients and zooplankton from the Bering Sea into the Chukchi Sea, creating better feeding opportunities for summer migrant fin whales.

In contrast to pull factors, potential push factors consist of poorer conditions in other reaches of the fin whale range, thereby sending fin whales into the Chukchi Sea in search of better conditions. Such areas include the Bering Sea and Gulf of Alaska, where fin whales are known to occur in the summer months (Moore et al., 1998, 2000; Stafford et al., 2007). Both 2014 and 2015 were significantly warmer years in comparison to historical records for the Bering Sea (Duffy-Anderson et al., 2017). Warm years in the Bering Sea result in poor recruitment in walleye pollock due to the prevalence of small, lipid-poor copepods (Kimmel et al., 2018). In 2015, an anomalously warm water mass, nicknamed the "Blob," pervaded the North Pacific, leading to declines in krill and to northward distribution shifts of multiple marine species (Cavole et al., 2016). Concurrent with the appearance of the Blob were reports of a mass mortality event of common murres (*Uria aalge*) in the Gulf of Alaska (Piatt et al., 2018). Additionally, 12 fin whales stranded on Kodiak Island, AK, between May and June 2015 (Savage, 2017). Though the causes of death for the whales were not determined, ecological conditions rather than anthropogenic factors (e.g. ship strikes) are thought to be the culprit (Savage, 2017). Warmer temperatures observed in 2015 may have affected prey availability in other fin whale summer feeding grounds, pushing fin whales into the Chukchi Sea in search of better feeding opportunities.

Another possible explanation for the increased observation of fin whale calls in 2015 is that the North Pacific population of fin whales is increasing (Zerbini et al., 2006), and thus may be reclaiming portions of its previous range (Clarke et al., 2013; Brower et al., 2018). An increased number of fin whales observed during annual surveys conducted by the Aerial Surveys of Arctic Marine Mammals Project (ASAMM) from 2008−2016 in comparison to 1982−1991 supports this theory (Brower et al., 2018). Brower et al. (2018) report seeing the most fin whales in the south-central Chukchi Sea in 2014 (44% of observations) and in 2015 (27%). However, it is difficult to evaluate habitat reclamation of fin whales using their calls alone given that only males are thought to produce the 20-Hz pulse and we could only detect vocal fin whales.

Limitations of the present study include limited spatial coverage of the study area with hydrophones located in only the east channel and north of the Bering Strait. Since there are no recent surveys on the western side of the Bering Strait or Chukchi Sea, our knowledge of fin whale habitat use in this region is limited. Given that the productive AW is typically found mainly in the west channel of the Bering Strait, it is possible that most fin whales may traverse through the strait on the western side. However, without adequate observation platforms covering both sides of the strait, the exact migration path of fin whales in the region remains unknown.

The results of this study corroborate patterns of interannual variation in fin whale presence observed by previous studies. Like the present study, Delarue et al., (2013) noted low fin whale detections in the northeast Chukchi Sea in 2009 and 2010, attributing diminished vocal activity to poorer feeding conditions. In contrast, more fin whales were heard in 2007, a particularly warm year in the Chukchi Sea with early ice retreat and low sea-ice extent, as well as high transport through the Bering Strait (Woodgate et al., 2010; Delarue et al., 2013). The

conditions in 2007 described by Delarue et al. (2013) are very similar to those we observed in 2015, when fin whale calls were the most abundant.

Our results present a preliminary examination of how environmental variations in the Bering Strait and southern Chukchi Sea may lead to interannual variability in the acoustic presence of fin whales. Though we were unable to identify a single environmental driver that explained the variation, differences in temperature, salinity, wind and water velocities likely played a role. There are potentially numerous combinations of environmental variables that create preferential feeding opportunities for fin whales. Delarue et al. (2013) hypothesize that perhaps the combination of environmental variables observed in 2007 (warm SSTs, low sea-ice concentrations, and high transport) created favorable conditions for fin whale prey. However, the abundance of calling fin whales in 2012, a period with colder water temperatures, low transport, and high spring sea-ice concentrations, suggests that alternative environmental drivers are also favorable for fin whale feeding.

Conditions in the Bering Sea may also be an important factor in determining fin whale occurrence in the Chukchi Sea. Comparing fin whale detections in the southern Chukchi Sea with those in the Bering Sea could help indicate whether fin whale presence in one region results in higher fin whale presence in the other. Also, examining environmental conditions in the Bering Sea for 2009−2015 could shed light on the patterns of fin whale occupation found in the present study. Continued monitoring of fin whale presence in the southern Chukchi and Bering seas in relation to oceanographic features is necessary for composing a more complete picture of how fin whale presence in the Pacific Arctic is changing in response to environmental shifts over time.

2.6 Acknowledgements

This material is based upon work supported by the National Science Foundation (NSF) Graduate Research Fellowship Program under grant number DGE-1256082. Any opinions, findings, and conclusions or recommendations expressed in this material are those of the author(s) and do not necessarily reflect the views of NSF. This work was also supported by the NSF Polar Programs Arctic Observing Network (R. Woodgate grant numbers PLR-1304052 and 1758565; K. Stafford grant number 1107106). A portion of the mooring work was supported by the Russian-American Long-term Census of the Arctic (RUSALCA), funded by the U. S. National Oceanic and Atmospheric Administration (NOAA) (grant numbers NA10OAR4320148, AM105, and AM133), the Applied Physics Laboratory at the University of Washington, and the National Science Foundation (grant number ARC-1107106). The Bering Strait mooring data are available at the permanent archives of the U.S. National Centers for Environmental Information/National Oceanographic Data Center, www.nodc.noaa.gov, and at: psc.apl.washington.edu/BeringStrait.html. This manuscript may be referenced through the North Pacific Research Board Arctic Integrated Ecosystem Research Program archives as ArcticIERP-13. We thank the four reviewers for their suggestions which improved the manuscript.

2.7 References

Baker, M., Kivva, K., Pisareva, M., Watson, J., Selivanova, J., this issue. Shifts in the physical environment in the Pacific Arctic and implications for ecological timing and conditions. Deep Sea Res. Part II Top. Stud. Oceanogr.

Beitsch, A., Kaleschke, L., Kern, S., 2014. Investigating high-resolution AMSR2 sea ice concentrations during the February 2013 fracture event in the Beaufort Sea. Remote Sens. 6, 3841–3856. https://doi.org/10.3390/rs6053841

Berline, L., Spitz, Y.H., Ashjian, C.J., Campbell, R.G., Maslowski, W., Moore, S.E., 2008. Euphausiid transport in the Western Arctic Ocean. Mar. Ecol. Prog. Ser. 360, 163–178.

Brower, A.A., Clarke, J.T., Ferguson, M.C., 2018. Increased sightings of subArctic cetaceans in the eastern Chukchi Sea, 2008–2016: population recovery, response to climate change, or increased survey effort? Polar Biol. 41, 1033–1039. https://doi.org/10.1007/s00300-018-2257-x

Cavalieri, D., 1996. Sea ice concentrations from Nimbus-7 SMMR and DMSP SSM/I-SSMIS passive microwave data, Version 1. https://doi.org/10.5067/8GQ8LZQVL0VL. [Date Accessed: 25 April 2017].

Cavalieri, D.J., Parkinson, C.L., 2012. Arctic sea ice variability and trends, 1979-2010. Cryosphere 6, 881–889. https://doi.org/10.5194/tc-6-881-2012

Cavole, L., Diner, R., Giddings, A., Koester, I., Pagniello, C., Paulsen, M.-L., Ramirez-Valdez, A., Schwenck, S., Yen, N., Zill, M., Franks, P., 2016. Biological impacts of the 2013–2015 warm-water anomaly in the Northeast Pacific: Winners, Losers, and the Future. Oceanography 29. https://doi.org/10.5670/oceanog.2016.32

Chenoweth, E., Gabriele, C., Hill, D., 2011. Tidal influences on humpback whale habitat selection near headlands. Mar. Ecol. Prog. Ser. 423, 279–289. https://doi.org/10.3354/meps08891

Clarke, J., Stafford, K., Moore, S., Rone, B., Aerts, L., Crance, J., 2013. Subarctic cetaceans in the southern Chukchi Sea: Evidence of recovery or response to a changing ecosystem. Oceanography 26, 136–149. https://doi.org/10.5670/oceanog.2013.81

Clarke, J.T., Ferguson, M.C., Curtice, C., Harrison, J., 2015. 8. Biologically important areas for cetaceans within U.S. waters – Arctic Region. Aquat. Mamm. 41, 94–103. https://doi.org/10.1578/AM.41.1.2015.94

Coachman, L.K., Aagaard, K., Tripp, R.B., 1975. Bering Strait: the regional physical oceanography. University of Washington Press, Seattle.

Comiso, J.C., Parkinson, C.L., Gersten, R., Stock, L., 2008. Accelerated decline in the Arctic sea ice cover. Geophys. Res. Lett. 35. https://doi.org/10.1029/2007GL031972

Croll, D.A., Clark, C.W., Acevedo, A., Tershy, B., Flores, S., Gedamke, J., Urban, J., 2002. Only male fin whales sing loud songs. Nature 417, 809.

Danielson, S.L., Eisner, L., Ladd, C., Mordy, C., Sousa, L., Weingartner, T.J., 2017. A comparison between late summer 2012 and 2013 water masses, macronutrients, and phytoplankton standing crops in the northern Bering and Chukchi Seas. Deep Sea Res. Part II Top. Stud. Oceanogr. 135, 7–26. https://doi.org/10.1016/j.dsr2.2016.05.024

Delarue, J., Martin, B., Hannay, D., Berchok, C.L., 2013. Acoustic occurrence and affiliation of fin whales detected in the northeastern Chukchi Sea, July to October 2007–10. Arctic 66, 159–172.

Duffy-Anderson, J.T., Stabeno, P.J., Siddon, E.C., Andrews, A.G., Cooper, D.W., Eisner, L.B., Farley, E.V., Harpold, C.E., Heintz, R.A., Kimmel, D.G., Sewall, F.F., Spear, A.H., Yasumishii, E.C., 2017. Return of warm conditions in the southeastern Bering Sea:

Phytoplankton - Fish. Plos One x12, e0178955. https://doi.org/10.1371/journal.pone.0178955

Edds-Walton, P.L., 1997. Acoustic communication signals of mysticete whales. Bioacoustics 8, 47–60. https://doi.org/10.1080/09524622.1997.9753353

Eisner, L., Hillgruber, N., Martinson, E., Maselko, J., 2013. Pelagic fish and zooplankton species assemblages in relation to water mass characteristics in the northern Bering and southeast Chukchi seas. Polar Biol. 36, 87–113. https://doi.org/10.1007/s00300-012-1241-0

Ershova, E., Hopcroft, R., Kosobokova, K., Matsuno, K., Nelson, R.J., Yamaguchi, A., Eisner, L., 2015. Long-Term Changes in Summer Zooplankton Communities of the Western Chukchi Sea, 1945–2012. Oceanography 28, 100–115. https://doi.org/10.5670/oceanog.2015.60

Flinn, R.D., Trites, A.W., Gregr, E.J., Perry, R.I., 2002. Diets of fin, sei, and sperm whales in British Columbia: an analysis of commercial whaling records, 1963-1967. Mar. Mamm. Sci. 18, 663–679. https://doi.org/10.1111/j.1748-7692.2002.tb01065.x

Frey, K.E., Moore, G.W.K., Cooper, L.W., Grebmeier, J.M., 2015. Divergent patterns of recent sea ice cover across the Bering, Chukchi, and Beaufort seas of the Pacific Arctic Region. Prog. Oceanogr. 136, 32–49. https://doi.org/10.1016/j.pocean.2015.05.009

Friday, N.A., Zerbini, A.N., Waite, J.M., Moore, S.E., Clapham, P.J., 2013. Cetacean distribution and abundance in relation to oceanographic domains on the eastern Bering Sea shelf, June and July of 2002 2008, and 2010. Deep Sea Res. Part II Top. Stud. Oceanogr. 94, 244–256. https://doi.org/10.1016/j.dsr2.2013.03.011

Grebmeier, J.M., Moore, S.E., Overland, J.E., Frey, K.E., Gradinger, R., 2010. Biological response to recent Pacific Arctic sea ice retreats, Eos, Trans., pp. 161–162. https://doi.org/10.1029/2010EO180001

Hasegawa, D., Lewis, M.R., Gangopadhyay, A., 2009. How islands cause phytoplankton to bloom in their wakes. Geophys. Res. Lett. 36. https://doi.org/10.1029/2009GL039743

Hauser, D.D.W., Laidre, K.L., Stafford, K.M., Stern, H.L., Suydam, R.S., Richard, P.R., 2017. Decadal shifts in autumn migration timing by Pacific Arctic beluga whales are related to delayed annual sea ice formation. Glob. Change Biol. 23, 2206–2217. https://doi.org/10.1111/gcb.13564

Hopcroft, R.R., Kosobokova, K.N., Pinchuk, A.I., 2010. Zooplankton community patterns in the Chukchi Sea during summer 2004. Deep Sea Res. Part II Top. Stud. Oceanogr. 57, 27–39. https://doi.org/10.1016/j.dsr2.2009.08.003

Jakobsson, M., L. A. Mayer, B. Coakley, J. A. Dowdeswell, S. Forbes, B. Fridman, H. Hodnesdal, R. Noormets, R. Pedersen, M. Rebesco, H.-W. Schenke, Y. Zarayskaya A, D. Accettella, A. Armstrong, R. M. Anderson, P. Bienhoff, A. Camerlenghi, I. Church, M. Edwards, J. V. Gardner, J. K. Hall, B. Hell, O. B. Hestvik, Y. Kristoffersen, C. Marcussen, R. Mohammad, D. Mosher, S. V. Nghiem, M. T. Pedrosa, P. G. Travaglini, Weatherall, P.,

The International Bathymetric Chart of the Arctic Ocean (IBCAO) Version 3.0, Geophys. Res. Lett., doi: 10.1029/2012GL052219.

Johnston, D., Thorne, L., Read, A., 2005a. Fin whales *Balaenoptera physalus* and minke whales *Balaenoptera acutorostrata* exploit a tidally driven island wake ecosystem in the Bay of Fundy. Mar. Ecol. Prog. Ser. 305, 287–295. https://doi.org/10.3354/meps305287

Johnston, D., Westgate, A., Read, A., 2005b. Effects of fine-scale oceanographic features on the distribution and movements of harbour porpoises *Phocoena phocoena* in the Bay of Fundy. Mar. Ecol. Prog. Ser. 295, 279–293. https://doi.org/10.3354/meps295279

Kaleschke, L., Lüpkes, C., Vihma, T., Haarpaintner, J., Bochert, A., Hartmann, J., Heygster, G., 2001. SSM/I Sea Ice Remote Sensing for Mesoscale Ocean-Atmosphere Interaction Analysis. Canadian Journal of Remote Sensing 27, 526–537. https://doi.org/10.1080/07038992.2001.10854892

Kaleschke, L., Tian-Kunze, X., 2016. "AMSR2 ASI 3.125 km Sea Ice Concentration Data, V0.1". Institute of Oceanography, University of Hamburg, Germany, digital media (ftp-projects.zmaw.de/seaice/) [1/1/2013 - 31/12/2015].

Kimmel, D.G., Eisner, L.B., Wilson, M.T., Duffy-Anderson, J.T., 2018. Copepod dynamics across warm and cold periods in the eastern Bering Sea: Implications for walleye pollock (*Gadus chalcogrammus*) and the Oscillating Control Hypothesis. Fish. Oceanogr. 27, 143–158. https://doi.org/10.1111/fog.12241

Kitamura, M., Amakasu, K., Kikuchi, T., Nishino, S., 2017. Seasonal dynamics of zooplankton in the southern Chukchi Sea revealed from acoustic backscattering strength. Cont. Shelf Res. 133, 47–58. https://doi.org/10.1016/j.csr.2016.12.009

Laidre, K.L., Heide-Jørgensen, M.P., 2012. Spring partitioning of Disko Bay, West Greenland, by Arctic and Subarctic baleen whales. ICES J. Mar. Sci. 69, 1226–1233. https://doi.org/10.1093/icesjms/fss095

Laidre, K.L., Stern, H., Kovacs, K.M., Lowry, L., Moore, S.E., Regehr, E.V., Ferguson, S.H., Wiig, Ø., Boveng, P., Angliss, R.P., Born, E.W., Litovka, D., Quakenbush, L., Lydersen, C., Vongraven, D., Ugarte, F., 2015. Arctic marine mammal population status, sea ice habitat loss, and conservation recommendations for the 21st century: Arctic Marine Mammal Conservation. Conserv. Biol. 29, 724–737. https://doi.org/10.1111/cobi.12474

Matsuno, K., Yamaguchi, A., Hirawake, T., Imai, I., 2011. Year-to-year changes of the mesozooplankton community in the Chukchi Sea during summers of 1991, 1992 and 2007, 2008. Polar Biol. 34, 1349–1360. https://doi.org/10.1007/s00300-011-0988-z

Markus, T., Stroeve, J.C., Miller, J., 2009. Recent changes in Arctic sea ice melt onset, freezeup, and melt season length. J. Geophys. Res. 114. https://doi.org/10.1029/2009JC005436

McDonald, M.A., Hildebrand, J.A., Webb, S.C., 1995. Blue and fin whales observed on a seafloor array in the Northeast Pacific. J. Acoust. Soc. Am. 98, 712–721. https://doi.org/10.1121/1.413565

Mellinger, D.K., Clark, C.W., 2000. Recognizing transient low-frequency whale sounds by spectrogram correlation. J. Acoust. Soc. Am. 107, 3518–29.

Mellinger, D., 2002. Ishmael 1.0 User's Guide. NOAA Technical Memorandum OAR PMEL-120. http://www.pmel.noaa.gov/pubs/PDF/mell2434/mell2434.pdf.

Mizroch, S.A., Rice, D.W., Breiwick, J.M., 1984. The fin whale, *Balaenoptera physalus*. Mar. Fish. Rev. 46, 20–24.

Mizroch, S.A., Rice, D.W., Zwiefelhofer, D., Waite, J., Perryman, W.L., 2009. Distribution and movements of fin whales in the North Pacific Ocean. Mammal Rev. 39, 193–227. https://doi.org/10.1111/j.1365-2907.2009.00147.x

Moore, S.E., George, J.C., Coyle, K.O., Weingartner, T.J., 1995. Bowhead whales along the Chukotka Coast in autumn. Arctic 48, 155–160.

Moore, S.E., Stafford, K.M., Dahlheim, M.E., Fox, C.G., Braham, H.W., Polovina, J.J., Bain, D.E., 1998. Seasonal variation in reception of fin whale calls at five geographic areas in the North Pacific. Mar. Mamm. Sci. 14, 617–627.

Moore, S.E., Waite, J., Mazzuca, L., Hobbs, R., 2000. Mysticete whale abundance and observations of prey associations on the central Bering Sea shelf. J. Cetac. Res. Manage. 2, 227–234.

Morris, B.A., 2019. Seasonality and forcing factors of the Alaskan Coastal Current in the Bering Strait from July 2011 to July 2012 (Thesis). University of Washington, Seattle, WA.

Nasu, K., 1960. Oceanographic investigation in the Chukchi Sea during the summer of 1958. Scientific Reports of the Whales Research Institute 15, 143–157.

Nemoto, T., 1959. Food of baleen whales with reference to whale movements. Scientific Reports of the Whales Research Institute 14, 149–290.

Nemoto, T., Kasuya, T., 1965. Foods of baleen whales in the Gulf of Alaska of the North Pacific. Scientific Reports of the Whales Research Institute 19, 45–51.

Nikulin, P.G., 1946. Distribution of cetaceans in the seas surrounding the Chukchi Peninsula. Izv. TINRO 22.

Ohashi, R., Yamaguchi, A., Matsuno, K., Saito, R., Yamada, N., Iijima, A., Shiga, N., Imai, I., 2013. Interannual changes in the zooplankton community structure on the southeastern Bering Sea shelf during summers of 1994–2009. Deep Sea Res. Part II Top. Stud. Oceanogr. 94, 44–56. https://doi.org/10.1016/j.dsr2.2013.03.018

Piatt, J., Springer, A., 2003. Advection, pelagic food webs and the biogeography of seabirds in Beringia. Mar. Ornithol. 31, 141–154.

Piatt, J., Jones, T., Kuletz, K., et al., 2018. Unprecedented scale of seabird mortality in the NE Pacific during the 2015-2016 marine heatwave. Presented at the Alaska Marine Science Symposium, Anchorage, Alaska.

Pike, G., 1950. Stomach contents of whales caught off the coast of British Columbia. Fisheries Research Board Canadian Pacific Progress Report 83, 27–28.

Pinchuk, A.I., Eisner, L.B., 2017. Spatial heterogeneity in zooplankton summer distribution in the eastern Chukchi Sea in 2012–2013 as a result of large-scale interactions of water masses. Deep Sea Res. Part II Top. Stud. Oceanogr. 135, 27–39. https://doi.org/10.1016/j.dsr2.2016.11.003

Pisareva, M.N., Pickart, R.S., Spall, M.A., Nobre, C., Torres, D.J., Moore, G.W.K., Whitledge, T.E., 2015. Flow of pacific water in the western Chukchi Sea: results from the 2009 RUSALCA expedition. Deep Sea Res. Part I Oceanogr. Res. Pap. 105, 53–73. https://doi.org/10.1016/j.dsr.2015.08.011

Pisareva, M.N., 2018. An overview of the recent research on the Chukchi Sea water masses and their circulation. Russ. J. Earth Sci. 18, 1–13.

Post, E., Alley, R.B., Christensen, T.R., Macias-Fauria, M., Forbes, B.C., Gooseff, M.N., Iler, A., Kerby, J.T., Laidre, K.L., Mann, M.E., Olofsson, J., Stroeve, J.C., Ulmer, F., Virginia, R.A., Wang, M., 2019. The polar regions in a 2°C warmer world. Sci. Adv. 5, eaaw9883. https://doi.org/10.1126/sciadv.aaw9883

Reynolds, R.W., Smith, T.M., Liu, C., Chelton, D.B., Casey, K.S., Schlax, M.G., 2007. Daily High-Resolution-Blended Analyses for Sea Surface Temperature. J. Clim. 20, 5473–5496. https://doi.org/10.1175/2007JCLI1824.1

Root, T.L., Price, J.T., Hall, K.R., Schneider, S.H., Rosenzweig, C., Pounds, J.A., 2003. Fingerprints of global warming on wild animals and plants. Nature 421, 57–60. https://doi.org/10.1038/nature01333

Savage, K., 2017. Alaska and British Columbia large whale unusual mortality event summary report. Protected Resources Division, National Oceanic and Atmospheric Administration, Juneau, AK.

Serreze, M.C., Barrett, A.P., Stroeve, J.C., Kindig, D.N., Holland, M.M., 2009. The emergence of surface-based Arctic amplification. Cryosphere 3, 11–19. https://doi.org/10.5194/tc-3-11-2009

Serreze, M.C., Crawford, A.D., Stroeve, J.C., Barrett, A.P., Woodgate, R.A., 2016. Variability, trends, and predictability of seasonal sea ice retreat and advance in the Chukchi Sea. J. Geophys. Res.: Oceans 121, 7308–7325. https://doi.org/10.1002/2016JC011977

Sigler, M.F., Mueter, F.J., Bluhm, B.A., Busby, M.S., Cokelet, E.D., Danielson, S.L., Robertis, A.D., Eisner, L.B., Farley, E.V., Iken, K., Kuletz, K.J., Lauth, R.R., Logerwell, E.A., Pinchuk, A.I., 2017. Late summer zoogeography of the northern Bering and Chukchi seas. Deep Sea Res. Part II Top. Stud. Oceanogr. 135, 168–189. https://doi.org/10.1016/j.dsr2.2016.03.005

Širović, A., Hildebrand, J.A., Wiggins, S.M., 2007. Blue and fin whale call source levels and propagation range in the Southern Ocean. J. Acoust. Soc. Am. 122, 1208–1215. https://doi.org/10.1121/1.2749452

Širović, A., Williams, L.N., Kerosky, S.M., Wiggins, S.M., Hildebrand, J.A., 2013. Temporal separation of two fin whale call types across the eastern North Pacific. Mar. Biol. 160, 47–57. https://doi.org/10.1007/s00227-012-2061-z

Sleptsov, M.M., 1961. O kolebaniakh chislennosti kitov v Chukotskom more v raznye gody. (On fluctuations in the number of whales in the Chukchi Sea in different years), in: Proceedings of the A.N. Severtsov Institute of Animal Morphology. Nauka, Moscow, pp. 54–64.

Spreen, G., Kaleschke, L., Heygster, G., 2008. Sea ice remote sensing using AMSR-E 89-GHz channels. J. Geophys. Res. 113, C02S03. https://doi.org/10.1029/2005JC003384

Springer, A.M., McRoy, C.P., 1993. The paradox of pelagic food webs in the northern Bering Sea—III. Patterns of primary production. Cont. Shelf Res. 13, 575–599. https://doi.org/10.1016/0278-4343(93)90095-F

Stabeno, P.J., Kachel, N.B., Moore, S.E., Napp, J.M., Sigler, M., Yamaguchi, A., Zerbini, A.N., 2012. Comparison of warm and cold years on the southeastern Bering Sea shelf and some implications for the ecosystem. Deep Sea Res. Part II Top. Stud. Oceanogr. 65–70, 31–45. https://doi.org/10.1016/j.dsr2.2012.02.020

Stabeno, P.J., Bell, S.W., Bond, N.A., Kimmel, D.G., Mordy, C.W., Sullivan, M.E., 2019. Distributed Biological Observatory Region 1: Physics, chemistry and plankton in the northern Bering Sea. Deep Sea Res. Part II Top. Stud. Oceanogr. 162, 8–21. https://doi.org/10.1016/j.dsr2.2018.11.006

Stafford, K.M., Mellinger, D.K., Moore, S.E., Fox, C.G., 2007. Seasonal variability and detection range modeling of baleen whale calls in the Gulf of Alaska, 1999–2002. J. Acoust. Soc. Am. 122, 3378–3390. https://doi.org/10.1121/1.2799905

Stroeve, J.C., Serreze, M.C., Holland, M.M., Kay, J.E., Malanik, J., Barrett, A.P., 2012. The Arctic's rapidly shrinking sea ice cover: a research synthesis. Climatic Change 110, 1005–1027. https://doi.org/10.1007/s10584-011-0101-1

Stroeve, J.C., Markus, T., Boisvert, L., Miller, J., Barrett, A., 2014. Changes in Arctic melt season and implications for sea ice loss. Geophys. Res. Lett. 41, 1216–1225. https://doi.org/10.1002/2013GL058951

Tomilin, A.G. 1957. Zveri SSSR i Prilezhashchikh Stran (The Mammals of the USSR and Adjacent Countries). Vol. IX. Kitoobraznye (Cetacea). Proceedings of the USSR Academy of Sciences. Nauk USSR, Moscow. 756 pp. [In Russian]

Tsujii, K., Otsuki, M., Akamatsu, T., Matsuo, I., Amakasu, K., Kitamura, M., Kikuchi, T., Miyashita, K., Mitani, Y., 2016. The migration of fin whales into the southern Chukchi Sea as monitored with passive acoustics. ICES J. Mar. Sci.: Journal du Conseil 73, 2085–2092. https://doi.org/10.1093/icesjms/fsv271

Vaughan, D. G., Comiso, J., Allison, I., Carrasco, J., Kaser, G., Kwok, R., et al., 2013. Observations: Cryosphere. In T. F. Stocker, D. Qin, G. K. Plattner, M. Tignor, S. K. Allen, J. Boschung, A. Nauels, et al., (Eds.), Climate change 2013: The physical science basis. Contribution of working group I to the fifth assessment report of the intergovernmental

panel on climate change Cambridge, United Kingdom and New York, NY, USA: Cambridge University Press.

Votrogov, L.M., and M.V. Ivashin. 1980. Sightings of fin and humpback whales in the Bering and Chukchi Seas. Report of the International Whaling Commission 30:247–248.

Walsh, J.E., Fetterer, F., Scott stewart, J., Chapman, W.L., 2017. A database for depicting Arctic sea ice variations back to 1850. Geogr. Rev. 107, 89–107. https://doi.org/10.1111/j.1931-0846.2016.12195.x

Wassmann, P., Duarte, C.M., Agustí, S., Sejr, M.K., 2011. Footprints of climate change in the Arctic marine ecosystem. Glob. Change Biol. 17, 1235–1249. https://doi.org/10.1111/j.1365-2486.2010.02311.x

Watkins, W.A., 1981. Activities and underwater sounds of fin whales. Scientific Reports of the Whales Research Institute 33, 83–117.

Watkins, W.A., Tyack, P., Moore, K.E., Bird, J.E., 1987. The 20-Hz signals of finback whales (*Balaenoptera physalus*). J. Acoust. Soc. Am. 82, 1901–1912.

Watkins, W.A., Daher, M.A., Repucci, G.M., George, J.E., Martin, D.L., Dimarzio, N.A., Gannon, D.P., 2000. Seasonality and distribution of whale calls in the North Pacific. Oceanography 13, 62–67.

Weingartner, T., 1997. A review of the physical oceanography of the northeastern Chukchi Sea. In: Reynolds, J. (Ed.), Fish Ecology in Arctic North America, American Fisheries Society Symposium. Bethesda, MD, pp. 40–59.

Weingartner, T.J., Danielson, S., Sasaki, Y., Pavlov, V., Kulakov, M., 1999. The Siberian Coastal Current: A wind- and buoyancy-forced Arctic coastal current. J. Geophys. Res. Oceans 104, 29697–29713. https://doi.org/10.1029/1999JC900161

Witteveen, B.H., Wynne, K.M., 2016. Trophic niche partitioning and diet composition of sympatric fin (Balaenoptera physalus) and humpback whales (*Megaptera novaeangliae*) in the Gulf of Alaska revealed through stable isotope analysis. Mar. Mamm. Sci. 32, 1319–1339. https://doi.org/10.1111/mms.12333

Wood, K., Wang, J., Salo, S., Stabeno, P., 2015a. The climate of the Pacific Arctic during the first RUSALCA decade 2004–2013. Oceanography 28, 24–35. https://doi.org/10.5670/oceanog.2015.55

Wood, K.R., Bond, N.A., Danielson, S.L., Overland, J.E., Salo, S.A., Stabeno, P.J., Whitefield, J., 2015b. A decade of environmental change in the Pacific Arctic region. Prog. Oceanogr. 136, 12–31. https://doi.org/10.1016/j.pocean.2015.05.005

Woodgate, R.A., Aagaard, K., Weingartner, T.J., 2005a. A year in the physical oceanography of the Chukchi Sea: Moored measurements from autumn 1990–1991. Deep Sea Res. Part II Top. Stud. Oceanogr. 52, 3116–3149. https://doi.org/10.1016/j.dsr2.2005.10.016

Woodgate, R.A., Aagaard, K., Weingartner, T.J., 2005b. Monthly temperature, salinity, and transport variability of the Bering Strait through flow. Geophys. Res. Lett. 32, n/a-n/a. https://doi.org/10.1029/2004GL021880

Woodgate, R., Stafford, K., Prahl, F., 2015. A synthesis of year-round interdisciplinary mooring measurements in the Bering Strait (1990–2014) and the RUSALCA years (2004–2011). Oceanography 28, 46–67. https://doi.org/10.5670/oceanog.2015.57

Woodgate, R.A., 2018. Increases in the Pacific inflow to the Arctic from 1990 to 2015, and insights into seasonal trends and driving mechanisms from year-round Bering Strait mooring data. Prog. Oceanogr. 160, 124–154. https://doi.org/10.1016/j.pocean.2017.12.007

Zerbini, A.N., Waite, J.M., Laake, J.L., Wade, P.R., 2006. Abundance, trends and distribution of baleen whales off Western Alaska and the central Aleutian Islands. Deep Sea Res. Part I Oceanogr. Res. Pap. 53, 1772–1790. https://doi.org/10.1016/j.dsr.2006.08.009

2.8 Tables

Table 2.1. Recording settings and positions of the three hydrophones. Dates are in the format 'mm/dd/yyyy.'

Mooring	Year	Latitude N	Latitude W	Record Start Date	Record End Date	Sampling Rate (Hz)	Hourly Duty Cycle
A2	2009	65.80°	168.80°	09/01/2009	01/16/2010	16384	12 min
	2010	65.80°	168.80°	08/11/2010	12/08/2010	16384	15 min
	2012	65.80°	168.80°	09/01/2012	05/15/2013	16384	10 min
	2013	65.78°	168.57°	07/15/2013	07/01/2014	8192	20 min
	2014	65.78°	168.57°	07/10/2014	07/04/2015	8192	20 min
	2015	65.78°	168.57°	07/05/2015	07/08/2016	8192	20 min
A3	2009	66.33°	168.97°	09/01/2009	03/03/2010	16384	12 min
	2010	66.33°	168.97°	08/11/2010	02/19/2011	16384	15 min
	2011	66.33°	168.97°	10/01/2011	05/25/2012	8192	10 min
	2012	66.33°	168.97°	09/01/2012	05/17/2013	16384	10 min
	2013	66.33°	168.97°	07/15/2013	07/02/2014	8192	20 min
	2014	66.33°	168.97°	07/10/2014	07/02/2015	8192	20 min
	2015	66.33°	168.97°	07/05/2015	07/08/2016	8192	20 min
A4	2012	65.75°	168.37°	09/01/2012	06/24/2013	16384	10 min
	2013	65.75°	168.26°	07/15/2013	07/02/2014	8192	20 min
	2014	65.75°	168.25°	07/10/2014	07/02/2015	8192	20 min
	2015	65.75°	168.25°	07/05/2015	07/08/2016	8192	20 min

Table 2.2. Fin whale detection data for the three moorings, including the dates of the first and last detection, and total number of days with fin whale calls present ('FW Days'). The '.' indicates periods when the hydrophone was not actively recording.

	A2			A3			A4		
Year	**First Detection Date**	**Last Detection Date**	**FW Days**	**First Detection Date**	**Last Detection Date**	**FW Days**	**First Detection Date**	**Last Detection Date**	**FW Days**
2009	1 Oct	5 Nov	4	23 Sep	8 Nov	33	.	.	.
2010	14 Oct	17 Oct	2	29 Sep	5 Nov	22	.	.	.
2011	.	.	.	1 Oct	18 Nov	28	.	.	.
2012	28 Oct	2 Nov	3	1 Sep	7 Nov	52	None	None	0
2013	22 Sep	15 Nov	7	23 Jul	9 Nov	28	None	None	0
2014	17 Oct	19 Oct	3	9 Aug	13 Nov	37	2 Nov	2 Nov	1
2015	30 Sep	19 Nov	14	8 Aug	20 Nov	71	11 Oct	8 Nov	7

Table 2.3. Wilcoxon rank-sum test results comparing fin whale hours (FWH) recorded at A3 in October of each year. The *p*-values are listed in the upper section above the diagonal, and the gray shaded area below the diagonal are the W statistics from the Wilcoxon rank-sum tests (**bold** W values indicate significant results). Significant *p*-values ($p < 0.05$) are in **bold*** and indicate that the distribution of FWHs significantly differed between the two years.

Year	2009	2010	2011	2012	2013	2014	2015
2009	.	0.736	0.147	**0.002***	0.42	**0.026***	**0.000***
2010	174.5	.	0.463	**0.002***	0.554	0.062	**0.000***
2011	186	220	.	**0.002***	0.566	**0.003***	**0.000***
2012	**69**	**77**	**76**	.	**0.003***	0.614	**0.007***
2013	223	185	98.5	**399.5**	.	**0.004***	**0.000***
2014	**96**	120.5	**57.5**	257.5	**47.5**	.	**0.006***
2015	**30**	**14**	**14.5**	**110**	**21**	**106**	.

Table 2.4. Sea ice statistics calculated for 2009–2015 for the study area and Chukchi Sea. Statistics for the study area include: melt initiation date ('Melt-Out Date'), melt period (number of days between 80% and 15% sea ice conc.), date when the study area was ice-free (<15% conc.; 'Ice-Free Date'), Freeze-up Period (number of days between 15% and 80% sea ice conc.), and mean sea ice concentration (%) in the study area on the last date fin whale calls were recorded ('Last FW'). Statistics for the Chukchi Sea include mean sea ice concentration (%) on the last date fin whale calls were recorded ('Last FW').

	Study Area							Chukchi Sea
Year	**Melt-Out Date**	**Ice-Free Date**	**Melt Period (# of days)**	**Freeze-up Date**	**Freeze-up Period (# of days)**	**Mean Nov. sea ice conc.**	**Last FW $\bar{x}$ sea ice conc.**	**Last FW $\bar{x}$ sea ice conc.**
2009	14 May	5 June	23	28 Nov	12	30.2%	0.9%	1.5%
2010	20 May	17 June	29	25 Dec	23	3.4%	1.3%	4.5%
2011	27 April	30 May	34	4 Dec	12	13.3%	0.8%	21.0%
2012	16 May	10 June	25	11 Dec	23	21.3%	1.9%	18.8%
2013	5 May	14 June	41	18 Dec	19	6.3%	3.1%	12.8%
2014	1 May	31 May	31	17 Dec	5	5.4%	4.1%	7.07%
2015	4 May	24 May	21	10 Dec	17	20.1%	4.9%	18.2%

Table 2.5. Summary of the overall monthly mean along-channel wind velocities (m/s) for October along with overall means for days with and without fin whale hours (FWH) in October. Wind velocities were measured at the data point at 67.5°N and 190°W. Values in parentheses are the Wilcoxon rank-sum *p*-values for the comparison between the overall October mean for each year (**bold***: significant $p < 0.05$).

Year	All October (m/s)	Days without FWH (m/s)	Days with ≥ 1 FWH (m/s)	Days with ≥6 FWH (m/s)	Days with ≥12 FWH (m/s)	Days with ≥ 18 FWH (m/s)
2009	-2.7	2.5 (**0.03***)	-5.2 (0.19)	-6.2 (0.07)	-6.6 (0.21)	NA
2010	-5.1	-3.2 (0.46)	-6.2 (0.58)	-7.3 (0.37)	-7.9 (0.25)	-9.5 (NA)
2011	-2.1	0.6 (0.12)	-4 (0.21)	-6.1 (**0.04***)	-8.7 (**0.02***)	NA
2012	-0.4	1.3 (0.97)	-0.5 (0.99)	-2.5 (0.45)	-3 (0.33)	-5.8 (NA)
2013	-6.2	-5.8 (0.88)	-6.7 (0.88)	-5.8 (0.84)	-7 (0.82)	NA
2014	-4.8	0.2 (**0.04***)	-6.2 (0.35)	-6.8 (0.25)	-7.9 (0.14)	-9.2 (NA)
2015	-4.0	5.5 (0.18)	-4.3 (0.86)	-4.7 (0.68)	-6 (0.255.3)	-7.1 (NA)

Table 2.6. Summary table of the Kendall's rank correlation test results for site A3. Correlation tests were conducted between the number of fin whale hours (FWH) recorded on days with fin whale calls (FWH > 0) and the daily means of: near-surface and near-bottom temperatures, along-channel wind and water velocities, water speeds, and SST. Two sets of tests were carried out: pooled data for all months for all years (2009−2015), and on October data only for all years at A3 (2009−2015).

Environmental Variable (Daily Means)	**Pooled data - all months (*n* = 271)**		**Oct only - all years pooled (*n* = 156)**	
	p	**τ**	***p***	**τ**
Near-surface Temperature	0.674	0.019	**0.012***	0.151
Near-surface Salinity	0.053	-0.087	0.851	-0.011
Near-bottom Temperature	0.82	0.01	0.129	0.084
Near-bottom Salinity	0.29	-0.044	0.507	0.037
Water Speed	**< 0.001***	**-0.167**	**< 0.001***	**-0.28**
SST	0.202	-0.054	**0.044***	**0.111**
Along-channel water velocity	**< 0.001***	**-0.15**	**< 0.001***	**-0.207**
Along-channel wind velocity	**< 0.001***	**-0.194**	**< 0.001***	**-0.231**

2.9 Figures

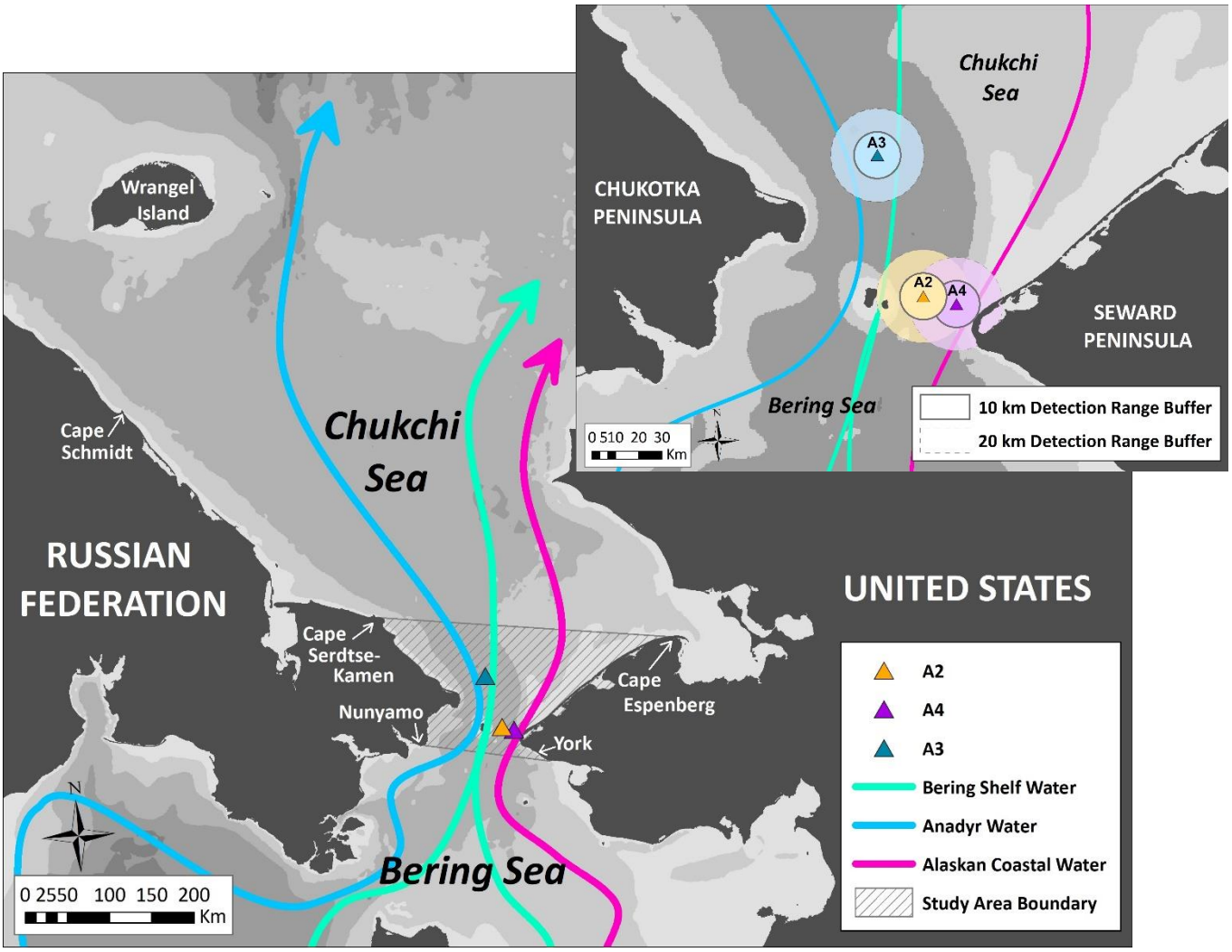

Fig. 2.1. Map of the study region with typical annual mean flow patterns of the three dominant water masses in the Bering Strait region and 20-m bathymetric contours (International Bathymetry Chart of the Arctic Ocean [IBCAO], *v.* 3; Jakobsson et al., 2012). Positions of the three moorings along with the boundaries of the study area polygon used in the sea ice concentration analysis are also displayed. Inset map shows estimated call detection range buffers around each mooring (10 and 20 km). Note that the Alaskan Coastal Water is only present seasonally.

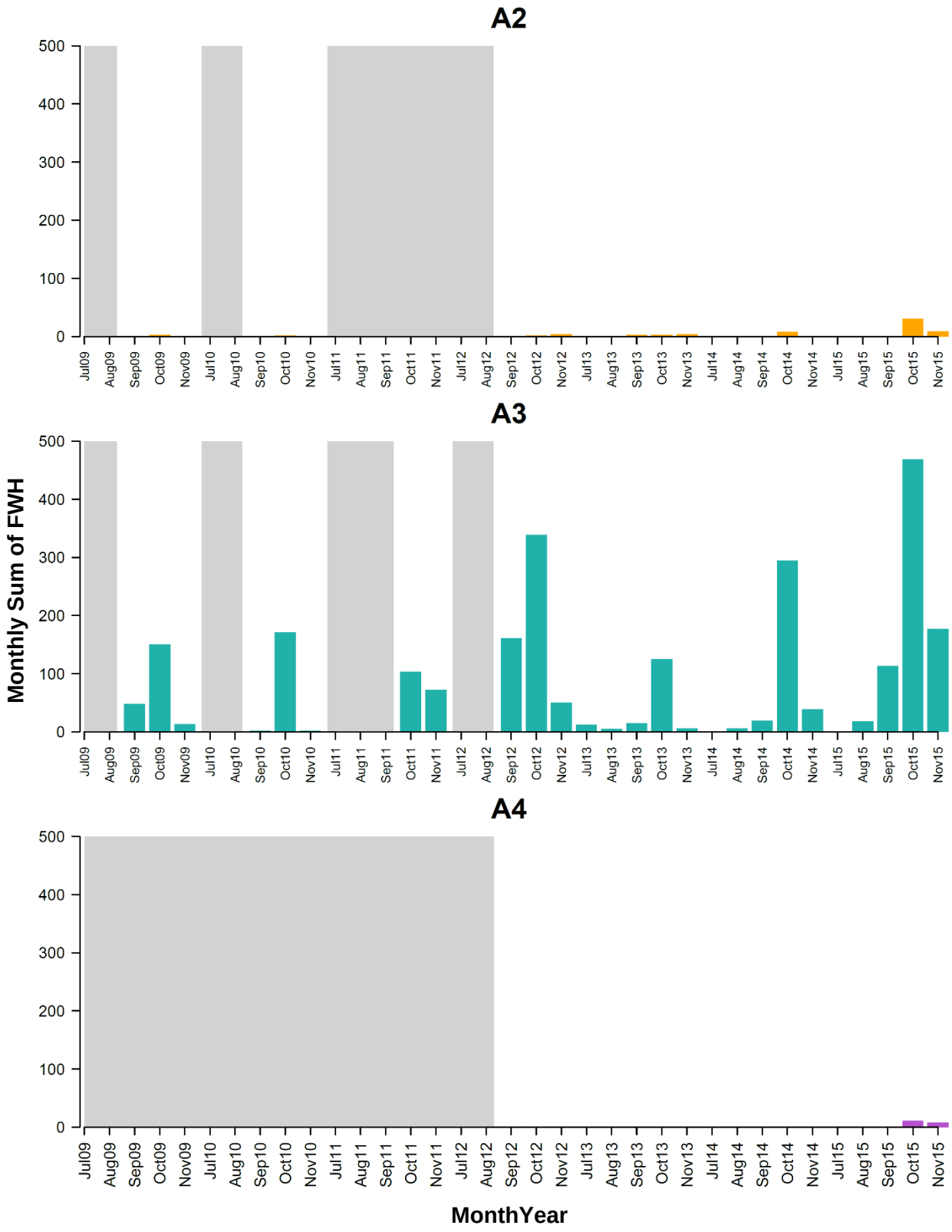

Fig. 2.2. Histograms of monthly sum of hours with fin whale calls ('FWH') recorded at the three mooring sites (A2, A3, and A4) within the Bering Strait region from 2009–2015. The gray-shaded boxes indicate periods when the hydrophones were not recording.

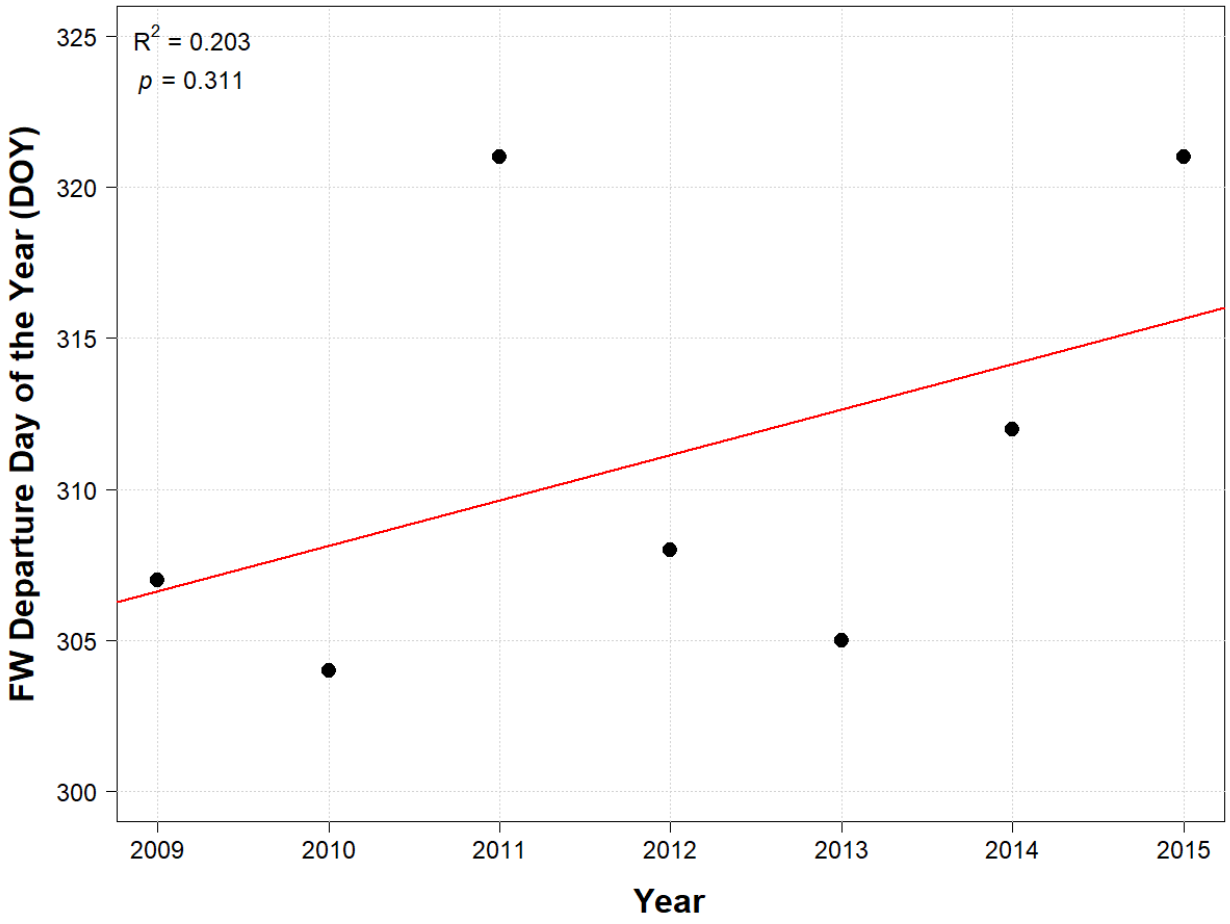

Fig. 2.3. Fin whale departure day of the year (DOY) for each year at the A3 mooring site, north of the Bering Strait, along with the line of best fit (R^2 = 0.203, p = 0.311).

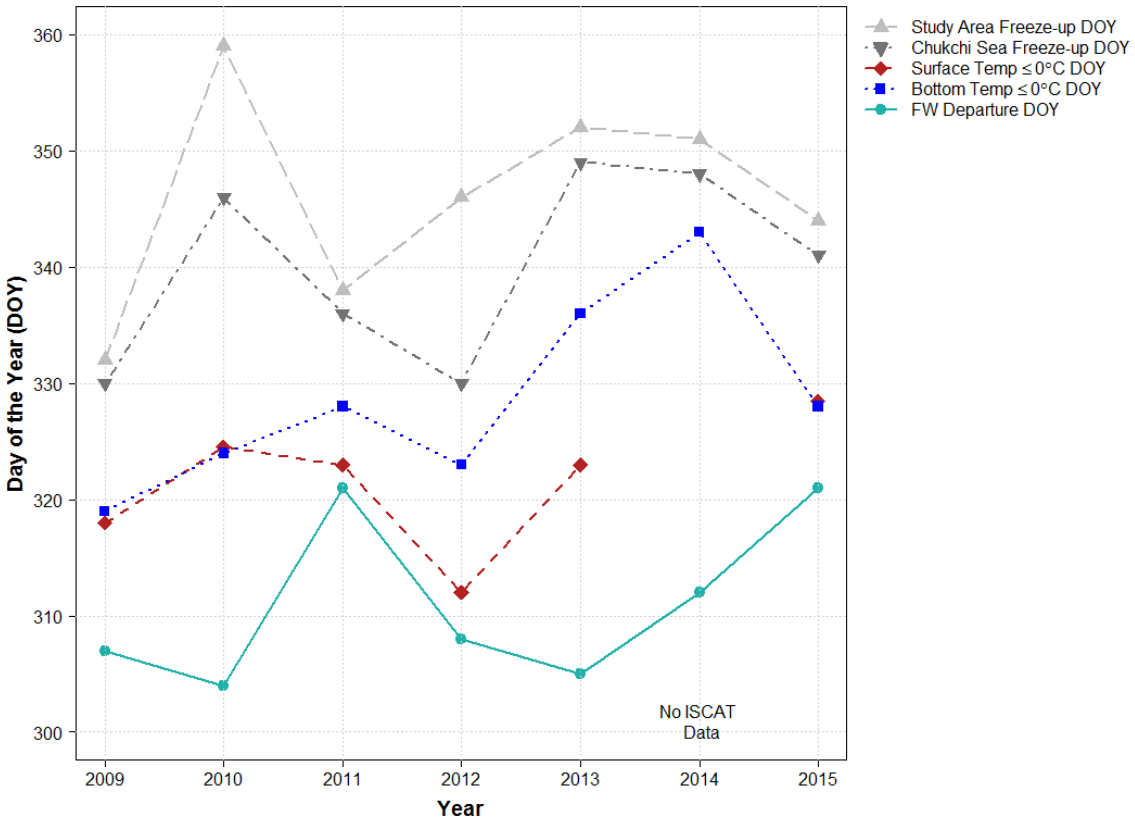

Fig. 2.4. Calculated fin whale departure days for each year at site A3 (light blue, solid line) with other non-solid lines indicating the day of the year (DOY) when the daily mean near-surface (ISCAT; red, medium-dashed line) and near-bottom (SBE; blue, dotted line) temperatures first reached ≤ 0 °C at the A3 mooring site. The light gray, long-dashed line represents the DOYs when sea ice concentration in the study area first reached ≥ 80% in each year, and the dark gray, dot-dashed line represents when sea ice concentration in the Chukchi Sea reached ≥ 80%. See Fig. 2.1 for boundaries of study area.

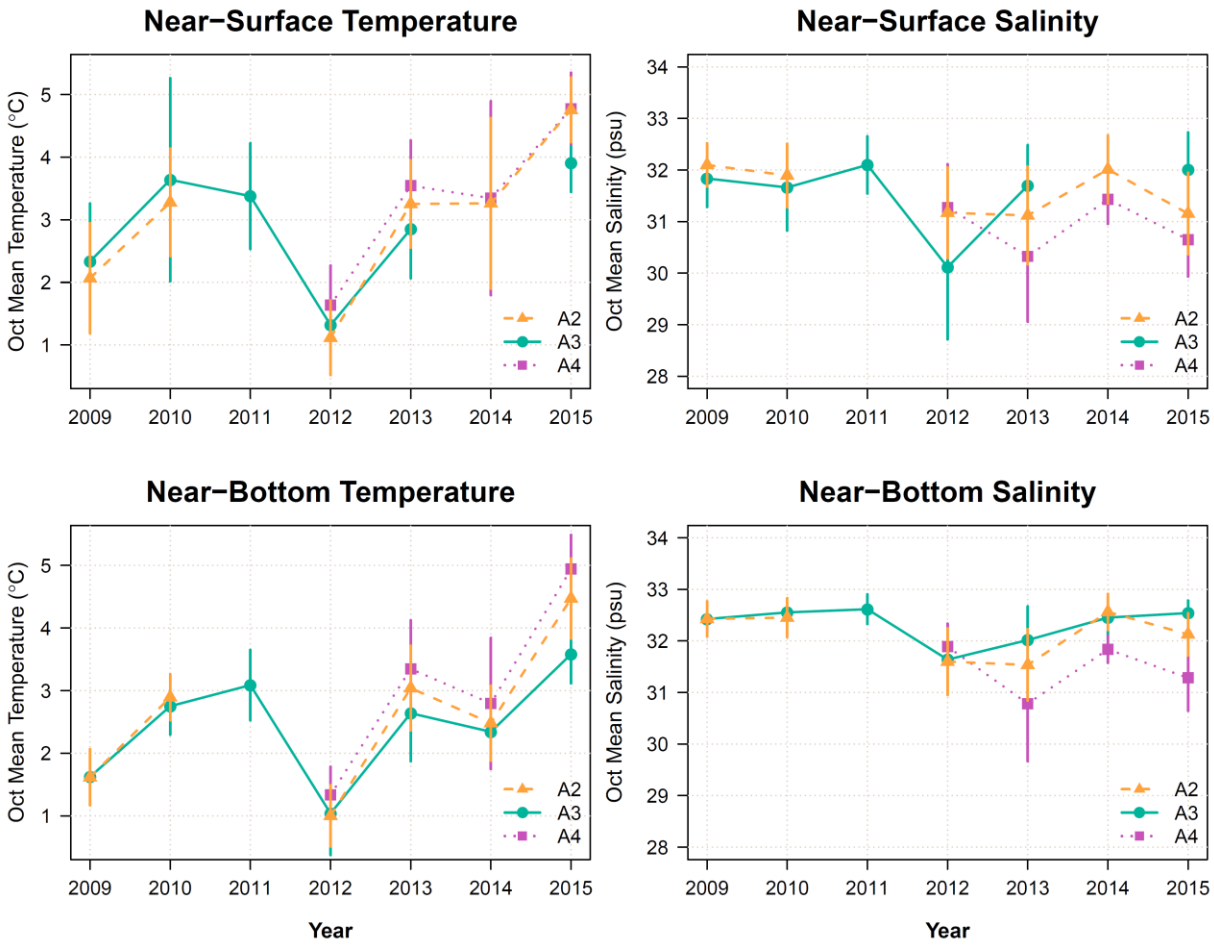

Fig. 2.5. Plots of the mean temperatures (°C) and salinities (psu) for October of each year for both the near-surface and near-bottom levels of the water column at each mooring site in the study area (A2, A3, and A4; see key for colors, symbols, and line styles). The vertical lines represent the standard deviation of the monthly means.

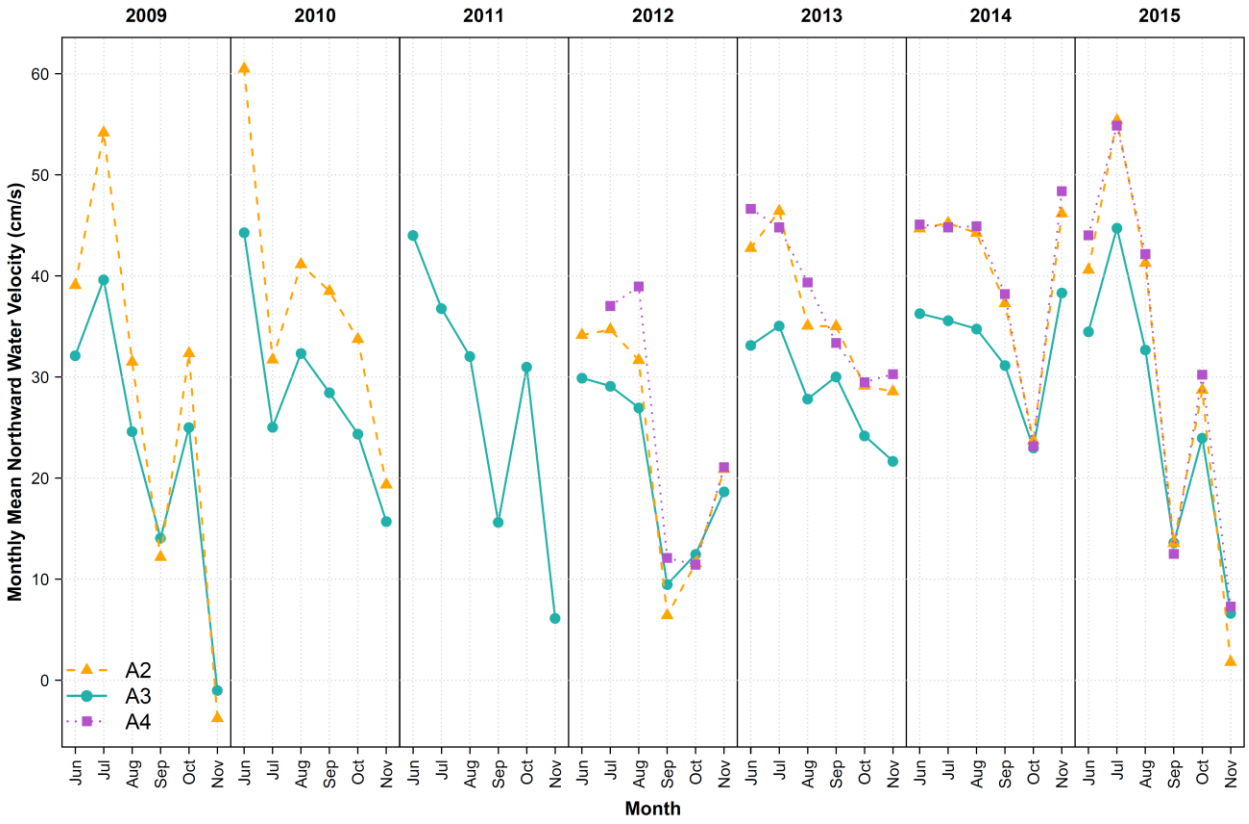

Fig. 2.6. Monthly mean northward water velocity (cm/s) for June through November at each mooring site in the Bering Strait region (A2, A3, and A4; see key for colors, symbols, and line styles). See Fig. 2.1 for mooring locations.

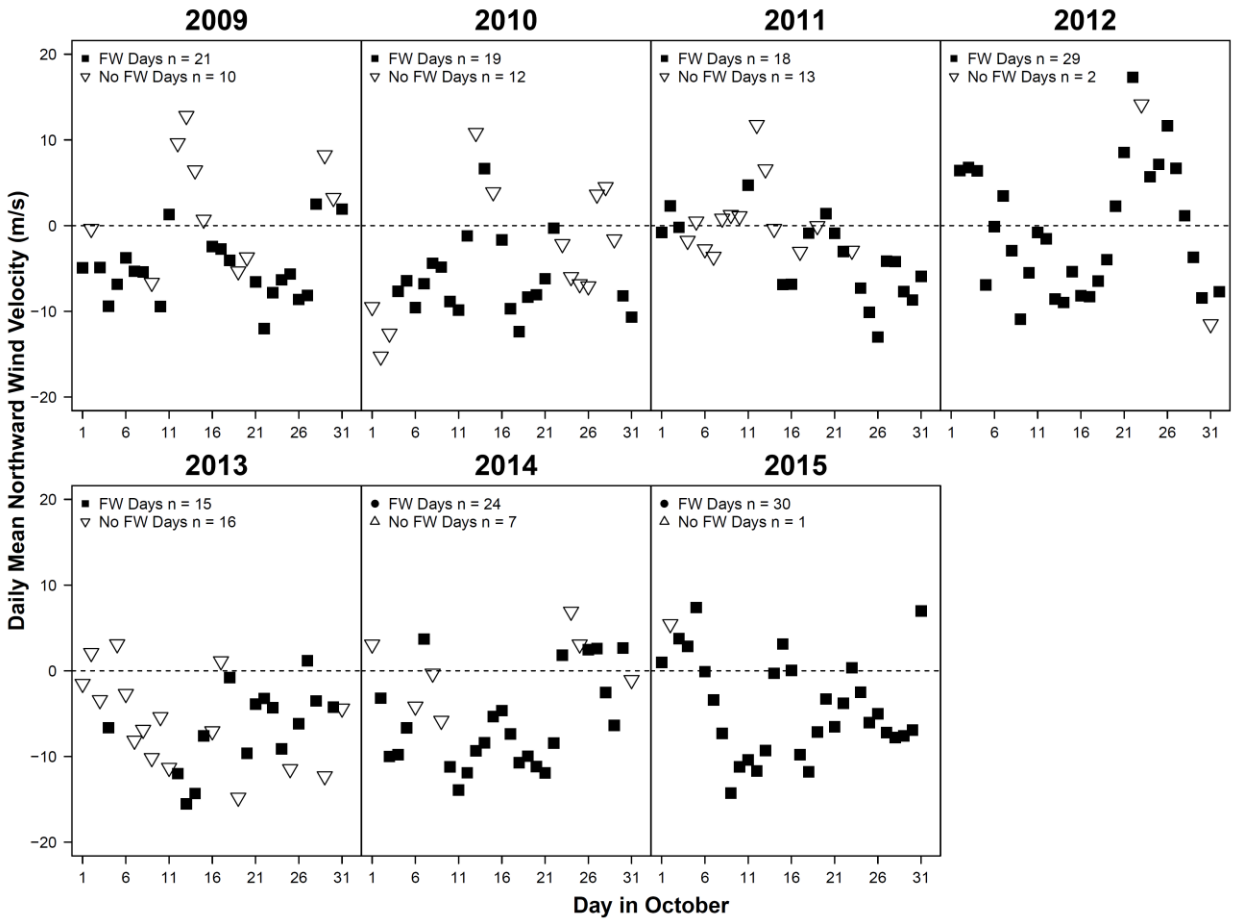

Fig. 2.7. Daily mean northward wind velocity for days with fin whale calls at site A3 ('FW Days', black squares) and days without fin whale calls ('No FW Days', white triangles) in October. Note that negative values signify southward wind velocities. The number of FW Days and No FW Days is included for reference.

2.10 Supplementary Tables and Figures

Table S2.1. Mooring instrument details for A2. Dates are given in the format 'mm/dd/yyyy.'

Year	Instrument	Record Frequency (min)	Instrument Depth (m)	Water Depth (m)	Record Start Date	Record End Date	Data Gap (# days)
2009	ISCAT	5	18	52	08/27/2009	08/02/2010	NA
	300kHz-ADCP	30	43	52	08/27/2009	08/01/2010	NA
	SBE16	60	47	52	08/27/2009	08/02/2010	NA
2010	ISCAT	5	19	53	08/04/2010	07/13/2011	2
	300kHz-ADCP	30	44	53	08/04/2010	07/13/2011	3
	SBE16	60	48	53	08/04/2010	07/13/2011	2
2012	ISCAT	5	19	53	07/14/2012	07/4/2013	367
	300kHz-ADCP	30	44	53	07/14/2012	07/4/2013	367
	SBE16	60	48	53	07/14/2012	07/4/2013	367
2013	ISCAT	30	15	54	07/06/2013	03/29/2014	2
	300kHz-ADCP	30	44	54	07/06/2013	07/01/2014	2
	SBE16	60	49	54	07/06/2013	07/01/2014	2
2014	ISCAT	5	16	53	07/03/2014	07/05/2015	96
	300kHz-ADCP	30	44	53	07/03/2014	07/04/2015	2
	SBE16	60	49	53	07/03/2014	07/05/2015	2
2015	ISCAT	30	14	54	07/05/2015	03/08/2016	0
	300kHz-ADCP	30	44	54	07/05/2015	07/08/2016	1
	SBE16	60	49	54	07/05/2015	07/08/2016	0

Table S2.2. Mooring instrument details for A3. Dates are given in the format 'mm/dd/yyyy.'

Year	Instrument	Record Frequency (min)	Instrument Depth (m)	Water Depth (m)	Record Start Date	Record End Date	Data Gap (# days)
2009	ISCAT	5	16	56	08/26/2009	08/03/2010	NA
	300kHz-ADCP	30	46	56	08/26/2009	08/02/2010	NA
	SBE37 Microcat	15	46	56	08/26/2009	08/03/2010	NA
2010	ISCAT	5	17	58	08/03/2010	07/14/2011	0
	600kHz-ADCP	30	44	58	08/03/2010	07/14/2011	1
	SBE37 Microcat	15	44	58	08/03/2010	07/14/2011	0
2011	ISCAT	30	15	57	07/14/2011	02/08/2012	0
	300kHz-ADCP	30	44	57	07/14/2011	07/13/2012	0
	SBE37 Microcat	15	44	57	07/14/2011	07/13/2012	0
2012	ISCAT	30	15	57	07/14/2012	03/04/2013	157
	600kHz-ADCP	30	44	57	07/14/2012	07/05/2013	1
	SBE37 Microcat	30	44	57	07/14/2012	07/05/2013	1
2013	ISCAT	5	16	56	07/05/2013	07/02/2014	123
	300kHz-ADCP	30	43	56	07/05/2013	07/02/2014	0
	SBE16	60	44	56	07/05/2013	07/02/2014	0
2014	ISCAT	30	15	56	07/02/2014	08/16/2014	0
	300kHz-ADCP	30	43	56	07/02/2014	07/03/2015	0
	SBE16	60	43	56	07/02/2014	07/03/2015	0
2015	ISCAT	30	15	56	07/03/2015	01/03/2016	321
	300kHz-ADCP	30	42	56	07/03/2015	07/08/2016	0
	SBE16	60	43	56	07/03/2015	07/08/2016	0

Table S2.3. Mooring instrument details for A4. Dates are given in the format 'mm/dd/yyyy.'

Year	Instrument	Record Frequency (min)	Instrument Depth (m)	Water Depth (m)	Record Start Date	Record End Date	Data Gap (# days)
2012	ISCAT	5	18	54	07/13/2012	07/04/2013	NA
	300kHz-ADCP	30	42	54	07/13/2012	07/04/2013	NA
	SBE16	60	45	54	07/13/2012	07/04/2013	NA
2013	ISCAT	30	16	47	07/06/2013	05/13/2014	2
	300kHz-ADCP	30	37	47	07/06/2013	07/01/2014	2
	SBE16	30	40	47	07/06/2013	07/01/2014	2
2014	ISCAT	30	15	47	07/03/2014	02/09/2015	51
	300kHz-ADCP	30	37	47	07/03/2014	07/03/2015	2
	SBE16	30	40	47	07/03/2014	07/03/2015	2
2015	ISCAT	30	14	47	07/04/2015	03/11/2016	145
	300kHz-ADCP	30	36	47	07/04/2015	07/08/2016	1
	SBE16	60	41	47	07/04/2015	07/08/2016	1

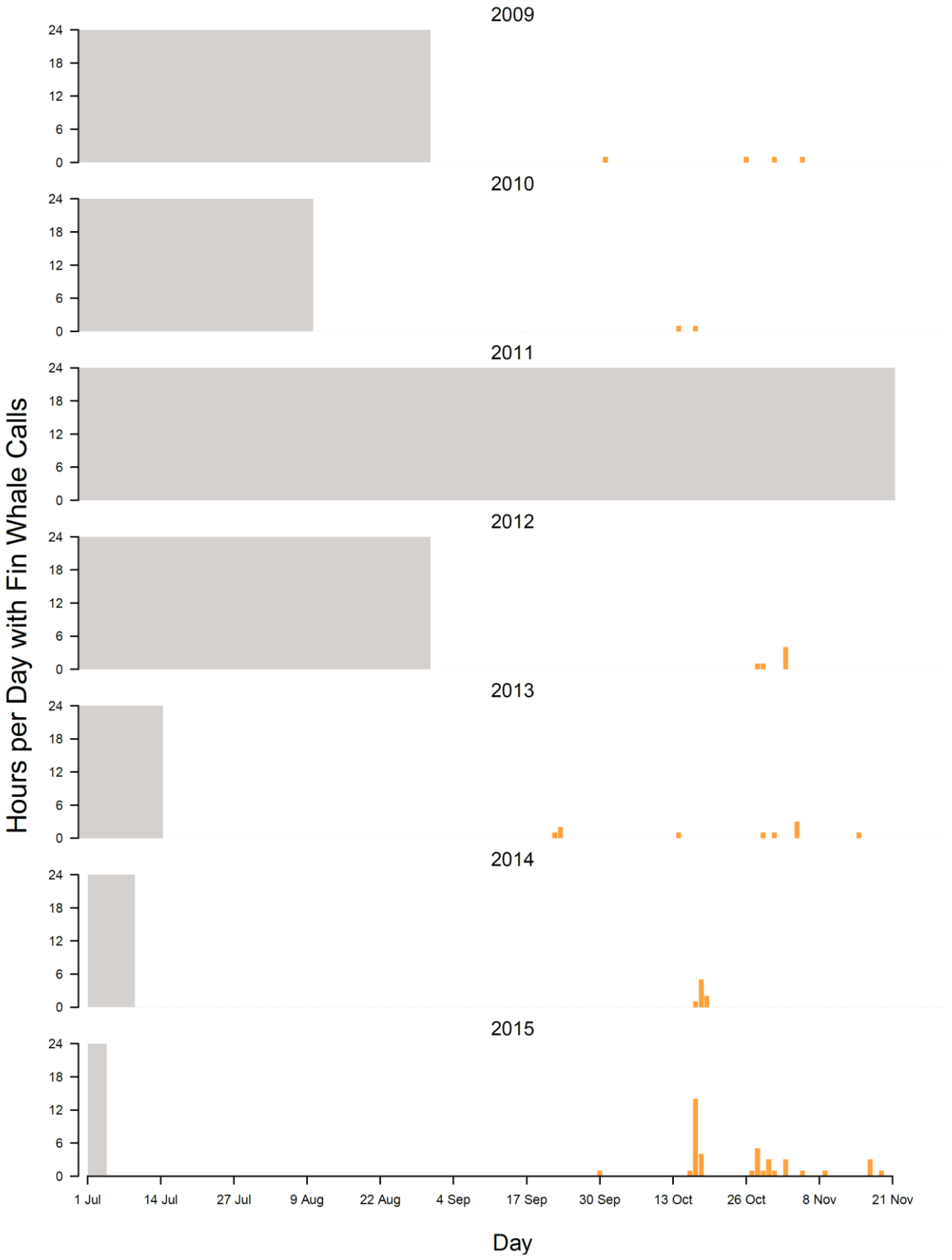

Fig. S2.1. The total number of fin whale hours is summed for each recording day at site A2 and plotted for each year. Gray-shaded areas indicate when the hydrophone was not recording.

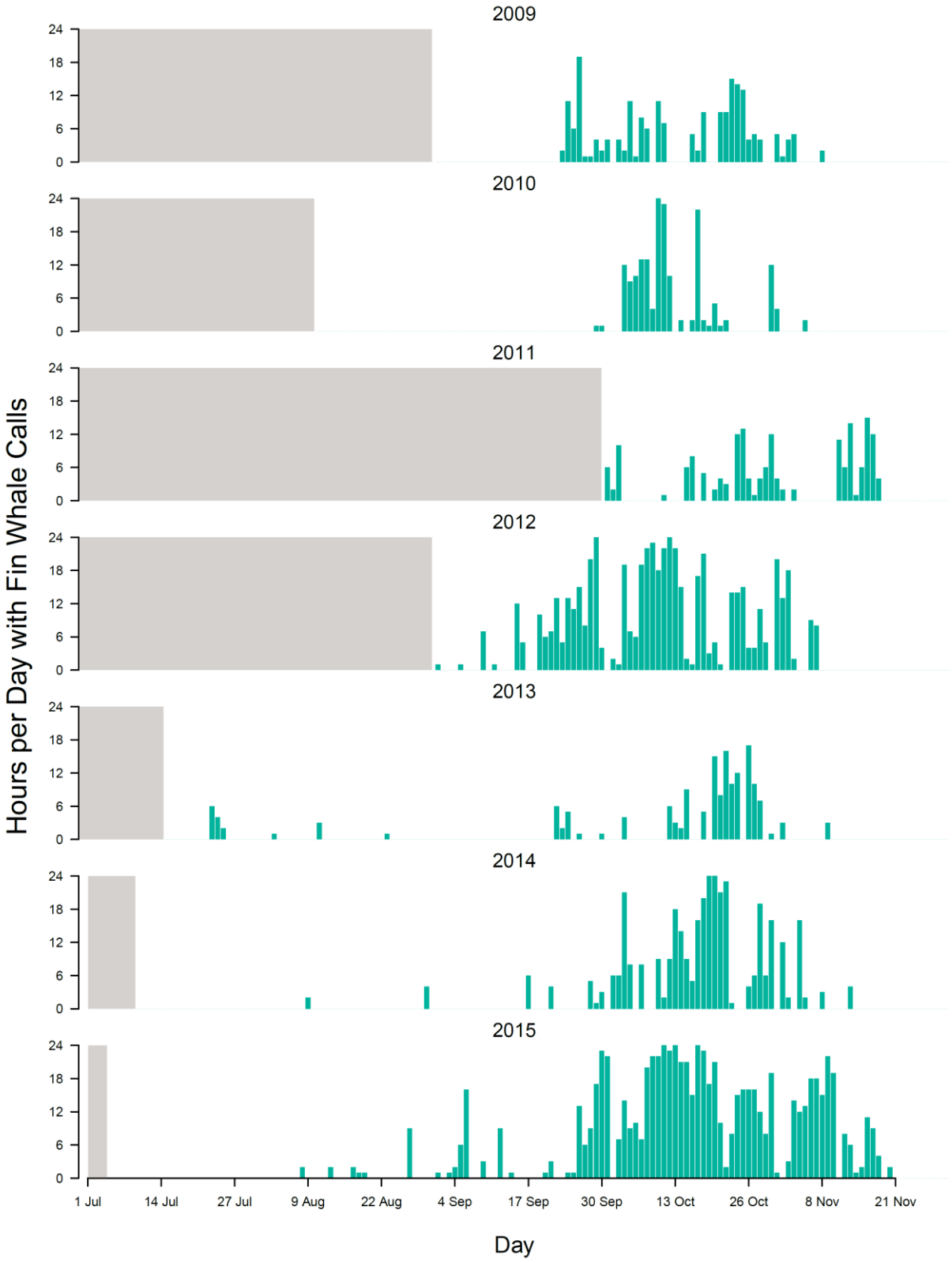

Fig. S2.2. The total number of fin whale hours is summed for each recording day at site A3 and plotted for each year. Gray-shaded areas indicate when the hydrophone was not recording.

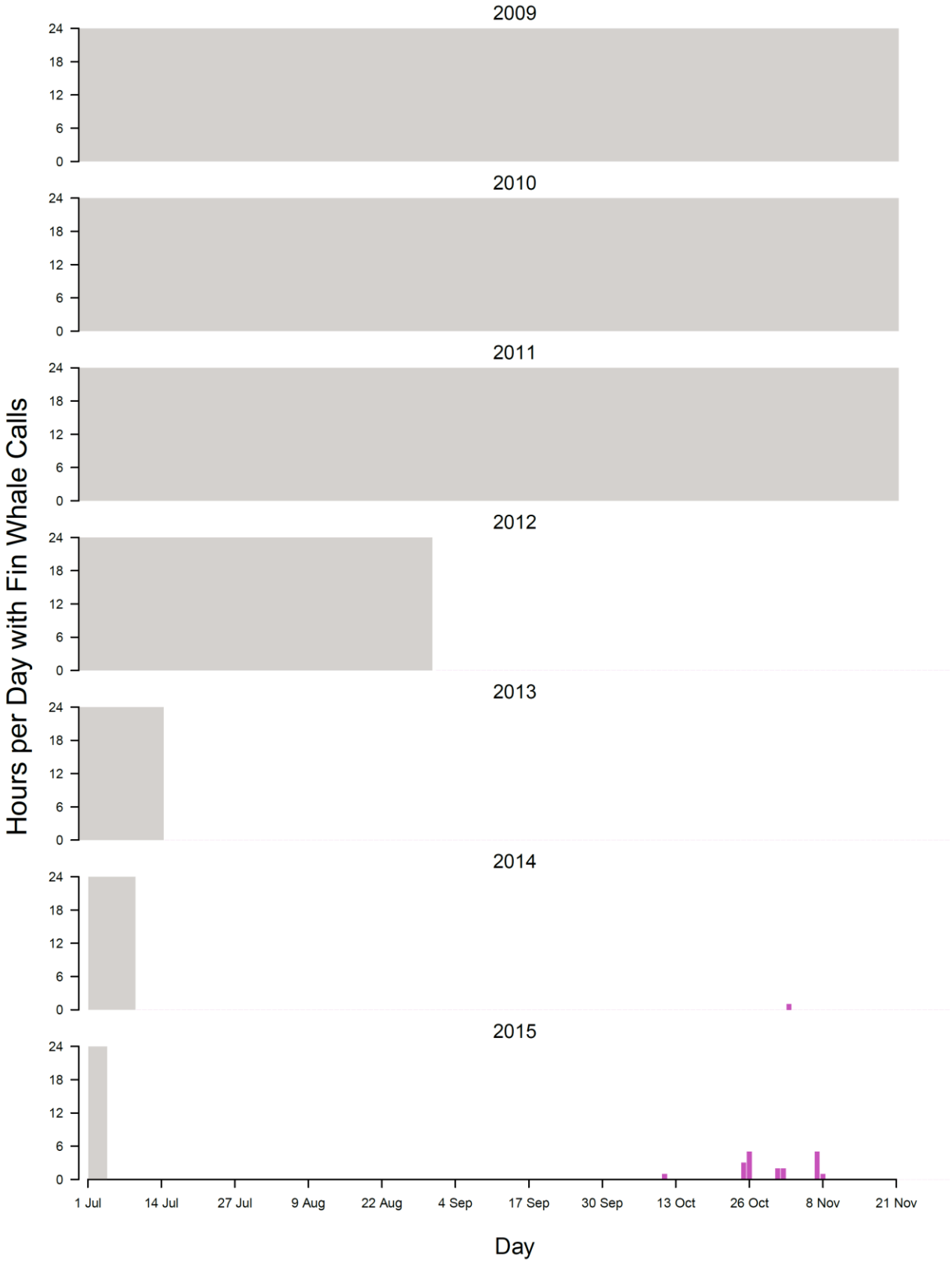

Fig. S2.3. The total number of fin whale hours is summed for each recording day at site A4 and plotted for each year. Gray-shaded areas indicate when the hydrophone was not recording.

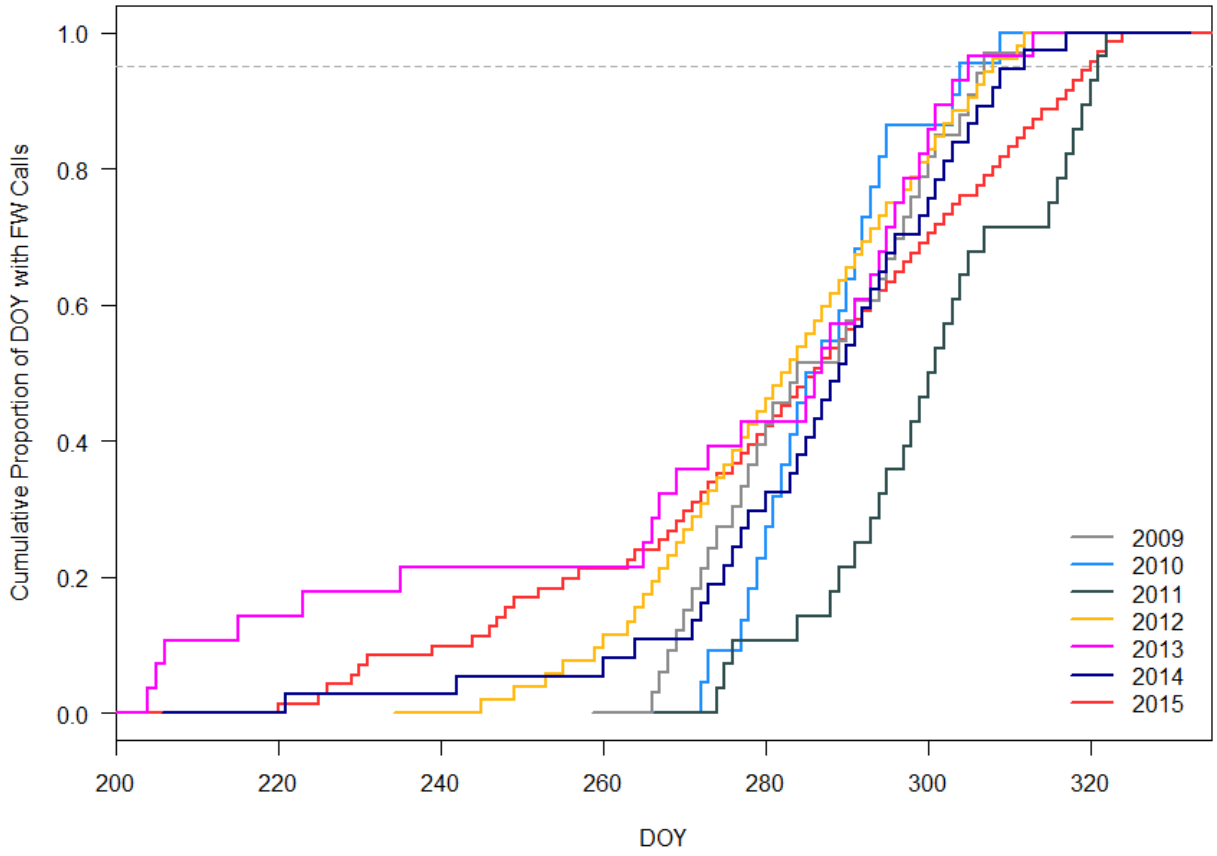

Fig. S2.4. Cumulative distribution of days of the year (DOY) with fin whale (FW) calls at A3. The gray dotted line marks the 95% quantile of the cumulative distribution.

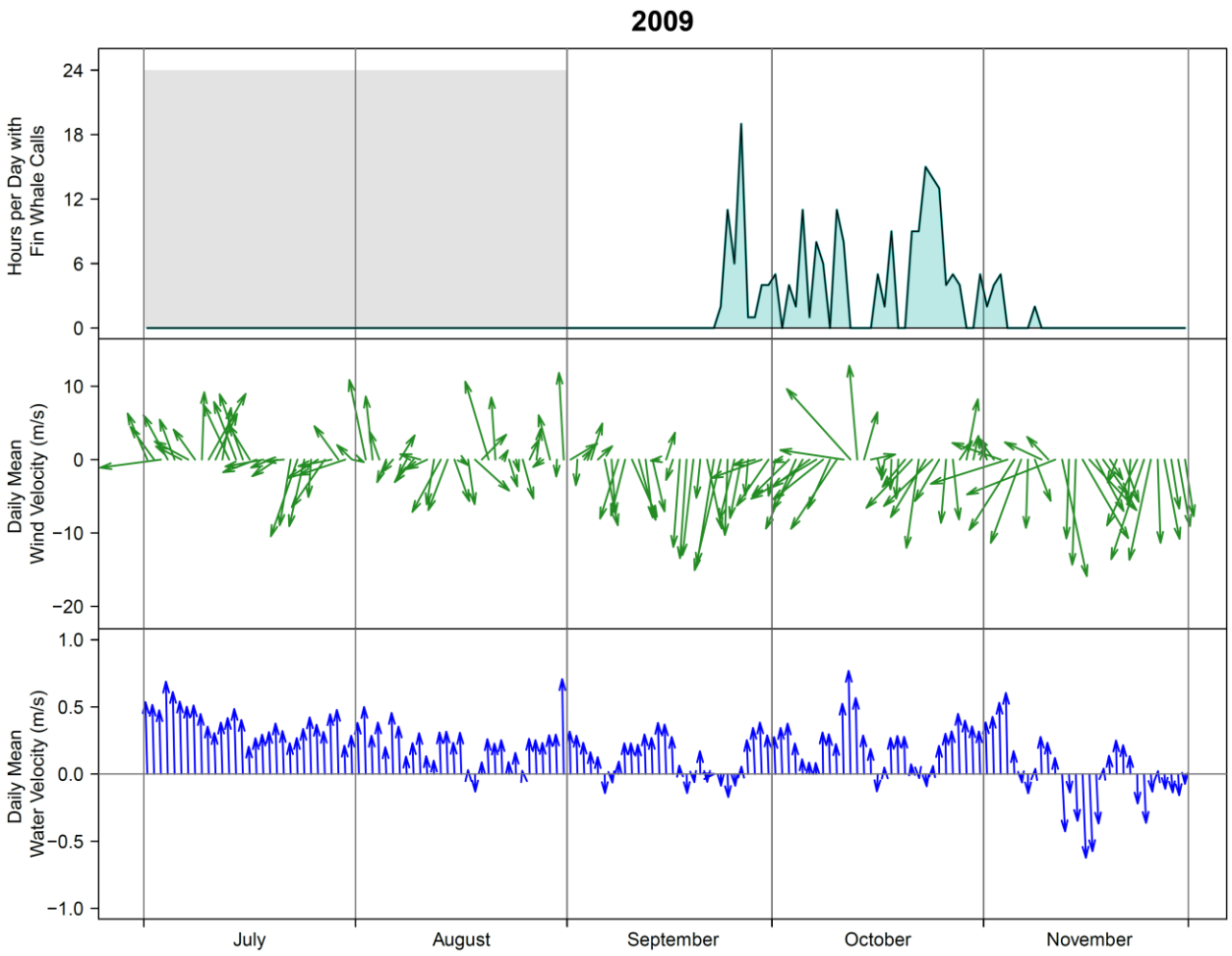

Fig. S2.5. Plot of northward wind (middle plot) and water (lower plot) velocities along with fin whale presence at site A3 for 2009.

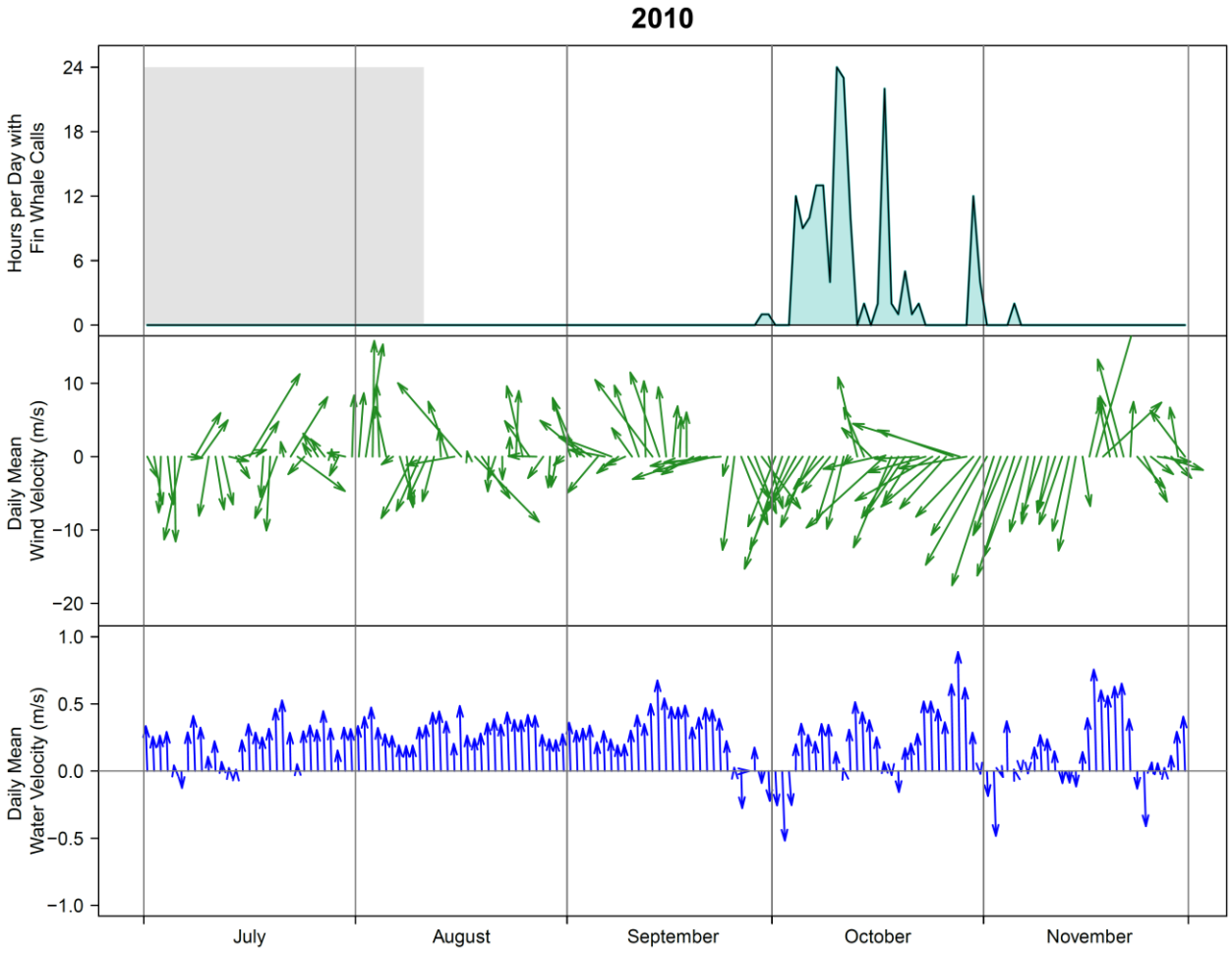

Fig. S2.6. Plot of northward wind (middle plot) and water (lower plot) velocities along with fin whale presence at site A3 for 2010.

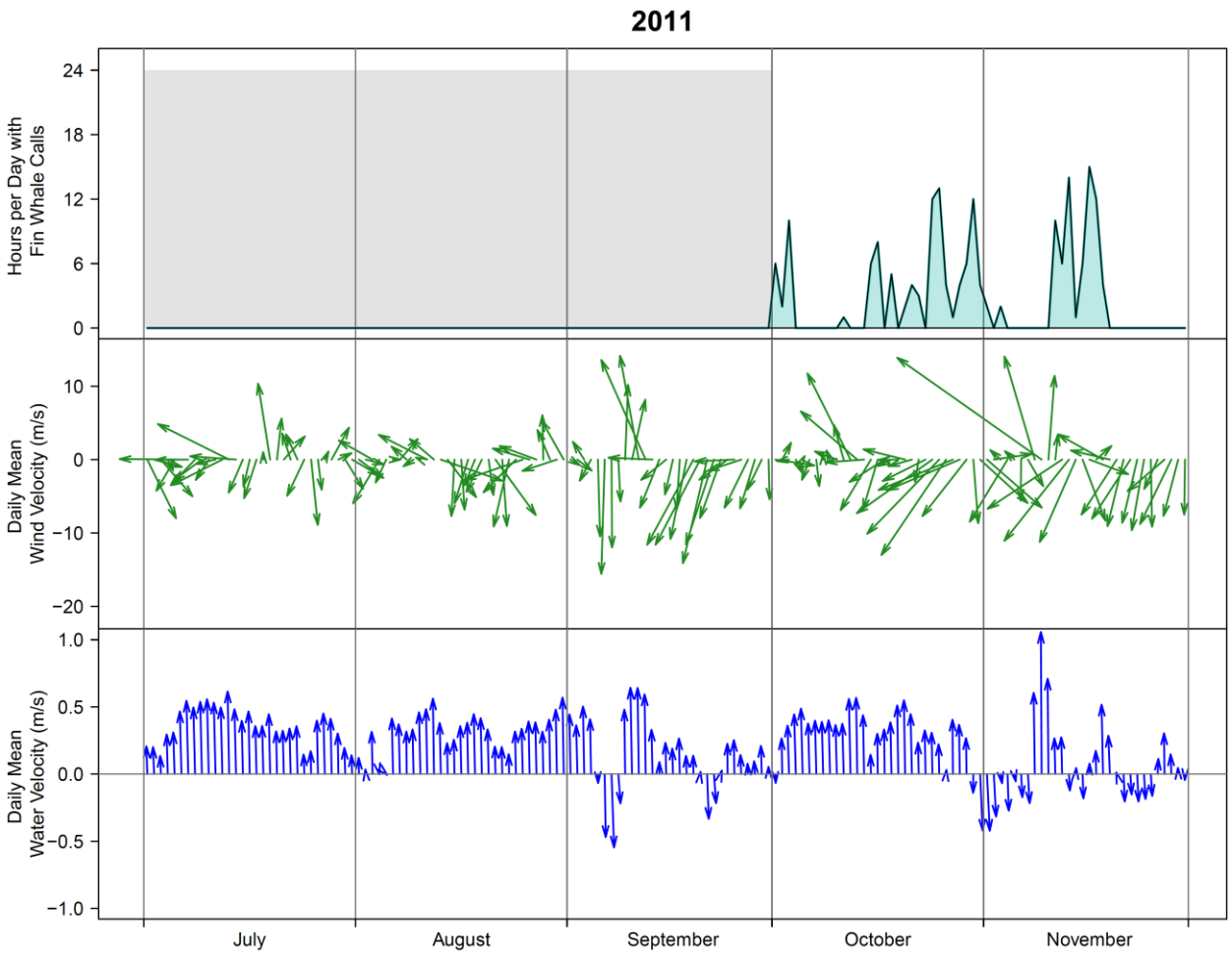

Fig. S2.7. Plot of northward wind (middle plot) and water (lower plot) velocities along with fin whale presence at site A3 for 2011.

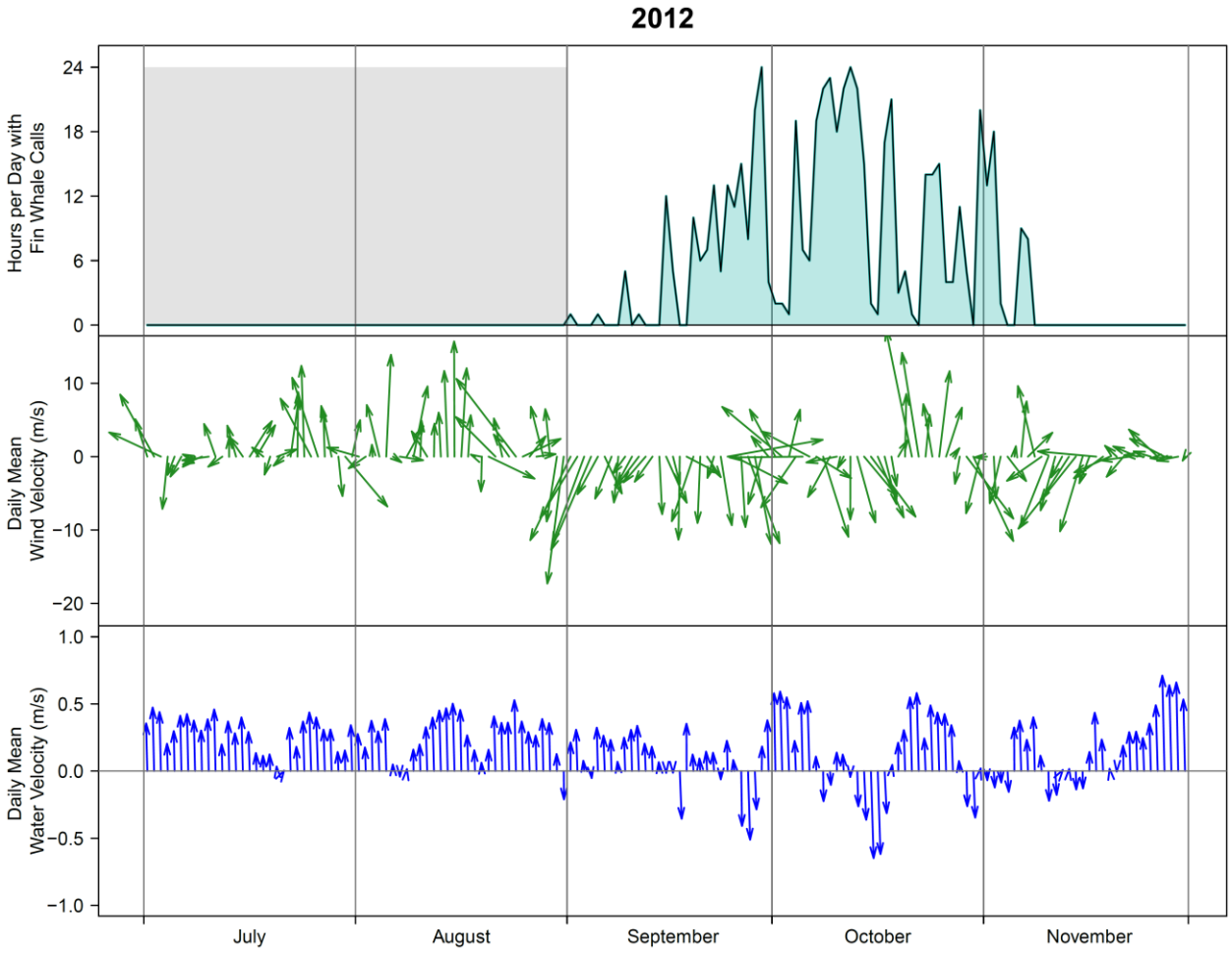

Fig. S2.8. Plot of northward wind (middle plot) and water (lower plot) velocities along with fin whale presence at site A3 for 2012.

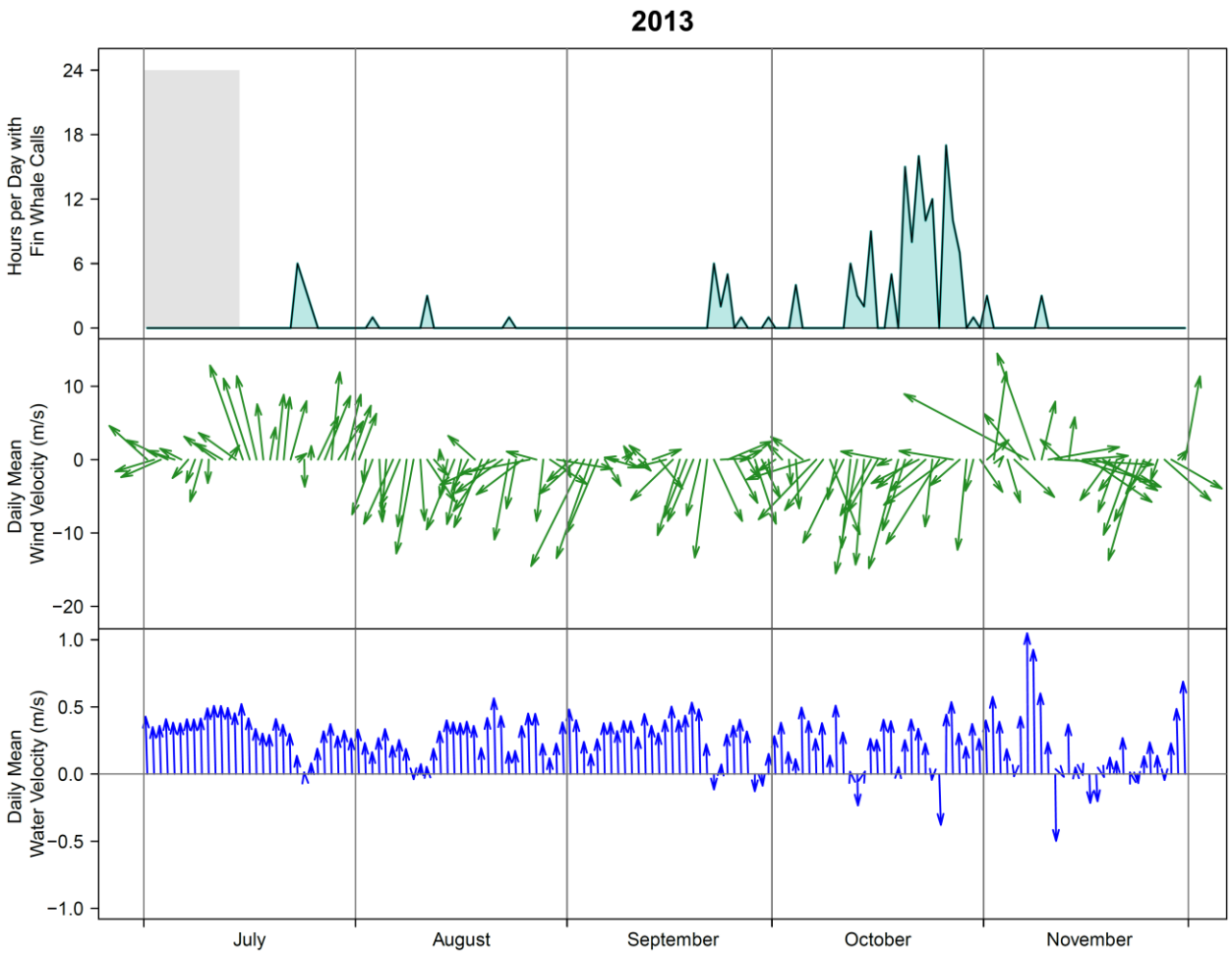

Fig. S2.9. Plot of northward wind (middle plot) and water (lower plot) velocities along with fin whale presence at site A3 for 2013.

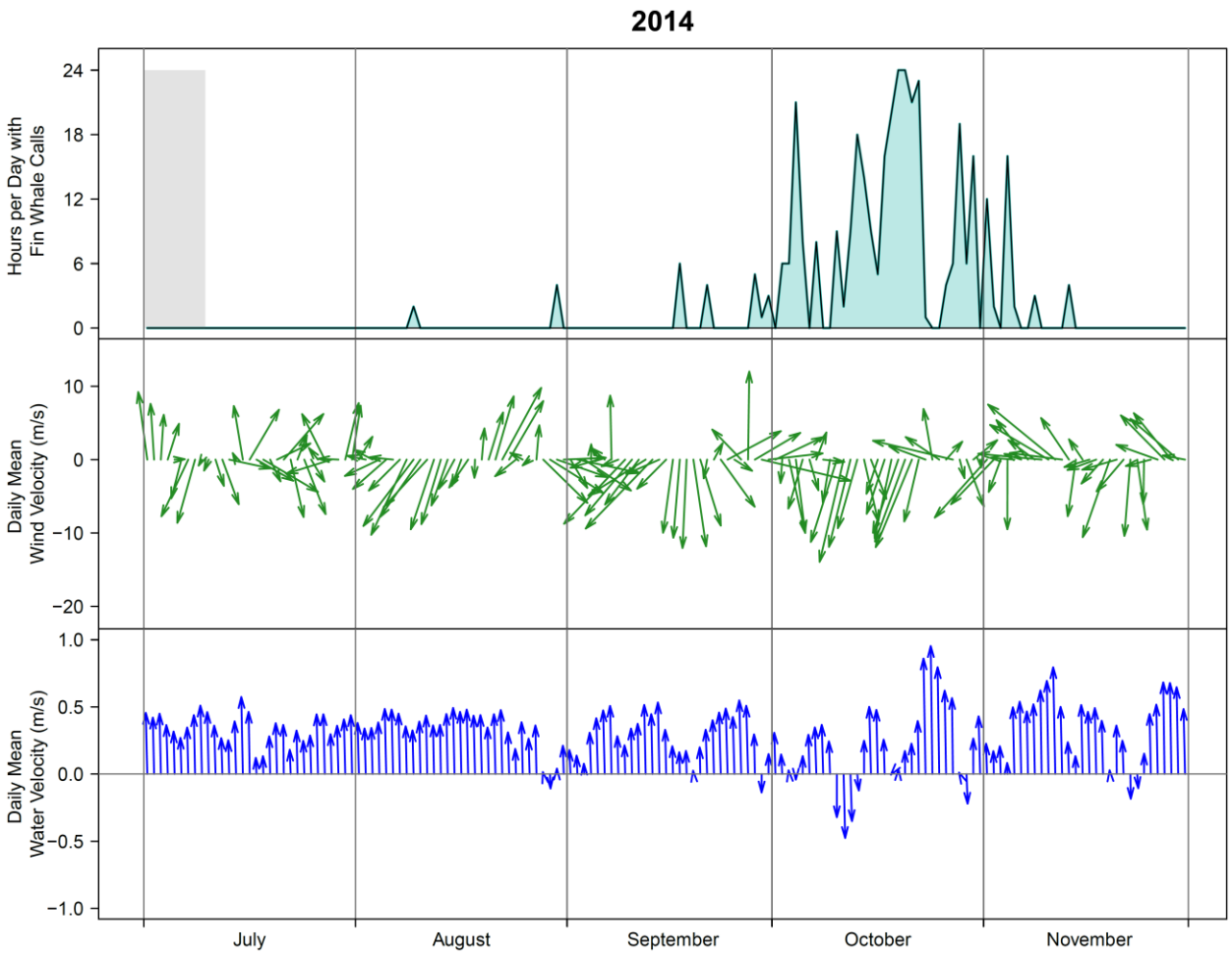

Fig. S2.10. Plot of northward wind (middle plot) and water (lower plot) velocities along with fin whale presence at site A3 for 2014.

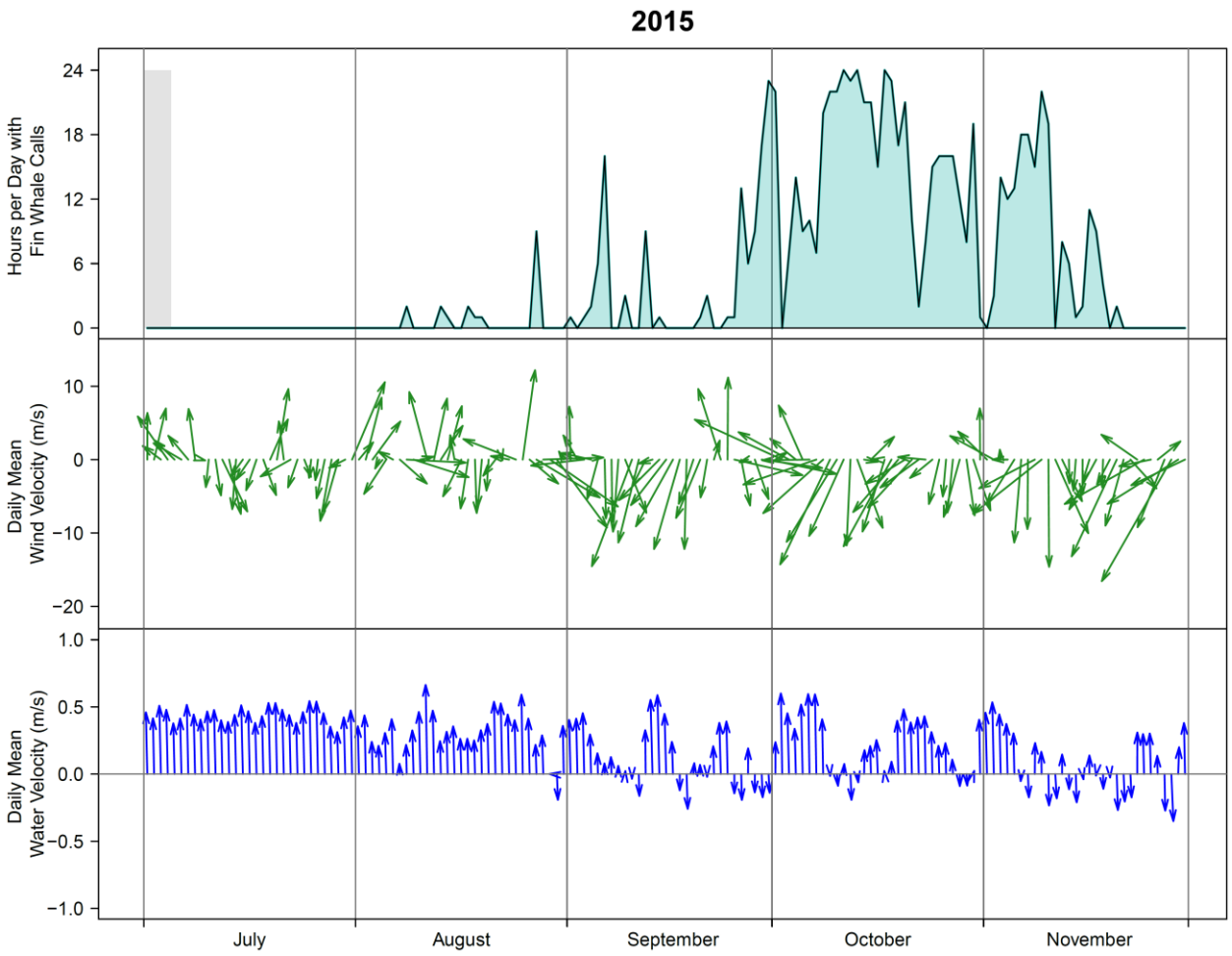

Fig. S2.11. Plot of northward wind (middle plot) and water (lower plot) velocities along with fin whale presence at site A3 for 2015.

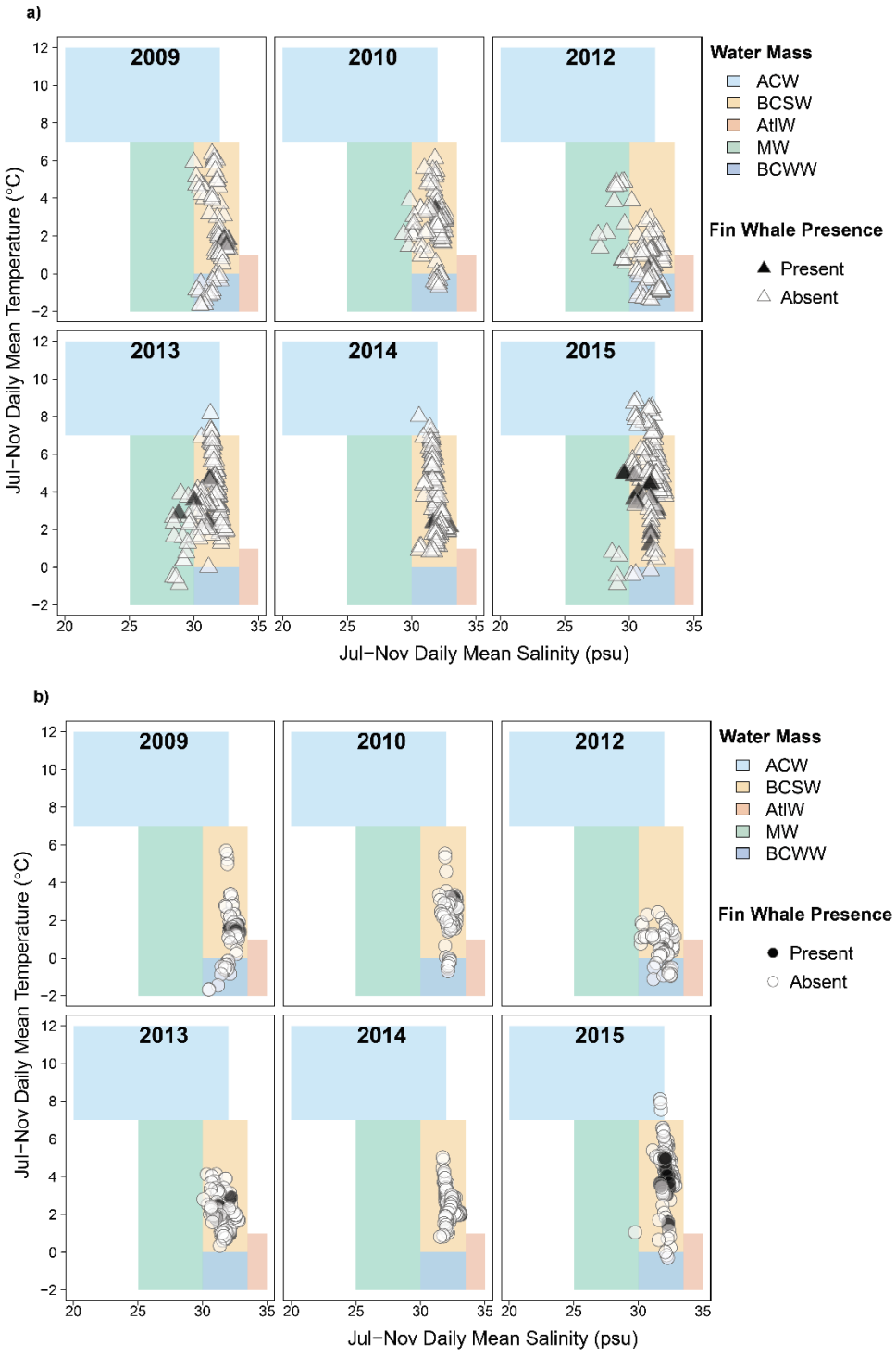

Fig. S2.12. Water mass composition at the A2 mooring site. The bounds for each water mass were calculated using daily mean temperatures and salinities from both the near-surface (triangles) and the near-bottom sensor. The icons are then shaded to convey the presence (black) or absence (white) of fin whale calls for that day. Note that 2011 was omitted since the hydrophone did not record data that year.

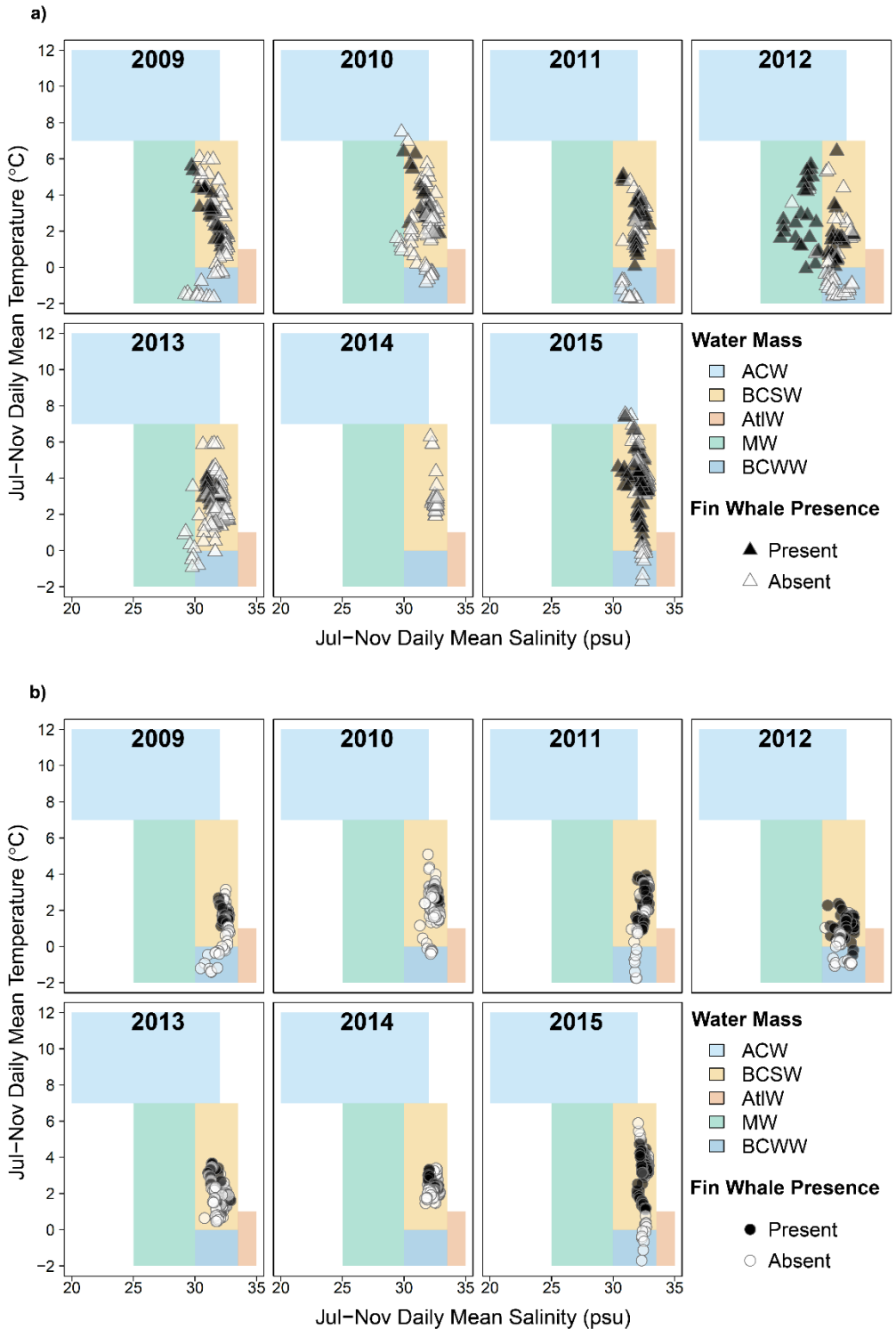

Fig. S2.13. Water mass composition at the A3 mooring site, ~35 km north of Bering Strait. The bounds for each water mass were calculated using daily mean temperatures and salinities from both the near-surface (triangles) and the near-bottom sensor (circles). The icons are then shaded to convey the presence (black) or absence (white) of fin whale calls for that day.

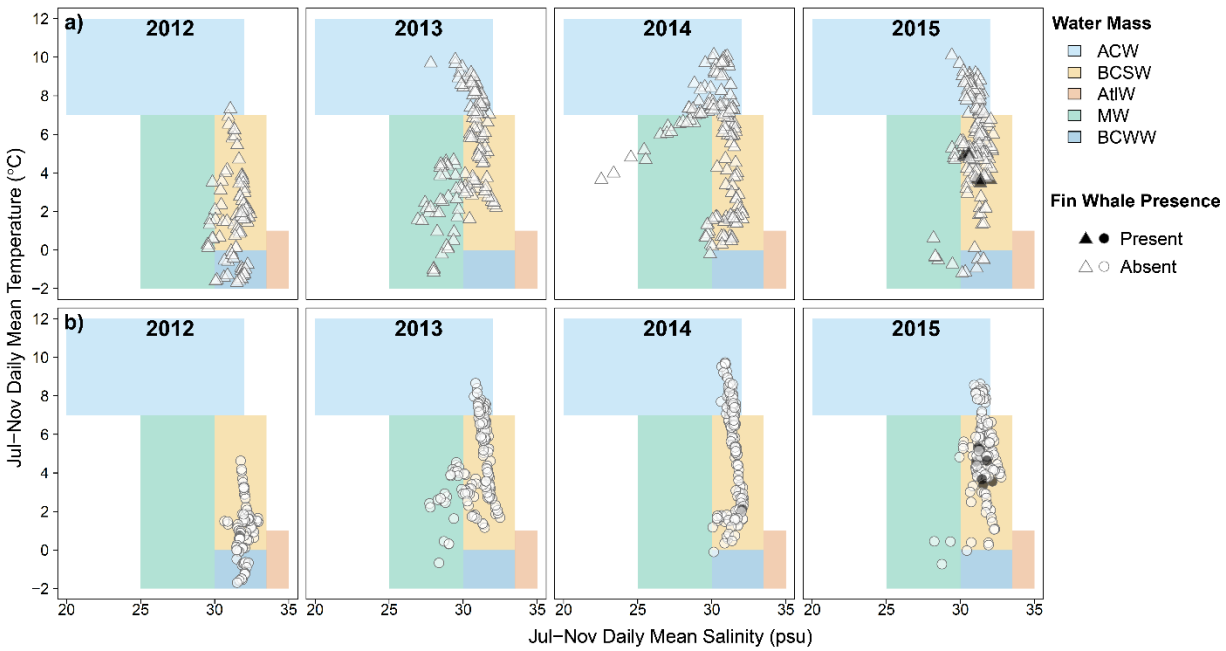

Fig. S2.14. Water mass composition at the A2 mooring site. The bounds for each water mass were calculated using daily mean temperatures and salinities from both the near-surface (triangles) and the near-bottom sensor. The icons are then shaded to convey the presence (black) or absence (white) of fin whale calls for that day. Note that years 2009–2011 were omitted since the hydrophone did not record data that year.

CHAPTER 3. The acoustic presence and migration timing of subarctic baleen whales in the Bering Strait in relation to environmental factors

3.1 Abstract

Subarctic baleen whales, including humpback (*Megaptera novaeangliae*), fin (*Balaenoptera physalus*), and gray whales (*Eschrichtius robustus*), migrate through the Bering Strait every summer to feed in the rich marine ecosystem of the Chukchi Sea. When and where the whales are found in the region likely reflects fluctuating environmental conditions. Using recordings collected between 2009–2018 from a moored hydrophone ~ 35 km north of the strait, we identified whale calls during the open-water season (May–December), examined the timing of migration, and investigated potential drivers of whale presence. The acoustic presence of fin and humpback whales varied across the years, with a peak in recordings with calls for all three species in October through November. We observed the highest proportion of recordings with humpback whale calls for the peak months of October–November in 2009, 2017, and 2018 (66–80% of recordings), and the highest proportion of recordings with fin whale calls for October–November in 2015, 2017, and 2018 (75–79% of recordings). We observed the highest proportion of recordings with gray whale calls for October–November in 2013 and 2015 (46 and 51% of recordings, respectively). Fin whales departed the Bering Strait ~ 3 days later per year over the duration of the study ($p = 0.02$). Both fin and humpback whales delayed their southward migration in years with warmer water temperatures in fall (Pearson $r \geq 0.71$, $p < 0.03$). Our models identified day of the year, water temperatures, and the lagged presence of a thermal front the previous month as drivers of the acoustic presence of all three species during the open-water season.

3.2 Introduction

Understanding the connection between species occurrence and environmental factors is crucial for predicting the effects of habitat shifts on recovering populations of marine mammals. Climate change in combination with other anthropogenic stressors—such as fishing gear entanglements, ship collisions, and increased ocean noise—may impact the recovery of baleen whale populations from commercial whaling that took place throughout the 20th century (Clapham 2016; Tulloch et al. 2019; Nelms et al. 2021). Moreover, changes in ocean conditions related to climate change and masking of calls from conspecifics by ocean noise may obscure the cues whales use to facilitate their migrations (Clark et al. 2009; Torres 2017). Identifying the drivers of baleen whale migration and distribution, therefore, is necessary to understand how baleen whales will respond to habitat shifts associated with climate change (Hazen et al. 2013; Abrahms et al. 2019; Meynecke et al. 2021). The present study seeks to characterize the occurrence of subarctic baleen whales in the Bering Strait and Chukchi Sea, including identifying migration timing and the factors that influence whale presence during the open-water season.

The Chukchi Sea is a shallow continental-shelf sea that owes its productivity to the influx of nutrient-rich Pacific waters that are advected northward by currents through the Bering Strait (Grebmeier et al. 2006; Fig. 3.1). The combination of abundant daylight during the polar summer along with a steady supply of advected nutrients make the Chukchi Sea one of the Arctic's most productive marine ecosystems (Grebmeier et al. 2006; Codispoti et al. 2013). High primary production rates outpace the grazing rates of pelagic zooplankton, thus much of the primary producer biomass is transported to the seafloor which supports rich benthic invertebrate communities (Grebmeier et al. 2006). In addition to nutrients, Pacific water masses also transport zooplankton, including large copepods (Eisner et al. 2013; Ershova et al. 2015; Pinchuk and

Eisner 2017; Spear et al. 2020) and euphausiids (Berline et al. 2008), as well as juvenile forage fish species (Levine et al. 2021) into the Chukchi Sea. Three dominant water masses flow through the north Bering Sea, through the Bering Strait, and into the Chukchi Sea. The cold, salty, and productive Anadyr Water flows on the western side of the north Bering Sea, the warmer and less salty Bering Sea Water flows through the center of the region, while the warm and fresher Alaskan Coastal Current flows along the eastern side against the Alaskan Coast in summer to early winter (Coachman et al. 1975; Grebmeier et al. 1989; Weingartner et al. 2005; Woodgate et al. 2005). Fronts form where these water masses meet (Coachman et al. 1975; Bluhm et al. 2007; Danielson et al. 2017), trapping zooplankton and small fish. Additionally, eddies form north of the strait in the wake of the Diomede Islands (Woodgate et al. 2015), vertically mixing the water column. The replenishment of nutrients to the surface by mixing promotes phytoplankton blooms (Hasegawa et al. 2009), which in turn creates feeding opportunities for upper trophic levels, including baleen whales.

Subarctic baleen whales—humpback (*Megaptera novaeangliae*), fin (*Balaenoptera physalus*), and gray whales (*Eschrichtius robustus*)—migrate into the Chukchi Sea during the late spring and summer months to take advantage of the seasonal abundance of prey. Fin and humpback whales are generalist pelagic predators, feeding primarily on euphausiids, including *Euphausia pacifica*, *Thysanoessa inermis*, *T. longipes*, and *T. spinifera* in the North Pacific as well as *T. raschii* in the Bering Sea (Nemoto 1959; Szabo 2015). Both fin and humpback whales are also known to prey on forage fish species such as capelin (*Mallotus villosus*), Pacific herring (*Clupea pallasii*), Pacific sand lance (*Ammodytes hexapterus*), and juvenile walleye pollock (*Gadus chalcogrammus*) (Nemoto 1959; Krieger and Wing 1986; Szabo 2014; Reidy et al. 2023). Fin and humpback whales prey switch depending on availability (Payne et al. 1990),

giving them greater flexibility in their diet. Additionally, both species exhibit niche partitioning in some regions of the North Pacific with fin whales consuming more euphausiids, while humpback whales consume more forage fish (Witteveen and Wynne 2016). In contrast, gray whales are primarily benthic grazers, specializing in tube-dwelling amphipods such as *Ampelisca macrocephala* (Highsmith and Coyle 1991) though they have been known to take a wide variety of prey throughout their range, including mysids and pelagic euphausiids (Nerini 1984; Moore et al. 2022). The relative occurrence of two pelagic predators (fin and humpback whales) and a benthic grazer (gray whales) can be used as an indicator of a shift from a benthic- to a pelagic-dominated ecosystem in the Chukchi Sea (Grebmeier 2012).

Previous studies have detected interannual variation in the presence of fin and humpback whales in the Chukchi Sea during the open-water season. More fin whale calls were recorded in the northeast Chukchi Sea in 2007 than in 2009–2010 by Delarue et al. (2013) while a study by Woodgate et al. (2015) indicated higher detection rates of fin whales in the southern Chukchi Sea in 2009 and 2012 than in 2010 and 2011. Similarly, more humpback whale calls were recorded in the southern Chukchi Sea in 2009 and 2012 than in 2010 and 2011 (Woodgate et al. 2015). Both studies attribute increases in the presence of the two species to warmer conditions, earlier sea-ice retreat coupled with low sea-ice extent, higher transport through the Bering Strait, and shifts in the distribution of the productive Anadyr Water mass (Delarue et al. 2013; Woodgate et al. 2015). While the presence of fin and humpback whales in the Chukchi Sea varies from year to year, gray whales are reliably observed in the region each summer (Clarke et al. 1989; Moore et al. 2000; Clarke and Moore 2002; Clarke et al. 2016; Brower et al. 2017; Moore et al. 2022). Declining sea ice may benefit gray whales in the short term since earlier ice melt in the spring allows them to forage earlier in the spring and delays in ice formation allows them to graze for

longer in the fall (Perryman et al. 2002). However, few observations have been collected on the timing of the southward migration of gray whales from the Chukchi Sea, so it is unclear if gray whales are extending their residence time in the Pacific Arctic.

Any variation in the presence of the three whale species is likely dependent on prey availability and environmental conditions in the Chukchi Sea. Environmental variability in the Chukchi Sea is driven by the presence and distribution of the major water masses, as well as changes in the Bering Strait throughflow, which in turn is dependent on local and far-field wind stress and ocean pressure gradients (Aagaard et al. 1985; Woodgate et al. 2012; Danielson et al. 2014; Peralta-Ferriz and Woodgate 2017; Woodgate 2018; Nguyen et al., 2020). Also, changes in sea-ice cover and melt timing along with storms affect the structure of the water column, and thus, the timing of phytoplankton blooms (Hunt et al. 2011; Sigler et al. 2014). Previous studies examining environmental influences on the presence of baleen whales found that primary production rates, and in turn, prey abundance along with sea surface temperatures, bathymetry, and sea surface height influenced the acoustic presence of baleen whales (Širović and Hildebrand 2011; Shabangu et al. 2017; Ryan et al. 2019; Szesciorka et al. 2020). In the northern Chukchi Sea, Ashjian et al. (2010) found that interannual variability in the distribution of bowhead whales (*Balaena mysticetus*) corresponded to both short-term (i.e., changes in wind speed and direction) and long-term environmental variability (i.e., sea ice and water mass distribution). What cues subarctic baleen whales use for finding food in the Pacific Arctic, however, remain unclear.

Using acoustic data along with *in situ* and satellite-derived environmental variables collected over a decade in the Bering Strait region (2009–2018), we examined whether fin, humpback, and gray whales shifted their migration timing in response to environmental conditions, and explored potential environmental influences on the presence of these species

during the open-water season (May through early December). We also examined the correlation between the abundance of recordings with whale calls and the seasonal abundance of prey sampled in the northern Bering Sea and the Chukchi Sea during the summer and fall months.

3.3 Methods

3.3.1 *Acoustic Data Collection*

Acoustic data were collected using an AURAL-M2 hydrophone (Autonomous Underwater Recorder for Acoustic Listening-Model 2, Multi-Électronique, Inc.) attached to an oceanographic mooring (Site A3) positioned ~ 35 km north of the strait in the southern Chukchi Sea (Fig. 3.1; Woodgate et al. 2015). The hydrophone was first installed on the mooring in September 2009, and serviced annually, yielding a recording time series from September 2009 through December 2018. Data gaps indicate periods when the hydrophone ran out of batteries, or when the hydrophone was serviced (no data available for fall 2016 through spring 2017 due to instrument failure). The hydrophone was set to record the first 10–20 minutes of every hour at a sampling rate of 8192 Hz or 16384 Hz depending on the year (16-bit resolution) with a gain of 16 dB (2009–2016) or 22 dB (2017–2018). The hydrophone was positioned 4–8 m above the seafloor (depth at the A3 mooring site ~ 56 m). See Table 3.1 for recording start/end dates, and the duty cycles for each year.

Spectrograms of the acoustic data were visualized in the software *Ishmael* (2014 version; Mellinger, 2002) using a fast Fourier transform size of 4096 samples, Hanning window, and spectrogram equalization enabled with a time constant of 30 s. Recordings with whale calls were identified by visually inspecting the spectrograms. For each calendar year, we scanned recordings from May, when sea ice typically retreats in the study area (Stroeve et al. 2014; Serreze et al. 2016; Grebmeier et al. 2018), through to freeze-up when sea ice concentration in

the Chukchi Sea first rose above 80% (typically late November to mid-December; see next section for sea ice methods). If a call from any of the three study species was captured in a recording, we counted that species as present for that hour. Note that we could not assume the absence of whales since we were only able to detect calling individuals using acoustic data.

3.3.2 *Environmental Data Collection*

We quantified sea-ice melt and formation dates in the Chukchi Sea to compare with the migration timing of whales in and out of the region. We defined the Chukchi Sea using boundaries defined by the International Hydrographic Organization (IHO, http://www.marineregions.org/gazetteer.php?p=details&id=4257; Fig. 3.1). Daily sea ice concentrations were obtained from the Special Scanning Microwave/Imager (SSM/I) dataset (25-km resolution; Cavalieri, 1996). We defined the initiation of sea ice melt-out as the day when sea ice concentration in the Chukchi Sea dropped below 80% for the last time that calendar year, while freeze-up onset was defined as the day when ice concentration reached above 80%. We defined an area as 'ice-free' if the mean sea ice concentration was ≤ 15%, a threshold commonly used to indicate the initiation of the open-water period (Serreze et al. 2009; Stroeve et al. 2012).

Environmental predictors were selected based on their hypothesized potential to influence the presence of baleen whales. *In-situ* environmental predictors were recorded by other sensors on the mooring and included near-bottom temperature and salinity (40–55 m depth) measured by Sea-Bird Electronics (SBE) sensors (model #16), and water velocity (cm s^{-1}) measured by Teledyne Workhorse Acoustic Doppler Current Profilers (ADCP; Woodgate 2018). We analyzed ADCP water velocities from the bin closest to ~ 30 m depth to avoid contamination by surface activity. Boxplots and Cleveland dot plots (Cleveland 1993) were generated for each

environmental covariate to identify outliers and violations of homogeneity. We removed any outliers before we calculated daily averages.

In addition to the *in-situ* mooring data, we also examined wind speed and direction, as well as satellite-derived sea-surface temperatures (SST). Daily mean wind speed (m s^{-1}) and direction were calculated from the National Centers for Environmental Prediction (NCEP) North American Regional Reanalysis 2 (NARR) 6-hourly wind data product (grid size of ~ 32 km; Mesinger et al. 2006). We calculated daily mean wind speed by taking the average of the northward (*v*) and eastward components (*u*) for the four NCEP-NARR 2 grid points nearest to the mooring site (Fig. 3.1). We then averaged the vectors across the four grid points, and used the mean vectors ($\bar{u}$ and $\bar{v}$) to calculate mean wind speed for a given day (*i*) using the following equation:

$$daily\ mean\ wind\ speed_i = \sqrt{(\bar{u}_i^2 + \bar{v}_i^2)}$$

Daily mean SST were calculated for the grid point closest to the mooring site using the National Oceanic and Atmospheric Administration (NOAA) Optimum Interpolation Sea Surface Temperature (OISST) gridded dataset (0.25° resolution; Reynolds et al. 2007).

3.3.3 *Migration Timing*

We estimated the arrival and departure of whales into the study region by calculating the 5% (arrival) and 95% quantiles (departure) of the cumulative distribution of days with whale calls present, similar to Hauser et al. (2017). We only had recordings in the spring for four years (2014–2016, and 2018), whereas we had nine years of fall recordings (2009–2015, 2017–2018). Therefore, we focused our statistical analyses on the fall departure dates. We tested the departure dates for annual trends using linear regressions, for correlations to freeze-up in the Chukchi Sea using Pearson correlation tests, and for correlations and linear relationships to seasonal

environmental conditions. We defined the four seasons using the solstices and equinoxes as the boundaries: winter = 21 December of previous year through 20 March, spring = 21 March through 20 June, summer = 21 June through 20 September, and fall = 21 September through 20 December. Seasonal means were calculated for near-bottom temperatures and salinities ('SBE Temp' and 'SBE Salt'), SST, water speeds, and wind speeds. Due to correlations between multiple seasonal means (Table S3.1), we built separate linear models for each predictor with departure dates (n = 9) as the response variable. As an example, we tested for a linear relationship between departure dates for fin whales (FW) and the spring mean of near-bottom temperatures for the corresponding year (i):

$$FW\ Departure\ Dates_i = \beta_0 + \beta_i(Spring\ SBE\ Temp)_i + \epsilon_i$$

3.3.4 *Prey Data Collection and Analyses*

Available prey datasets for our study period and area included forage fish density (kg per km^2) collected using surface rope trawls by the NOAA Bering Arctic Subarctic Integrated Survey (BASIS; 2009–2018); zooplankton abundance (number per m^3) from the NOAA Ecosystems and Fisheries Oceanography Coordinated Investigations (EcoFOCI) joint research program (Years: 2012–2015, 2017–2018); and benthic zooplankton abundance (number per m^2) collected using four van Veen grabs per station during the Distributed Biological Observatory surveys (DBO; https://www.pmel.noaa.gov/dbo/; Years: 2012–2017) led by Grebmeier and Cooper (2019a, 2019b), hereafter referred to as 'benthic data' (Table S3.2). Data collection for all prey datasets was restricted to the area east of the international date line.

The EcoFOCI data were collected in the southeastern and eastern Chukchi Sea in August through October 2012–2018 (Fig. 3.3A; Table S3.2). We only used data from samples collected using oblique bongo tows with a 153-µm net mesh size to standardize the sampling method

across years (tows were deployed ~ 10 m from the seafloor; see Eisner et al. 2018 for complete sampling methods). We then reduced the zooplankton to previously identified fin and humpback prey species (Nemoto 1959; Witteveen and Wynne 2016). True euphausiid abundance is likely underestimated in the EcoFOCI dataset due to small net size along with net avoidance behavior exhibited by adults (Pinchuk and Eisner 2017; Eisner et al. 2018). Therefore, we examined the influence of *Calanus* spp. copepod abundance on the presence of fin and humpback since both species are known to prey on copepods in the North Pacific and Gulf of Alaska (Nemoto 1957; Nemoto and Kasuya 1965; Witteveen and Wynne 2016). The EcoFOCI dataset combined *Calanus marshallae* and *C. glacialis* copepods into one category, and we further combined the later life stages (C3–C6) together to form one *Calanus* copepod abundance value per day.

The BASIS data were collected at multiple sampling locations within the northern Bering Sea, defined here as the area north and east of St. Lawrence Island to the Bering Strait (Fig. 3.2A). BASIS data were mostly collected in September with some sampling dates in August and October 2009–2018 (Table S3.2). See Moss et al. (2009) for a complete description of the sampling methods for the BASIS dataset. As with the zooplankton dataset, the BASIS dataset was reduced to previously identified fin and humpback prey species, including: sand lance, capelin, juvenile pollock (age-0 and age-1), and Pacific herring (Nemoto 1959).

The benthic data were collected along multiple DBO transect lines in the Bering and Chukchi seas in July (2012–2015) and late August to early September (2017; Fig. 3.2B). The benthic dataset was reduced to amphipod species and genera previously identified as gray whale prey using the descriptions of gray whale diet by Nerini (1984), and Yablokov and Bogoslovskaya (1984) as guides.

The number of sampling stations for each dataset varied from year to year; to standardize effort, we calculated the average density over all stations within select zones for each year. We grouped sampling stations into zones (Fig. 3.2B) based on the hydrography of the region as well as the DBO sampling regions (Grebmeier et al. 2019; see Fig. S3.1 for DBO sampling regions). Species averages were then calculated across all sampling stations within a zone to generate one abundance value per zone, per year for each dataset. Not all sampling zones had the same years of data available. For the EcoFOCI dataset, the Beaufort zone only had *Calanus* spp. data for 2014–2018 and the S Chukchi zone did not have *Calanus* data for 2015. The benthic dataset did not have amphipod data for 2012 for the Beaufort and Barrow zones.

3.3.5 *Correlation Between Whale Presence and Prey Data*

The three prey datasets were not collected at the same location and time as the acoustic data, leading to a potential spatial and temporal mismatch between the prey and acoustic datasets (see Fig. S3.2 for a chart of the sampling periods). The EcoFOCI and the benthic datasets were sampled in the Chukchi Sea during the late summer months (August through early October) when subarctic whales have been observed feeding in the region (Brower et al. 2018). However, we hypothesized that high copepod and amphipod abundance in the Chukchi Sea would attract more whales to the area to feed, leading to a high abundance of whale calls in the Bering Strait during the fall outmigration period (October through November). In contrast, the BASIS data were sampled south of the Bering Strait in September when we expect most whales to be north of the strait. We therefore hypothesized that high forage fish abundance would result in whales milling around the hydrophone during their southward migration to feed on fish that were advected through the Bering Strait. Given the different sampling periods, we used the outmigration period (October through November) as our analysis window for the EcoFOCI

copepod and benthic amphipod data, and September as our analysis window for the BASIS fish data.

We used a proxy for whale abundance and Pearson correlation tests to examine the influence of forage fish and zooplankton abundance on the acoustic occurrence of fin and humpback whales, and the influence of benthic amphipod abundance on gray whales. To create the whale abundance proxy, we reduced the acoustic dataset to the same years as the prey datasets (BASIS: 2009–2018, excluding 2016; EcoFOCI: 2012–2015, 2017–2018; Benthic: 2012–2015, 2017). We then calculated the whale abundance proxy (W_i) as the proportion of recordings with whale calls during October through November for a given year (i) for the EcoFOCI and benthic datasets, resulting in one abundance value per species per year, e.g.:

$$W_i = \frac{(Total\ \#\ of\ recordings\ with\ at\ least\ one\ whale\ call\ for\ Oct-Nov)_i}{(Total\ \#\ of\ recordings\ for\ Oct-Nov)_i}$$

For the BASIS dataset, we calculated the proxy using September data only (2011 was excluded since it did not have recordings in September). We then conducted Pearson correlation tests between the whale abundance proxy for each species and the seasonal mean prey abundance for each dataset. All analyses were performed using *R* (*v.* 4.1.0; R Core Team, 2021).

3.3.6 *Modeling the Relationship Between Whale Presence and Environmental Covariates*

We conducted an exploratory modeling analysis to determine potential temporal and environmental covariates associated with the probability of observing whale calls (p) during the open-water season. Our analyses included examining the influence of time of year (day of the year, DOY), and environmental conditions at the mooring site on the acoustic presence of each whale species. For the response variable, the acoustic data were converted into counts of recordings with calls present ("Detected") along with the number of recordings that did not have calls present ("Not Detected") for each day.

Conditions at the mooring site included daily means for: temperature and salinity near the bottom ('SBE Temp' and 'SBE Salt'), SST, water speed (cm s^{-1}), wind speed (m s^{-1}), and wind direction (as a categorical variable). Sea ice extent for the Chukchi Sea was considered for the models, however preliminary correlation tests found that sea ice extent was highly correlated with both SST and near-bottom temperatures. Since all three species are typically in the study region when it is ice-free, we omitted sea ice extent as an explanatory variable, and retained SST and near-bottom water temperatures. Ocean-basin scale indices such as the Arctic Oscillation, Pacific Decadal Oscillation, and the North Pacific Gyre Oscillation were also considered for the models, however preliminary tests with these covariates resulted in large models that were likely overfitting the data. Moreover, factors relevant to the indices such as sea-surface temperature were already included in the models. Therefore, ocean-scale indices were not included in our models.

Fronts form important feeding habitats for baleen whales (Bluhm et al. 2007; Bost et al. 2009; Scales et al. 2014; Bassoi et al. 2020), and can be identified using horizontal gradients in water temperature, salinity, chlorophyll concentration, and sea surface height (Bluhm et al. 2007). We used high-resolution SST data from the Group for High Resolution Sea Surface Temperature (GHRSST) Level 4 sea surface temperature analysis product (0.054°, ~ 6-km resolution) to calculate the maximum gradient in SST in any direction within a 30-km area around the mooring site. The magnitude of the maximum SST gradient represents the presence and strength of any thermal fronts within 30-km of the mooring site (see Fig. 3.1 for buffer). The 30-km radius was chosen since this is the midpoint of the detection range estimated for fin whale calls in the northeast Chukchi Sea (14–74 km; Delarue et al. 2013). Fin whales produce the lowest frequency calls of the three species at ~ 20 Hz (Watkins 1981; Watkins et al. 1987) and

lower frequency calls travel farther underwater than higher frequency calls. Therefore the 30-km radius likely captures the maximum detection ranges for all three species in the shallow Chukchi Sea. In addition to the daily value for the 30-km SST gradient, we also included a one-month lag of the SST gradient in our model to test for a lag between the presence of a front and whale presence.

Given that the probability of a calling whale being present on a given hour or day was likely influenced by whether a calling whale was present the previous hour/day, our model choice was driven by the need to account for overdispersion in our response variable. Overdispersion occurs when the variance of a response variable is greater than assumed by the model, and is caused when Bernoulli outcomes are not independent. Unlike the binomial distribution, the beta-binomial distribution does not assume independent Bernoulli outcomes and is a good choice when zero-inflation is a concern, i.e., in our case, when there are more recording hours with zero calls than expected (Hisakado et al. 2006; Martin et al. 2011). We did not know a priori the functional form of the relationship between whale presence and the predictors, therefore we also required a non-parametric model fitting algorithm that could accommodate a beta-binomial distribution. Generalized additive models for location, shape, and scale (GAMLSS) are robust to more complex distributions, such as beta-binomial, and allow for nonparametric predictors.

We generated our beta-binomial GAMLSS models using the *gamlss* package in *R* (Rigby and Stasinopoulos 2005), and ran separate models for each species with all years combined (2009–2018, excluding 2016 due to recorder failure). Following Monnahan et al. (2014), we fit the same predictors for the probability of observing whale calls on a given day (p) and the over-

dispersion parameter (σ). We used cubic splines (cs) for the environmental variables, and penalized b-spline smoothers (pb) for DOY:

$$\begin{aligned}\text{logit}(\hat{p}) = {} & \text{pb(DOY)} + \text{cs(SBE Temp)} + \text{cs(SBE Salt)} + \text{cs(SST)} + \text{cs(Water Speed)} \\ & + \text{cs(Wind Speed)} + \text{factor(Wind Direction)} + \text{cs(SST Gradient)} \\ & + \text{cs(SST Gradient Lagged)}\end{aligned}$$

$$\begin{aligned}\log(\hat{\sigma}) = {} & \text{pb(DOY)} + \text{cs(SBE Temp)} + \text{cs(SBE Salt)} + \text{cs(SST)} + \text{cs(Water Speed)} \\ & + \text{cs(Wind Speed)} + \text{factor(Wind Direction)} + \text{cs(SST Gradient)} \\ & + \text{cs(SST Gradient Lagged)}\end{aligned}$$

Note that all variables except for wind direction were continuous; wind direction was included as a categorical variable. The type of smoother used as well as model selection were based on the Akaike information criterion score (AIC) with a correction for small sample sizes (AICc; Akaike 1973). To avoid multicollinearity among the model parameters, we tested pairs of variables using Pearson's correlation tests and eliminated any predictor variables with a correlation factor > 0.7, following Širović and Hildebrand (2011). Predictors were selected using the *stepGAIC* function (Rigby and Stasinopoulos 2005) applied to the full model in *R*, which performed backwards stepwise selection using Generalized AIC (GAIC) as the model selection criterion. Next, we applied the *drop1* function from the *stats* package in *R* to the final model for each species to check for any spurious covariates. The *drop1* function systematically removes one variable at a time and compares the AIC score of the reduced model to that of the full model. Any variables that did not significantly decrease the likelihood relative to the full model ($p > 0.05$) were removed. Finally, we assessed the relative importance of each predictor variable in the final model using incremental R^2, where the incremental R^2 for a predictor variable equals the increase in R^2 when the predictor is last predictor added the model (Cohen et al. 2003). For the

incremental R^2 tests, we calculated the Cox and Snell R^2 (Cox and Snell 1989) for each model using the *Rsq* function from the *gamlss* package.

When fitting a smoothed nonparametric term, you cannot interpret the effect of the predictor variable on the response variable using the coefficients. Instead, the influence of a predictor variable must be interpreted using the whole smoothing function (Stasinopoulos et al. 2017). We used the *term.plot* function from *gamlss* to plot the additive smoothing fits to evaluate the influence of each predictor on the probability of acoustic occurrence (*p*). The relative direction of the curve for an explanatory variable represents the effect of the variable on *p*. The *y*-axis is unitless, and we used different scales for the *y*-axis to aid in legibility of each explanatory variable's effect. Increasing values represent a positive effect of the explanatory variable on *p*, while declining values signify a negative effect.

3.4 Results

3.4.1 *Acoustic Detections*

We scanned a total of 33,371 audio files recorded at Site A3 from 1 May to freeze-up in November and December (see Table 3.2 for freeze-up dates). Humpback whales were the most common species across the ten years with 20% of all recordings (2009–2018) containing humpback whale calls. Fin whales were detected in 12% of all recordings, and gray whales in 7% of all recordings. Humpback and fin whale calls peaked in October whereas gray whale calls were heard throughout the open-water season at low levels with a peak in June–August (Fig. 3.4).

We calculated the proportion of recordings with whale calls for October through November for each year to compare acoustic occurrence across the years. October and November were chosen since all years had recordings for these two months, and both months

capture peak whale vocalization activity (Fig. 3.4). The years 2009, 2017, and 2018 had the highest proportion of recordings with humpback vocalizations with 66%, 75%, and 80% of the total recordings for October–November containing humpback whale calls, respectively (Fig. 3.5). For fin whales, 2015, 2017, and 2018 had the highest proportion of recordings with fin whale vocalizations, with 77%, 75%, and 79% of the total recordings for October–November containing fin whale calls, respectively. We observed the highest proportion of recordings with gray whale calls for October–November in 2015 (51%) followed by 2013 (46%; Fig. 3.5).

3.4.2 *Environmental Conditions*

Sea ice conditions in the Chukchi Sea varied from year to year, with melt-out initiation (< 80% ice concentration) as early as 23 April 2018 and as late as 6 June 2013 (Table 3.2; Fig. 3.6). The Chukchi Sea was typically ice-free by late June to early July, except for 2012 when the open-water period did not start until 22 July. Freeze-up (≥ 80% ice concentration) typically occurred in late November to mid-late December, with the earliest freeze-up on 28 November 2009 and the latest on 2 January 2018 (for winter 2017–2018; Table 3.2; Fig. 3.6). The open-water period ranged from as short as 99 days in 2012 to as long as 152 days in 2014 and 2017 (Table 3.2).

Environmental conditions at the mooring site were similarly variable, with some interesting patterns emerging in some years (Fig. 3.7A). Both 2017 and 2018 had abnormally warm winter temperatures in comparison to the other years (~ 0.3 °C warmer than the winter median surface and near-bottom temperatures for all nine years combined). Warmer temperatures persisted into spring for both years, with SST > 0 °C and near-bottom temperatures ≥ −0.5 °C. Summer temperatures varied across the years with mean near-bottom temperatures hovering between 1 and 4 °C while mean SST ranged from 4 to 7 °C (Fig. 3.7A). Water

temperatures at both depths began cooling in fall, except for 2018 when both near-bottom and surface temperatures remained above 3 °C throughout the fall season.

Patterns in near-bottom salinities were relatively consistent across seasons, except for winter (Fig. 3.7B). The year 2017 had abnormally fresh near-bottom salinities throughout the winter (0.7 psu lower than the winter median near-bottom salinity for the study period). The years 2015 and 2018 also had relatively low salinities during the winter, indicating a freshening of the near-bottom waters in winter, also noted by Woodgate and Peralta-Ferriz (2021). In spring, near-bottom salinities increased to values > 32 psu, with 2012 as an abnormal year with a seasonal mean salinity of 33 psu. Salinities stabilized in summer, with seasonal means hovering around 32.5 psu for all years (Fig. 3.7B). Fall near-bottom salinities were more variable, with fresher salinities observed in 2012, 2013, and 2018 (31.8–31.9 psu).

Transport through the Bering Strait at the mooring site was northwestward throughout the year for all study years, with some occasional flow reversals observed in fall and winter (Fig. S3.3). As observed by Woodgate and Peralta-Ferriz (2021), water speeds at the mooring site gradually increased over the study period (0.15 cm s^{-1} per year; $p = 0.02$). Water speeds throughout the seasons were highly variable with standard deviations ranging from 13 cm s^{-1} to 27 cm s^{-1}. Before 2017 and 2018, the fastest seasonal water speeds were observed in spring and summer, except for 2012 which had slower water speeds (Fig. S3.4). In 2017, water speeds were highest in fall which carried over into winter of 2018, which could explain the late ice freeze-up for winter 2017–2018 (Table 3.2).

Winds in the Bering Strait region during the study period exhibited a general pattern of strong southward winds during the winter, switching to weaker southward winds in the spring and early summer (Fig. S3.5). Winds were mostly southward in the fall with speeds increasing as

winter approaches. Wind speeds rarely exceeded 10 m s^{-1} during the year with annual mean wind speeds ranging between 6–7 m s^{-1} (SD = 3.1–3.5 m s^{-1}).

Surface thermal fronts, indicated by higher SST gradients, within 30-km of the mooring were evident starting in June, though the strongest fronts (higher SST gradients) were observed in August (Figs. S3.6−S3.8). The year 2014 had the highest SST gradient (~ 5 °C) which occurred in late August, followed by 2013 which had a ~ 4 °C SST gradient in late August.

3.4.3 *Migration Timing*

Gray whales had the earliest arrival dates of the three species, with arrival dates ranging from 7 May to 12 June for the years that had spring data available (2014–2016 and 2018; Fig. 3.8A). Humpback whale calls were typically seen starting in early June with arrival dates ranging from 8 June to 25 July. Fin whales were first heard later in the summer with arrival dates ranging from 17 August to 13 September.

According to the fall detection data (2009–2018, excluding 2016), all three species typically began to depart the Bering Strait region in late October. Humpback whales were typically the first to leave the study area, with departure dates starting in late October (mean departure 4 November; Fig. 3.8B). Fin whales typically left the region in early to mid-November (mean departure 10 November), and gray whales were typically the last to leave with departure dates from mid to late November (mean departure 18 November; Fig. 3.8B). Over time, fin whales departed the Bering Strait 3 days later over the study period (± 1 day standard error, R^2 = 0.57, p = 0.02; Fig. 3.8B), but trends for the other two species were not significant, nor were there significant correlations between the departure dates for the three species and freeze-up dates for the Chukchi Sea (all Pearson $r \leq 0.38$, $p \geq 0.31$). We did, however, find significant positive relationships between departure dates for fin and humpback whales and seasonal mean

near-bottom temperatures for all four seasons (all Pearson $r \geq 0.71$, all $p < 0.02$; Fig. 3.9). We also found significant positive correlations between departure dates for fin and humpback whales and seasonal mean SSTs for all four seasons (all Pearson $r \geq 0.74$, all $p < 0.02$; Fig. 3.9), except between fin whale departure dates and summer SSTs ($p = 0.15$). Departure dates for fin whales were also positively correlated to higher water speeds in the previous winter ($r = 0.83$, $p = 0.006$; Fig. 3.10). The were no significant relationships between gray whale departure dates and seasonal mean environmental conditions at the mooring site.

3.4.4 *Correlation Between Whale Presence and Prey Data*

The Pearson correlation tests between the fin and humpback whale abundance proxies and forage fish abundance (for September) did not produce any significant results. We also did not find any significant correlations between the abundance proxies for fin and humpback whales for the outmigration period (October–November) and mean *Calanus* spp. abundance for any of the sampling zones (all zones: Pearson $|r| \leq 0.58$, $p \geq 0.31$; see Fig. 3.3A for the sampling zones). We observed the highest *Calanus* mean abundance for all EcoFOCI sampling zones in 2012 (Fig. 3.3B), which also had high abundance of recordings with fin and humpback whales during the outmigration period (October–November; Fig. 3.5). However, two other years with high abundance of fin and humpback whale calls, 2017 and 2018, only had moderate to low *Calanus* copepod densities (Fig. 3.3B). The correlation tests between the gray whale abundance proxy for the outmigration period and seasonal mean amphipod density only produced significant results for the Barrow transect (2013–2015, 2017; Pearson $r = 0.96$, $p = 0.04$; see Fig. 3.2B for the sampling zones). Correlations between gray whale abundance and amphipod density were insignificant for the other four sampling zones.

3.4.5 *Modeling Results*

Six models were within 10 AICc units of the best model for each species (Table S3.4) Among these models, day of the year (DOY), daily mean near-bottom temperatures ('SBETemp'), SST, water speed, and the lagged SST gradient ('SST Gradient Lagged,' lagged by one month) were included in all three species models (Table 3.3).

The probability of observing fin whale calls increased with DOY, peaking between early September (DOY 250) and mid-November (~ DOY 325; Fig. 3.11). The probability of calling fin whales being present increased with increasing near-bottom temperatures, with a peak between 4–5 °C, and calling fin whales were more likely to be heard on days with sea-surface temperatures ranging from 1–4 °C. Removing near-bottom temperature from the fin whale model resulted in a 6% decrease in R^2 , making it the third most important predictor in the model. The code produced an error when SST and SST Gradient variables were removed from the model, therefore we were unable to calculate the change in R^2 for these predictors. Water speed was the most important predictor for the fin whale model with a −15% change in R^2 when the variable was removed from the model (Table 3.4). The probability of a calling fin whale being present decreased with faster water speeds (> 30 cm s^{-1}), which likely was due to higher water speeds causing strumming noise which obscures whale calls in the spectrograms. The relationship between probability of calling fin whales being present and SST Gradient was negative, with probability decreasing as the SST gradient increased. This could be due to the lack of strong fronts during the fall when most calling fin whales were detected (Fig. S3.6). In contrast, more recordings with fin whale calls occurred when the SST gradient was within 2−4 °C the previous month, indicating that the presence of a thermal front earlier in the season may attract calling fin whales.

Like with fin whales, the probability of observing humpback whale calls increased with DOY, particularly between early September (DOY 250) and early November (~ DOY 305; Fig. 3.12). Day of the year was the most important predictor for the humpback model, with a −12% change in the R^2 value according to the incremental R^2 test (Table 3.4). There was a bimodal relationship between near-bottom temperature and humpback calls, with a peak between 0–2 °C and another between 4–5 °C. Calling humpback whales were more likely to be present on days with warmer SST (> 2 °C). Removing temperature for the humpback model resulted in a −3% change in R^2 (Table 3.4). The probability of calling humpback whales being present decreased with increasing near-bottom salinity with a slight peak between 32 and 32.5 psu, though removal of near-bottom salinity only resulted in a 2% decrease in R^2. Similar to fin whales, humpback whales were less likely to be heard on days with high winds and water speeds, likely because high wind and water speeds inhibit detection of humpback calls. Both SST Gradient and Lagged SST Gradient were included in the final humpback model, though both predictors were less important for the fit of the model according to the incremental R^2 test (−2% change). The plot for SST Gradient shows a mostly negative relationship between the probability of calling humpbacks being present and the daily maximum SST gradient, similar to fin whales. However, the probability of a calling humpback being present increased with lagged SST gradients between 2−4 °C, with greater uncertainty towards higher gradients.

There were two final gray whale models according to AICc (with equal R^2), therefore we chose the more parsimonious model (Table S3.4). The probability of a calling gray whale being present had a negative relationship with DOY, and DOY had a low impact on R^2 with a −2% change (Table 3.4). The probability of observing calling gray whales increased with increasing near-bottom temperatures (Fig. 3.13), while the relationship with SST was bimodal with a slight

peak in probability at ~ 1 °C and another around 7 °C. Removal of either temperature variables had a weak impact on R^2 with a 2% decrease. The probability of calling gray whales being present slightly decreased with increasing near-bottom salinities with higher probabilities around 31–32 psu (Fig. 3.12). Similar to the temperature variables, removing near-bottom salinity only resulted in a −2% change in R^2. Lagged SST gradient was included in the gray whale model with higher probability of calling gray whales being present when the lagged SST gradient was low (0−1 °C). Calling gray whales were more likely to be heard on days with slower water and wind speeds (Fig. 3.12), though water speed was far more important with a −67% change in R^2 in comparison to a −2% change for wind speed.

3.5 Discussion

3.5.1 *Acoustic Presence*

Similar to previous studies (Sleptsov 1961; Clarke et al. 2013; Delarue et al. 2013; Woodgate et al. 2015; Melnikov 2019), we found that the acoustic presence of fin and humpback whales varied from year to year in the Bering Strait. Both fin and humpback whales had a pronounced peak in their calls around late September to October which likely corresponds with increased vocal activity among males in association with the approaching breeding season (Winn and Winn 1978; Tyack 1981; Watkins et al. 2000; Darling and Bérubé 2001; Stafford et al. 2007). Additionally, feeding fin and humpback whales are commonly observed in the southern Chukchi Sea during the late summer to early fall months (August to October; Clarke et al. 2013; Brower et al. 2018; Melnikov 2019). High zooplankton biomass in the southern Chukchi Sea in late summer to early fall (August to November; Tsujii et al. 2016) could also explain the peaks in acoustic presence for both fin and humpback whales during this period (Fig. 3.4).

In comparison to fin and humpback whales, the acoustic presence of gray whales was relatively consistent across the years, except for 2010 when gray whale calls were only heard in 7% of recordings for October–November (compared to 26–51% in other years). The year 2010 had the second shortest open-water season (114 days) due to a long melt-out period (Table 3.2), which could explain why gray whale detections were relatively low. Also of note, Moore et al. (2022) report that 2010 had the lowest number of gray whale sightings in the south and northeast Chukchi Sea during the 2009–2019 Aerial Surveys of Arctic Marine Mammals (ASAMM). Unlike fin and humpback whales, the pattern in the acoustic occurrence of gray whales during the open-water season was more pulsed. In years with both spring and fall recordings (2013–2015, 2018), there is a clear spring peak in recordings with gray whale calls (~ June–July) and a clear fall peak (~ November). This pattern likely reflects the migration of gray whales in and out of the study area given that the most common gray whale call we saw, the 'M3' call, is associated with migration (Crane and Lashkari 1996; Guazzo et al. 2017).

3.5.2 *Migration Timing*

Gray whales were the first of the three species to arrive in the study area (calls heard starting in early May), which aligns well with observations by Urbán et al. (2021) of tagged gray whales arriving in the Chirikov Basin in May, as well as historical eyewitness accounts of gray whales entering the Bering Strait as early as the end of April (Sleptsov 1961). Humpback whales were the second species detected at our mooring site with the earliest humpback whale vocalizations recorded at the start of June. Fin whales were the last to arrive at the Bering Strait with the earliest fin whale calls detected in July. While observations of fin and humpback whales north of the Bering Strait in the spring months are lacking, land-based surveys conducted along the Chukotka Peninsula have observed humpback whales in the Gulf of Anadyr as early as the end

of April (Melnikov 2019). By June, small pods of humpback whales can be seen along the east coast of the Chukotka Peninsula, including the Bering Strait area (Melnikov 2019). Soviet whalers regularly observed fin whales in the Chukchi Sea starting in mid-June in the mid-20th century (Nikulin 1946). More contemporary observations indicate that fin whales are typically in the Chukchi Sea region by July (Clarke et al. 2013; Delarue et al. 2013).

Historical observations for the Chukchi Sea indicate that all three species typically departed the Chukchi Sea in October with gray whales sometimes leaving in November (Nikulin 1946; Berzin 1984; Sleptsov 1961) although the accuracy of these historical observations were restricted by sea ice, weather, and reduced daylight. In the present study, fin whale departure dates for 2009–2017 ranged from 31 October to 17 November, however in 2018, fin whale calls were heard well into early December (departure date = 3 December). Humpback whales similarly were last heard in the study region in late October and early November, with the latest departure date on 24 November 2018. Gray whales were typically the last to leave the study area with departure dates ranging from 12 November to 24 November. The departure dates for gray whales we calculated are 1–2 months later than those observed by Moore et al. (2022) using acoustic data recorded at a point ~ 78 km southwest of Point Hope in the Chukchi Sea (~ 179 km north of our mooring site). The difference in departure dates could be due to the gradual movement of gray whales southward during their fall migration. Additionally, fewer gray whale calls were recorded at the Point Hope location for 2018 in comparison to 2012–2017 (Moore et al. 2022), whereas 2018 was a good year for gray whale detections at our mooring site, A3 (Fig. S3.9). Possible explanations for this discrepancy include the limited spatial coverage of hydrophones in the Chukchi Sea and imperfect detection associated with acoustic data (Moore et al. 2022). Whales must vocalize to be detected using passive acoustics, and it is possible that

calling gray whales could have been out of range of either hydrophone during the fall migration period.

Fin whales left the study region an average of 3 days later each year, while humpback whales left the study region 2 days later each year, however the trend was not significant. Gray whales departed the study region around the same time each year and did not have any significant correlations to any environmental variables. Our results support the hypothesis set forth by Guazzo et al. (2019) that gray whale migration may be driven by instinct and their biological clocks rather than the environment.

We did not find a significant correlation between the departure dates and freeze-up dates (when sea-ice concentration > 80%). Instead, the departure of fin and humpback whales from the study region was influenced by water temperature. Note that fin whale departure dates were also significantly correlated with mean water speeds from the previous winter, however this relationship is likely driven by 2017 and 2018 which had abnormally high water speeds in winter. Strong northward water speeds coupled with warmer temperatures in summer and fall 2017 delayed sea-ice formation in the Chukchi Sea (Wang et al. 2021), allowing whales to stay for longer in the region that fall. Similarly, strong water speeds along with warmer temperatures during the winter of 2017−18 likely prevented sea ice from forming as far south as in previous years, reducing total sea-ice extent for the region, and allowing whales to remain in the Chukchi Sea for longer in fall 2018.

Tsujii et al. (2016) found that the departure of fin whales from the southern Chukchi Sea corresponded to a decrease in water temperatures and salinities, implying that changes in temperature may trigger the southward migration of fin whales. It is possible, then, that the lack of such a cold-water signal in 2017 and 2018 in the Chukchi Sea resulted in later departure dates

for fin whales. However, whether the connection between fin whale departure dates and temperature is determined by thermal tolerances, decreased feeding opportunities in the fall, or other environmental conditions associated with temperature is unclear. Given that fin whales were regularly observed among sea ice in the Pacific Arctic in the past (Sleptsov 1961), it is likely that other changes in the environment related to warmer temperatures affected the whales' migration timing, rather than any physiological limitations.

Instead, warmer temperatures could extend the ice-free period in areas where subarctic whales feed in the fall. Both the Bering and Chukchi shelves have experienced rapid warming over the past decade, which in turn, has affected ice patterns in the region. Danielson et al. (2020) found that the warming rate for the Chukchi Sea tripled from 0.14 ± 0.07 °C decade^{-1} to 0.43 ± 0.35 °C decade^{-1} from 1990 to 2018. Warmer ocean temperatures impact the formation of sea ice in winter and ice retention in spring (Serreze et al. 2019; Kodaira et al. 2020), leading to unprecedented low winter and spring ice cover in the Pacific Arctic (Danielson et al. 2020). The Bering Strait inflow has also warmed over 1990–2018 (0.05 ± 0.02 °C year^{-1}) with longer durations of the warm-water period (from 5.5 months in the 1990s to > 7 months in 2017) on account of earlier warming (1.3 ± 0.7 days year^{-1}; Woodgate 2018; Woodgate and Peralta-Ferriz 2021). Warmer seasonal temperatures are extending the ice-free period in the Chukchi Sea, potentially allowing fin and humpback whales to delay their southward migration.

Alternatively, and perhaps concurrently, warmer conditions throughout the Pacific could mean reduced quality and quantity of prey for subarctic baleen whales (Arimitsu et al. 2021). The occurrence of an unusual mortality event (UME) for fin whales in 2015 following a heatwave in the North Pacific (2014–2016) suggests that warmer conditions are leading to poorer feeding conditions elsewhere in their range, leading to starvation (Savage 2017). Humpback

whales in the Hawaii Distinct Population Segment have exhibited declines in reproductive rates between 2013 and 2018, possibly in connection to the North Pacific heatwave (Cartwright et al. 2019). Therefore, both species may be staying longer in the Chukchi Sea to acquire more fat reserves before migrating south.

3.5.3 *Whale Presence and Prey Density*

Our analysis of the relationship between the acoustic presence of fin, humpback, and gray whales and prey density was constrained by the fact that the acoustic recordings were not collected where the whales are commonly observed feeding in the Chukchi Sea (e.g., southwest of Point Hope, or in the northeastern Chukchi Sea; Clarke et al. 2013; Brower et al. 2018). Moreover, the prey data were not collected at the same time and place as the acoustic recordings. Consequently, we compared whale recording densities in the Bering Strait to prey abundance elsewhere in the Bering and Chukchi seas, finding no relationships.

Correlation tests between fin and humpback whale proxies for September and mean forage fish abundance (mostly collected in September) were not significant. Without visual observations of fin and humpback whales feeding in areas with known aggregations of forage fish, it is difficult to determine which forage fish species either species targets in the Chukchi Sea.

We did not find a significant correlation between mean *Calanus* abundance (collected August–September) and the abundance proxies for humpback and fin whales (calculated for October–November), consequently whether copepods are a target prey for fin and humpback whales remains unclear. Although there is evidence that fin whales eat copepods in the North Pacific (Nemoto 1957; Nemoto and Kasuya 1965; Flinn et al. 2002; Witteveen and Wynne 2016), they may primarily target concentrations of euphausiids in the Chukchi Sea given their

preference for euphausiids elsewhere in their range (Mizroch et al. 1984; Laidre et al. 2010). Also, euphausiids are an important fall food source for bowhead whales feeding near Utqiaġvik, Alaska (Lowry et al. 2004), therefore it is likely that fin and humpback whales similarly prey on euphausiids in the Chukchi Sea. In their study of large baleen whales in West Greenland, Laidre et al. (2010) found that the relationship between the presence of whales and euphausiid abundance was significant only when both datasets were collected simultaneously. Laidre et al. (2010) concluded that perhaps the quickly changing environment of the West Greenland continental shelf diminished the relevancy of time lags in prey abundance. The Bering Strait is equally dynamic, especially given strong flow during the summer and fall months. Without accurate data on euphausiid distribution and abundance in addition to concurrent observations of whales, whether fin and humpback whales are feeding on euphausiids in the Chukchi Sea remains to be seen.

We found a significant correlation with our gray whale abundance proxy (calculated for October–November) and benthic amphipod densities (collected in July, and August–September) in the Barrow zone only. The region around the Barrow transect is known to be a foraging hotspot for gray whales (Moore and Ljungblad 1984; Kuletz et al. 2015; Clarke et al. 2016; Brower et al. 2017; Moore et al. 2022). Despite being a historical foraging hotspot (Highsmith et al. 2007), amphipod abundance in the DBO 2 transect in Chirikov Basin did not have a significant correlation to gray whale occurrence. Recent declines in amphipod abundance in the Chirikov Basin suggest that this feeding area is in decline (Moore et al. 2022). Additionally, gray whale abundance at Site A3 was not correlated to amphipod densities in the southern Chukchi area, even though feeding gray whales are regularly seen in this region (Clarke et al. 2016;

Moore et al. 2022). Again, without concurrent prey collection along with observations of whale presence, it is difficult to draw any conclusions from this analysis.

3.5.4 *Environmental Influence on Whale Presence*

The importance of day of the year (DOY) in the fin and humpback models suggests that time of the year is highly influential in determining the probability of a calling whale being present for both species. The peaks in fin and humpback detections in October and November are likely connected to increases in vocalization rates by male fin and humpback whales (Stafford et al. 2007; Kowarski et al. 2019). Visual observations of fin and humpback whales in the Bering Strait region also indicate that both species depart the area in fall (Sleptsov 1961; Melnikov et al. 2019). In contrast, DOY had low importance in the gray whale model, suggesting that time of the year has little effect on the probability of hearing a gray whale call. Also, gray whales have low vocalization rates (0.74 calls hr^{-1}; Cummings et al. 1968), which likely contributed to low detection throughout the open-water season.

Near-bottom temperature was included in all three species' models, while near-bottom salinity was only included in the humpback and gray whale models. The range of near-bottom water temperatures (~ 1–4 °C) and salinities (31–32 psu) identified by models as contributing to higher probability of calling whales align with typical temperatures and salinities observed at A3 (Woodgate 2018; Fig. 3.7). Similarly, the range of SST that had the highest probabilities of a calling fin whale being present match the range of fall mean SST at Site A3 (Woodgate 2018; Fig. 3.7A). Therefore, it is unclear if the models identified preferred temperature and salinity ranges for whales, or simply reflect seasonal conditions at the mooring site. The effect of SST for humpback and gray whale acoustic occurrence exhibited different patterns, likely due to the difference in detection densities for the two species. Unlike fin whales, who were mostly

detected in fall, humpback whales were heard throughout the summer when SST are higher on average (Fig. 3.7A). Therefore, the probability of calling humpback whales being present increased with increasing SST. The effect of SST on gray whale acoustic occurrence had a somewhat bimodal shape, with an increase in probability of gray whale occurrence at SSTs around 1 °C and a lower secondary peak around 7 °C (Fig. 3.7A). The first peak associated with colder SSTs could reflect the increase in gray whale detections in spring when colder temperatures prevail (Woodgate 2018; Fig. 3.A), while the second peak was likely driven by warmer SSTs in summer. Additionally, 2017 and 2018 had high SST throughout the open-water period and higher abundances of recordings with whale calls (Fig. 3.5), likely driving the relationship between water temperature and the presence of calling whales.

Along with day of the year, water speed was among the most important variables with calling whales more likely to be present at the mooring site when water speeds were low to moderate (< 20 cm s^{-1}). The most likely explanation is that instrument strumming caused by water flowing past the mooring could have obscured calls in the spectrograms, leading to lower detection rates when water speeds were high. Though we scanned the spectrograms to identify calls rather than using an automated detector, missed detections are a factor when recording in the Bering Strait due to the presence of strong northward currents throughout the open-water season (Woodgate et al. 2005; Woodgate 2018). Also, singing fin and humpback whales are known to swim more slowly than non-singing whales, maintaining speeds of 1.1 m s^{-1} to 3.9 m s^{-1} in the case of fin whales (McDonald et al. 1995; Soule and Wilcock 2013; Varga et al. 2018; Clark et al. 2019; Guazzo et al. 2021) and 0.4–0.5 m s^{-1} for humpback whales (Frankel et al. 1995). Whales may therefore choose to cease vocalizing when water speeds are strong to conserve energy.

Whale acoustic presence was also impacted by wind speeds according to the humpback and gray models, with low to moderate wind speeds (≤ 10 m s^{-1}) more favorable for detection of calls. Wind and water speeds in the Bering Strait are often correlated, with faster flow speeds linked to stronger wind speeds (Woodgate et al. 2005). It is no surprise then that slower wind speeds were indicated by the models as increasing the probability of detection. Also, most days during the study period had wind speeds ≤ 10 m s^{-1}, therefore low wind speeds are more common during the open-water season in the strait.

The presence and strength of a thermal front near the A3 mooring site in the previous month ('SST Gradient Lagged') was included in all three models, though the relationship between the gradient and detection probability varied for the three species. Though its intensity and presence changes over the season, a front reliably forms off the coast of Point Hope, Alaska, where fin, humpback, and gray whales are often seen feeding (Bluhm et al. 2007; Clarke et al. 2013; Clarke et al. 2016; Brower et al. 2018; Moore et al. 2022). The location and intensity of fronts created by water masses in the Chukchi Sea are likely important factors that drive patterns in subarctic baleen whale occurrence, and should be explored in future research.

3.4.5 *Conclusions*

Our goal for this study was to better understand the connection between the presence of subarctic whales and environmental factors in the Pacific Arctic. We found that the years with the highest detections of subarctic whales were also the warmest and had the highest water speeds, supporting the hypotheses put forth by Delarue et al (2013) and Woodgate et al. (2015) that increases in transport through the Bering Strait along with warmer temperatures would lead to increases in the occurrence of subarctic whales in the region. Though we observed interannual variation in the occurrence and abundance of the three species, as estimated by their vocal

activity, all three species regularly travel through the Bering Strait and thus, are an important part of the Chukchi Sea ecosystem during the open-water period.

Our study was conducted over a decade of intense warming for the Arctic; the ten warmest years on record for the entire Arctic all occurred after 2011 (Ballinger et al. 2022). From 2014 to 2018, the Pacific Arctic experienced increasingly warmer temperatures with increased heat flux into the Bering and Chukchi seas (Danielson et al. 2020) which coincided with a strong El Niño event and heatwave in the North Pacific in 2015–2016 (Joh and Di Lorenzo 2017). Despite warmer conditions, portions of the northern Bering Sea still had spring sea ice prior to 2018 (Stabeno and Bell 2019), allowing for the formation of both an ice-edge bloom and an open-water bloom in the Bering Strait (Kikuchi et al. 2020). However, that all changed with the winter of 2017–2018 which had the lowest sea-ice extent on record in the northern Bering Sea (Stabeno and Bell 2019). Reduced ice cover in winter 2018 led to a contraction in the areal extent of the ice-edge bloom and delayed the open-water bloom (Duffy-Anderson et al. 2019; Kikuchi et al. 2020), which likely had cascading impacts on the food web. The loss of springtime ice in 2018 followed by another ice-free spring in 2019 added further evidence to a hypothesized regime change underway in the Pacific Arctic (Huntington et al. 2020; Ballinger and Overland 2022). Whether the changes in sea ice and warmer temperatures will lead to better conditions for subarctic baleen whales in this region, however, remains to be seen (Moore and Huntington 2008; Moore 2016). Our results suggest that subarctic baleen whales are already modifying their behavior in response to changes in the Pacific Arctic, including shifting the timing of their fall migrations, and suggest that we can expect more changes to come.

3.6 Acknowledgements

This study is based upon work supported by the National Science Foundation (NSF) Graduate Research Fellowship Program under grant number DGE-1256082. Any opinions, findings, and conclusions or recommendations expressed in this material are those of the author(s) and do not necessarily reflect the views of NSF. We also thank the University of Washington School of Aquatic and Fishery Sciences for providing funding for the primary author. Additional funding for this study was provided to K. Stafford from the North Pacific Research Board Arctic IERP (A94-00), the Office of Naval Research Marine Mammals and Biology Program N000141712274, and the National Science Foundation Polar Programs ARC-1107106; and to R. Woodgate from the NSF Arctic Observing Network PLR-1304052, 1758565 and 2153942. We would like to thank the crew of the R/V *Norseman II* for their support in retrieving and deploying the moorings. Many thanks to Alex Hornof, Trevor Branch, and Lisa Eisner whose feedback greatly improved earlier versions of this manuscript. The Bering Strait mooring data can be accessed in the permanent archives of the U.S. National Centers for Environmental Information/National Oceanographic Data Center (www.ncei.noaa.gov), and at: psc.apl.washington.edu/BeringStrait.html.

3.7 References

Aagaard K, Roach AT, Schumacher JD (1985) On the wind-driven variability of the flow through Bering Strait. Journal of Geophysical Research 90:7213. https://doi.org/10.1029/JC090iC04p07213

Abrahms B, Hazen EL, Aikens EO, et al (2019) Memory and resource tracking drive blue whale migrations. Proceedings of the National Academy of Sciences USA 116:5582–5587. https://doi.org/10.1073/pnas.1819031116

Akaike H (1973) Maximum likelihood identification of Gaussian autoregressive moving average models. Biometrika 60:255–265. https://doi.org/10.1093/biomet/60.2.255

Arimitsu ML, Piatt JF, Hatch S, et al (2021) Heatwave-induced synchrony within forage fish portfolio disrupts energy flow to top pelagic predators. Global Change Biology 27:1859–1878. https://doi.org/10.1111/gcb.15556

Ashjian CJ, Braund SR, Campbell RG, et al (2010) Climate variability, oceanography, bowhead whale distribution, and Iñupiat subsistence whaling near Barrow, Alaska. Arctic 63:179–194

Ballinger TJ, Overland JE (2022) The Alaskan Arctic regime shift since 2017: A harbinger of years to come? Polar Science 32:100841. https://doi.org/10.1016/j.polar.2022.100841

Ballinger TJ, Overland JE, Wang M, et al (2022) Surface Air Temperature. Arctic Report Card 2022, Druckenmiller ML, Thoman RL, Moon TA (Eds.). https://doi.org/10.25923/13qm-2576

Bassoi M, Acevedo J, Secchi ER, et al (2020) Cetacean distribution in relation to environmental parameters between Drake Passage and northern Antarctic Peninsula. Polar Biology 43:1–15. https://doi.org/10.1007/s00300-019-02607-z

Berline L, Spitz YH, Ashjian CJ, et al (2008) Euphausiid transport in the Western Arctic Ocean. Marine Ecology Progress Series 360:163–178

Berzin AA (1984) Soviet studies on the distribution and numbers of the gray whale in the Bering and Chukchi Seas from 1968 to 1982. In: Jones ML, Swartz SL, Leatherwood S (eds) The Gray Whale: *Eschrichtius robustus*. Academic Press, Massachusetts, pp 409–419

Bluhm BA, Coyle KO, Konar B, Highsmith R (2007) High gray whale relative abundances associated with an oceanographic front in the south-central Chukchi Sea. Deep Sea Research Part II: Topical Studies in Oceanography 54:2919–2933. https://doi.org/10.1016/j.dsr2.2007.08.015

Bost CA, Cotté C, Bailleul F, et al (2009) The importance of oceanographic fronts to marine birds and mammals of the southern oceans. Journal of Marine Systems 78:363–376. https://doi.org/10.1016/j.jmarsys.2008.11.022

Brower AA, Clarke JT, Ferguson MC (2018) Increased sightings of subArctic cetaceans in the eastern Chukchi Sea, 2008–2016: population recovery, response to climate change, or increased survey effort? Polar Biolgy 41:1033–1039. https://doi.org/10.1007/s00300-018-2257-x

Brower AA, Ferguson MC, Schonberg SV, et al (2017) Gray whale distribution relative to benthic invertebrate biomass and abundance: Northeastern Chukchi Sea 2009–2012. Deep Sea Research Part II: Topical Studies in Oceanography 144:156–174. https://doi.org/10.1016/j.dsr2.2016.12.007

Cartwright R, Venema A, Hernandez V, et al (2019) Fluctuating reproductive rates in Hawaii's humpback whales, *Megaptera novaeangliae*, reflect recent climate anomalies in the North Pacific. Royal Society Open Science 6:181463. https://doi.org/10.1098/rsos.181463

Clapham P (2016) Managing leviathan: conservation challenges for the great whales in a post-whaling world. Oceanography 29:214–225. https://doi.org/10.5670/oceanog.2016.70

Clark C, Ellison W, Southall B, et al (2009) Acoustic masking in marine ecosystems: intuitions, analysis, and implication. Marine Ecology Progress Series 395:201–222. https://doi.org/10.3354/meps08402

Clark CW, Gagnon GJ, Frankel AS (2019) Fin whale singing decreases with increased swimming speed. Royal Society Open Science 6:180525. https://doi.org/10.1098/rsos.180525

Clarke J, Moore S (2002) A note on observations of gray whales in the southern Chukchi and northern Bering Seas, August-November, 1980-89. Journal of Cetacean Research and Management 4:283–288

Clarke J, Stafford K, Moore S, et al (2013) Subarctic cetaceans in the southern Chukchi Sea: evidence of recovery or response to a changing ecosystem. Oceanography 26:136–149. https://doi.org/10.5670/oceanog.2013.81

Clarke JT, Kennedy AS, Ferguson MC (2016) Bowhead and gray whale distributions, sighting rates, and habitat associations in the Eastern Chukchi Sea, summer and fall 2009–15, with a retrospective comparison to 1982–91. Arctic 69:359. https://doi.org/10.14430/arctic4597

Clarke JT, Moore SE, Ljungblad DK (1989) Observations on gray whale (*Eschrichtius robustus*) utilization patterns in the northeastern Chukchi Sea, July-October 1982-1987. Canadian Journal of Zoology 67:2646–2654

Cleveland W (1993) Visualizing data. Hobart Press, Summit, NJ

Coachman LK, Aagaard K, Tripp RB (1975) Bering Strait: the regional physical oceanography. University of Washington Press, Seattle

Codispoti LA, Friederich GE, Sakamoto CM, Gordon LI (1991) Nutrient cycling and primary production in the marine systems of the Arctic and Antarctic. Journal of Marine Systems 2:359–384. https://doi.org/10.1016/0924-7963(91)90042-S

Cohen J, Cohen J, West SG, Aiken LS (2003) Applied multiple regression/correlation analysis for the behavioral sciences, 3rd Ed. Erlbaum, Mahwah, NJ

Cox DR, Snell EJ (1989) Analysis of Binary Data, Second Ed. Chapman & Hall

Crane NL, Lashkari K (1996) Sound production of gray whales, *Eschrichtius robustus*, along their migration route: A new approach to signal analysis. Journal of the Acoustical Society of America 100:1878–1886. https://doi.org/0001-4966/96/100(3)/1878/9/$10.00

Cummings WC, Thompson PO, Cook R (1968) Underwater sounds of migrating gray whales, *Eschrichtius glaucus*. Journal of the Acoustical Society of America 44: 1278-1281

Danielson SL, Ahkinga O, Ashjian C, et al (2020) Manifestation and consequences of warming and altered heat fluxes over the Bering and Chukchi Sea continental shelves. Deep Sea

Research Part II: Topical Studies in Oceanography 177:104781. https://doi.org/10.1016/j.dsr2.2020.104781

Danielson SL, Eisner L, Ladd C, et al (2017) A comparison between late summer 2012 and 2013 water masses, macronutrients, and phytoplankton standing crops in the northern Bering and Chukchi Seas. Deep Sea Research Part II: Topical Studies in Oceanography 135:7–26. https://doi.org/10.1016/j.dsr2.2016.05.024

Danielson SL, Weingartner TJ, Hedstrom KS, et al (2014) Coupled wind-forced controls of the Bering–Chukchi shelf circulation and the Bering Strait throughflow: Ekman transport, continental shelf waves, and variations of the Pacific–Arctic sea surface height gradient. Progress in Oceanography 125:40–61. https://doi.org/10.1016/j.pocean.2014.04.006

Darling JD, Berube M (2001) Interactions of singing humpback whales with other males. Marine Mammal Sci 17:570–584. https://doi.org/10.1111/j.1748-7692.2001.tb01005.x

Delarue J, Martin B, Hannay D, Berchok CL (2013) Acoustic occurrence and affiliation of fin whales detected in the northeastern Chukchi Sea, July to October 2007–10. Arctic 66:159–172

Eisner L, Hillgruber N, Martinson E, Maselko J (2013) Pelagic fish and zooplankton species assemblages in relation to water mass characteristics in the northern Bering and southeast Chukchi seas. Polar Biology 36:87–113. https://doi.org/10.1007/s00300-012-1241-0

Eisner LB, Pinchuk AI, Kimmel DG, et al (2018) Seasonal, interannual, and spatial patterns of community composition over the eastern Bering Sea shelf in cold years. Part I: zooplankton. ICES Journal of Marine Science 75:72–86. https://doi.org/10.1093/icesjms/fsx156

Ershova E, Hopcroft R, Kosobokova K, et al (2015) Long-term changes in summer zooplankton communities of the Western Chukchi Sea, 1945–2012. Oceanography 28:100–115. https://doi.org/10.5670/oceanog.2015.60

Environmental Systems Research Institute, ESRI, 2019. ArcGIS Desktop: Release 10.8. Redlands, CA: Environmental Systems Research Institute.

Flinn RD, Trites AW, Gregr EJ, Perry RI (2002) Diets of fin, sei, and sperm whales in British Columbia: an analysis of commercial whaling records, 1963–1967. Marine Mammal Science 18:663–679. https://doi.org/10.1111/j.1748-7692.2002.tb01065.x

Frankel AS, Clark CW, Herman LM, Gabriele CM (1995) Spatial distribution, habitat utilization, and social interactions of humpback whales, *Megaptera novaeangliae*, off Hawai'i, determined using acoustic and visual techniques. Canadian Journal of Zoology 73:1134–1146. https://doi.org/10.1139/z95-135

Grebmeier JM, Cooper LW (2019a) Benthic macroinfaunal samples collected from the Canadian Coast Guard Ship (CCGS) Sir Wilfrid Laurier, Northern Bering Sea to Chukchi Sea, 2012−2015. https://arcticdata.io/catalog

Grebmeier JM, Cooper LW (2019b) Benthic macroinfaunal samples collected from the (USCGC) Healy Northern Bering Sea to Chukchi Sea, 2017. https://arcticdata.io/catalog/view/doi%3A10.18739%2FA27M0414K

Grebmeier J, Frey K, Cooper L, Kędra M (2018) Trends in benthic macrofaunal populations, seasonal sea ice persistence, and bottom water temperatures in the Bering Strait region. Oceanography 31:136–151. https://doi.org/10.5670/oceanog.2018.224

Grebmeier JM (2012) Shifting patterns of life in the Pacific Arctic and Sub-Arctic seas. Annual Review of Marine Science 4:63–78. https://doi.org/10.1146/annurev-marine-120710-100926

Grebmeier JM, Feder HM, McRoy CP (1989) Pelagic-benthic coupling on the shelf of the northern Bering and Chukchi Seas. III. Benthic food supply and carbon cycling. Marine Ecology Progress Series 51:253–268

Grebmeier JM, Moore SE, Cooper LW, Frey KE (2019) The Distributed Biological Observatory: A change detection array in the Pacific Arctic – An introduction. Deep Sea Research Part II: Topical Studies in Oceanography 162:1–7. https://doi.org/10.1016/j.dsr2.2019.05.005

Grebmeier JM, Overland JE, Moore SE, et al (2006) A major ecosystem shift in the northern Bering Sea. Science 311:1461–1464

Guazzo R, Schulman-Janiger A, Smith M, et al (2019) Gray whale migration patterns through the Southern California Bight from multi-year visual and acoustic monitoring. Marine Ecology Progress Series 625:181–203. https://doi.org/10.3354/meps12989

Guazzo RA, Durbach IN, Helble TA, et al (2021) Singing fin whale swimming behavior in the Central North Pacific. Frontiers in Marine Science 8:696002. https://doi.org/10.3389/fmars.2021.696002

Guazzo RA, Helble TA, D'Spain GL, et al (2017) Migratory behavior of eastern North Pacific gray whales tracked using a hydrophone array. PLoS ONE 12:e0185585. https://doi.org/10.1371/journal.pone.0185585

Hasegawa D, Lewis MR, Gangopadhyay A (2009) How islands cause phytoplankton to bloom in their wakes. Geophysical Research Letters 36:L20605. https://doi.org/10.1029/2009GL039743

Hazen EL, Jorgensen S, Rykaczewski RR, et al (2013) Predicted habitat shifts of Pacific top predators in a changing climate. Nature Climate Change 3:234–238. https://doi.org/10.1038/nclimate1686

Highsmith RC, Coyle KO (1991) Amphipod life histories: community structure, impact of temperature on decoupled growth and maturation rates, productivity, and P:B ratios. American Zoologist 31:861-873

Highsmith RC, Coyle KO, Bluhm BA, Konar B (2007) Gray whales in the Bering and Chukchi seas. In: Estes JA, DeMaster DP, Doak DF, et al. (eds) Whales, whaling, and ocean ecosystems. University of California Press, Berkeley, pp 303–313

Hisakado M, Kitsukawa K, Mori S (2006) Correlated binomial models and correlation structures. Journal of Physics A: Mathematical and General 39:15365–15378. https://doi.org/10.1088/0305-4470/39/50/005

Hunt GL, Coyle KO, Eisner LB, et al (2011) Climate impacts on eastern Bering Sea foodwebs: a synthesis of new data and an assessment of the Oscillating Control Hypothesis. ICES Journal of Marine Science 68:1230–1243. https://doi.org/10.1093/icesjms/fsr036

Huntington HP, Danielson SL, Wiese FK, et al (2020) Evidence suggests potential transformation of the Pacific Arctic ecosystem is underway. Nature Climate Change 10:342–348. https://doi.org/10.1038/s41558-020-0695-2

Joh Y, Di Lorenzo E (2017) Increasing coupling between NPGO and PDO leads to prolonged marine heatwaves in the Northeast Pacific. Geophysical Research Letters 44:11,663-11,671. https://doi.org/10.1002/2017GL075930

Kikuchi G, Abe H, Hirawake T, Sampei M (2020) Distinctive spring phytoplankton bloom in the Bering Strait in 2018: A year of historically minimum sea ice extent. Deep Sea Research Part II: Topical Studies in Oceanography 181–182:104905. https://doi.org/10.1016/j.dsr2.2020.104905

Kodaira T, Waseda T, Nose T, Inoue J (2020) Record high Pacific Arctic seawater temperatures and delayed sea ice advance in response to episodic atmospheric blocking. Scientific Reports 10:20830. https://doi.org/10.1038/s41598-020-77488-y

Krieger KJ, Wing BL (1986) Hydroacoustic monitoring of prey to determine humpback whale movements. Auke Bay Laboratory, Northwest and Alaska Fisheries Center. National Oceanic and Atmospheric Administration

Kuletz KJ, Ferguson MC, Hurley B, et al (2015) Seasonal spatial patterns in seabird and marine mammal distribution in the eastern Chukchi and western Beaufort seas: identifying biologically important pelagic areas. Progress in Oceanography 136:175–200. https://doi.org/10.1016/j.pocean.2015.05.012

Laidre K, Heide-Jørgensen M, Heagerty P, et al (2010) Spatial associations between large baleen whales and their prey in West Greenland. Marine Ecology Progress Series 402:269–284. https://doi.org/10.3354/meps08423

Levine RM, De Robertis A, Grünbaum D, et al (2021) Autonomous vehicle surveys indicate that flow reversals retain juvenile fishes in a highly advective high-latitude ecosystem. Limnology and Oceanography 66:1139–1154. https://doi.org/10.1002/lno.11671

Lowry LF, Sheffield G, George JC (2023) Bowhead whale feeding in the Alaskan Beaufort Sea, based on stomach contents analyses. Journal of Cetacean Research and Management 6:215–223. https://doi.org/10.47536/jcrm.v6i3.763

Martin J, Royle JA, Mackenzie DI, et al (2011) Accounting for non-independent detection when estimating abundance of organisms with a Bayesian approach: Correlated behaviour and abundance. Methods in Ecology and Evolution 2:595–601. https://doi.org/10.1111/j.2041-210X.2011.00113.x

McDonald MA, Hildebrand JA, Webb SC (1995) Blue and fin whales observed on a seafloor array in the northeast pacific. Journal of the Acoustical Society of America 98:712–721

Mellinger D (2002) Ishmael 1.0 User's Guide. NOAA Technical Memorandum OAR PMEL-120. http://www.pmel.noaa.gov/pubs/PDF/mell2434/mell2434.pdf.

Melnikov VV (2019) Observation of humpback whales (*Megaptera novaeangliae*) in the waters adjacent to the Chukotka Peninsula with comparisons to historical sighting data. Open Access Library Journal 6:e5407

Mesinger F, DiMego G, Kalnay E, et al (2006) North American Regional Reanalysis. Bulletin of the American Meteorological Society 87:343–360. https://doi.org/10.1175/BAMS-87-3-343

Meynecke J-O, de Bie J, Barraqueta J-LM, et al (2021) The role of environmental drivers in humpback whale distribution, movement and behavior: a review. Frontiers in Marine Science 8:720774. https://doi.org/10.3389/fmars.2021.720774

Mizroch SA, Rice DW, Breiwick JM (1984) The fin whale, *Balaenoptera physalus*. Marine Fisheries Review 46:20–24

Monnahan CC, Branch TA, Stafford KM, et al (2014) Estimating historical eastern North Pacific blue whale catches using spatial calling patterns. PLoS ONE 9:e98974. https://doi.org/10.1371/journal.pone.0098974

Moore SE (2016) Is it 'boom times' for baleen whales in the Pacific Arctic region? Biology Letters 12:20160251. https://doi.org/10.1098/rsbl.2016.0251

Moore SE, Clarke JT, Okkonen SR, et al (2022) Changes in gray whale phenology and distribution related to prey variability and ocean biophysics in the northern Bering and eastern Chukchi seas. PLoS ONE 17:e0265934. https://doi.org/10.1371/journal.pone.0265934

Moore SE, deMaster DP, Dayton PK (2000) Cetacean habitat selection in the Alaskan Arctic during summer and autumn. Arctic 53:432–447

Moore SE, Huntington HP (2008) Arctic marine mammals and climate change: impacts and resilience. Ecological Applications 18:S157–S165

Moore SE, Ljungblad DK (1984) Gray whales in the Beaufort, Chukchi, and Bering seas: distribution and sound production. In: Jones ML, Swartz SL, Leatherwood S (eds) The gray whale, *Eschrichtius robustus*. Academic Press, San Diego, California, pp 543–559

Moss JH, Farley EV, Feldmann AM, Ianelli JN (2009) Spatial distribution, energetic status, and food habits of Eastern Bering Sea age-0 walleye pollock. Transactions of the American Fisheries Society 138:497–505. https://doi.org/10.1577/T08-126.1

Nelms S, Alfaro-Shigueto J, Arnould J, et al (2021) Marine mammal conservation: over the horizon. Endangered Species Research 44:291–325. https://doi.org/10.3354/esr01115

Nemoto T (1959) Food of baleen whales with reference to whale movements. Scientific Report of the Whales Research Institute 14:149–290

Nemoto T (1957) Foods of baleen whales in the northern Pacific. Scientific Reports of the Whales Research Institute Tokyo 12:33–89

Nemoto T, Kasuya T (1965) Foods of baleen whales in the Gulf of Alaska of the North Pacific. Scientific Reports of the Whales Research Institute 19:45–51

Nerini M (1984) A review of gray whale feeding ecology. In: Jones ML, Swartz SL, Leatherwood S (eds) The Gray Whale *Eschrichtius Robustus*. Academic Press, Florida, pp 423–450

Nguyen AT, Woodgate RA, Heimbach P (2020) Elucidating large-scale atmospheric controls on Bering Strait throughflow variability using a data-constrained ocean model and its adjoint. Journal of Geophysical Research: Oceans 125:NA–NA. https://doi.org/10.1029/2020JC016213

Nikulin PG (1946) Distribution of cetaceans in the seas surrounding the Chukchi Peninsula. Izv TINRO 22

Payne PM, Wiley DN, Young SB, et al (1990) Recent fluctuations in the abundance of baleen whales in the southern Gulf of Maine in relation to changes in selected prey. Fishery Bulletin (Washington, DC) 88:687–696

Perryman WL, Donahue MA, Perkins PC, Reilly SB (2002) Gray whale calf production 1994–2000: are observed fluctuations related to changes in seasonal ice cover? Marine Mammal Science 18:121–144. https://doi.org/10.1111/j.1748-7692.2002.tb01023.x

Peralta-Ferriz C, Woodgate RA (2017) The dominant role of the east Siberian Sea in driving the oceanic flow through the Bering Strait—conclusions from GRACE ocean mass satellite data and in situ mooring observations between 2002 and 2016. Geophysical Research Letters 44:NA–NA. https://doi.org/10.1002/2017GL075179

Pinchuk AI, Eisner LB (2017) Spatial heterogeneity in zooplankton summer distribution in the eastern Chukchi Sea in 2012–2013 as a result of large-scale interactions of water masses. Deep Sea Research Part II: Topical Studies in Oceanography 135:27–39. https://doi.org/10.1016/j.dsr2.2016.11.003

R Core Team. (2021). R: A language and environment for statistical computing. R Foundation for Statistical Computing, Vienna, Austria. https://www.R-project.org/.

Reidy R, Gauthier S, Doniol-Valcroze T, et al (2023) Integrating technologies provides insight into the subsurface foraging behaviour of a humpback whale (*Megaptera novaeangliae*) feeding on walleye pollock (*Gadus chalcogrammus*) in Juan de Fuca Strait, Canada. PLoS ONE 18:e0282651. https://doi.org/10.1371/journal.pone.0282651

Reynolds RW, Smith TM, Liu C, et al (2007) Daily high-resolution-blended analyses for sea surface temperature. Journal of Climate 20:5473–5496. https://doi.org/10.1175/2007JCLI1824.1

Rigby RA, Stasinopoulos DM (2005) Generalized additive models for location, scale and shape. Journal of the Royal Statistical Society Series C-Applied Statistics 54:507–544

Ryan JP, Cline DE, Joseph JE, et al (2019) Humpback whale song occurrence reflects ecosystem variability in feeding and migratory habitat of the northeast Pacific. PLoS ONE 14:e0222456. https://doi.org/10.1371/journal.pone.0222456

Savage K (2017) Alaska and British Columbia large whale unusual mortality event summary report. Protected Resources Division, National Oceanic and Atmospheric Administration, Juneau, AK

Scales KL, Miller PI, Hawkes LA, et al (2014) On the Front Line: frontal zones as priority at-sea conservation areas for mobile marine vertebrates. Journal of Applied Ecology 51:1575–1583. https://doi.org/10.1111/1365-2664.12330

Serreze MC, Barrett AP, Crawford AD, Woodgate RA (2019) Monthly variability in Bering Strait oceanic volume and heat transports, links to atmospheric circulation and ocean temperature, and implications for sea ice conditions. Journal of Geophysical Research: Oceans 124:9317–9337. https://doi.org/10.1029/2019JC015422

Serreze MC, Barrett AP, Stroeve JC, et al (2009) The emergence of surface-based Arctic amplification. The Cryosphere 3:11–19. https://doi.org/10.5194/tc-3-11-2009

Serreze MC, Crawford AD, Stroeve JC, et al (2016) Variability, trends, and predictability of seasonal sea ice retreat and advance in the Chukchi Sea. Journal of Geophysical Research: Oceans 121:7308–7325. https://doi.org/10.1002/2016JC011977

Shabangu FW, Yemane D, Stafford KM, et al (2017) Modelling the effects of environmental conditions on the acoustic occurrence and behaviour of Antarctic blue whales. PLoS ONE 12:e0172705. https://doi.org/10.1371/journal.pone.0172705

Sigler MF, Stabeno PJ, Eisner LB, et al (2014) Spring and fall phytoplankton blooms in a productive subarctic ecosystem, the eastern Bering Sea, during 1995–2011. Deep Sea Research Part II: Topical Studies in Oceanography 109:71–83. https://doi.org/10.1016/j.dsr2.2013.12.007

Širović A, Hildebrand JA (2011) Using passive acoustics to model blue whale habitat off the Western Antarctic Peninsula. Deep Sea Research Part II: Topical Studies in Oceanography 58:1719–1728. https://doi.org/10.1016/j.dsr2.2010.08.019

Sleptsov MM (1961) O kolebaniakh chislennosti kitov v Chukotskom more v raznye gody. (On fluctuations in the number of whales in the Chukchi Sea in different years). In: Proceedings of the A.N. Severtsov Institute of Animal Morphology. Nauka, Moscow, pp 54–64

Soule DC, Wilcock WSD (2013) Fin whale tracks recorded by a seismic network on the Juan de Fuca Ridge, Northeast Pacific Ocean. Journal of the Acoustical Society of America 133:1751–1761. https://doi.org/10.1121/1.4774275

Spear A, Napp J, Ferm N, Kimmel D (2020) Advection and in situ processes as drivers of change for the abundance of large zooplankton taxa in the Chukchi Sea. Deep Sea Research Part II: Topical Studies in Oceanography 177:104814. https://doi.org/10.1016/j.dsr2.2020.104814

Stabeno PJ, Bell SW (2019) Extreme conditions in the Bering Sea (2017–2018): record-breaking low sea-ice extent. Geophysical Research Letters 46:8952–8959. https://doi.org/10.1029/2019GL083816

Stafford KM, Mellinger DK, Moore SE, Fox CG (2007) Seasonal variability and detection range modeling of baleen whale calls in the Gulf of Alaska, 1999–2002. Journal of the Acoustical Society of America 122:3378–3390. https://doi.org/10.1121/1.2799905

Stasinopoulos D, Rigby RA, Heller G, et al (2017) Flexible Regression and Smoothing: Using GAMLSS in R. Chapman and Hall, Boca Raton, FL

Stroeve JC, Markus T, Boisvert L, et al (2014) Changes in Arctic melt season and implications for sea ice loss. Geophysical Research Letters 41:1216–1225. https://doi.org/10.1002/2013GL058951

Stroeve JC, Serreze MC, Holland MM, et al (2012) The Arctic's rapidly shrinking sea ice cover: a research synthesis. Climatic Change 110:1005–1027. https://doi.org/10.1007/s10584-011-0101-1

Szabo A (2015) Immature euphausiids do not appear to be prey for humpback whales (*Megaptera novaeangliae*) during spring and summer in Southeast Alaska. Marine Mammal Science 31:677–687. https://doi.org/10.1111/mms.12183

Szesciorka AR, Ballance LT, Širović A, et al (2020) Timing is everything: drivers of interannual variability in blue whale migration. Scientific Reports 10:7710. https://doi.org/10.1038/s41598-020-64855-y

Torres LG (2017) A sense of scale: Foraging cetaceans' use of scale-dependent multimodal sensory systems. Marine Mammal Science 33:1170–1193. https://doi.org/10.1111/mms.12426

Tsujii K, Otsuki M, Akamatsu T, et al (2016) The migration of fin whales into the southern Chukchi Sea as monitored with passive acoustics. ICES Journal of Marine Science: Journal du Conseil 73:2085–2092. https://doi.org/10.1093/icesjms/fsv271

Tyack P (1981) Interactions between singing Hawaiian humpback whales and conspecifics nearby. Behavioral Ecology and Sociobiology 8:105–116

Urbán R J, Jiménez-López E, Guzmán HM, Viloria-Gómora L (2021) Migratory behavior of an eastern North Pacific gray whale from Baja California Sur to Chirikov Basin, Alaska. Frontiers in Marine Science 8:619290. https://doi.org/10.3389/fmars.2021.619290

Wang Y, Liu N, Zhang Z (2021) Sea Ice Reduction During Winter of 2017 due to oceanic heat supplied by Pacific Water in the Chukchi Sea, west Arctic Ocean. Frontiers in Marine Science 8:650909. https://doi.org/10.3389/fmars.2021.650909

Watkins WA (1981) Activities and underwater sounds of fin whales. Scientific Report of the Whales Research Institute 33:83–117

Watkins WA, Daher MA, Repucci GM, et al (2000) Seasonality and distribution of whale calls in the North Pacific. Oceanography 13:62–67

Watkins WA, Tyack P, Moore KE, Bird JE (1987) The 20-Hz signals of finback whales (*Balaenoptera physalus*). Journal of the Acoustical Society of America 82:1901–1912

Weingartner T, Aagaard K, Woodgate R, et al (2005) Circulation on the north central Chukchi Sea shelf. Deep Sea Research Part II: Topical Studies in Oceanography 52:3150–3174. https://doi.org/10.1016/j.dsr2.2005.10.015

Winn HE, Winn LK (1978) The song of the humpback whale *Megaptera novaeangliae* in the West Indies. Marine Biology 47:97–114. https://doi.org/10.1007/BF00395631

Witteveen BH, Wynne KM (2016) Trophic niche partitioning and diet composition of sympatric fin (*Balaenoptera physalus*) and humpback whales (*Megaptera novaeangliae*) in the Gulf of Alaska revealed through stable isotope analysis. Marine Mammal Science 32:1319–1339. https://doi.org/10.1111/mms.12333

Woodgate RA (2018) Increases in the Pacific inflow to the Arctic from 1990 to 2015, and insights into seasonal trends and driving mechanisms from year-round Bering Strait mooring data. Progress in Oceanography 160:124–154. https://doi.org/10.1016/j.pocean.2017.12.007

Woodgate RA, Aagaard K, Weingartner TJ (2005) A year in the physical oceanography of the Chukchi Sea: Moored measurements from autumn 1990–1991. Deep Sea Research Part II: Topical Studies in Oceanography 52:3116–3149. https://doi.org/10.1016/j.dsr2.2005.10.016

Woodgate RA, Weingartner TJ, Lindsay R (2012) Observed increases in Bering Strait oceanic fluxes from the Pacific to the Arctic from 2001 to 2011 and their impacts on the Arctic Ocean water column. Geophysical Research Letters 39:L24603. https://doi.org/10.1029/2012GL054092

Woodgate R, Stafford K, Prahl F (2015) A synthesis of year-round interdisciplinary mooring measurements in the Bering Strait (1990–2014) and the RUSALCA years (2004–2011). Oceanography 28:46–67. https://doi.org/10.5670/oceanog.2015.57

Woodgate R, Peralta-Ferriz C (2021) Warming and freshening of the Pacific inflow to the Arctic from 1990-2019 implying dramatic shoaling in Pacific winter water ventilation of

the Arctic water column. Geophysical Research Letters 48:e2021GL092528. https://doi.org/10.1029/2021GL092528

Yablokov AV, Bogoslovskaya LS (1984) A review of Russian research on the biology and commercial whaling of the gray whale. In: Jones ML, Swartz SL, Leatherwood S (eds) The Gray Whale: *Eschrichtius robustus*. Academic Press, Massachusetts, pp 465–485

3.8 Tables

Table 3.1. Hydrophone deployment data, positions, and recording settings (duty cycle refers to the recording time per hour). Dates are in the format 'YYYY-MM-DD.' The "Record Start/End" dates indicate when the hydrophone started and stopped recording, however we only analyzed recordings for the open-water season (May through freeze-up in November/December of each year).

Deployment Year	Latitude N	Latitude W	Record Start Date	Record End Date	Sampling Rate (Hz)	Hourly Duty Cycle
2009	66.33°	168.97°	2009-09-01	2010-03-03	16384	12 min
2010	66.33°	168.97°	2010-08-11	2011-02-19	16384	15 min
2011	66.33°	168.97°	2011-10-01	2012-05-25	8192	10 min
2012	66.33°	168.97°	2012-09-01	2013-05-17	16384	10 min
2013	66.33°	168.97°	2013-07-15	2014-07-02	8192	20 min
2014	66.33°	168.97°	2014-07-10	2015-07-02	8192	20 min
2015	66.33°	168.97°	2015-07-05	2016-07-08	8192	20 min
2017	66.33°	168.95°	2017-08-17	2018-07-25	8192	20 min
2018	66.33°	168.95°	2018-08-12	2019-09-07	8192	20 min

Table 3.2. Melt-out (sea-ice concentration < 80%) and freeze-up (sea-ice conc. ≥ 80%) initiation dates along with the start/end dates and length of the open-water period for the Chukchi Sea (boundaries in Fig. 3.1).

Year	Melt-out Initiation Date	Open-water Start Date	Open-water End Date	Freeze-up Initiation Date	Open-water Period Length (days)
2009	21 May	3 Jul	14 Nov	28 Nov	134
2010	20 May	16 Jul	7 Nov	13 Dec	114
2011	18 May	25 Jun	16 Nov	2 Dec	144
2012	3 Jun	22 Jul	29 Oct	25 Nov	99
2013	6 Jun	10 Jul	12 Nov	17 Dec	125
2014	11 May	2 Jul	1 Dec	15 Dec	152
2015	13 May	22 Jun	17 Nov	7 Dec	148
2016	17 May	6 Jul	21 Nov	28 Dec	138
2017	2 May	23 Jun	22 Nov	2 Jan	152
2018	23 Apr	27 Jun	25 Nov	14 Dec	151

Table 3.3. List of variables included in the best model for each species (model with lowest AICc score). A check mark (✓) indicates that the variable was included in the model. Smoothers are: cs = cubic spline, pb = penalized b-spline smoothers. Variables in **bold** text were included in all three species' models.

Variable	Fin Whales	Humpback Whales	Gray Whales
pb(DOY)	✓	✓	✓
cs(SBE Temp)	✓	✓	✓
cs(SBE Salt)		✓	✓
cs(SST)	✓	✓	✓
cs(Water Speed)	✓	✓	✓
cs(Wind Speed)		✓	✓
cs(SST Gradient)	✓	✓	
cs(SST Gradient Lagged)	✓	✓	✓

Table 3.4. Results of the incremental R^2 test on the final models for each species. The R^2 value listed for each predictor variable is the R^2 for the full model with that variable removed. The ΔR^2 indicates the change in R^2 from that of the full model, and the percent (%) change indicates how much the full-model R^2 changed with that variable removed. The R^2 values were calculated using the Cox-Snell equation (Cox and Snell 1989).

Fin Whale Final Model R^2 = 0.51			
Variable	R^2	ΔR^2	**% change**
Water speed	0.44	-0.08	15
DOY	0.44	-0.07	13
SBE Temp	0.49	-0.03	6
SST Gradient Lagged	0.5	-0.02	4

Humpback Whale Final Model R^2 = 0.60			
Variable	R^2	ΔR^2	**% change**
DOY	0.53	-0.07	12
Water Speed	0.57	-0.03	5
SBE Temp	0.58	-0.02	3
SST	0.58	-0.02	3
Wind Speed	0.58	-0.02	3
SBE Salt	0.59	-0.01	2
SST Gradient	0.59	-0.01	2
SST Gradient Lagged	0.59	-0.01	2

Gray Whale Final Model R^2 = 0.45			
Variable	R^2	ΔR^2	**% change**
Water Speed	0.15	-0.3	67
DOY	0.44	-0.01	2
SBE Temp	0.44	-0.01	2
SBE Salt	0.44	-0.01	2
SST	0.44	-0.01	2
Wind Speed	0.44	-0.01	2
SST Gradient Lagged	0.44	-0.01	2

3.9 Figures

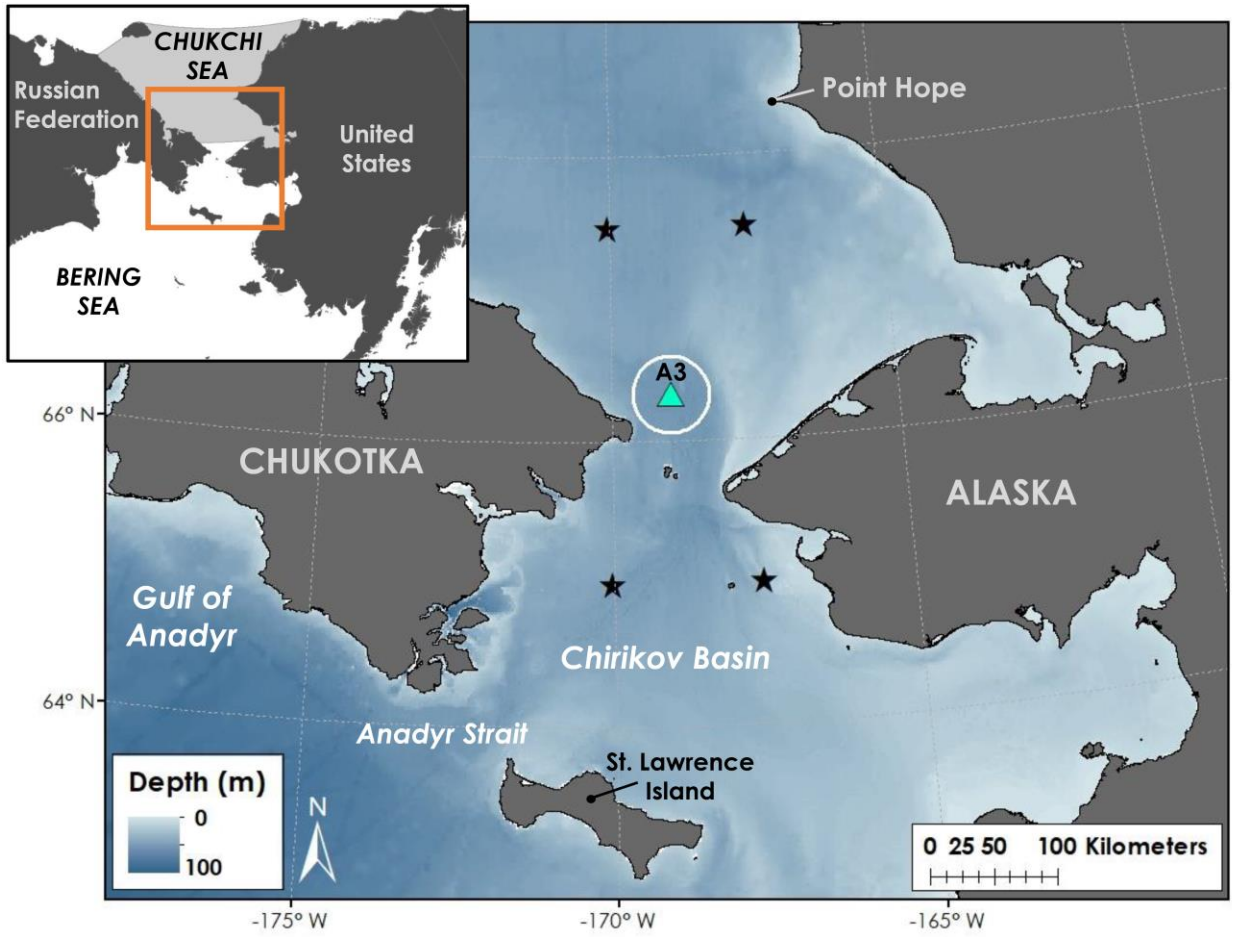

Fig. 3.1. Map of study area and the Bering Strait region. The white circle around A3 indicates the extent of the 30-km buffer which we used to calculate the sea-surface temperature gradient for indicating the presence of a thermal front near A3. The four wind data points from NOAA's National Center for Atmospheric Prediction (NCEP) North American Regional Reanalysis (NARR) dataset are included (stars). The inset map shows the study area (orange box) along with the boundaries for the Chukchi Sea as defined by the International Hydrographic Organization (IHO, http://www.marineregions.org/gazetteer.php?p=details&id=4257).

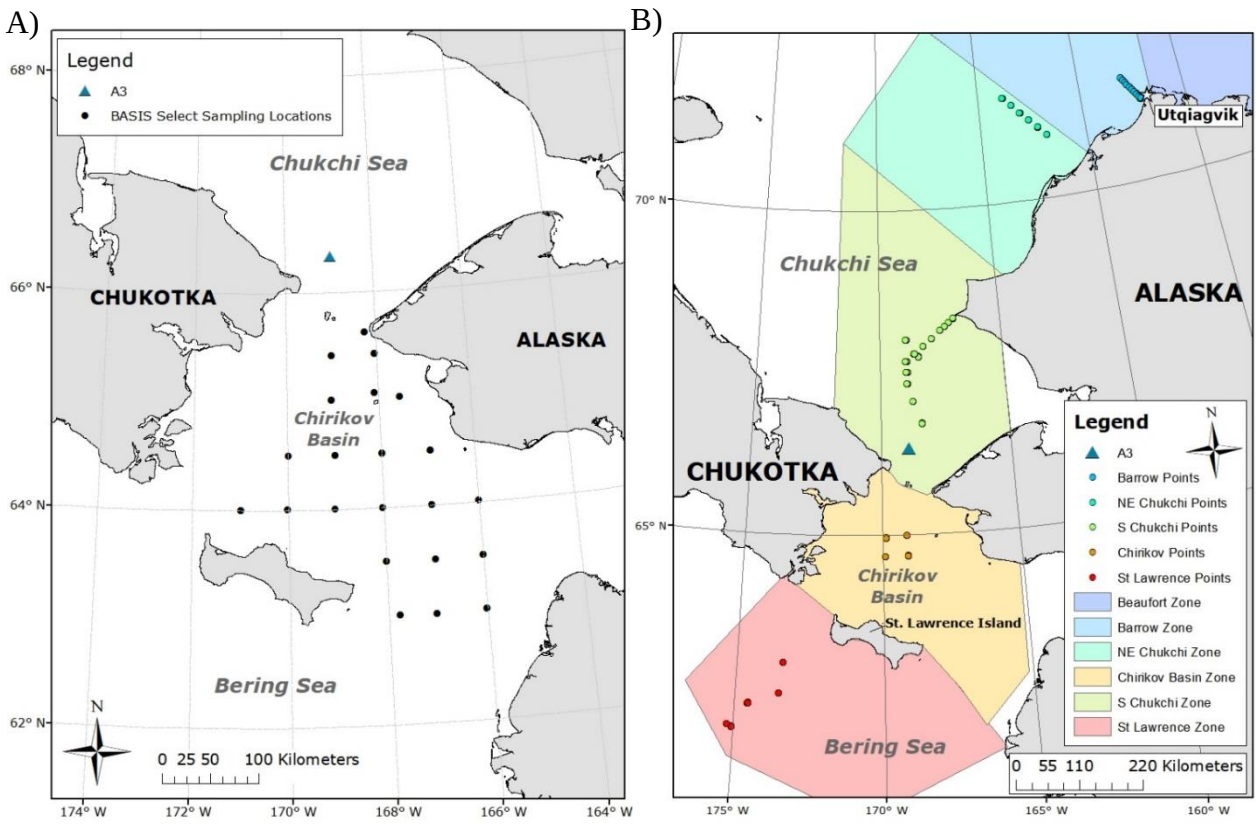

Fig. 3.2. Sampling stations for (A) the Bering Arctic Subarctic Integrated Survey (BASIS), and (B) the benthic invertebrate dataset (Grebmeier and Cooper 2019a, 2019b).

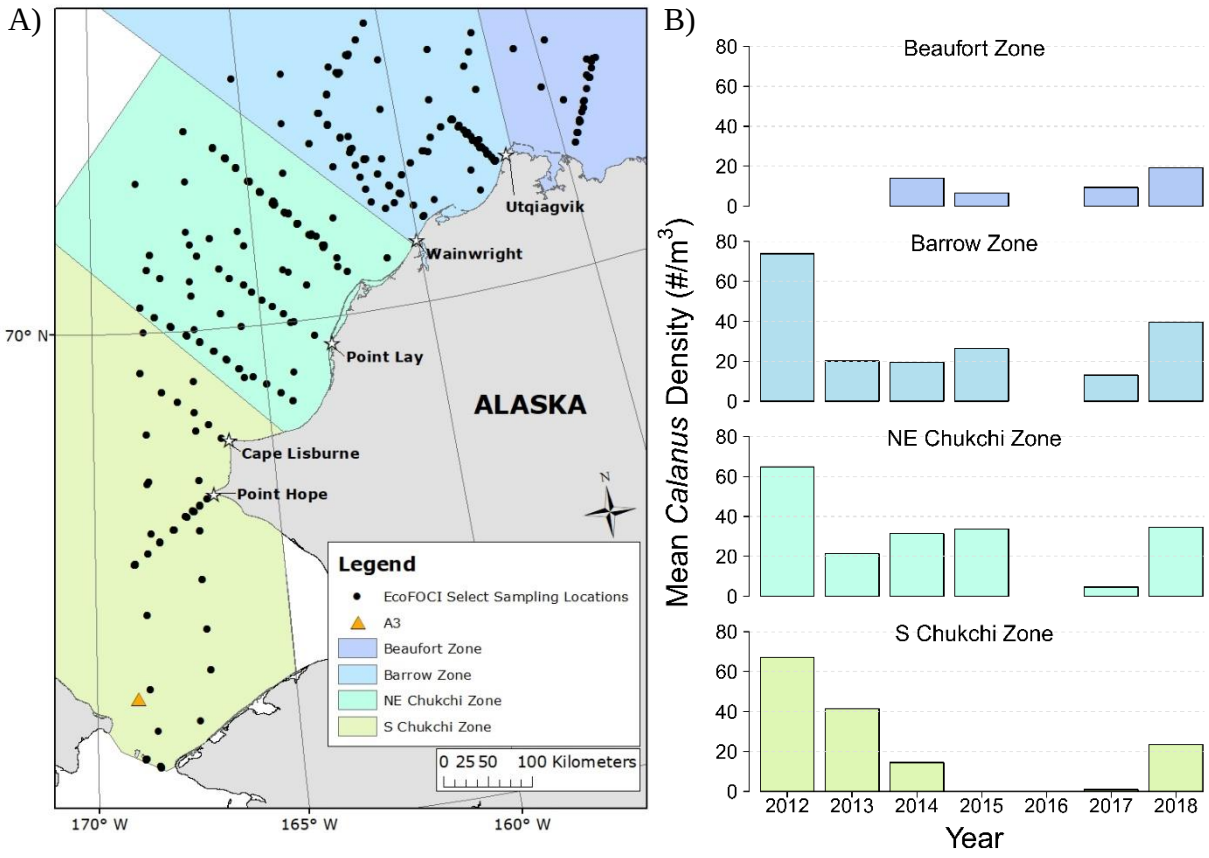

Fig. 3.3. (A) Sampling stations for the NOAA EcoFOCI zooplankton dataset. (B) Annual mean density (number per m^3) of *Calanus* spp. copepods in the four sampling zones.

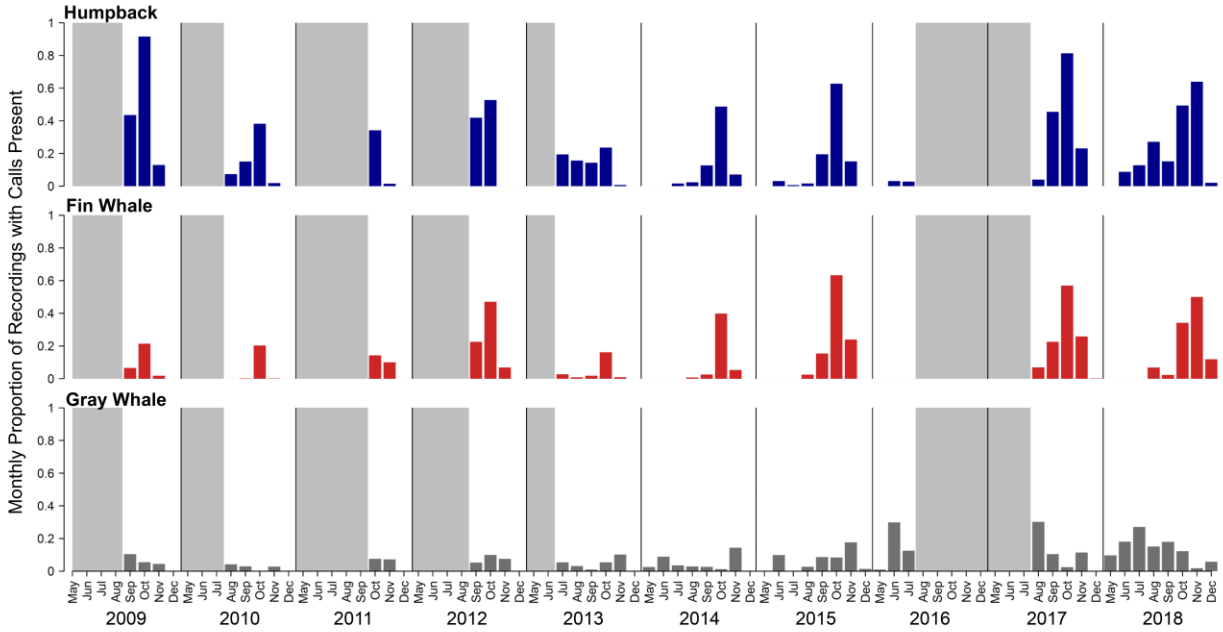

Fig. 3.4. Proportion of hourly recordings with whale calls by month during the open-water season for humpback whales, fin whales, and gray whales at the A3 mooring site. Vertical lines separate each year while the gray shaded areas indicate periods with no recordings.

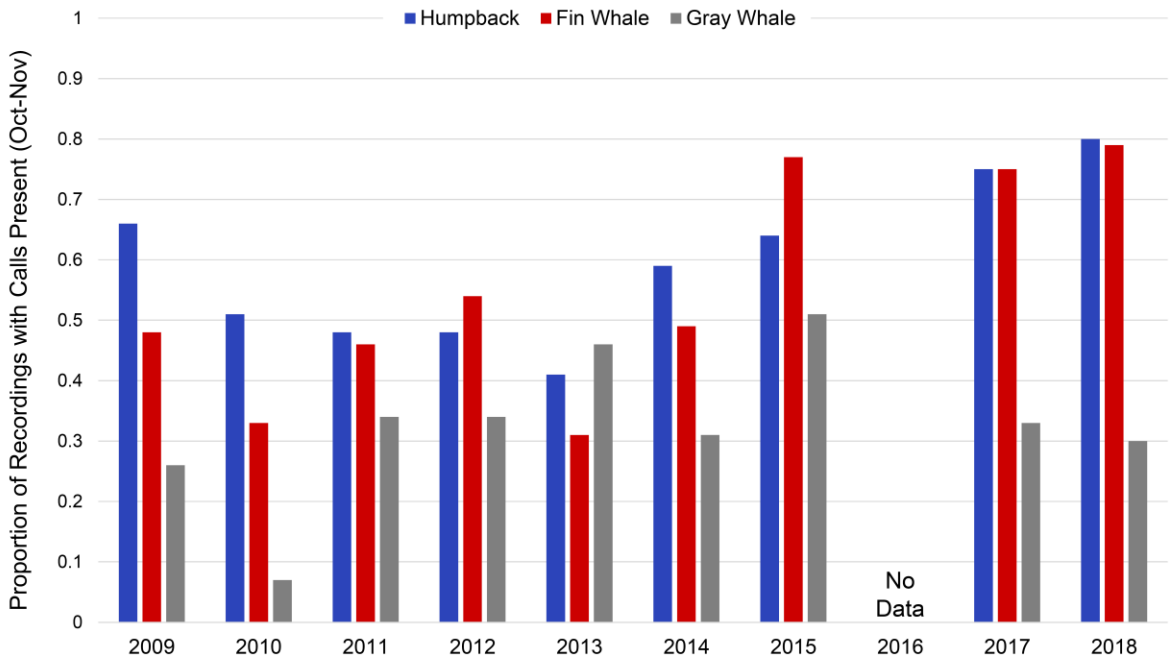

Fig. 3.5. Proportion of October–November recordings with whale calls by year for each species.

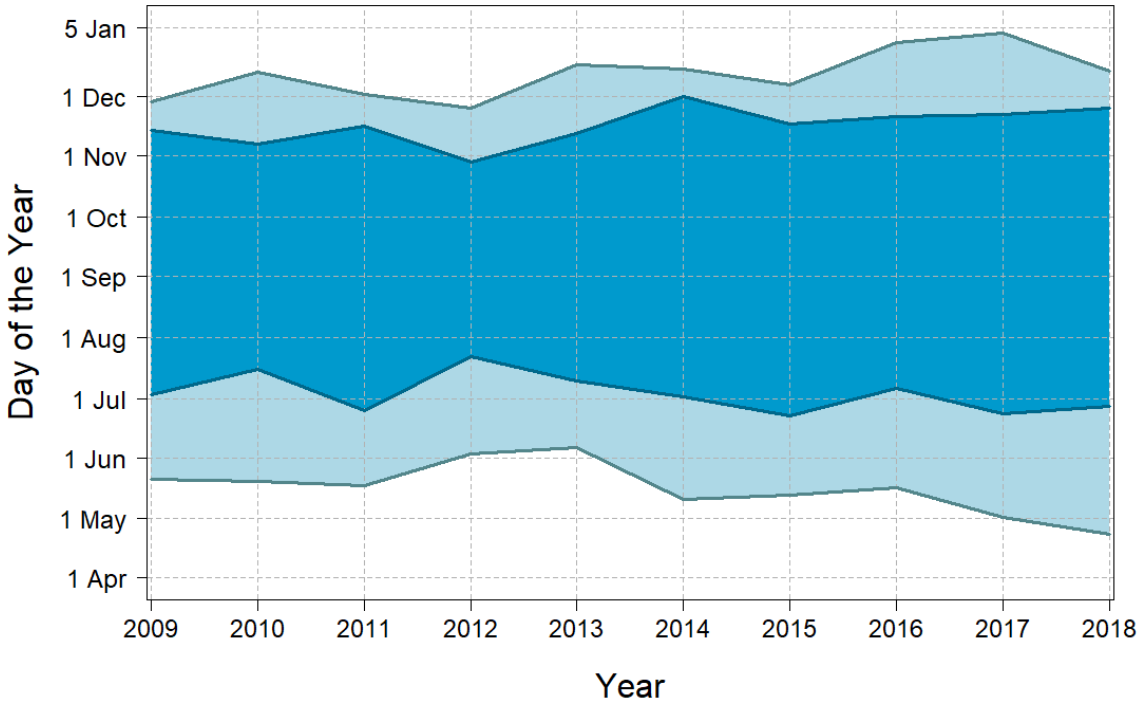

Fig. 3.6. Graphical representation of Chukchi Sea ice melt-out (< 80% concentration) in the spring, and freeze-up (≥ 80% concentration) in the fall for the study period (2009–2018) (light blue). The dark blue area represents the open-water period (sea-ice concentration ≤ 15%).

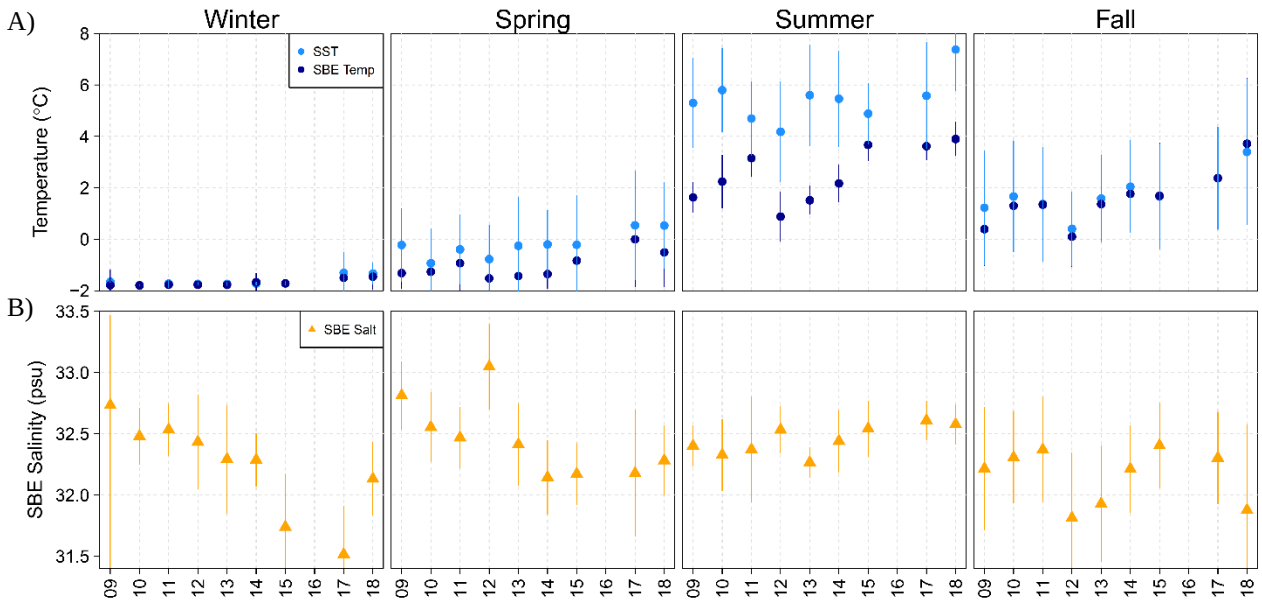

Fig. 3.7. Plots of (A) seasonal mean near-bottom ('SBE Temp') and sea-surface (SST) temperatures, and (B) near-bottom salinities ('SBE Salt').

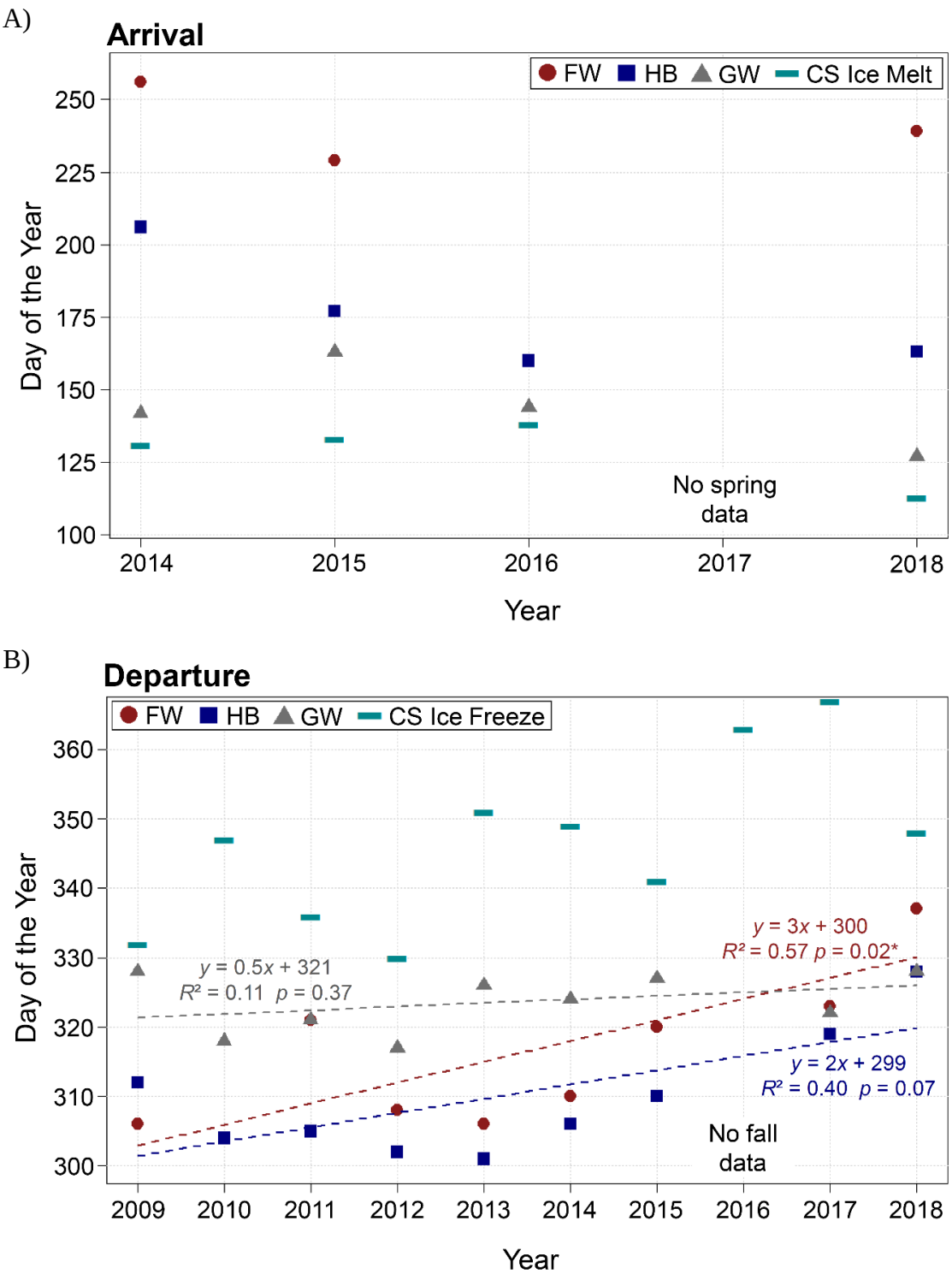

Fig. 3.8. (A) Arrival and (B) departure days of the year for fin whales (FW; circles), humpback whales (HB; squares), and gray whales (GW; triangles). Arrival dates shown for the years that had recordings available in spring (2014–2016, 2018). Linear regressions are shown as dotted. The days of the year when sea ice concentrations reached < 80% in the Chukchi Sea ('CS Ice Melt') and ≥ 80% concentration ('CS Ice Freeze') are included with the arrival and departure dates for illustrative purposes (dashes).

Fin whales

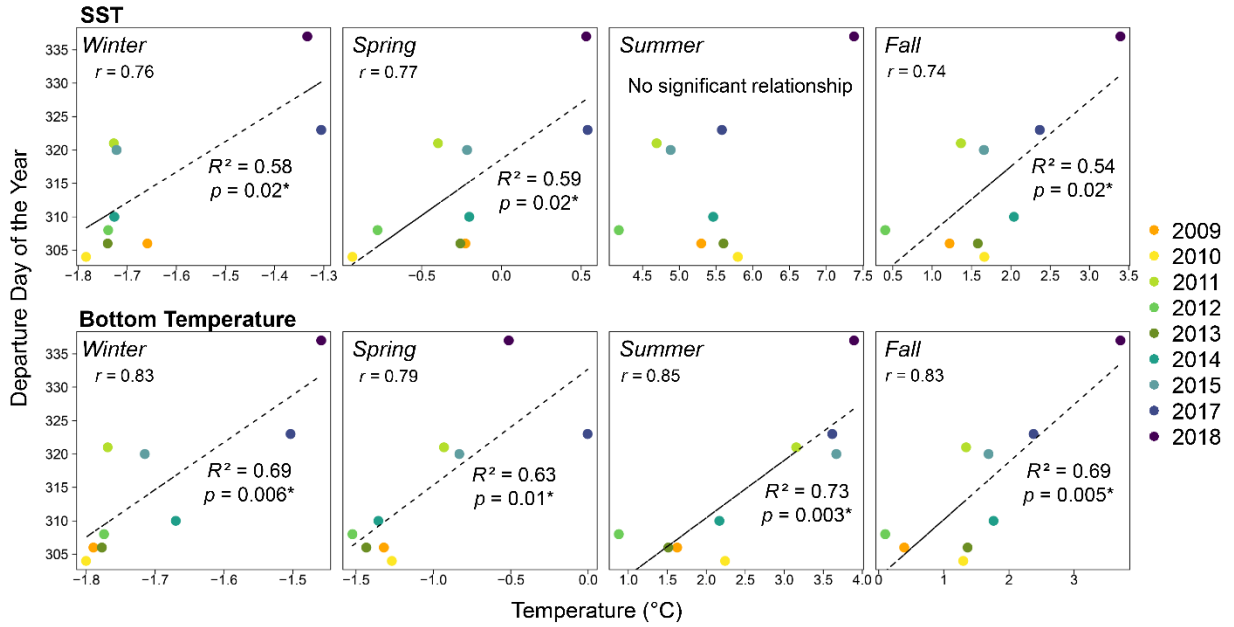

Humpback whales

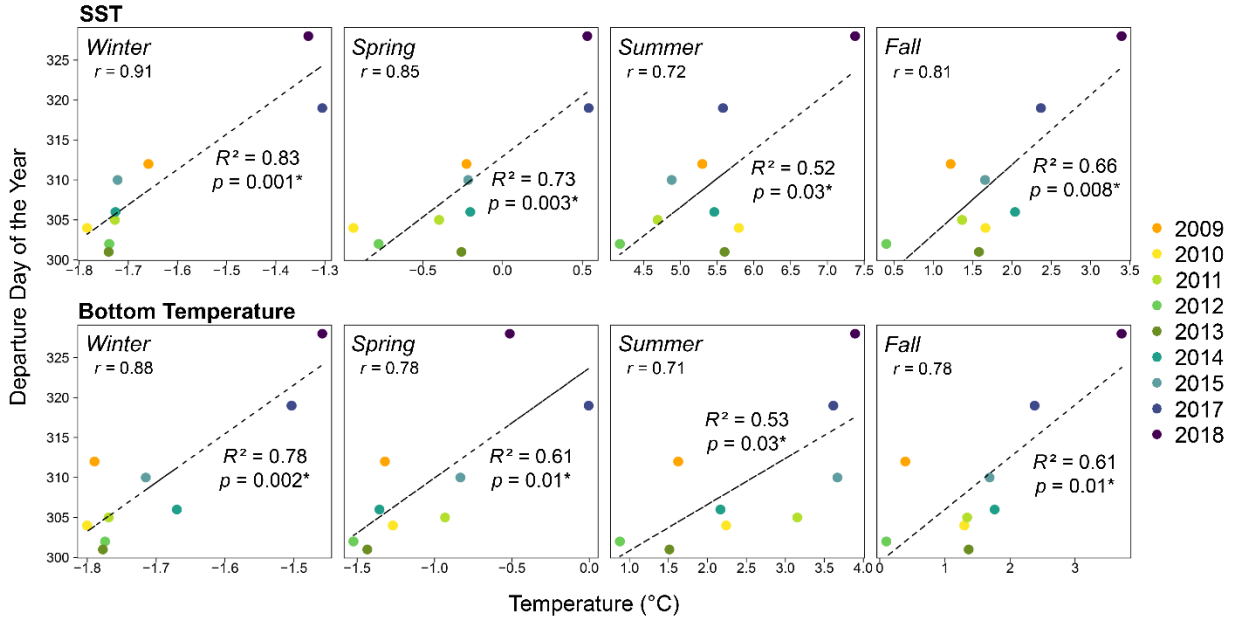

Fig. 3.9. Results from the Pearson correlation tests (*r*) and linear regression between departure days for fin whales (top) and humpback whales (bottom) and seasonal mean sea-surface temperatures (SST; from the NOAA Optimum Interpolation Sea Surface Temperature [OISST] dataset; °C), and near-bottom temperatures (from SBE-16 instrument; °C). Seasons were defined as follows: winter = 21 Dec–20 Mar, spring = 21 Mar–20 Jun, summer = 21 Jun–20 Sep, and fall = 21 Sep–20 Dec. See Table S3.3 for the linear equations.

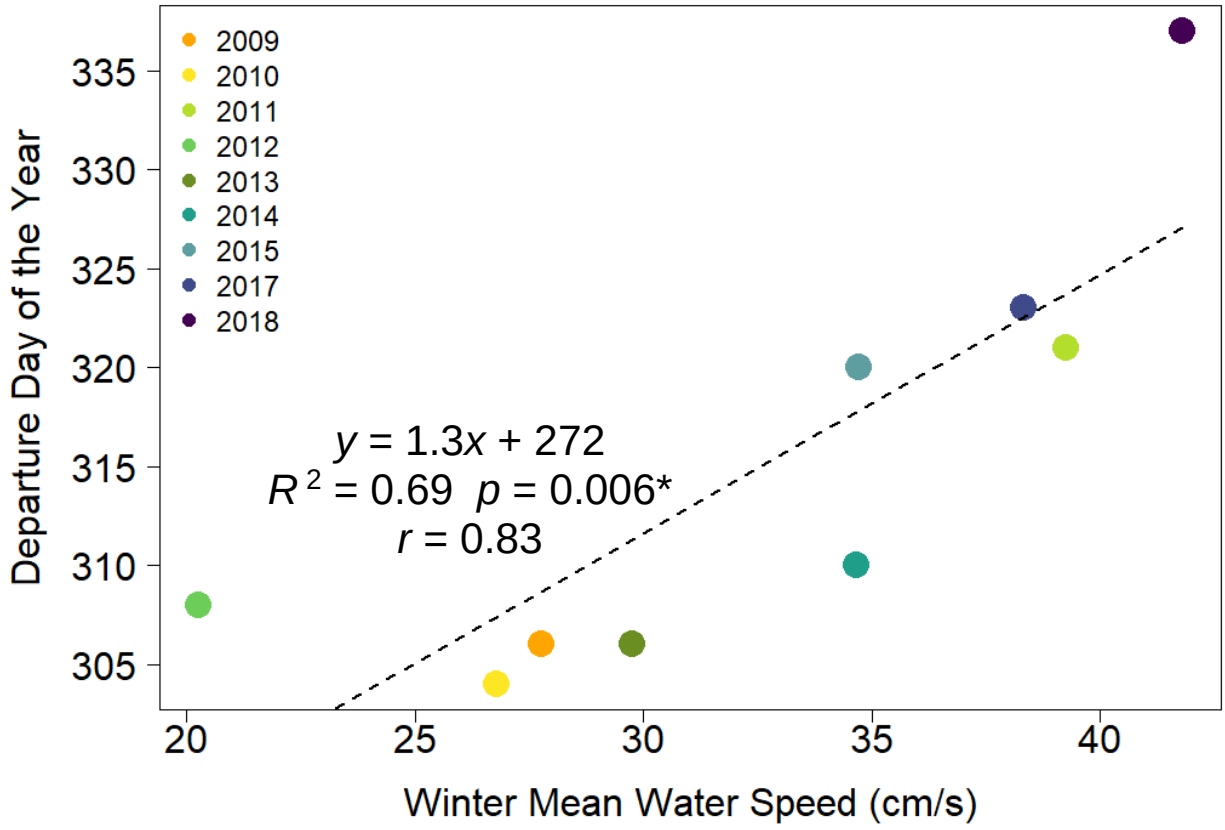

Fig. 3.10. Results from the Pearson correlation test (*r*) and linear regression between fin whale departure days and winter mean water speeds (ADCP data; cm s^{-1}). Winter was defined by the period 21 December–20 March.

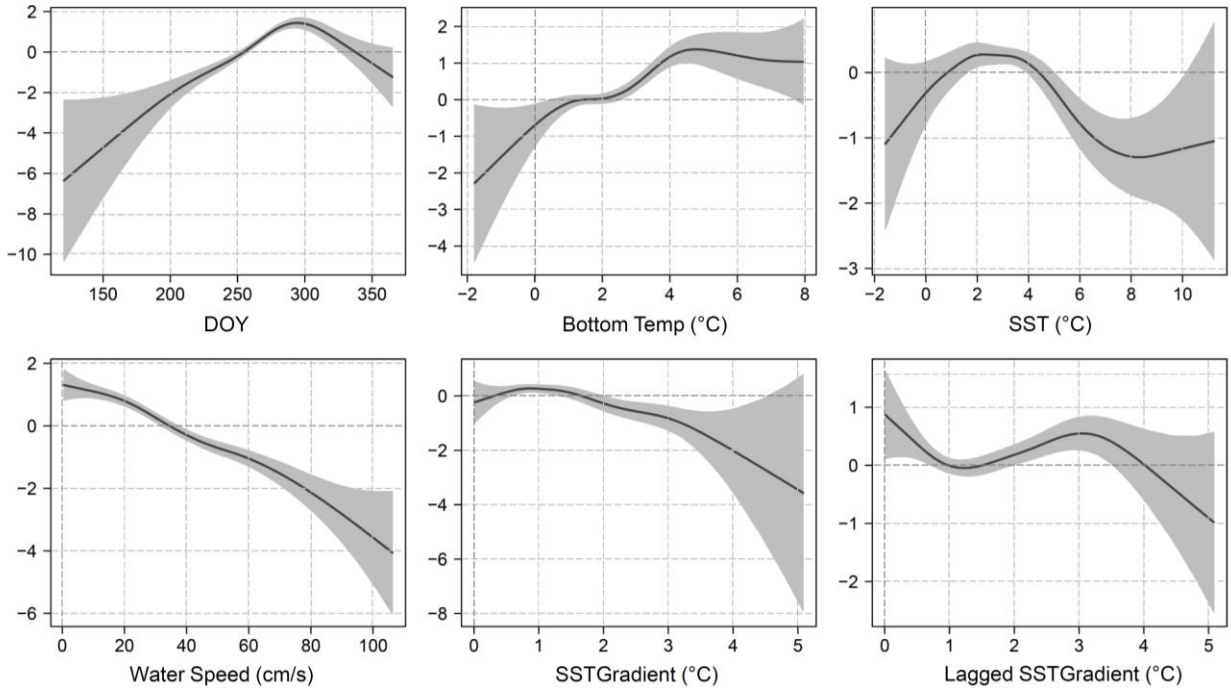

Fig. 3.11. Plots of the additive smoothing fits for the best fin whale model with the smoothed functions for the daily probability of a calling fin whale being present in relation to temporal (day of the year, DOY), and environmental conditions. Daily means were used for the environmental covariates, including near-bottom temperature, sea surface temperatures (SST), and water speed. The 'SST Gradient' represents the maximum difference in daily mean SSTs between grid cells within a 30-km buffer around site A3, which was then lagged by one month ('Lagged SST Gradient'). The lines indicate the effect of the covariate on the probability and the gray areas represent the standard errors for the effect of the smoothed term.

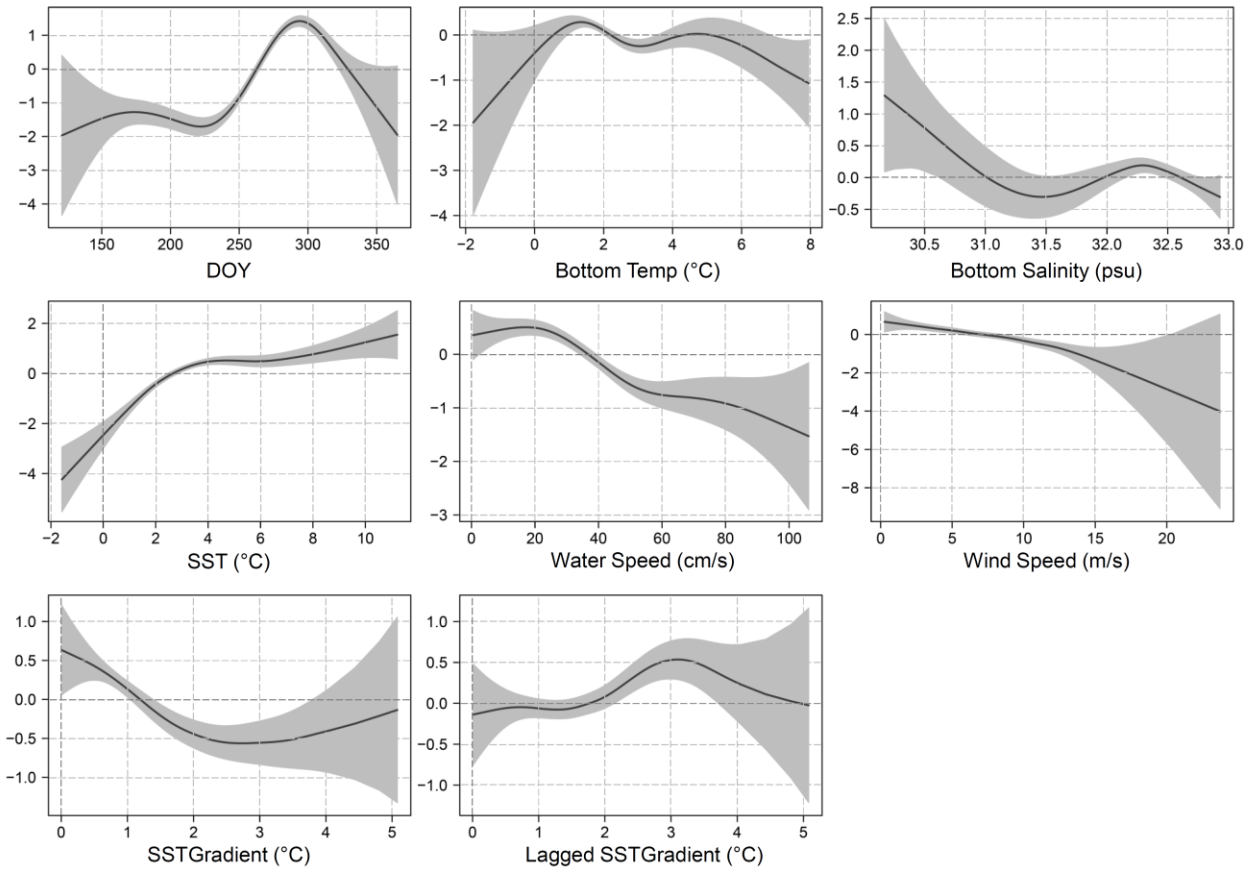

Fig. 3.12. Plots of the additive smoothing fits for the best humpback whale model with the smoothed functions for the daily probability of a calling humpback whale being present in relation to temporal (day of the year, DOY), and environmental conditions. Daily means were used for the environmental covariates, including near-bottom temperature and salinity, sea-surface temperatures (SST), water speed, and wind speed. The 'SST Gradient' represents the maximum difference in daily mean SSTs between grid cells within a 30-km buffer around site A3, which was then lagged by one month ('Lagged SST Gradient'). The lines indicate the effect of the covariate on the probability and the gray areas represent the standard errors for the effect of the smoothed term.

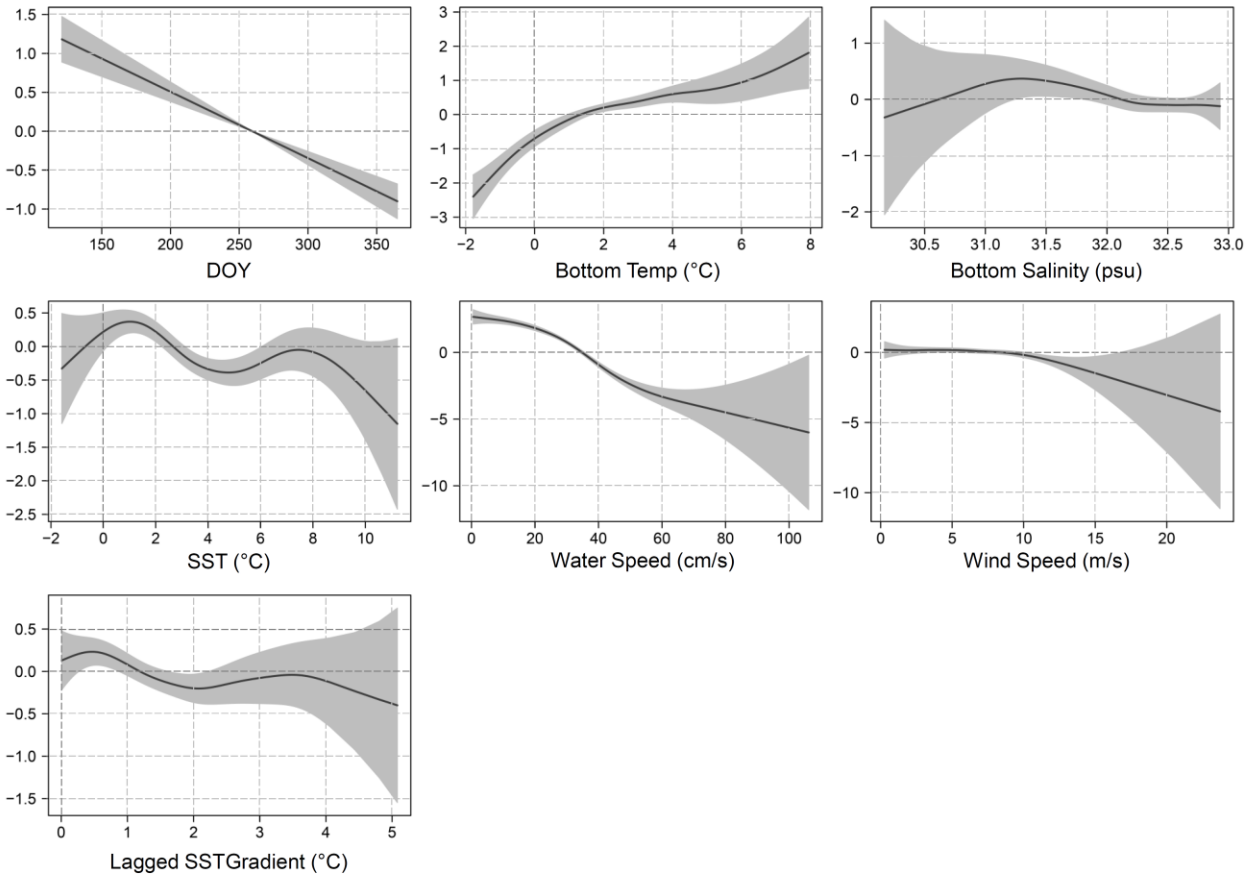

Fig. 3.13. Plots of the additive smoothing fits for the best gray whale model with the smoothed functions for the daily probability of a calling gray whale being present in relation to temporal (day of the year, DOY), and environmental conditions. Daily means were used for the environmental covariates including near-bottom temperature and salinity, sea-surface temperatures (SST), water speed, and wind speed. The 'Lagged SST Gradient' represents the maximum difference in daily mean SSTs between grid cells within a 30-km buffer around site A3 lagged by one month. The lines indicate the effect of the covariate on the probability and the gray areas represent the standard errors for the effect of the smoothed term.

3.10 Supplementary Tables and Figures

Table S3.1. Results of the Pearson correlation tests between seasonal means for near-bottom temperature and salinities ('SBE Temp' and 'SBE Salt'), sea-surface temperatures (SST), water speeds, and wind speeds. Pink shading denotes correlations with an absolute value > 0.7.

	SST Winter	SBE Temp Winter	SBE Salt Winter	Water Winter	Wind Winter	SST Spring	SBE Temp Spring	SBE Salt Spring	Water Spring	Wind Spring	SST Summer	SBE Temp Summer	SBE Salt Summer	Water Summer	Wind Summer	SST Fall	SBE Temp Fall	SBE Salt Fall	Water Fall	Wind Fall
SST Winter	1	0.93	-0.58	0.61	-0.62	0.9	0.86	-0.38	0.4	0.55	0.62	0.62	0.69	-0.37	-0.56	0.74	0.74	-0.14	0.57	-0.15
SBE Temp Winter	0.93	1	-0.66	0.71	-0.48	0.9	0.82	-0.58	0.57	0.48	0.67	0.7	0.74	-0.19	-0.5	0.85	0.87	-0.14	0.58	-0.01
SBE Salt Winter	-0.58	-0.66	1	-0.48	0.55	-0.62	-0.77	0.68	-0.38	-0.26	-0.17	-0.65	-0.66	-0.03	0.51	-0.48	-0.57	-0.21	-0.31	0.41
Water Winter	0.61	0.71	-0.48	1	-0.25	0.77	0.75	-0.8	0.83	0.17	0.53	0.89	0.33	0.43	-0.32	0.8	0.84	0.32	0.31	0.28
Wind Winter	-0.62	-0.48	0.55	-0.25	1	-0.49	-0.71	0.05	-0.31	-0.44	0.1	-0.48	-0.82	0.4	0.56	-0.12	-0.15	-0.28	-0.09	0.24
SST Spring	0.9	0.9	-0.62	0.77	-0.49	1	0.8	-0.6	0.54	0.19	0.6	0.67	0.58	-0.11	-0.55	0.79	0.78	-0.05	0.48	-0.04
SBE Temp Spring	0.86	0.82	-0.77	0.75	-0.71	0.8	1	-0.58	0.58	0.56	0.41	0.86	0.66	-0.03	-0.59	0.67	0.72	0.29	0.43	-0.19
SBE Salt Spring	-0.38	-0.58	0.68	-0.8	0.05	-0.6	-0.58	1	-0.74	0.05	-0.45	-0.75	-0.21	-0.63	0.46	-0.74	-0.76	-0.42	-0.36	-0.1
Water Spring	0.4	0.57	-0.38	0.83	-0.31	0.54	0.58	-0.74	1	0.13	0.4	0.81	0.41	0.52	-0.48	0.68	0.67	0.54	0.2	0.53
Wind Spring	0.55	0.48	-0.26	0.17	-0.44	0.19	0.56	0.05	0.13	1	0.41	0.44	0.48	-0.34	-0.16	0.38	0.43	-0.07	0.19	-0.02
SST Summer	0.62	0.67	-0.17	0.53	0.1	0.6	0.41	-0.45	0.4	0.41	1	0.47	0.12	0.08	-0.27	0.9	0.82	-0.23	0.38	0.36
SBE Temp Summer	0.62	0.7	-0.65	0.89	-0.48	0.67	0.86	-0.75	0.81	0.44	0.47	1	0.51	0.38	-0.39	0.74	0.81	0.45	0.14	0.24
SBE Salt Summer	0.69	0.74	-0.66	0.33	-0.82	0.58	0.66	-0.21	0.41	0.48	0.12	0.51	1	-0.44	-0.42	0.36	0.43	-0.07	0.19	-0.08
Water Summer	-0.37	-0.19	-0.03	0.43	0.4	-0.11	-0.03	-0.63	0.52	-0.34	0.08	0.38	-0.44	1	0.01	0.21	0.21	0.65	-0.19	0.43
Wind Summer	-0.56	-0.5	0.51	-0.32	0.56	-0.55	-0.59	0.46	-0.48	-0.16	-0.27	-0.39	-0.42	0.01	1	-0.44	-0.32	-0.47	-0.59	0.21
SST Fall	0.74	0.85	-0.48	0.8	-0.12	0.79	0.67	-0.74	0.68	0.38	0.9	0.74	0.36	0.21	-0.44	1	0.97	0	0.48	0.29
SBE Temp Fall	0.74	0.87	-0.57	0.84	-0.15	0.78	0.72	-0.76	0.67	0.43	0.82	0.81	0.43	0.21	-0.32	0.97	1	-0.02	0.42	0.24
SBE Salt Fall	-0.14	-0.14	-0.21	0.32	-0.28	-0.05	0.29	-0.42	0.54	-0.07	-0.23	0.45	-0.07	0.65	-0.47	0	-0.02	1	-0.05	0.09
Water Fall	0.57	0.58	-0.31	0.31	-0.09	0.48	0.43	-0.36	0.2	0.19	0.38	0.14	0.19	-0.19	-0.59	0.48	0.42	-0.05	1	-0.41
Wind Fall	-0.15	-0.01	0.41	0.28	0.24	-0.04	-0.19	-0.1	0.53	-0.02	0.36	0.24	-0.08	0.43	0.21	0.29	0.24	0.09	-0.41	1

Table S3.2. Summary of sampling dates and units for the prey datasets: National Oceanic and Atmospheric Administration (NOAA) Bering Arctic Subarctic Integrated Survey (BASIS); NOAA Ecosystems and Fisheries Oceanography Coordinated Investigations joint research program (EcoFOCI); and benthic zooplankton density collected during Distributed Biological Observatory surveys (DBO; https://www.pmel.noaa.gov/dbo/; Grebmeier and Cooper 2019a, 2019b). See Figs. 2 and 3 for sampling locations. *The National Oceanic and Atmospheric Administration (NOAA) EcoFOCI dataset was compiled by Dr. David Kimmel (NOAA – National Marine Fisheries Service).

Name	Years and Dates	Sampling Units	Method
NOAA BASIS (N. Bering)	2009: 8–13 Sep 2010: 21–23 Sep, 27 Sep–1 Oct 2011: 6, 8–11, 13–17 Sep 2012: 10–16, 18–19 Sep 2013: 7 Aug; 10–15, 17–19 Sep 2014: 4–7, 9–11 Sep 2015: 8–10, 12–16 Sep 2016: 8–12 Sep 2017: 5–9 Sep 2018: 8–17 Sep	Fish total weight (kg) per km^2	Surface rope trawl
Benthic	2012: 14–16 Jul 2013: 13–23 Jul 2014: 14–23 Jul 2015: 14–21 Jul 2017: 29–31 Aug; 1–5, 7–10, 12–13 Sep	Amphipod density ($\#/m^2$)	van Veen grab
NOAA EcoFOCI Cruises*	2012: 17–27 Aug 2013: 12 Aug–17 Sep 2014: 4 Sep–12 Oct 2015: 6 Aug–25 Sep 2017: 27 Aug–6 Oct 2018: 8 Aug–18 Sep	Estimated number of individuals per m^3	Bongo net with 153-µm mesh size

Table S3.3. Results of the linear regression for the departure dates (y) for each species vs. seasonal means of environmental variables (x). Only the variables with a significant, linear relationship to the departure dates ($p < 0.05$) are listed below, including seasonal means for sea-surface temperatures (SST, °C), near bottom temperatures (measured with SBE-16 instrument, °C), and water speeds (measured by ADCP instrument, cm s^{-1}). Seasons were defined as follows: winter = 21 Dec–20 Mar, spring = 21 Mar–20 Jun, summer = 21 Jun–20 Sep, and fall = 21 Sep–20 Dec. Winter here indicates the previous winter to the arrival of the whales to the Bering Strait.

Fin Whales			
Variable (x)	**R^2**	**p**	**Equation**
Bottom Temp Winter	0.69	0.006	$y = 70.9x + 435.1$
Bottom Temp Spring	0.63	0.01	$y = 17.4x + 332.7$
Bottom Temp Summer	0.73	0.003	$y = 8.6x + 293.2$
Bottom Temp Fall	0.69	0.005	$y = 8.6x + 301.6$
SST Winter	0.58	0.02	$y = 45.7x + 389.8$
SST Spring	0.59	0.02	$y = 16.9x + 318.6$
SST Fall	0.54	0.02	$y = 9.8x + 297.9$
Water Speed Winter	0.69	0.006	$y = 1.3x + 272.3$
Humpback Whales			
Variable (x)	**R^2**	**p**	**Equation**
Bottom Temp Winter	0.78	0.002	$y = 61x + 413.1$
Bottom Temp Spring	0.61	0.01	$y = 13.8x + 323.7$
Bottom Temp Summer	0.53	0.03	$y = 5.8x + 295.1$
Bottom Temp Fall	0.61	0.01	$y = 6.6x + 299.4$
SST Winter	0.83	0.001	$y = 44.1x + 381.8$
SST Spring	0.73	0.003	$y = 15.2x + 312.9$
SST Summer	0.52	0.03	$y = 7.2x + 270.7$
SST Fall	0.66	0.008	$y = 8.7x + 294.4$

Table S3.4. Best models for each species according to Akaike information criterion with a correction for small sample sizes (AICc) along with their R^2 values (Cox-Snell). Other models that had ΔAICc < 10 are also listed. Note that the two models for gray whale had the same AICc score and R^2 value, thus we chose the model with fewer variables. The smoothing terms are specified next to the variable names: cs = cubic spline, pb = penalized b-spline smoothers. DOY = day of the year; SBE Temp = daily mean near-bottom temperatures; SBE Salt = daily mean near-bottom salinities; Water Speed = daily mean water speeds; Wind Speed = daily mean wind speeds; SST Grad = SST gradient (represents presence of a thermal front); SST Grad Lagged = SST Gradient lagged by one month.

AICc	Fin Whale Model	ΔAICc	R^2
3320	pb(DOY) + cs(SBE Temp) + cs(SST) + cs(Water Speed) + cs(SSTGrad) + cs(SST Grad Lagged)	0	0.51
3324	pb(DOY) + cs(SBE Temp) + cs(SST) + cs(Water Speed) + cs(Wind Speed) + cs(SST Grad) + cs(SST Grad Lagged)	4	0.51
3329	pb(DOY) + cs(SBE Temp) + cs(SST) + cs(Water Speed) + cs(SST Grad)	9	0.5
AICc	**Humpback Whale Models**	**ΔAICc**	**R^2**
4454	pb(DOY) + cs(SBE Temp) + cs(SBE Salt) +cs(SST) + cs(Water Speed) + cs(Wind Speed) + cs(SST Grad) + cs(SST Grad Lagged)	0	0.6
4455	pb(DOY) + cs(SBE Temp) +cs(SST) + cs(Water Speed) + cs(Wind Speed) + cs(SST Grad) + cs(SST Grad Lagged)	1	0.59
4460	pb(DOY) + cs(SBE Temp) +cs(SST) + cs(Water Speed) + cs(Wind Speed) + cs(SST Grad Lagged)	6	0.59
4462	pb(DOY) + cs(SBE Temp) + cs(SBE Salt) +cs(SST) + cs(Water Speed) + cs(Wind Speed) + cs(SST Grad Lagged)	8	0.59
AICc	**Gray Whale Models**	**ΔAICc**	**R^2**
3087	pb(DOY) + cs(SBE Temp) + cs(SBE Salt) + cs(SST) + cs(Water Speed) + cs(Wind Speed) + cs(SST Grad Lagged)	0	0.45
3087	pb(DOY) + cs(SBE Temp) + cs(SBE Salt) + cs(SST) + cs(Water Speed) + cs(Wind Speed) + cs(SST Grad) + cs(SST Grad Lagged)	0	0.45

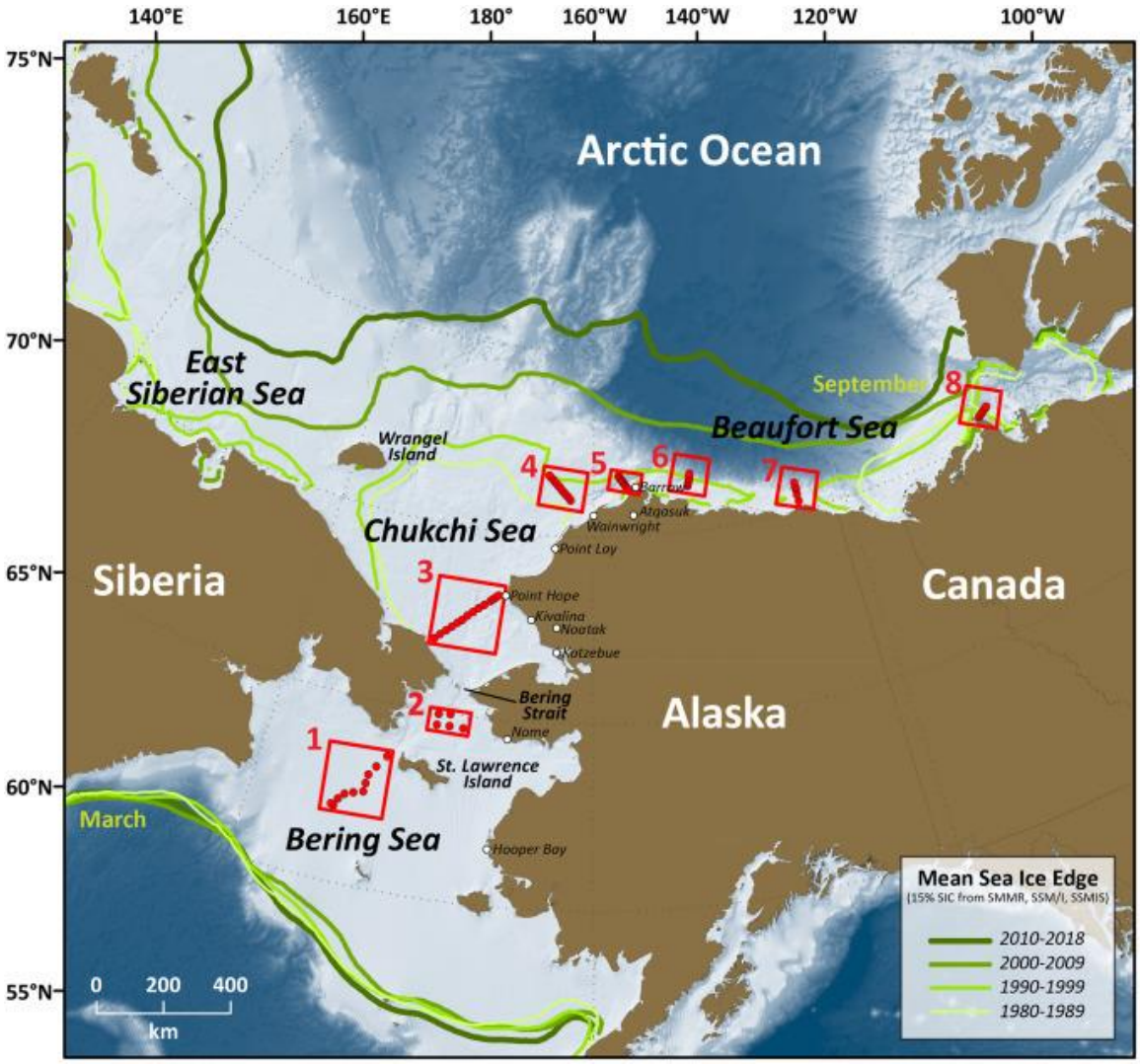

Fig. S3.1. Map of the Distributed Biological Observatory (DBO) sampling regions (figure from Grebmeier et al. 2019).

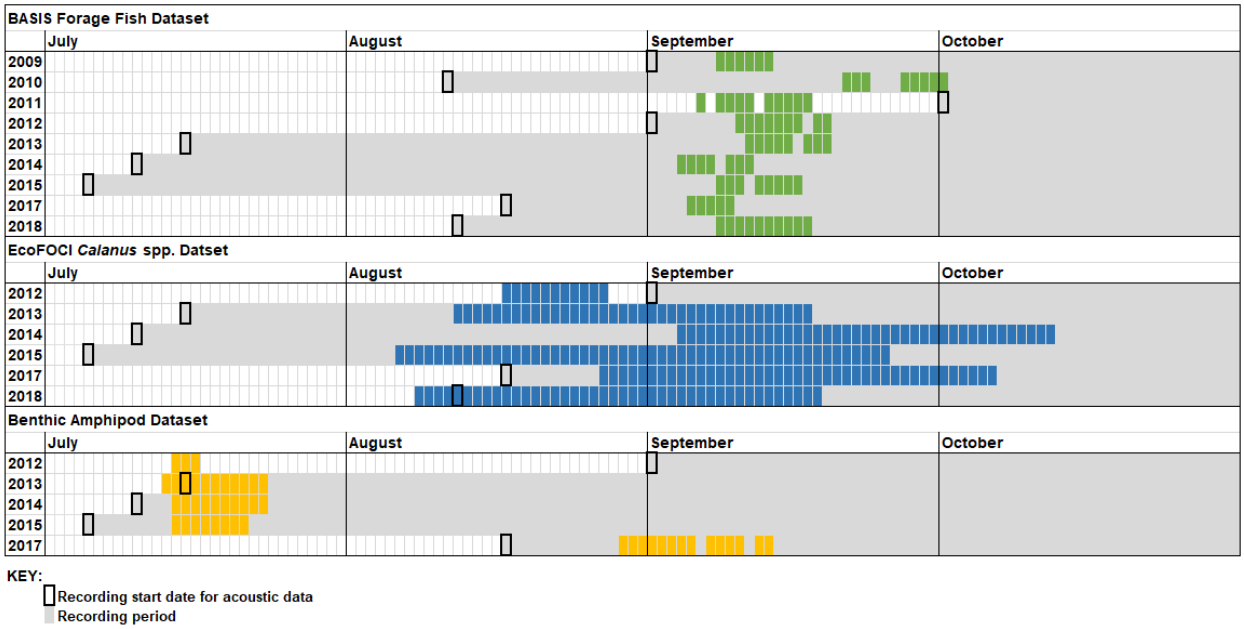

Fig. S3.2. Chart of the sampling periods for all three prey datasets: BASIS forage fish dataset (top, green squares), EcoFOCI *Calanus* spp. dataset (middle, blue squares), and the benthic amphipod dataset (bottom, yellow squares). The start dates of the hydrophone recordings are represented by the bold squares and the gray shading represents the recording periods.

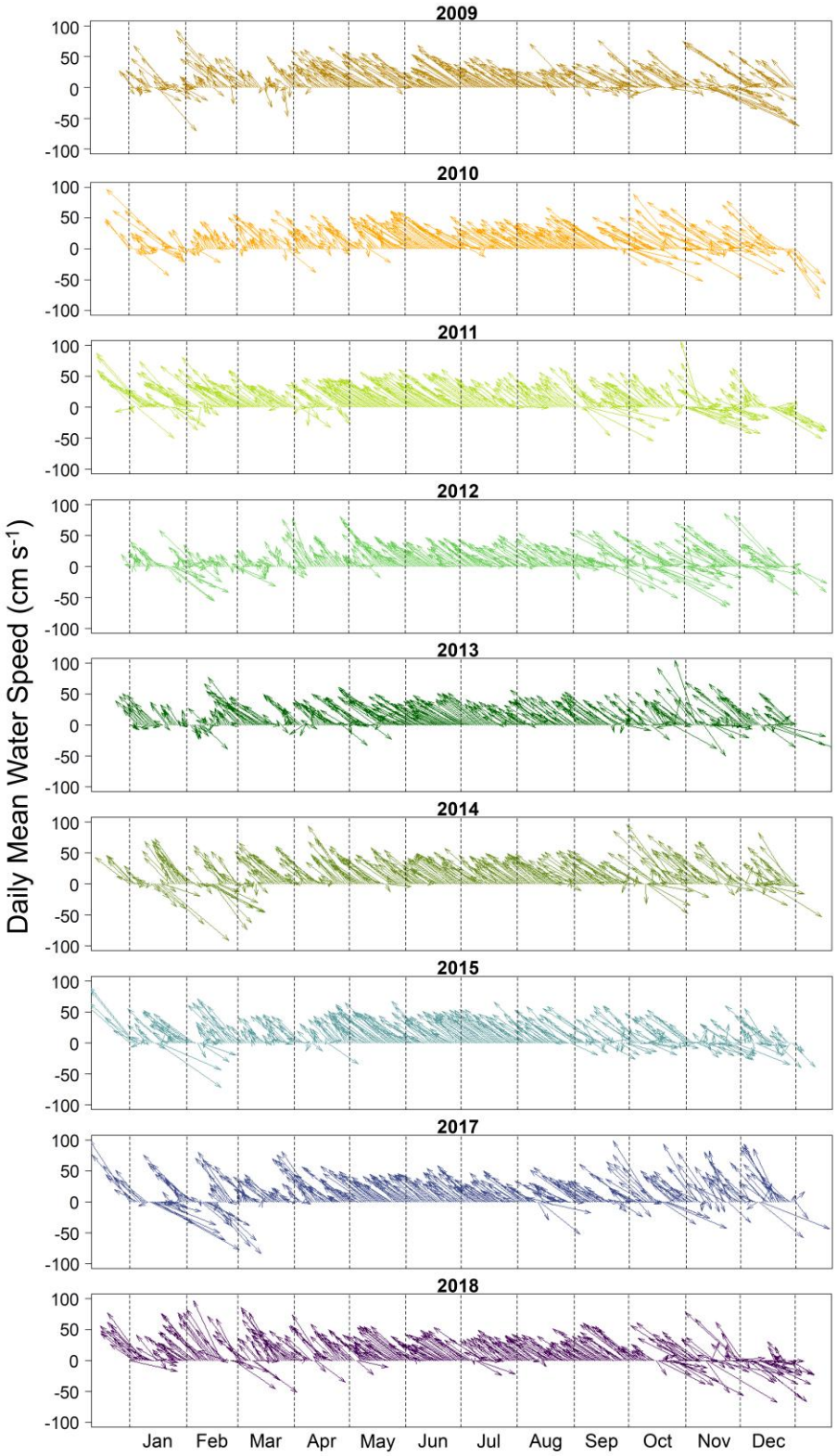

Fig. S3.3. Vector plots of daily mean water speed (cm s^{-1}) at the A3 mooring site.

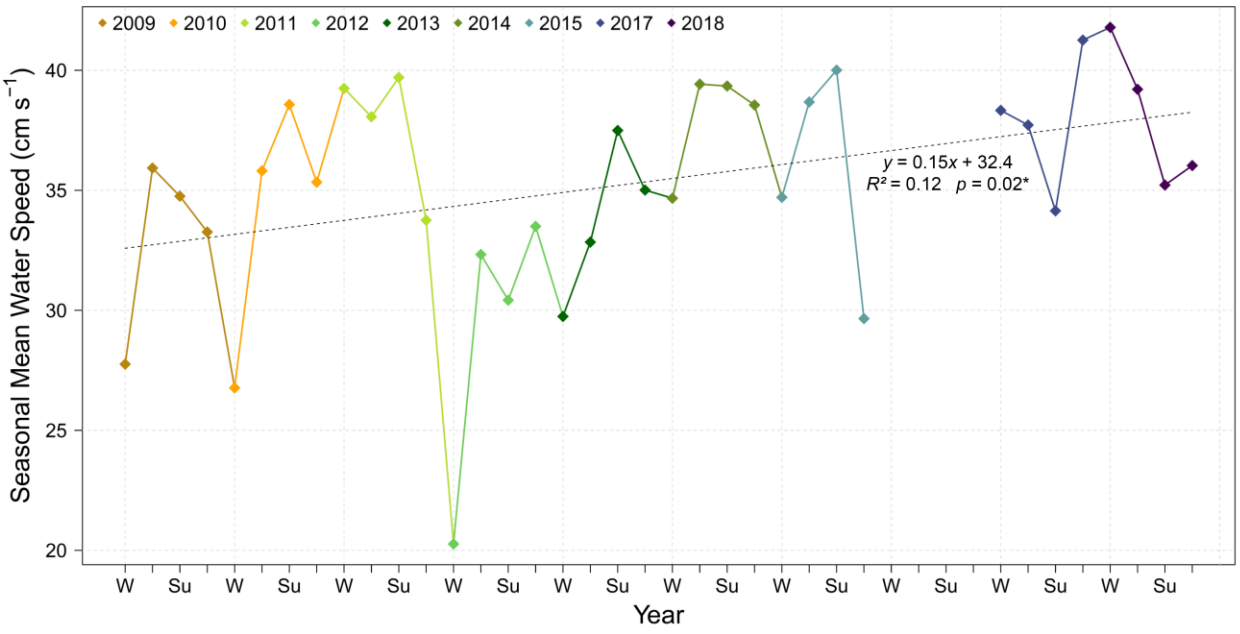

Fig. S3.4. Seasonal means for water speed (cm s^{-1}) measured at the A3 mooring site. Note that 2016 was omitted since we do not have acoustic data for that year. The seasons were defined as follows: Winter ('W') = 21 Dec–20 Mar; Spring = 21 Mar–20 Jun; Summer ('Su') = 21 Jun–20 Sep; Fall = 21 Sep–20 Dec. Water speeds throughout the seasons were highly variable with standard deviations ranging from 13 cm s^{-1} to 27 cm s^{-1}. A linear regression of the seasonal means with year shows a significant increasing trend over the study period (p = 0.02).

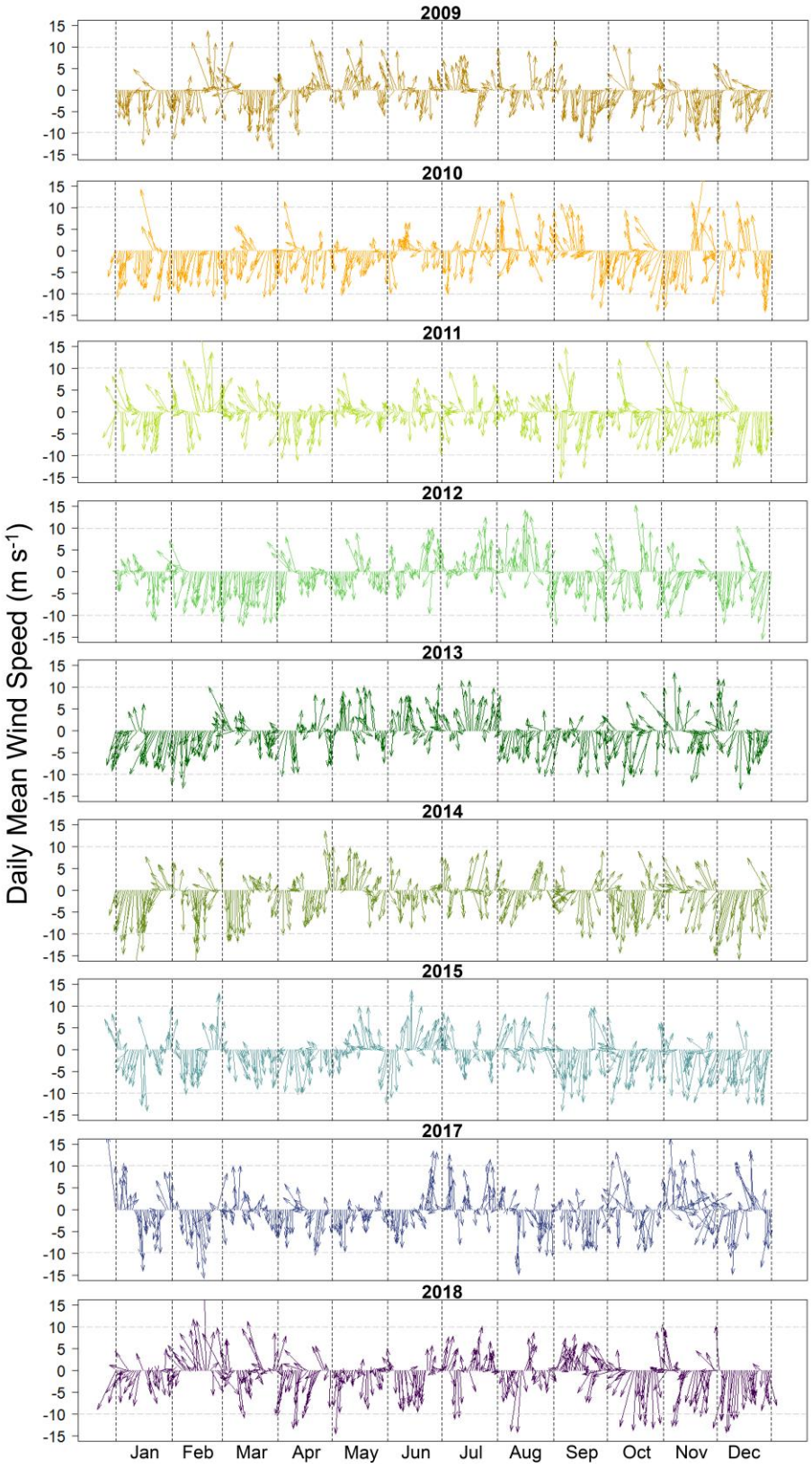

Fig. S3.5. Vector plots of daily mean wind speed (cm s^{-1}) at the A3 mooring site. The gray dashed line at 10 m s^{-1} indicates strong wind speeds.

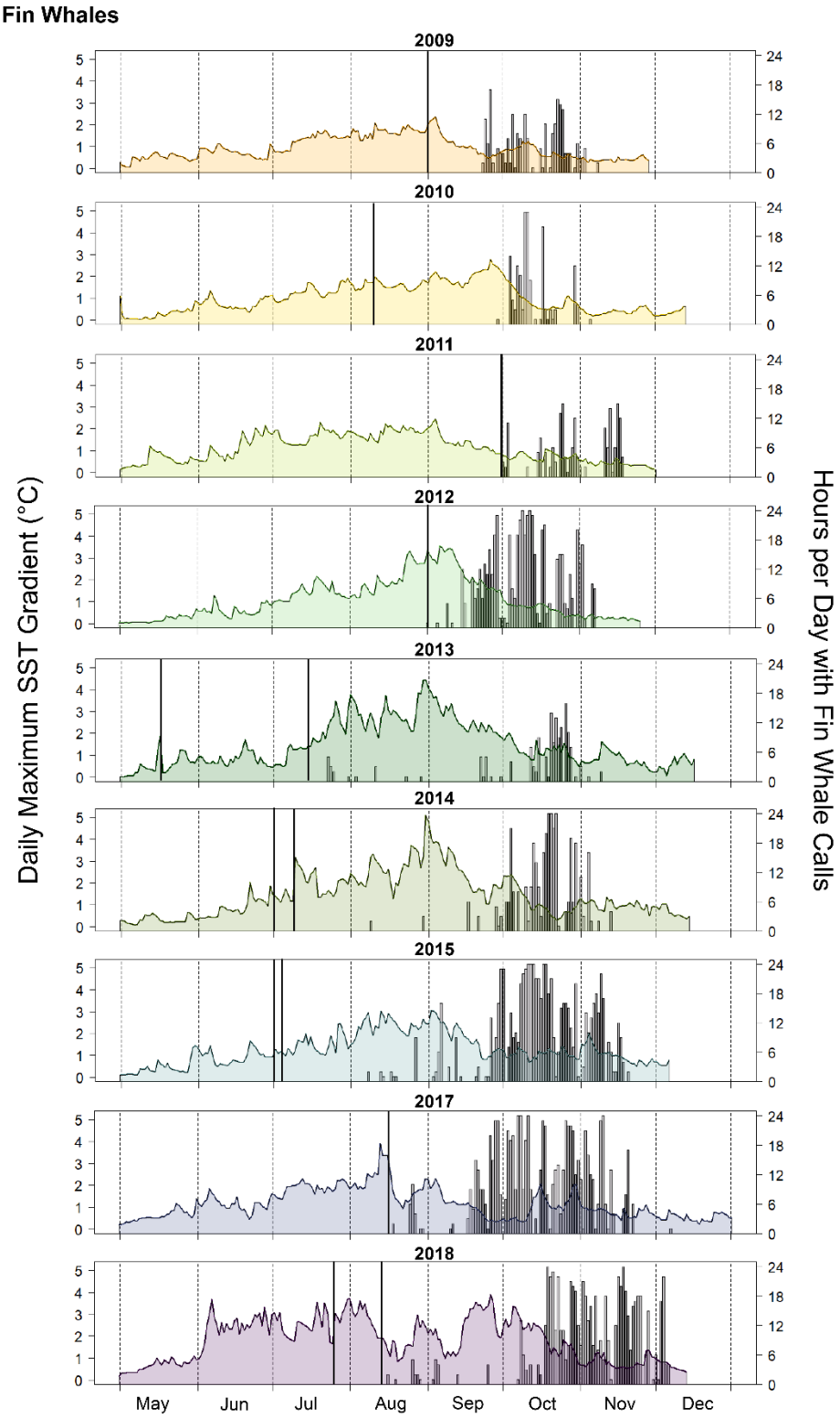

Fig. S3.6. Plot of the daily maximum sea-surface temperature (SST) gradient (°C) within a 30-km radius of the A3 mooring site for the open-water season (1 May through freeze-up; see Table 3.2). The SST gradient is a proxy for the presence of a thermal front—the higher the gradient, the stronger the front. The plot is overlaid with a bar plot of the hours per day with fin whale calls with bold lines indicating the start and end of the recording period.

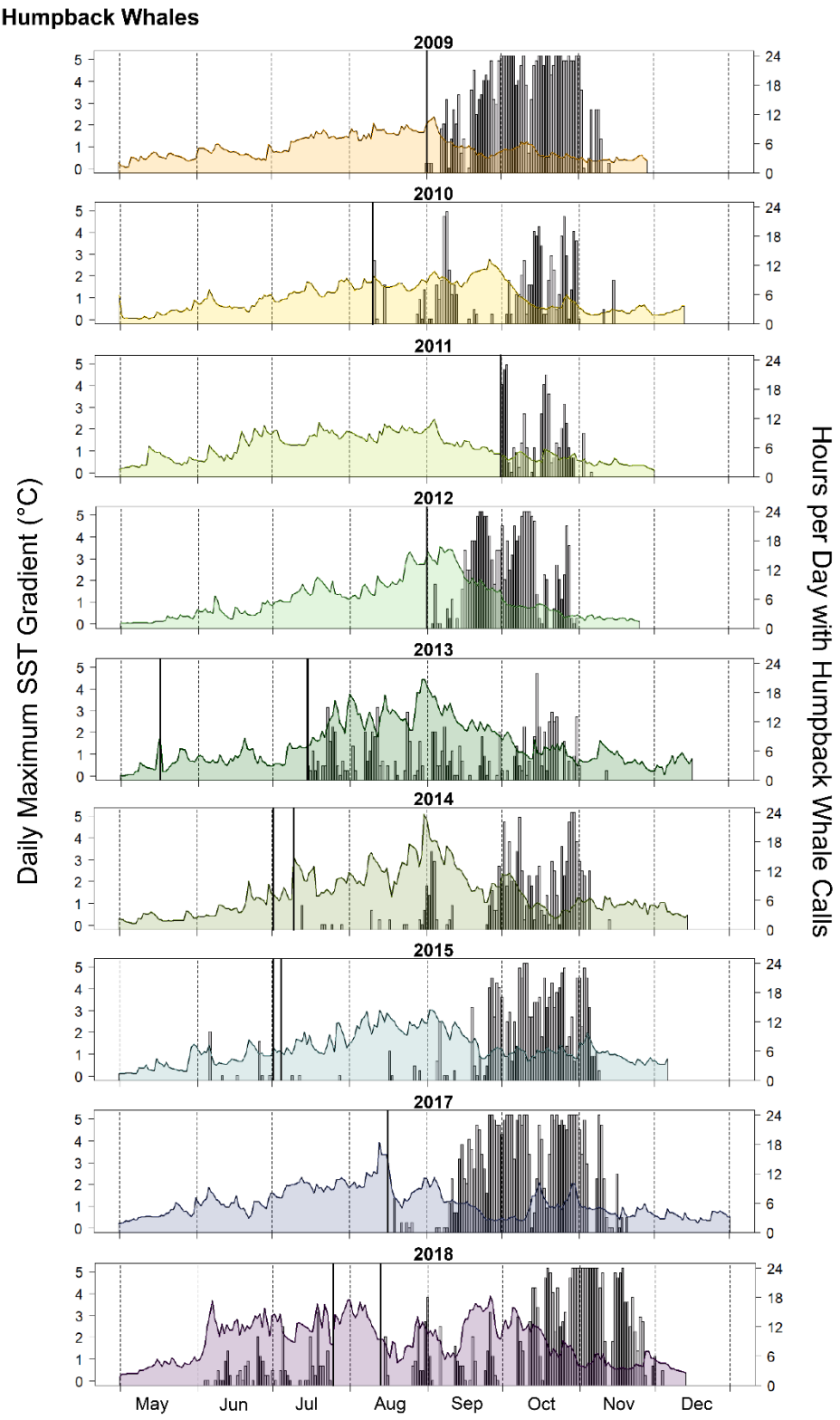

Fig. S3.7. Plot of the daily maximum sea-surface temperature (SST) gradient (°C) within a 30-km radius of the A3 mooring site for the open-water season (1 May through freeze-up; see Table 3.2). The SST gradient is a proxy for the presence of a thermal front—the higher the gradient, the stronger the front. The plot is overlaid with a bar plot of the hours per day with humpback whale calls with bold lines indicating the start and end of the recording period.

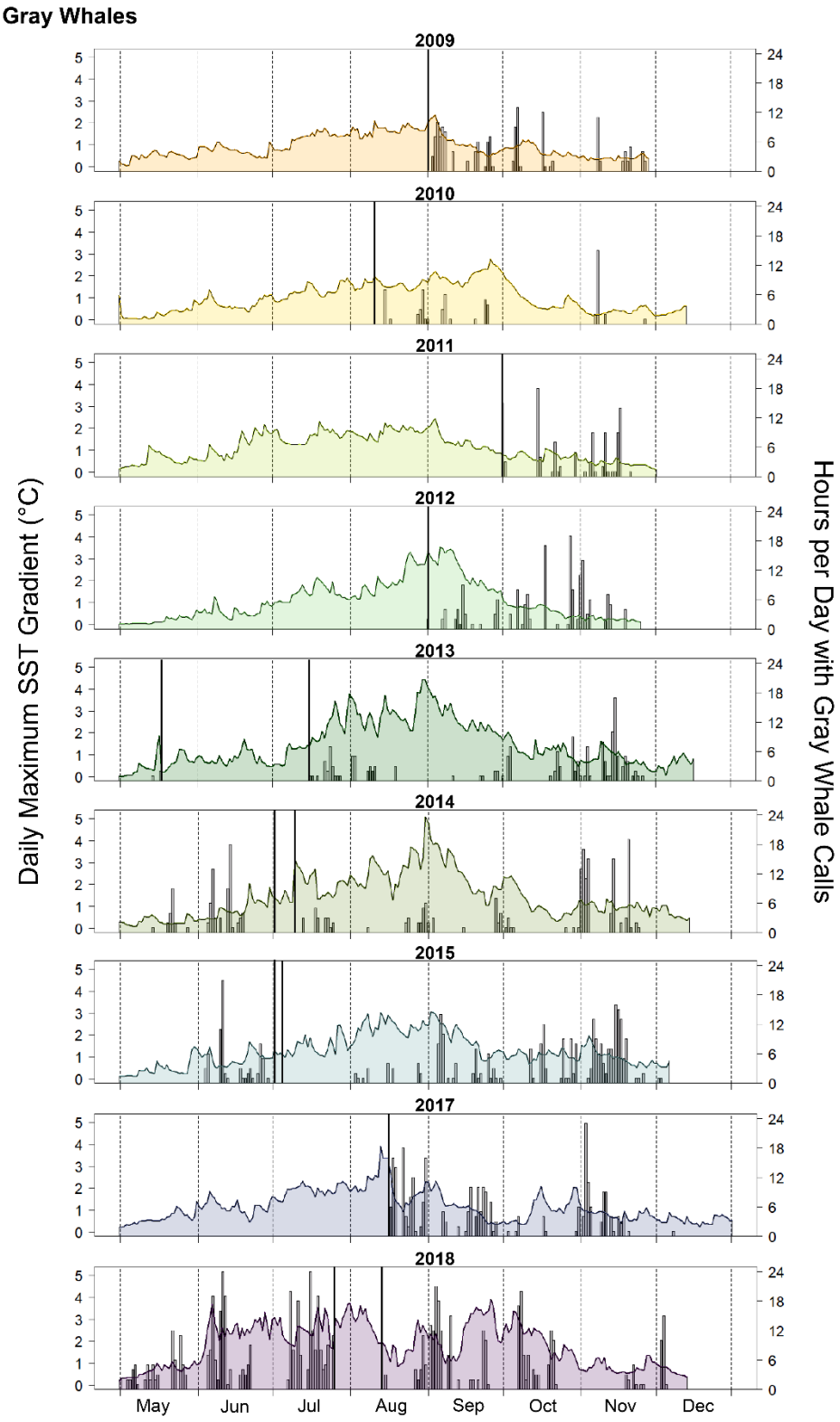

Fig. S3.8. Plot of the daily maximum sea-surface temperature (SST) gradient (°C) within a 30-km radius of the A3 mooring site for the open-water season (1 May through freeze-up; see Table 3.2). The SST gradient is a proxy for the presence of a thermal front—the higher the gradient, the stronger the front. The plot is overlaid with a bar plot of the hours per day with gray whale calls with bold lines indicating the start and end of the recording period.

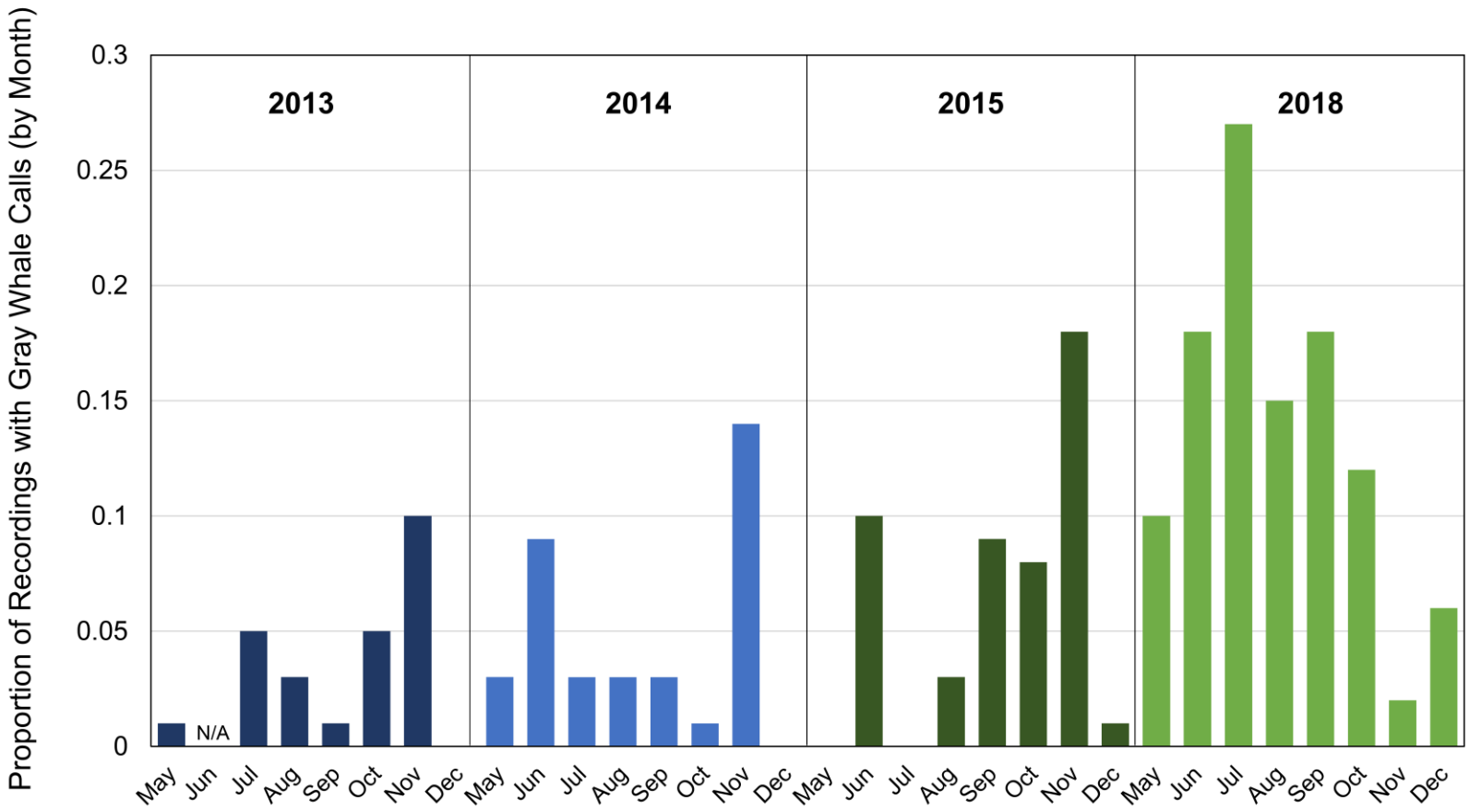

Fig. S3.9. Proportion of recordings with gray whale calls by month. Only the years with both spring and fall recordings are shown. In some years, particularly 2013 and 2014, a peak in gray whale calls is evident in the spring and fall, possibly reflecting the spring and fall migration of gray whales into and from the study region.

CHAPTER 4. Quantifying the effect of ship noise on the acoustic environment of the Bering Strait

[Escajeda ED, Stafford KM, Woodgate RA, Laidre KL (2023) Quantifying the effect of ship noise on the acoustic environment of the Bering Strait. Marine Pollution Bulletin 187:114557. https://doi.org/10.1016/j.marpolbul.2022.114557]

4.1 Abstract

The narrow Bering Strait provides the only gateway between the Pacific Ocean and the Arctic, bringing migrating marine mammals in close proximity to ships transiting the strait. We characterized ship activity in the Bering Strait during the open-water season (July–November) for 2013–2015 and quantified the impact of ship noise on third-octave sound levels (TOLs) for bands used by baleen whales (25–1000 Hz). Peak ship activity occurred in July–September with the greatest overlap in ship noise and whale vocalizations observed in October. Ships elevated sound levels by ~ 4 dB on average for all TOL bands combined, and 250-Hz TOLs exceeding 100 dB re 1 µPa were recorded from two large vessels over 11 km away from the hydrophones. Our results show that ship noise has the potential to impact baleen whales in the Bering Strait and serve as a baseline for measuring future changes in ship activity in the region.

4.2 Introduction

Declining sea ice is opening the Arctic to increased ship activity (Eguíluz et al, 2016), potentially impacting the acoustic habitat of Arctic and subarctic marine mammals (Moore et al., 2012; Halliday et al., 2017, 2021a; Hauser et al., 2018). Known impacts of ship noise on marine mammals include masking of important biological signals (Clark et al., 2009; Pine et al., 2018), elevating stress hormone levels (Rolland et al., 2012; Lemos et al., 2022), and provoking avoidance behavior (Finley et al., 1990; Nowacek et al., 2007; Southall et al., 2007; Martin et al., 2022). The two major Arctic shipping routes—the Northwest Passage through the Canadian

Arctic Archipelago, and the Northern Sea Route along the northern coast of Eurasia—are expected to see a sharp increase in trans-Arctic ship transits by 2050 (Stephenson et al., 2011, 2013; Smith and Stephenson, 2013). Both sea routes pass through the Bering Strait, making it an important region for studying the effects of ship noise on the marine soundscape.

The Bering Strait connects the Bering Sea to the south with the Chukchi Sea to the north (Fig. 4.1). The region is shallow (30–60 m), and narrow, spanning only ~ 80 km at its narrowest point. The marine ecosystem of the Chukchi Sea is one of the richest in the world, home to dense aggregations of benthic invertebrates and swarms of lipid-rich zooplankton that attract marine mammals to the region (Grebmeier et al., 2006; Eisner et al., 2013; Ershova et al., 2015). Marine mammals endemic to the Arctic and commonly observed in the Chukchi Sea include bowhead whales (*Balaena mysticetus*), belugas (*Delphinapterus leucas*), walrus (*Odobenus rosmarus*), bearded seals (*Erignathus barbatus*), and ringed seals (*Pusa hispida*), all of which are important subsistence species for the Chukchi, Iñupiaq, St. Lawrence Island Yupik, Siberian Yupik, and Yup'ik Peoples of the coastal Pacific Arctic (Huntington et al., 2015).

The seasonal migrations of species through the Bering Strait region are driven by the melting of sea ice in spring (~ May), and the formation of sea ice in late fall and early winter (November–December; Frey et al., 2015; Serreze et al., 2016; Grebmeier et al., 2006, 2018). When the sea ice disappears in the summer, subarctic baleen whales, namely gray whales (*Eschrichtius robustus*), humpback whales (*Megaptera novaeangliae*), fin whales (*Balaenoptera physalus*), and minke whales (*B. acutorostrata*), migrate northward into the Chukchi Sea to feed on seasonally-abundant prey (Clarke et al., 2013; Woodgate et al., 2015; Brower et al., 2018; Escajeda et al., 2020). Marine mammals rely on sound as their primary sense (Richardson et al.,

1995); consequently, the intrusion of ships into the Pacific Arctic presents a potential threat to the acoustic habitat of these animals.

Despite the potential for increased ship noise, little work has been done to quantify the impact of ships on sound levels in the Bering Strait region. Southall et al. (2020) examined sound levels produced by three vessels that passed within 10 km of two recorders, one in the Bering Strait and the other at a site north of St. Lawrence Island, and found that the ships produced sound levels below or higher than monthly average conditions depending on the proximity of the ship. A follow-up study by McKenna et al. (2021) examined the impact of ship noise on annual median sound levels measured for third-octave frequency bands at a site west of St. Lawrence Island in the northern Bering Sea. They found that radiated sounds measured from ships traveling at speeds > 5 knots within 10 km of their hydrophone had negligible impact on year-round sound levels (< 1 dB difference between median sound levels with ships present and annual median sound levels for third-octave frequency bands between 100 and 1000 Hz). Instead, wind and sea ice were the most significant contributors to annual sound levels (except for the 1000-Hz third-octave band; McKenna et al., 2021). Most vessels are only able to transit the Pacific Arctic when its waters are ice-free (June–November), necessitating an examination of how ships affect ambient sound levels of the region specifically during the open-water season.

In this study, we characterized the acoustic effects of ship activity in the Bering Strait during the open-water season (June through November) for 2013–2015 using three moored hydrophones within the Bering Strait. Specifically, we quantified the contribution of ship noise above ambient sound levels, with a focus on frequency bands used by baleen whales (25–1000 Hz; Southall et al., 2007; Moore et al., 2012). Our results reveal how ship noise is affecting the

acoustic environment of the Bering Strait, and serve as a baseline for measuring future changes in ship activity for the region.

4.3 Methods

4.3.1 *Acoustic Data Collection*

We collected acoustic recordings from AURAL-M2 hydrophones (Autonomous Underwater Recorder for Acoustic Listening-Model 2; Multi-Électronique, Inc.) attached to three moorings positioned within the Bering Strait. Site A2 was in the center of the eastern channel and Site A4 on the east side of the eastern channel. Site A3 was located ~ 35 km north of the strait in the southern Chukchi Sea (Fig. 4.1). The mooring sites were originally established in 1990 for measuring the physical properties of the oceanic throughflow through the strait (Woodgate et al., 2015; Woodgate, 2018). Hydrophone sensitivity was –155 dB re 1 V/µPa with a gain of 16 dB and the recordings were made using a 16-bit resolution. Each hydrophone was positioned 4–8 m above the seafloor and sampled at 8192 Hz, with a 20-min (2013 and 2014) or 22-min (2015) duty cycle, and varying deployment periods (Table 4.1). All recordings were timed to start at the top of the hour.

We focused our analyses on recordings from June through November of each year since the Bering Strait is typically ice-free during this period (Serreze et al., 2016; Grebmeier et al., 2018). We also noted the presence of ships in May and December; however, we did not analyze recordings for either month due to the abundance of vocalizing bearded seals and sea ice, which would make isolating ship sounds difficult. Note that acoustic data were unavailable for June 2013 at Sites A2 and A3, therefore we began our analysis in July for 2013. Recordings were visualized in the *Ishmael* software program (2014 version; Mellinger, 2002) using a fast Fourier transform (FFT) size of 4096 samples with a Hamming window and spectrogram equalization

enabled (time constant of 30 s). Recordings with ship sounds, as well as biotic sounds (e.g., whale calls) and line strumming created by water rushing past the mooring were identified by manually analyzing spectrograms in *Ishmael*. We quantified the number of recordings that matched three scenarios: 1) recordings with only ship noise present, 2) recordings with ship noise together with baleen whale vocalizations, and 3) recordings with baleen whale vocalizations only.

Marine mammals are sensitive to changes in frequency among third octaves, therefore summarizing sound amplitude using third-octave bands is useful for approximating sound levels for a range of frequencies (Richardson et al., 1995). Third-octave bands have a lower frequency limit, an upper frequency limit that is equivalent to $2^{1/3}$ of the lower frequency, and a central frequency roughly equivalent to the square-root of the product of the lower and upper frequencies. Third-octave bands are referred to by their central frequencies; for example, the 250-Hz third-octave band has a central frequency of 250 Hz and covers the frequency band from 223 to 281 Hz. We calculated the root-mean-square (RMS) sound pressure levels integrated over the 17 standard third-octave frequency bands between 25 and 1000 Hz for each recording using *PAMGuide* software in *MATLAB* (FFT with a 1-s long Hann window and 50% overlap; Merchant et al., 2015). We hereafter refer to third-octave sound levels as TOLs.

4.3.2 *Effects of Wind and Water Speed on Sound Levels*

We examined the impact of wind and water speed on TOLs commonly used to quantify radiated sound from ships, specifically TOLs with center frequencies of 63 Hz, 125 Hz, and 250 Hz (Van der Graaf et al., 2012; Dekeling et al., 2014; Merchant et al., 2014), to understand how wind and water speed may affect sounds recorded by our hydrophones. Wind is an important contributor to ambient sound levels during the open-water season (Wenz, 1962; Hildebrand,

2009; Roth et al., 2012; Insley et al., 2017; Stafford et al., 2018; Halliday et al., 2021b; McKenna et al., 2021), and thus, should be taken into consideration when quantifying the impact of ship noise. The Bering Strait has high water speeds, with hourly mean northward water speeds occasionally exceeding 130 cm/s (Woodgate, 2018), which can lead to flow noise and/or mooring line strumming (McKenna et al., 2021). Consequently, it was also important to consider how water speeds contribute to sound levels recorded by the hydrophones in the three third-octave frequency bands. Both flow noise and line strumming result from water flowing past the mooring, and therefore are not considered features of the broader acoustic environment (Robinson et al., 2014).

We analyzed ambient sound recordings—recordings without ship noise, line strumming, or biotic sounds—to isolate the effect of wind and water speeds on third-octave sound levels recorded by the hydrophones. We computed TOLs for the three third-octave bands (63 Hz, 125 Hz, and 250 Hz) over 1-s time windows and then time-averaged the sound levels over the full duration of the recording (~ 20 min in 2013 and 2014: 1199 s; ~ 22 min in 2015: 1399 s). We assumed that sound levels recorded when the hydrophones were on (i.e., during the first 20–22 min of the hour) were representative of the entire hour. We then calculated the daily median for each TOL band. Surface wind speed and direction were taken from the National Centers for Environmental Predication (NCEP) North American Regional Reanalysis 2 (NARR) wind data product (grid size of ~ 32 km; Mesinger et al., 2006) calculated for the closest grid point to the strait, ~110 km southwest of the moorings (65°N, 170°W; Fig. 4.1). We calculated daily mean water speeds using hourly water velocity data measured at 30-m depth by Acoustic Doppler Current Profilers (ADCP) attached to each mooring (Woodgate, 2018).

Given that the daily median TOLs for a given day could be correlated to the daily median TOLs from the previous day, we used generalized least squares (GLS) regression to examine the influence of daily mean wind and water speeds on daily median TOLs for the three bands. GLS regression accounts for correlation between the model residuals, making the method a good choice when temporal correlation in the response variable is a concern (Aitken, 1936). We built individual models for each third-octave band using data from each mooring site with all three years combined (e.g., we created a separate model for the 63 Hz TOLs recorded at Site A2 in 2013–2015, etc.) using the *nlme* package in *R* (*v*. 4.1.0; R Core Team, 2021; Pinheiro et al., 2022). We included a first-order autoregressive correlation structure in each model using a continuous time variable (day number) and the Pearson correlation coefficient taken from correlation tests between daily median TOLs as inputs (Table 4.2). We defined a day as a 24-h period starting at 00:00 UTC and assumed that daily means for wind and water speeds were independent. We used a significance threshold of 0.05 for all statistical tests.

4.3.3 *Characterizing Ship Activity*

We used Automatic Identification System (AIS) vessel tracking data to characterize the presence of ships throughout the open-water season (June–November) in the Bering Strait region, which we defined as within 100 km of the A2 and A3 moorings (see Fig. 4.1 for boundaries). Note that the 100-km buffer around A4 covered the same region as the 100-km buffer around A2, therefore we used the merged buffer for A2 and A3 to filter the AIS data. AIS data were obtained from the Nationwide Automatic Identification System (NAIS) dataset managed by the United States Coast Guard (https://marinecadastre.gov/ais/). The NAIS dataset is collected by land-based receivers every minute and includes vessel name (2015 only), status (2015 only), length, width, draft, a unique Maritime Mobile Service Identity (MMSI) number,

vessel type, latitude and longitude, speed over ground (in knots), course over ground, and heading. The vessel types identified in the NAIS dataset are based on the U.S. Coast Guard's Authoritative Vessel Identification Service (AVIS) database (https://marinecadastre.gov/ais/; Lee et al., 2019). The International Maritime Organization (IMO) only requires large vessels (> 300 gross tonnage), passenger vessels (vessels ≥ 100 gross tons and carrying a minimum of 12 passengers; U.S. Code of Federal Regulations, Title 46), and large fishing vessels to carry AIS transponders (IMO International Convention for the Safety of Life at Sea, 1974). Consequently, AIS is not a reliable tool for tracking the presence of small vessels (Hermannsen et al., 2019).

We filtered the AIS data to include only transmissions from vessels observed within a 100-km buffer around moorings A2 and A3. We identified unique vessels using their MMSI number and removed any transmissions that were missing a MMSI number from the dataset as we could not verify the source of these data (whether the transmissions were from unique ships). We then summed the number of unique ships by vessel type (provided by the AIS data) and by year. Finally, we calculated the average speed for each vessel using the reported speed over ground (SOG). See Fig. 4.2 for a flowchart of our approach for filtering the AIS data.

4.3.4 *Comparison Between Vessel Noise and Ambient Sound Levels*

Recordings with identified ship noise were paired with AIS transmissions from a single moving vessel (reported SOG > 5 knots) that passed within 10 km of the recorder (n = 156 recordings), following McKenna et al. (2021). Any ship recordings that did not match with AIS data or that had other sound sources present (e.g., whale calls) were excluded from the analysis. We refer to a ship recording that matched with the closest pass of a single unique vessel by the mooring as a "ship event" (unique vessels were identified using their MMSI number). AIS transmissions for each ship event were visualized in *ArcMap* (v. 10.8; Environmental Systems

Research Institute, ESRI, 2020) to ensure that the vessel was in a reasonable position relative to the mooring (i.e., not behind a landmass), and that the vessel was moving during the recording window.

We quantified ambient and ship noise levels as the TOLs for third-octave bands with standard center frequencies between 25 and 1000 Hz averaged over the full duration of the recording. Both wind speeds and water flowing past the mooring are known to affect received sound levels (McDonald et al., 2006; Insley et al., 2017; Halliday et al., 2021b; McKenna et al., 2021), therefore we separated the ship and ambient recordings into categories based on the mean wind speed from the NCEP-NARR dataset for the day of the recording and the hourly mean water speed from the ADCP instrument on the mooring (see Fig. 4.3 for a flowchart of our procedure). Recordings on days with mean wind speeds < 10 knots (~ 5 m/s) were labeled as "Low Wind" recordings since the effect of wind speed on ambient sound levels was found to decrease when winds were below this level (McDonald et al., 2006). Recordings with water speeds < 40 cm/s were labeled as "Low Water" since strumming noise was reduced below this level. We then compared median ambient third-octave SPLs to the median third-octave SPLs for the ship recordings for all sites and years combined by wind-water speed category: "Low Water/Low Wind," "Low Water/High Wind," "High Water/Low Wind," "High Water/High Wind" (Fig. 4.3).

4.3.5 *Ship Received Levels vs. Range*

We investigated the spatial impact of ship noise on the Bering Strait using received levels (RLs) for ship events where one vessel was present. Using the dataset of ship events from the ship noise vs. ambient analysis (see Section 4.3.4), we examined the AIS transmissions for each vessel and eliminated any ship events with fewer than three AIS transmissions during the 20/22-

minute recording window. We then eliminated duplicate ship events where the same vessel was detected at two mooring sites by selecting the recording from the closest hydrophone to the ship's track. In the case of repeat recordings of the same ship by the same hydrophone, we kept the recording from the closest pass of the vessel (total n = 73 ship events; Fig. 4.2).

We quantified the RLs for each ship event as the root-mean-square pressure for the 250-Hz TOL band time-averaged over 60-s intervals to match the same time resolution as the AIS transmissions. The 250-Hz band was chosen since it is less likely to be contaminated with flow noise than lower frequency TOL bands (Merchant et al., 2014). We then calculated the slant range between the recorder and each point from the ship's AIS transmissions using the hydrophone depth and straight-line distance between the ship and the recorder. Given that background noise levels could have contributed to the RLs, we corrected for background noise using the following equation (ANSI, 2009):

$$L_S = 10log_{10}\left[10^{\left(\frac{L_T}{10}\right)} - 10^{\left(\frac{L_B}{10}\right)}\right]$$

where L_S is the RL attributed to the ship (in dB), L_T is the total sound level in dB which consists of the ship and background noise, and L_B is background noise. Background TOLs were calculated from recordings that did not have any detectable sound sources present and that were recorded on the same day as the corresponding ship event (or as close to the day as possible).

We examined plots of background noise-corrected RLs for the 250-Hz band as a function of slant range for all the ship events. We then partitioned the ships by vessel type and examined the ship event with the maximum TOLs for the 250-Hz band for each vessel type.

4.4 Results

We analyzed 41,866 recordings combined across the three sites and years. There were 2,992 recordings with ship noise in total, with 1,031 recordings at Site A2, 1,000 recordings at

Site A3, and 961 recordings at Site A4. Out of the recordings with ship noise, 4% (A2), 17% (A3), and 3% (A4) also had baleen whale vocalizations present (Table 4.3). October had the highest number of recordings with both whale vocalizations and ship noise detected (44% of recordings from October had both ship noise and whale sounds present), followed by September (20%) and August (13%). In total, there were 93 days with ship noise present in 2013, 103 days in 2014, and 131 days in 2015. Most of the ships detected at Site A3 were also detected at Sites A2 and A4, and the AIS transmissions were closer to A2 and A4. Consequently, we focused our analyses only on Sites A2 and A4 (see Fig. 4.1 for map of mooring sites).

4.4.1 *Effects of Wind and Water Speed on Sound Levels*

All models indicated that both wind and water speeds influence sound levels for all three TOL bands (63 Hz, 125 Hz, and 250 Hz) at Sites A2 and A4 (Table 4.4). The relationship between sound levels for the three third-octave bands, and wind and water speeds were all significant (all $p < 0.05$) and positive, indicating that daily median sound levels in the three TOL bands increased with increasing daily mean wind and water speeds at Sites A2 and A4 (Table 4.4). The water speed coefficients were higher for 63-Hz TOL band at both sites (A2: increase of 0.56 dB per cm/s increase in water speed, A4: increase of 0.44 dB per cm/s) and the coefficients were barely higher than zero for the 250-Hz TOL band (A2: 0.02 dB per cm/s, A4: 0.04 dB per cm/s), indicating very little change in sound levels measured at this band in response to changes in wind and water speed. Conversely, the highest coefficients for wind speed were at the 250-Hz band (A2: increase of 0.86 dB per m/s increase in wind speed, A4: increase of 0.86 dB per m/s) and lowest at the 63-Hz band (A2: 0.47 dB per m/s, A4: 0.48 dB per m/s), suggesting that wind speeds have a greater effect on the 250-Hz TOL band while water speeds have a greater effect on the 63-Hz and 125-Hz TOL bands.

4.4.2 *Ship Activity in the Bering Strait*

A total of 412 unique AIS-transmitting vessels entered the Bering Strait region from May to November 2013–2015. The highest number of unique vessel passages occurred in 2013 with 153 vessels, compared to 123 vessels in 2014, and 136 vessels in 2015 (Table 4.5). Peak ship activity occurred in the months of July through September (Fig. 4.4), with the earliest AIS transmissions occurring in early May and the latest in mid-December. We did not analyze ship recordings from May or December due to the increased acoustic presence of marine mammals and sea ice. Two cargo ships and a military vessel traveled north of Site A3 on 4–6 May 2015, and the latest passage in the open-water season was made by a Russian icebreaker which transited northward through the western channel on 17 December 2015. A summary of the vessel types observed in the Bering Strait region can be found in Table 4.5. Cargo ships were the most common vessel type (139 unique vessels, 34%), followed by tugboats (n = 85 vessels, 21%), and vessels labeled as "other" in the NAIS dataset (n = 46 vessels, 11%). A total of 33 vessels had an unknown vessel type (i.e., vessel type was not listed in the NAIS dataset). Average speed over ground (SOG) for all vessel types ranged from 5 knots (tugboat) to 13.1 knots (law enforcement vessel), with an average of 9.1 knots (SD: ± 2.1 knots; Table 4.6).

4.4.3 *Comparison Between Vessel Noise and Ambient Sound Levels*

Median sound levels when a ship was present were higher than ambient sound levels for the majority of the third-octave frequency bands, regardless of water and wind speeds (mean difference for all wind/water speed categories and TOL frequency bands combined = ~ 4 dB ± 3 dB SD; range: –3 to 15 dB; Fig. 4.5). Ambient and ship median sound levels recorded on days with low water and low wind speeds had the greatest differences with ships elevating sound levels by 2–15 dB above ambient with an average difference of ~ 7 dB (Fig. 4.5A). The smallest

differences between ship and ambient median TOLs were observed in recordings with high wind speeds (high wind and low/high water speed) with an average difference of 3 dB ± 2 dB SD (range: –3 to 5 dB; Fig. 4.5). The highest median received levels were observed in the recordings with high water speeds (Fig. 4.5B), reflecting the influence of flow noise on sound levels recorded by the hydrophones (Section 4.4.1; Table 4.4).

4.4.4 *Ship Received Levels vs. Range*

Received levels (RL) measured at the 250-Hz TOL band for the select ship events (n = 73) show a general declining trend with higher RLs closer to the recorder, and lower RLs as the ships move away from the recorder (Fig. 4.6). The loudest vessel was a 102-m long ship in the "other" category. The ship was traveling at an average of 13 knots during the recording and produced RLs > 110 dB re 1 µPa at ~ 4.5 km from the recorder, and RLs > 100 dB re 1 µPa over 11 km away from the recorder (Fig. 4.6). The second loudest ship, a 122-m long military vessel, produced RLs > 100 dB re 1 µPa from ~ 5.5 km to ~ 11 km away from the recorder. Other loud vessels included three "other" ships of various lengths (Fig. 4.6), a cargo ship (225 m), a tugboat (32 m), and an offshore supply vessel (82 m). Speed over ground (SOG) ranged from 6 knots ("other" ship) to 14 knots (cargo ship).

4.5 Discussion

Our goal was to quantify how ship noise affects the soundscape of the Bering Strait during the open-water season. We found that ships elevated ambient sound levels by ~ 7 dB on average for calm days with low water/low wind speeds (range: 2 to 15 dB; Fig. 4.5A). On days with high water and high wind speeds, the mean increase over background levels was smaller (mean: 2 dB, range: –3 to 5 dB), however recordings with ship noise still had higher median TOLs (Fig. 4.5B). We also observed an increase in the number of days with ship noise over our

study period, which could be a reflection of increasing ship activity in the Bering Strait. Wind and water speeds were found to affect sound levels in third-octave bands commonly used to quantify ship noise with increases of 0.02–0.73 dB per unit change in wind/water speeds, emphasizing the importance of correcting for background noise and choosing a band that is less influenced by water speed when flow noise is a concern.

McKenna et al., (2021) conducted a similar study using a single hydrophone west of St. Lawrence Island and found that median third-octave sound levels (100–1000 Hz) produced by ships traveling at speeds > 5 knots within 10 km of their recorder were < 1 dB higher than annual median ambient sound levels. Given that ships are only able to transit the strait during the open-water season, we felt it was necessary to examine how ship noise affected median sound levels during this specific period. We observed sound levels 2–12 dB (mean: ~ 6 dB) above ambient for third-octave frequency bands between 100 and 1000 Hz on days with low wind and low water speeds during the open-water season in the Bering Strait (Fig. 4.5A). Note that the values given here are slightly different from the mean and range stated in the previous paragraph as the frequency range is different. While they may contribute a negligible amount of sound in comparison to annual median sound levels, ships are a major contributor of anthropogenic noise during the open-water season.

Our analysis of ship received levels as a function of range represents a preliminary approximation of the spatial impact of ship noise in the Bering Strait. The two loudest ships, a 102-m long “other” ship and a 122-m long military vessel, produced received levels that exceeded 100 dB re 1 μPa out to 11.1 km and ~ 10.9 km away from the recorder, respectively (Fig. 4.6). These distances indicate that ships could affect marine mammals well beyond the immediate vicinity of the traveling ships. Previous studies have demonstrated the long-range

impacts of ship noise on marine mammals in the Arctic. For example, Martin et al., (2022) observed that tagged belugas increased their swimming speeds and their lateral and vertical movements when ships were within 13–43 km. Other flee behaviors such as diving and swimming close to sea ice were observed by Finley et al., (1990) when ships were > 10 km away, suggesting that belugas are likely disturbed by ship noise rather than the ships themselves. We quantified the impact of ship noise with only one vessel present within 10 km of the recorders. Noise from multiple ships would certainly exacerbate any negative effects and should be the focus of a future study.

Most of the ships detected in the Bering Strait during our study period were cargo ships and tugboats, reflecting an increasing trend in commercial shipping in the Arctic. The Bering Strait has served as a corridor for large vessels transiting to the Arctic from the Pacific since the late 1800s when commercial whaling vessels first sailed its waters (Bockstoce, 1986). In the 20th century, the majority of vessels in this region were small cargo ships, tugboats, tankers, and barges en route to support coastal Arctic communities in the Chukchi and Beaufort seas (AMSA, 2009). With increased industrial activity and resource extraction in the western Arctic, the number of cargo ships and tankers observed in the region increased between 2008 and 2013 (AMSA, 2009; Huntington et al., 2015). Along with cargo transport, ship-based tourism in the Arctic is expected to increase in the 21st century (AMSA, 2009). Only 6% of the vessels observed in the Bering Strait region from 2013 to 2015 were identified as passenger vessels or pleasure crafts in the NAIS dataset (Table 4.5), however we anticipate that these numbers will grow in the future. It is also important to note that pleasure crafts and smaller passenger vessels (< 100 gross tons) are not required to carry AIS transponders by the IMO, and consequently, are underrepresented by the AIS data.

Most of the ship transits through the strait occurred in the summer and early fall months (July–September; Fig. 4.4), similar to Eguíluz et al. (2016) and Halliday et al. (2021a) who noted the highest numbers of Arctic transits in July–October. The peak in ship activity overlaps with the migrations of subarctic baleen whales through the strait (Clarke et al., 2013; Woodgate et al., 2015; Escajeda et al., 2020), increasing the probability of interactions between ships and whales. We observed the greatest overlap in ship noise and whale vocalizations in October, followed by September and August. Therefore, ships transiting through the Bering Strait during the month of October should be aware of migrating whales in the region and slow down when whales are observed.

Another key finding was how much both wind and water speeds affect sound levels in the third-octave bands used for quantifying ship noise. The European Union (E.U.) currently recommends using the 63-Hz and 125-Hz third-octave band for measuring ship noise (Van der Graaf et al., 2012; Dekeling et al., 2014). However, both bands exhibited significant, positive relationships to wind and water speed (Table 4.4), suggesting that sound levels for the 63-Hz and 125-Hz bands recorded by the hydrophone on days with strong currents may be artificially high (change of 0.25–0.56 dB per cm/s increase in water speed). Additionally, we found that median ambient sound levels for the 63-Hz band exceeded 100 dB re 1 μPa, the threshold for ambient noise set by the E.U. (Tasker et al., 2010), on days with high wind and water speeds (Fig. 4.5B). This result indicates that sound levels in the 63-Hz band may be higher on days with high wind and water speeds, regardless of ship activity. The difference for the 250-Hz band, on the other hand, was negligible (change of 0.02–0.04 dB per cm/s increase in water speed), suggesting that the 250-Hz band may be a better choice for quantifying ship noise when flow noise is a concern.

As the presence of ships continues to increase in the Bering Strait region, ship noise will become a greater threat for marine species that rely on sound for critical life functions (Erbe and Farmer, 2000; Halliday et al., 2017, 2020). Even relatively small changes in background sound levels could impact communication among Arctic and subarctic baleen whales given their documented sensitivity to changes in the soundscape. In Glacier Bay National Park, Alaska, humpback whales raised the source levels of their vocalizations by 0.81 dB and were 9% less likely to call for every for every 1 dB increase in ambient sound levels (Fournet et al., 2018). Gray whales similarly increased the source level of their calls along with their vocalization rate when exposed to increased vessel noise in their breeding grounds (Dahlheim and Castellote, 2016). As for fin whales, the features of their 20-Hz song notes, including note duration and peak frequency, changed when exposed to increased background noise (Castellote et al., 2012). Our findings that ship noise elevated sound levels as much as 15 dB in the frequency bands used by baleen whales indicates that increased noise levels due to ships could interrupt baleen whale communication during the open-water season in the Bering Strait.

Recommendations for mitigating the negative impacts of ships include limiting the travel of commercial ships to a specific route through the strait as well as encouraging vessel speed limits (Halliday et al., 2017, 2020). In late 2018, the IMO approved a joint proposal from the U.S. Coast Guard and the Russian Federation for a two-way route for large ships in the western and eastern channels of the Bering Strait (Fletcher et al., 2020). The routing measures also include multiple “Areas to be Avoided,” including the coastal region surrounding St. Lawrence Island, south of the Bering Strait. The routes are voluntary for vessels of 400 gross-tons and above, however a 2019 study by the Nuka Research and Planning Group found that compliance

was high among large commercial vessels, including bulk carriers, tankers, and cargo ships (Fletcher et al., 2020).

Shipping routes through the Bering Strait region are a good first step to managing vessel traffic in this sensitive area, however they do not address the issue of ship noise. Previous studies suggest that reducing the speed of ships could reduce noise levels (MacGillivray et al., 2019; ZoBell et al., 2021). We found that large vessels transiting the Bering Strait are already traveling at speeds around or below the 13-knot speed limit currently enforced in Glacier Bay National Park (ships in this study had a mean speed through water = 9.1 knots ± 2.1 knots SD; Code of Federal Registrations [CFR] 36 CFR 13.65, 2001; Frankel and Gabriele, 2017). Installing a voluntary speed limit through the strait is therefore likely to have high compliance among ship operators since ships are already transiting at relatively slow speeds and are already largely compliant with current Bering Strait routing measures (Fletcher et al., 2020). Additionally, decreasing the speed of vessels traveling the strait would have the added benefits of reducing the risk and lethality of vessel strikes for whales (Vanderlaan and Taggart, 2007) and lowering carbon emissions (Leaper, 2019). Moreover, voluntary speed limits are already in place in other regions of the Arctic. The Inuvialuit Settlement Region in the western Canadian Arctic established a voluntary speed limit of 10 knots with the goal of reducing the risk of vessel strikes and underwater noise (Fisheries and Oceans Canada, 2022). Therefore, a similar speed limit could be pursued for the Bering Strait region.

Coordinated efforts among multiple governments and agencies are required to reduce the potential harm to marine organisms from the expansion of economic activity in the Arctic. It is also important to realize that noise pollution is just one impact of increased shipping in the Arctic. Ship strikes, oil spills (leaks or major accidents), introduction of invasive species, and

disruption of marine mammal behavior such as feeding and migration (AMSA, 2009) will negatively affect sensitive species that are already being pushed to their limits by changing habitat conditions brought on by climate change (Laidre et al., 2008; Hauser et al., 2018; Halliday et al., 2020). The results presented here can serve as a baseline for measuring future impacts of shipping on the acoustic environment of the Bering Strait. More research is needed, however, to understand, anticipate, and mitigate the impacts of ships on the marine environment of the Pacific Arctic.

4.6 Acknowledgements

This study is based upon work supported by the National Science Foundation (NSF) Graduate Research Fellowship Program under grant number DGE-1256082. Any opinions, findings, and conclusions or recommendations expressed in this material are those of the author(s) and do not necessarily reflect the views of NSF. We also thank the University of Washington School of Aquatic and Fishery Sciences for providing funding for the primary author. This research was supported in part through the North Pacific Research Board Arctic Integrated Ecosystem Research Program, Baker et al., (2020); https://www.nprb.org/arctic-program/); this is manuscript ArcticIERP-52. Additional funding for this study was provided to K. Stafford from the North Pacific Research Board Arctic IERP (A94-00), the Office of Naval Research Marine Mammals and Biology Program N000141712274, and the National Science Foundation Polar Programs ARC-1107106; and to R. Woodgate from the NSF Arctic Observing Network PLR-1304052, 1758565 and 2153942. We would like to thank Alexander Hornof for his help in refining the methods; the crew of the *RV Norseman II* for their support in retrieving and deploying the moorings; as well as two anonymous reviewers whose comments and edits improved the manuscript. The Bering Strait mooring data can be accessed in the permanent

archives of the U.S. National Centers for Environmental Information/National Oceanographic Data Center (www.ncei.noaa.gov), and at:

http://psc.apl.washington.edu/HLD/Bstrait/bstrait.html.

4.7 References

Aitken, A.C. (1936). On Least Squares and Linear Combination of Observations. Proc. R. Soc. Edinb. 55, 42–48. https://doi.org/10.1017/S0370164600014346

AMSA (2009). *Arctic marine shipping assessment*. Arctic Council.

ANSI (2009). Quantities and Procedures for Description and Measurements of Underwater Sound from Ships – Part 1: General Requirements. Technical report, Acoustical Society of America Standards Secretariat.

Bockstoce, J. R. (1986). *Whales, ice, and men: the history of whaling in the western Arctic*, University of Washington Press in association with the New Bedford Whaling Museum, Massachusetts, Seattle, 1st ed., 400 pages.

Brower, A. A., Clarke, J. T., Ferguson, M. C. (2018). Increased sightings of subarctic cetaceans in the eastern Chukchi Sea, 2008–2016: population recovery, response to climate change, or increased survey effort? Polar Biol. 41, 1033–1039. doi:10.1007/s00300-018-2257-x

Castellote, M., Clark, C.W., Lammers, M.O. (2012). Acoustic and behavioural changes by fin whales (*Balaenoptera physalus*) in response to shipping and airgun noise. Biol. Conserv. 147, 115–122. doi: 10.1016/j.biocon.2011.12.021

Clark, C., Ellison, W., Southall, B., Hatch, L., Van Parijs, S., Frankel, A., Ponirakis, D. (2009). Acoustic masking in marine ecosystems: intuitions, analysis, and implication. Mar. Ecol. Prog. Ser. 395, 201–222. doi:10.3354/meps08402

Clarke, J., Stafford, K., Moore, S., Rone, B., Aerts, L., Crance, J. (2013). Subarctic cetaceans in the southern Chukchi Sea: evidence of recovery or response to a changing ecosystem. Oceanography 26, 136–149. doi:10.5670/oceanog.2013.81

Dahlheim, M., Castellote, M. (2016). Changes in the acoustic behavior of gray whales *Eschrichtius robustus* in response to noise. Endang. Species. Res. 31, 227–242. doi: 10.3354/esr00759

Dekeling, R., Tasker, M., Van Der Graaf, S., Ainslie, M., Andersson, M., André, M., Borsani, J., Brensing, K., Castellote, M., Cronin, D., Dalen, J., Folegot, T., Leaper, R., Pajala, J., Redman, P., Robinson, S., Sigray, P., Sutton, G., Thomsen, F., Werner, S., Wittekind, D., Young, J. (2014). *Monitoring guidance for underwater noise in European seas: a guidance document within the common implementation strategy for the Marine Strategy Framework Directive. Part II, Monitoring guidance specifications.*, European Commission. Joint

Research Centre. Institute for Environment and Sustainability, Publications Office, LU. Retrieved from https://data.europa.eu/doi/10.2788/27158

Eguíluz, V. M., Fernández-Gracia, J., Irigoien, X., Duarte, C. M. (2016). A quantitative assessment of Arctic shipping in 2010–2014. Sci. Rep. 6, 30682. doi:10.1038/srep30682

Eisner, L., Hillgruber, N., Martinson, E., Maselko, J. (2013). Pelagic fish and zooplankton species assemblages in relation to water mass characteristics in the northern Bering and southeast Chukchi seas. Polar Biol. 36, 87–113. doi:10.1007/s00300-012-1241-0

Erbe, C., and Farmer, D. M. (2000). Zones of impact around icebreakers affecting beluga whales in the Beaufort Sea. J. Acoust. Soc. Am. 108, 1332. doi:10.1121/1.1288938

Ershova, E., Hopcroft, R., Kosobokova, K., Matsuno, K., Nelson, R. J., Yamaguchi, A., Eisner, L. (2015). Long-term changes in summer zooplankton communities of the western Chukchi Sea, 1945–2012. Oceanography 28, 100–115. doi:10.5670/oceanog.2015.60

Escajeda, E., Stafford, K. M., Woodgate, R. A., Laidre, K. L. (2020). Variability in fin whale (*Balaenoptera physalus*) occurrence in the Bering Strait and southern Chukchi Sea in relation to environmental factors. Deep Sea Res. Part II 177, 104782. doi:10.1016/j.dsr2.2020.104782

Finley, K. J., Miller, G. W., Davis, R. A., Greene, C. R. (1990). Reactions of belugas, (*Delphinapterus leucas*), and narwhals (*Monodon monoceros*), to ice-breaking ships in the Canadian High Arctic. Canadian Bulletin of Fisheries and Aquatic Sciences 224, 97– 117.

Fletcher, S., Higman, B., Chartier, A., Robertson, T. (2020). *Adherence to Bering Strait Vessel Routing Measures in 2019* Seldovia, AK: Nuka Research and Planning Group LLC, p. 39. Retrieved from https://www.pewtrusts.org/-/media/assets/2020/04/200131nukaberingstraitroutingstudy.pdf

Fournet, M., Matthews, L., Gabriele, C., Haver, S., Mellinger, D., Klinck, H. (2018). Humpback whales *Megaptera novaeangliae* alter calling behavior in response to natural sounds and vessel noise. Mar. Ecol. Prog. Ser. 607, 251–268. doi:10.3354/meps12784

Frankel, A., Gabriele, C. (2017). Predicting the acoustic exposure of humpback whales from cruise and tour vessel noise in Glacier Bay, Alaska, under different management strategies. Endang. Species. Res. 34, 397–415. doi:10.3354/esr00857

Frey, K. E., Moore, G. W. K., Cooper, L. W., Grebmeier, J. M. (2015). Divergent patterns of recent sea ice cover across the Bering, Chukchi, and Beaufort seas of the Pacific Arctic Region. Prog. Oceanogr. 136, 32–49. doi:10.1016/j.pocean.2015.05.009

Grebmeier, J. M., Cooper, L. W., Feder, H. M., Sirenko, B. I. (2006). Ecosystem dynamics of the Pacific-influenced Northern Bering and Chukchi Seas in the Amerasian Arctic. Prog. Oceanogr., 71, 331–361. doi:10.1016/j.pocean.2006.10.001

Grebmeier, J., Frey, K., Cooper, L., Kędra, M. (2018). Trends in Benthic Macrofaunal Populations, Seasonal Sea Ice Persistence, and Bottom Water Temperatures in the Bering Strait Region. Oceanogr., 31. doi:10.5670/oceanog.2018.224

Halliday, W. D., Insley, S. J., Hilliard, R. C., de Jong, T., Pine, M. K. (2017). Potential impacts of shipping noise on marine mammals in the western Canadian Arctic. Mar. Pollut. Bull. 123, 73–82. doi:10.1016/j.marpolbul.2017.09.027

Halliday, W. D., Pine, M. K., Insley, S. J. (2020). Underwater noise and Arctic marine mammals: review and policy recommendations. Environ. Rev. 28, 438–448. doi:10.1139/er-2019-0033

Halliday, W. D., Pine, M. K., Citta, J. J., Harwood, L., Hauser, D. D. W., Hilliard, R. C., Lea, E. V., et al. (2021a). Potential exposure of beluga and bowhead whales to underwater noise from ship traffic in the Beaufort and Chukchi Seas. Ocean Coast. Manag. 204, 105473. doi:10.1016/j.ocecoaman.2020.105473

Halliday, W.D., Barclay, D., Barkley, A.N., Cook, E., Dawson, J., Hilliard, R.C., Hussey, N.E., Jones, J.M., Juanes, F., Marcoux, M., Niemi, A., Nudds, S., Pine, M.K., Richards, C., Scharffenberg, K., Westdal, K., Insley, S.J. (2021b). Underwater sound levels in the Canadian Arctic, 2014–2019. Mar. Pollut. Bull. 168, 112437. https://doi.org/10.1016/j.marpolbul.2021.112437

Hauser, D. D. W., Laidre, K. L., Stern, H. L. (2018). Vulnerability of Arctic marine mammals to vessel traffic in the increasingly ice-free Northwest Passage and Northern Sea Route. Proc. Natl. Acad. Sci. U.S.A. 115, 7617–7622. doi:10.1073/pnas.1803543115

Hermannsen, L., Mikkelsen, L., Tougaard, J., Beedholm, K., Johnson, M., Madsen, P. T. (2019). Recreational vessels without Automatic Identification System (AIS) dominate anthropogenic noise contributions to a shallow water soundscape. Sci. Rep. 9, 15477. doi:10.1038/s41598-019-51222-9

Hildebrand, J. (2009). Anthropogenic and natural sources of ambient noise in the ocean. Mar. Ecol. Prog. Ser. 395, 5–20. doi:10.3354/meps08353

Huntington, H. P., Daniel, R., Hartsig, A., Harun, K., Heiman, M., Meehan, R., Noongwook, G., et al. (2015). Vessels, risks, and rules: Planning for safe shipping in Bering Strait. Mar. Policy 51, 119–127. doi:10.1016/j.marpol.2014.07.027

Insley, S. J., Halliday, W. D., De Jong, T. (2017). Seasonal patterns in ocean ambient noise near Sachs Harbour, Northwest Territories. Arctic 70, 239. doi:10.14430/arctic4662

International Maritime Organization (IMO), International Convention for the Safety of Life At Sea, 1 November 1974, 1184 UNTS 3, available at: https://www.refworld.org/docid/46920bf32.html [Accessed 7 September 2022]

Jakobsson, M., Mayer, L., Coakley, B., Dowdeswell, J. A., Forbes, S., Fridman, B., Hodnesdal, H., et al. (2012). The International Bathymetric Chart of the Arctic Ocean (IBCAO) Version 3.0. Geophys. Res. Lett. 39, n/a-n/a. doi:10.1029/2012GL052219

Laidre, K. L., Stirling, I., Lowry, L. F., Wiig, Ø., Heide-Jørgensen, M. P., Ferguson, S. H. (2008). Quantifying the sensitivity of arctic marine mammals to climate-induced habitat change. Ecol. Appl. 18, S97–S125. doi:10.1890/06-0546.1

Leaper, R. (2019). The role of slower vessel speeds in reducing greenhouse gas emissions, underwater noise and collision risk to whales. Front. Mar. Sci. 6, 505. doi:10.3389/fmars.2019.00505

Lee, E., Mokashi, A.J., Moon, S.Y., Kim, G. (2019). The Maturity of Automatic Identification Systems (AIS) and Its Implications for Innovation. J. Mar. Sci. Eng. 7, 287. doi:10.3390/jmse7090287

Lemos, L.S., Haxel, J.H., Olsen, A., Burnett, J.D., Smith, A., Chandler, T.E., Nieukirk, S.L., Larson, S.E., Hunt, K.E., Torres, L.G., 2022. Effects of vessel traffic and ocean noise on gray whale stress hormones. Sci. Rep. 12, 18580. https://doi.org/10.1038/s41598-022-14510-5

MacGillivray, A.O., Li, Z., Hannay, D.E., Trounce, K.B., Robinson, O.M. (2019). Slowing deep-sea commercial vessels reduces underwater radiated noise. J. Acoust. Soc. Am. 146, 340–351. doi:10.1121/1.5116140

Martin, M.J., Halliday, W.D., Storrie, L., Citta, J.J., Dawson, J., Hussey, N.E., Juanes, F., Loseto, L.L., MacPhee, S.A., Moore, L., Nicoll, A., O'Corry-Crowe, G., Insley, S.J.(2022). Exposure and behavioral responses of tagged beluga whales (*Delphinapterus leucas*) to ships in the Pacific Arctic. Mar. Mamm. Sci. 12978. doi:10.1111/mms.12978

McKenna, M. F., Ross, D., Wiggins, S. M., Hildebrand, J. A. (2012). Underwater radiated noise from modern commercial ships. J. Acoust. Soc. Am. 131, 92–103. doi:10.1121/1.3664100

McKenna, M. F., Southall, B. L., Chou, E., Robards, M., Rosenbaum, H. C. (2021). An integrated underwater soundscape analysis in the Bering Strait region. J. Acoust. Soc. Am. 150, 1883–1896. doi:10.1121/10.0006099

Mellinger, D. (2002). *Ishmael 1.0 User's Guide*. NOAA Technical Memorandum OAR PMEL-120. http://www.pmel.noaa.gov/pubs/PDF/mell2434/mell2434.pdf.

Merchant, N. D., Pirotta, E., Barton, T. R., Thompson, P. M. (2014). Monitoring ship noise to assess the impact of coastal developments on marine mammals. Mar. Pollut. Bull. 78, 85–95. doi:10.1016/j.marpolbul.2013.10.058

Merchant, N. D., Fristrup, K. M., Johnson, M. P., Tyack, P. L., Witt, M. J., Blondel, P., Parks, S. E. (2015). Measuring acoustic habitats. (D. Hodgson, Ed.) Methods Ecol. Evol. 6, 257–265. doi:10.1111/2041-210X.12330

Mesinger, F., DiMego, G., Kalnay, E., Mitchell, K., Shafran, P. C., Ebisuzaki, W., Jović, D., et al. (2006). North American Regional Reanalysis. Bull. Amer. Meteor. Soc. 87, 343–360. doi:10.1175/BAMS-87-3-343

Moore, S. E., Reeves, R. R., Southall, B. L., Ragen, T. J., Suydam, R. S., Clark, C. W. (2012). A new framework for assessing the effects of anthropogenic sound on marine mammals in a rapidly changing Arctic. BioScience 62, 289–295. doi:10.1525/bio.2012.62.3.10

Notices to Mariners – Monthly Western Edition (Edition No. 06/2022), (2022). Canadian Coast Guard Programs: Aids to Navigation and Waterways. Fisheries and Oceans Canada, Montreal, Canada.

Nowacek, D. P., Thorne, L. H., Johnston, D. W., Tyack, P. L. (2007). Responses of cetaceans to anthropogenic noise. Mammal Rev. 37, 81–115. doi:10.1111/j.1365-2907.2007.00104.x

Pine, M. K., Hannay, D. E., Insley, S. J., Halliday, W. D., Juanes, F. (2018). Assessing vessel slowdown for reducing auditory masking for marine mammals and fish of the western Canadian Arctic. Mar. Pollut. Bull. 135, 290–302. doi:10.1016/j.marpolbul.2018.07.031

Pinheiro, J., Bates, D., R Core Team. (2022). *nlme*: Linear and Nonlinear Mixed Effects Models. R package version 3.1-160, https://CRAN.R-project.org/package=nlme.

R Core Team. (2021). R: A language and environment for statistical computing. R Foundation for Statistical Computing, Vienna, Austria. https://www.R-project.org/.

Richardson, W. J., Greene, Jr., C. R., Malme, C. I., Thomson, D. H. (1995). *Marine mammals and noise*, Academic Press, San Diego, California.

Robinson, S. P., Lepper, P. A., Hazelwood, R. A. (2014). *Good Practice Guide for Underwater Noise Measurement*. Technical report, National Measurement Office, Marine Scotland, The Crown Estate.

Rolland, R. M., Parks, S. E., Hunt, K. E., Castellote, M., Corkeron, P. J., Nowacek, D. P., Wasser, S. K., et al. (2012). Evidence that ship noise increases stress in right whales. Proc. Royal Soc. B. 279, 2363–2368. doi:10.1098/rspb.2011.2429

Ross, D. (1976). *Mechanics of underwater noise*, Pergamon, New York.

Serreze, M. C., Crawford, A. D., Stroeve, J. C., Barrett, A. P., Woodgate, R. A. (2016). Variability, trends, and predictability of seasonal sea ice retreat and advance in the Chukchi Sea. J. Geophys. Res. Oceans 121, 7308–7325. doi:10.1002/2016JC011977

Smith, L. C., Stephenson, S. R. (2013). New Trans-Arctic shipping routes navigable by midcentury. Proc. Natl. Acad. Sci. U.S.A. 110, E1191–E1195. doi:10.1073/pnas.1214212110

Southall, B. L., Bowles, A. E., Ellison, W. T., Finneran, J. J., Gentry, R. L., Greene, C. R., Kastak, D., et al. (2007). Marine mammal noise exposure criteria: initial scientific recommendations. Aquat. Mamm. 33, 411–521. doi:10.1578/AM.33.4.2007.411

Southall, B.L., Southall, H., Antunes, R., Nichols, R., Rouse, A., Stafford, K.M., Robards, M., Rosenbaum, H.C., (2020). Seasonal trends in underwater ambient noise near St. Lawrence Island and the Bering Strait. Mar. Pollut. Bull. 157, 111283. doi:10.1016/j.marpolbul.2020.111283

Stafford, K.M., Castellote, M., Guerra, M., Berchok, C.L. (2018). Seasonal acoustic environments of beluga and bowhead whale core-use regions in the Pacific Arctic. Deep-Sea Res. II: Top. Stud. Oceanogr. 152, 108–120. doi:10.1016/j.dsr2.2017.08.003

Stephenson, S. R., Smith, L. C., Agnew, J. A. (2011). Divergent long-term trajectories of human access to the Arctic. Nat. Clim. Chang. 1, 156–160. doi:10.1038/nclimate1120

Stephenson, S. R., Smith, L. C., Brigham, L. W., Agnew, J. A. (2013). Projected 21st-century changes to Arctic marine access. Clim. Change 118, 885–899. doi:10.1007/s10584-012-0685-0

Tasker, M. L., Amundin, M., André, M., Hawkins, A., Lang, W., Merck, T., et al. (2010). *Marine Strategy Framework Directive Task Group 11 Report: Underwater Noise and Other Forms of Energy*. Ispra: Joint Research Centre. doi: 10.2788/87079

Van der Graaf, A., Ainslie, M.A., Andre, M., Brensing, K., Dalen, J., Dekeling, R., Robinson, S., Tasker, M., Thomsen, F., Werner, S. (2012). European Marine Strategy Framework Directive–Good Environmental Status (MSFD GES): Report of the Technical Subgroup on Underwater Noise and Other Forms of Energy. http://ec.europa.eu/environment/marine/pdf/MSFD_reportTSG_Noise.pdf.

Vanderlaan, A. S. M., Taggart, C. T. (2007). Vessel collisions with whales: the probability of lethal injury based on vessel speed. Marine Mammal Sci. 23, 144–156. doi:10.1111/j.1748-7692.2006.00098.x

Wenz, G. M. (1962). Acoustic ambient noise in the Ocean: spectra and sources. J. Acoust. Soc. Am. 34, 1936–1956. doi:10.1121/1.1909155

Woodgate, R. A. (2018). Increases in the Pacific inflow to the Arctic from 1990 to 2015, and insights into seasonal trends and driving mechanisms from year-round Bering Strait mooring data. Prog. Oceanogr. 160, 124–154. doi:10.1016/j.pocean.2017.12.007

Woodgate, R., Stafford, K., Prahl, F. (2015). A synthesis of year-round interdisciplinary mooring measurements in the Bering Strait (1990–2014) and the RUSALCA years (2004–2011). Oceanography 28, 46–67. doi:10.5670/oceanog.2015.57

ZoBell, V. M., Frasier, K. E., Morten, J. A., Hastings, S. P., Peavey Reeves, L. E., Wiggins, S. M., Hildebrand, J. A. (2021). Underwater noise mitigation in the Santa Barbara Channel through incentive-based vessel speed reduction. Sci. Rep. 11, 18391. doi:10.1038/s41598-021-96506-1

4.8 Tables

Table 4.1. Hydrophone deployment data, including latitude and longitude (in decimal degrees) and recording settings. Dates are in the format ‘yyyy-mm-dd.’ Mooring names are from the Bering Strait mooring program (Woodgate et al., 2015). See Fig. 4.1 for the mooring locations.

Mooring	Deployment Year	Latitude N	Latitude W	Record Start Date	Record End Date	Hydrophone Depth (m)	Water Depth (m)	Sampling Rate (Hz)	Hourly Duty Cycle
A2	2013	65.78°	168.57°	2013-07-15	2014-07-01	48	54	8192	20 min
	2014	65.78°	168.57°	2014-07-10	2015-07-04	49	53	8192	20 min
	2015	65.78°	168.57°	2015-07-05	2016-07-08	49	54	8192	22 min
A3	2013	66.33°	168.97°	2013-07-15	2014-07-02	52	56	8192	20 min
	2014	66.33°	168.97°	2014-07-10	2015-07-02	50	56	8192	20 min
	2015	66.33°	168.97°	2015-07-05	2016-07-08	48	56	8192	22 min
A4	2013	65.75°	168.26°	2013-07-15	2014-07-02	42	47	8192	20 min
	2014	65.75°	168.25°	2014-07-10	2015-07-02	42	47	8192	20 min
	2015	65.75°	168.25°	2015-07-05	2016-07-08	41	47	8192	22 min

Table 4.2. Correlation coefficients and *p*-values from Pearson correlation tests between daily median third-octave sound levels measured for the 63-Hz, 125-Hz, and 250-Hz bands. The correlation coefficients were used in the autoregressive correlation factors for the generalized least squares regression models (See Section 4.3.2).

	A2			A4		
	63 Hz	**125 Hz**	**250 Hz**	**63 Hz**	**125 Hz**	**250 Hz**
Correlation Coefficient	0.51	0.5	0.54	0.5	0.5	0.5
***p*-value**	< 0.001	< 0.001	< 0.001	< 0.001	< 0.001	< 0.001

Table 4.3. Total numbers of recordings with ship noise, baleen whale vocalizations, or a combination of both for each mooring. Note that there were ship recordings with other marine mammal species present, we focus on whales only here.

	A2	**A3**	**A4**
Total number of recordings with ship noise	1031	1000	961
Number of recordings with ship noise ONLY	936	757	911
Number of recordings with ship noise AND whale calls	39	165	33
Number of recordings with whale calls ONLY	1672	5444	1306

Table 4.4. Coefficients ("Coef.") and *p*-values from the generalized least squares (GLS) regression models examining the relationship between daily mean wind (m/s) and water speeds (cm/s), and daily median sound levels recorded for the 63-Hz, 125-Hz, and 250-Hz third-octave bands at Sites A2 and A4 (2013–2015 combined). All *p*-values were significant (significance threshold = 0.05).

	A2						**A4**					
	63 Hz		**125 Hz**		**250 Hz**		**63 Hz**		**125 Hz**		**250 Hz**	
	Coef.	***p***	**Coef.**	***p***	**Coef.**	***p***	**Coef.**	***p***	**Coef.**	***p***	**Coef.**	***p***
Intercept	66.2	< 0.001	68.1	< 0.001	76.2	< 0.001	68.8	< 0.001	69.3	< 0.001	75.1	< 0.001
Water Speed	0.56	< 0.001	0.29	< 0.001	0.02	0.02	0.44	< 0.001	0.25	< 0.001	0.04	< 0.001
Wind Speed	0.47	< 0.001	0.73	< 0.001	0.86	< 0.001	0.48	< 0.001	0.71	< 0.001	0.86	< 0.001

Table 4.5. Total counts of vessels by type observed in the Bering Strait region (i.e., within 100-km of Sites A2 and A3) during May–November for the years 2013–2015 according to the U.S. Coast Guard's Nationwide Automatic Identification System (NAIS) data. The vessel types were defined by the NAIS dataset and are based on the U.S. Coast Guard's Authoritative Vessel Identification Service (AVIS) database. Note that only large vessels (> 300 gross tonnage), passenger vessels (≥ 100 gross tons and carrying a minimum of 12 passengers), and large fishing vessels are required to carry AIS transponders by the International Maritime Organization (IMO). Sailing and smaller vessels are not required to carry AIS transponders, and consequently, their numbers may be underrepresented in the totals presented here.

Vessel Type	**2013**	**2014**	**2015**	**Totals**
Cargo	51	43	45	**139**
Tug	27	23	35	**85**
Other	23	22	1	**46**
Tanker	21	11	10	**42**
NA	14	12	8	**34**
Passenger	7	5	6	**18**
Research Vessel	0	0	9	**9**
Offshore Supply Vessel	0	0	9	**9**
Fishing	4	1	2	**7**
Public Vessel	0	0	7	**7**
Pleasure Craft/Sailing	2	2	2	**6**
Military	3	1	0	**4**
Search and Rescue	1	2	0	**3**
Offshore Drilling Unit	0	0	2	**2**
Law Enforcement	0	1	0	**1**
Totals	**153**	**123**	**136**	**412**

Table 4.6. Number of unique vessels by type (total n = 378) along with the average speed over ground (SOG, knots) and the standard deviation in parentheses calculated using all unique vessels combined for each vessel type. Note that there were 34 ships with unknown vessel type that were not included in the table below.

Vessel Type	***n***	**Mean SOG (knots)**
Cargo	139	11.2 (± 2.5)
Tug	85	7.4 (± 2.2)
Other	46	9.2 (± 2.9)
Tanker	42	11.4 (± 2.6)
Passenger	18	8.7 (± 2.6)
Research Vessel	9	9.1 (± 2)
Offshore Supply Vessel	9	7 (± 2.4)
Fishing	7	8.3 (± 2.1)
Public Vessel	7	11 (± 5.2)
Pleasure Craft/Sailing	6	9.2 (± 3.4)
Military	4	8 (± 3.6)
Search and Rescue	3	8.8 (± 1.4)
Offshore Drilling Unit	2	5 (± 0.3)
Law Enforcement	1	13.1

4.9 Figures

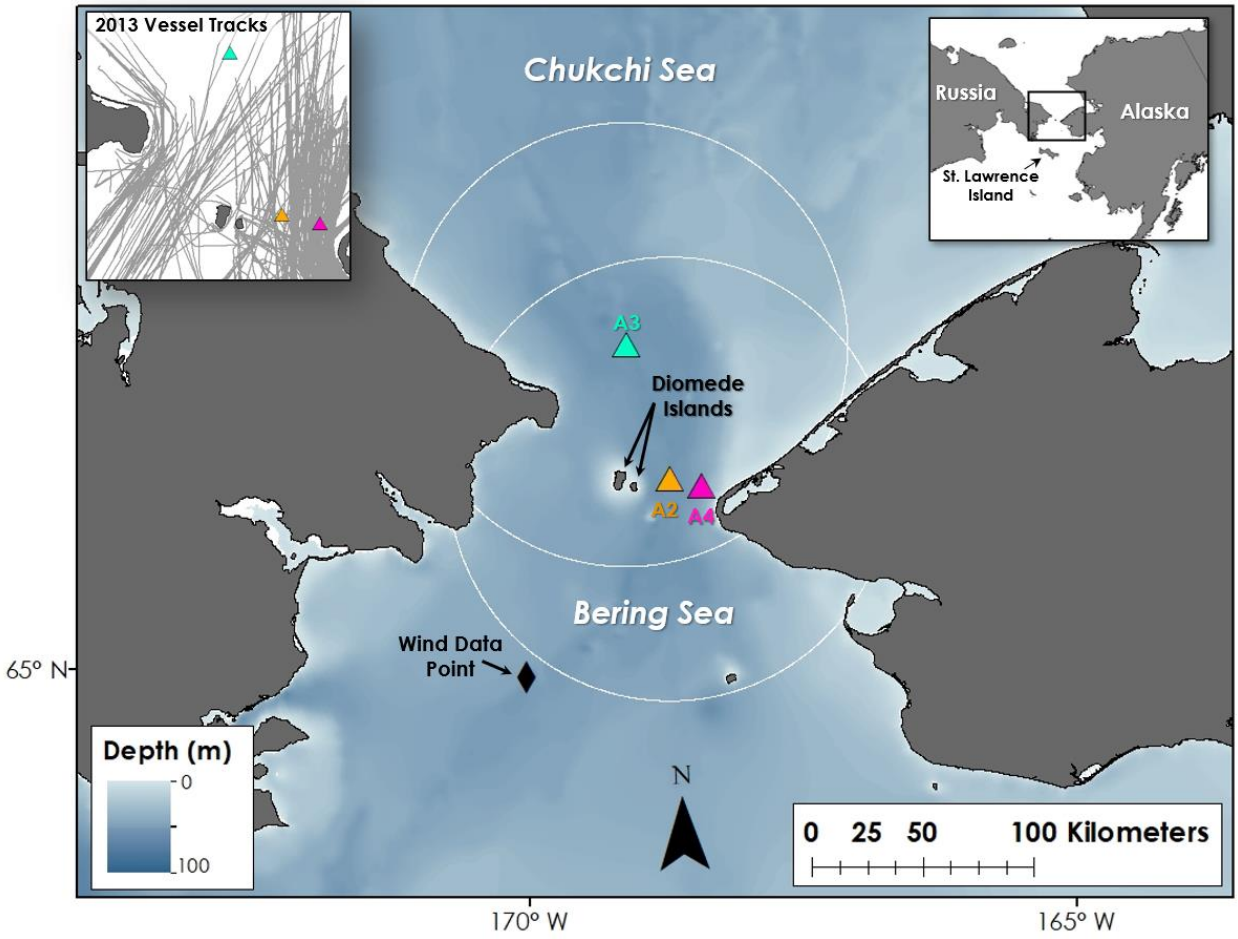

Fig. 4.1. Map of the study area with the three mooring locations—Sites A2 and A4 in the eastern channel of the strait, and Site A3 north of the strait. The nearest NCEP-NARR wind data point is located southwest of the strait (65°N, 170°W; Mesinger et al., 2006). The two white circles represent 100-km buffers around Sites A2 and A3, respectively, and were used for identifying ships within the Bering Strait region. Depth data were taken from the International Bathymetric Chart of the Arctic Ocean version 3.0 (500-m resolution; Jakobsson et al., 2012). The top left inset shows the tracklines for all vessels that transited the Bering Strait between June–November 2013.

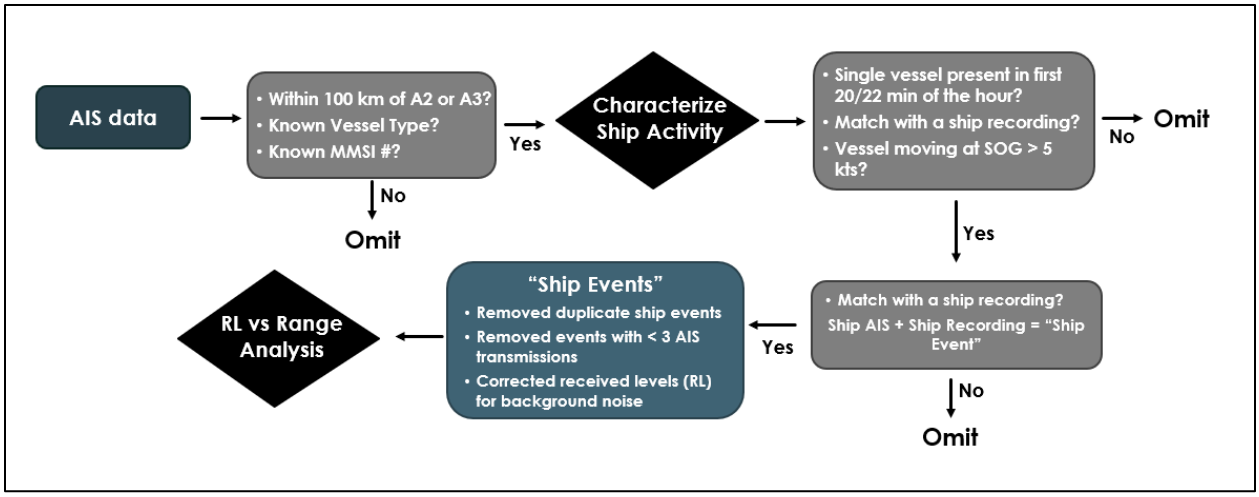

Fig. 4.2. Summary of our approach for selecting the ship transmissions from the AIS data for characterizing ship activity in the Bering Strait and for the received level (RL) vs. range to receiver analysis. SOG = speed over ground in knots; MMSI = Maritime Mobile Service Identity number.

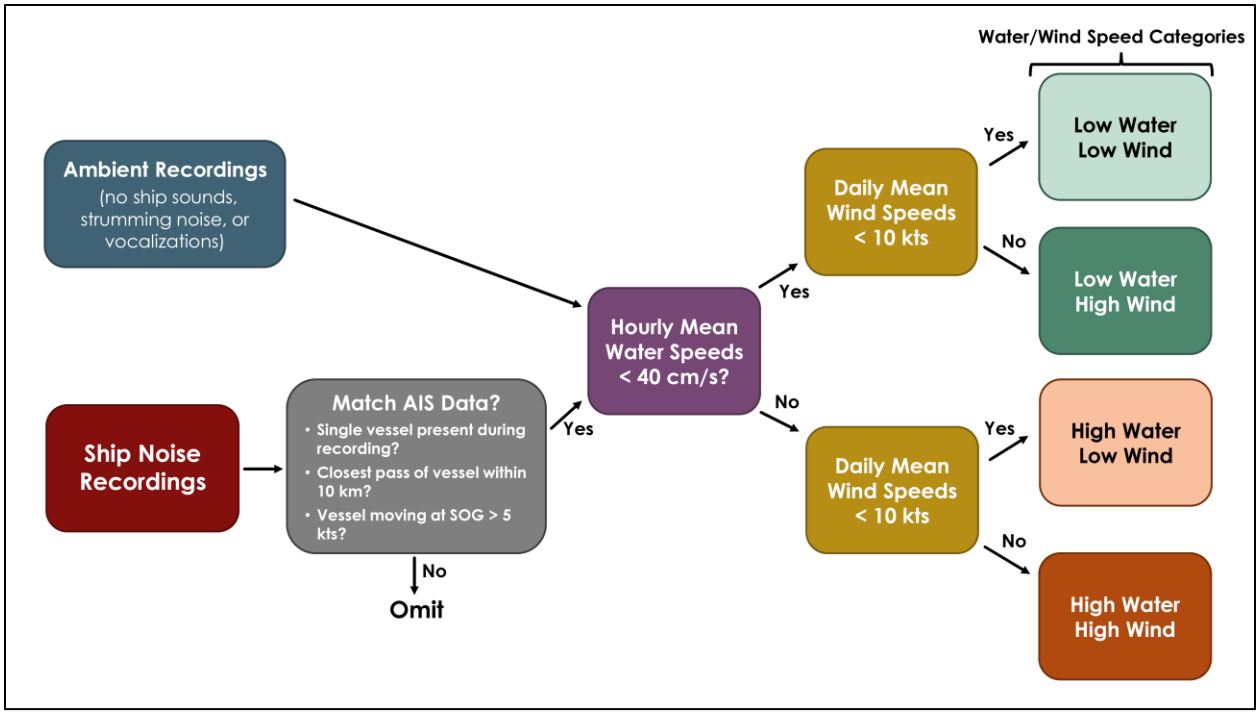

Fig. 4.3. Summary of our approach to dividing the ambient and ship acoustic files into wind and water speed categories for the ship vs. ambient sound level analysis.

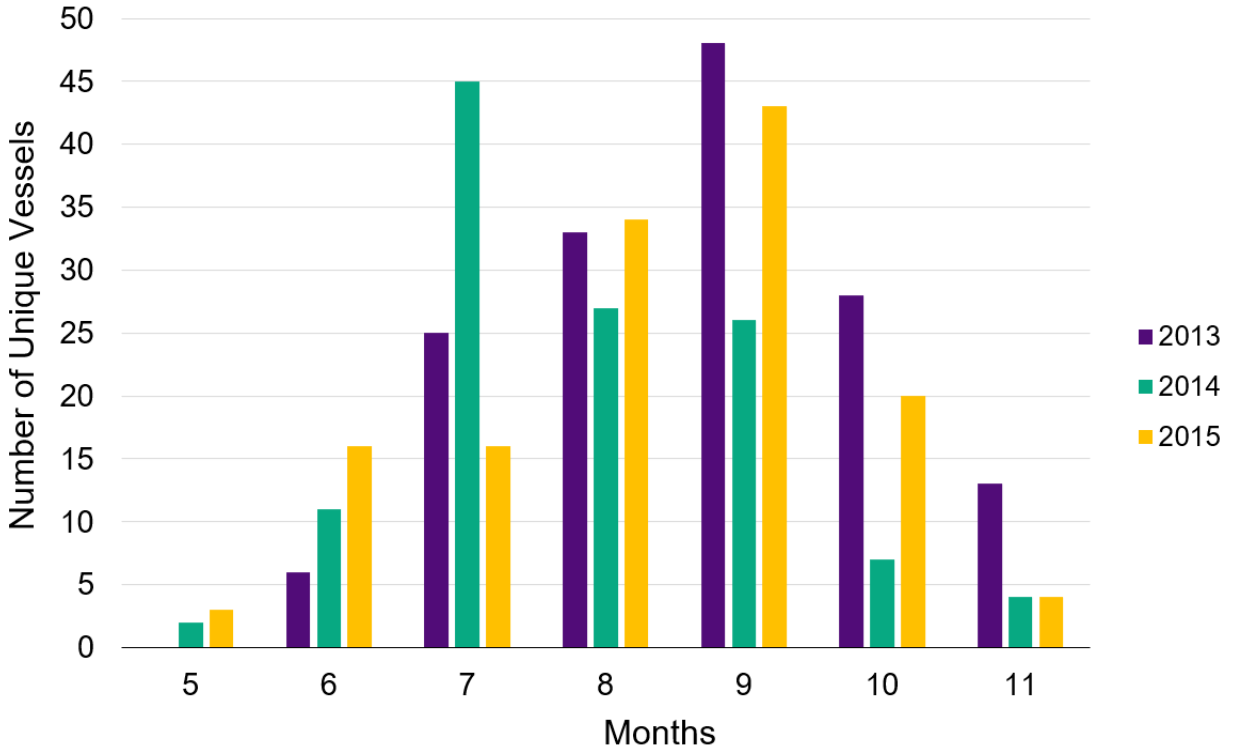

Fig. 4.4. Total counts of unique vessels that transited within 100 km of the Bering Strait region (*n* = 412 vessels), defined as merged 100-km buffers around Sites A2 and A3 (see Fig. 4.1). Note that the totals are likely underestimates since not all vessels are required to carry AIS transponders.

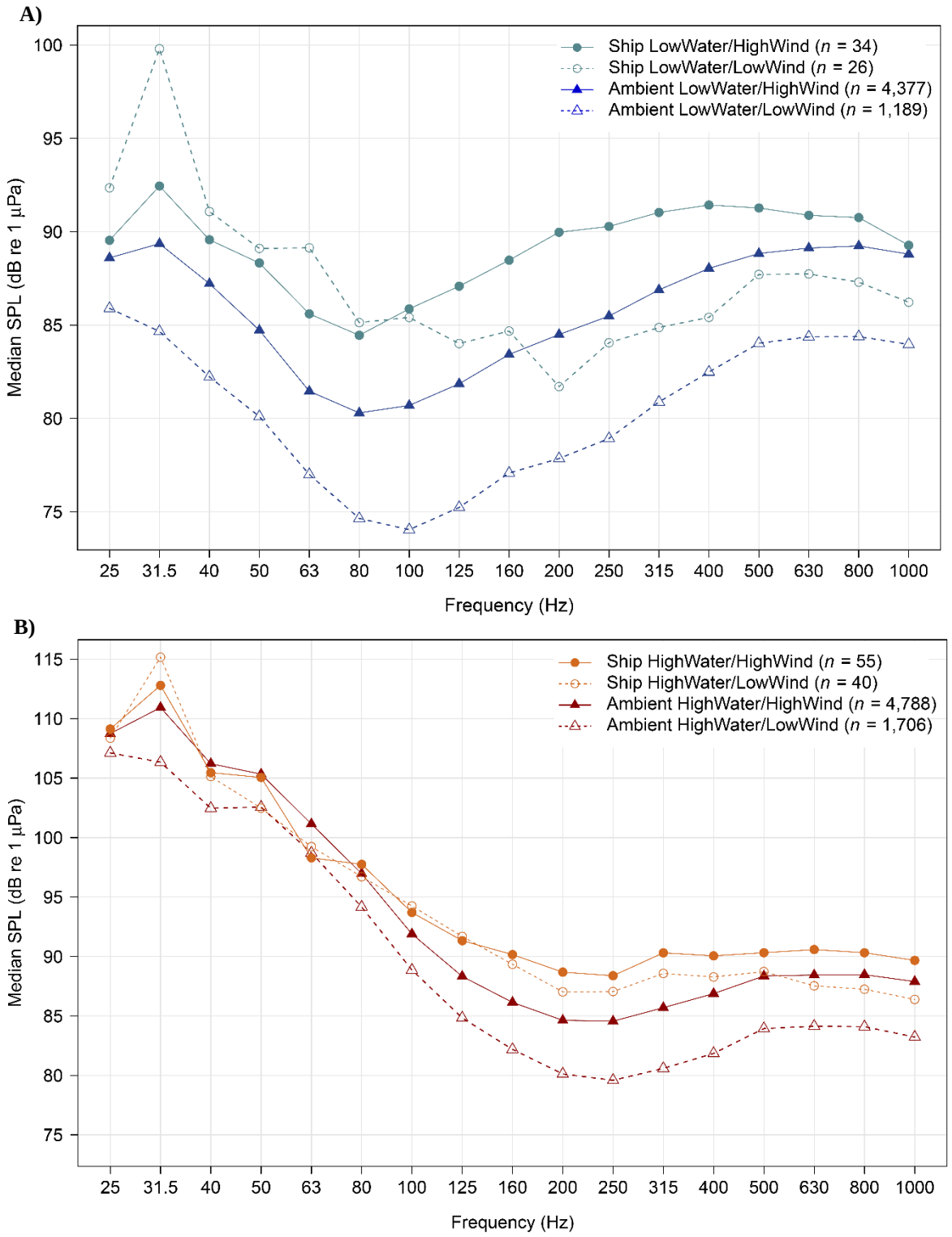

Fig. 4.5. Median sound pressure levels (SPL) measured across third-octave frequency bands (Hz) for recordings with ship noise (circles) plotted against ambient SPLs (triangles) for (A) days with low water speeds (≤40 cm/s), and (B) days with high water speeds (>40 cm/s) visualized by whether the recording occurred on a day with high wind speeds (>10 knots; solid lines and

points), or low wind speeds (≤10 knots; dotted lines and hollow points). Total sample sizes for the ship recordings are as follows: low water/high wind = 34 recordings; low water/low wind = 26 recordings; high water/high wind = 55 recordings; and high water/low wind = 40 recordings. Ambient sample sizes are as follows: low water/high wind = 4,377 recordings; low water/low wind = 1,189 recordings; high water/high wind = 4,788 recordings; and high water/low wind = 1,706 recordings. Note that the *x*-axis is log-scaled.

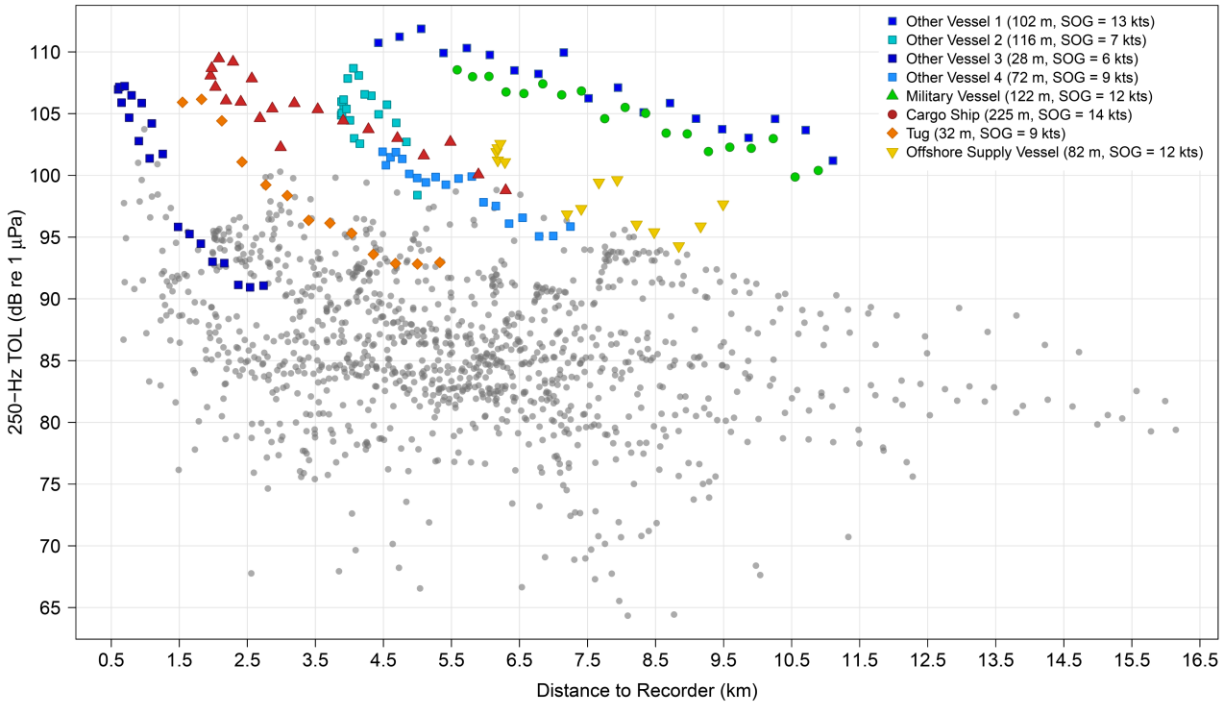

Fig. 4.6. Received levels (RL) for the 250-Hz third-octave frequency band (TOL) vs. slant range to the recorder (km) for the loudest vessels from the select dataset of unique ship events (n = 8; color points) plotted against the RLs for all select ship events (total n = 73; gray points). A 'ship event' is a ship recording matched with the AIS tracks of a single vessel that was traveling at speeds > 5 knots and passed within 10 km of the mooring (see Section 4.3.5). Vessel type is listed for each of the loudest vessels along with its length and mean speed over ground (SOG) in knots (kts). Each point represents the RL measured over each minute of the ship event recording and corresponds to an AIS transmission.